

MINISTRY OF EDUCATION AND SCIENCE UKRAINE

ODESSA I. I. MECHNIKOV NATIONAL UNIVERSITY

# **ФОТОЭЛЕКТРОНИКА**

**PHOTOELECTRONICS  
INTER-UNIVERSITIES SCIENTIFIC ARTICLES**

Founded in 1986

Number 27

ODESSA  
ONU  
2018

**«PHOTOELECTRONICS»**  
**№ 27 – 2018**

**INTER-UNIVERSITIES SCIENTIFIC  
ARTICLES**

Founded in 1986

*Certificate of State Registration*  
*KB № 15953*

**«ФОТОЭЛЕКТРОНИКА»**  
**№ 27–2018**

**МЕЖВЕДОМСТВЕННЫЙ НАУЧНЫЙ  
СБОРНИК**

Основан в 1986 г.

*Свидетельство о Государственной  
регистрации KB № 15953*

UDC 621.315.592:621.383.51:537.221

The results of theoretical and experimental studies in problems of the semiconductor and micro-electronic devices physics, opto- and quantum electronics, quantum optics, spectroscopy and photophysics of nucleus, atoms, molecules and solids are presented in the issue. New directions in the photoelectronics, stimulated by problems of the super intense laser radiation interaction with nuclei, atomic systems and substance, are considered. Scientific articles «Photoelectronics» collection abstracted in ВИНИТИ and «Джерело»

Scientific articles «Photoelectronics» collection abstracted in: Scientific Periodicals in National Library of Ukraine Vernadsky, Ukrainian Abstract Journal, Україніка наукова, ВИНИТИ, Джерело, Українські наукові журнали: The issue is introduced to the List of special editions of the Ukrainian Higher Certification Commission in physics-mathematics and technical sciences.

For lecturers, scientists, post-graduates and students

У збірнику наведено результати теоретичних і експериментальних досліджень з питань фізики напівпровідників та мікроелектронних приладів, опто- та квантової електроніки, квантової оптики, спектроскопії та фотофізики ядра, атомів, молекул та твердих тіл. Розглянуто нові напрямки розвитку фотоелектроніки, пов'язані із задачами взаємодії надінтенсивного лазерного випромінювання з ядром, атомними системами, речовиною.

Збірник включено до Переліку спеціальних видань ВАК України з фізико-математичних та технічних наук.

Збірник реферується: Scientific Periodicals in National Library of Ukraine Vernadsky, Ukrainian Abstract Journal, Україніка наукова, ВИНИТИ, Джерело, Українські наукові журнали

Для викладачів, наукових працівників, аспірантів, студентів

В сборнике приведены результаты теоретических и экспериментальных исследований по вопросам физики полупроводников и микроэлектронных приборов, опто- и квантовой электроники, квантовой оптики, спектроскопии и фотофизики ядра, атомов, молекул и твердых тел. Рассмотрены новые направления развития фотоэлектроники, связанные с задачами взаимодействия сверхинтенсивного лазерного излучения с ядром, атомными системами, веществом.

Сборник включен в Список специальных изданий ВАК Украины по физико-математическим и техническим наукам. Сборник «Photoelectronics» реферируется в Scientific Periodicals in National Library of Ukraine Vernadsky, Ukrainian Abstract Journal, Україніка наукова, ВИНИТИ, Джерело, Українські наукові журнали

Для преподавателей, научных работников, аспирантов, студентов

Editorial board «Photoelectronics»:

Editor-in-Chief V. A. Smyntyna  
Kutalova M. I. (Odessa, Ukraine, responsible editor);  
Vaksman Yu. F. (Odessa, Ukraine);  
Litvchenko V. G. (Kiev, Ukraine);  
Mokrickiy V. A. (Odessa, Ukraine);  
Starodub N. F. (Kiev, Ukraine);  
Vikulin I. M. (Odessa, Ukraine).  
Kurmachov Ch.D.(Odessa,Ukraine)  
Vorshcak V.A.(Odessa,Ukraine)  
Address of editorial board:

Odessa I. I. Mechnikov National University 42, Pasteur str., Odessa, 65026, Ukraine  
Information is on the site: <http://phys.onu.edu.ua/journals/photoele/>  
[http://experiment.onu.edu.ua/exp\\_ru/files/](http://experiment.onu.edu.ua/exp_ru/files/)  
e – mail: [photoelectronics@onu.edu.ua](mailto:photoelectronics@onu.edu.ua).

© Odessa I. I. Mechnikov National University, 2018

## TABLE OF CONTENTS:

<i>A. P. Chebanenko, A. V. Polischuk</i> ELECTRICAL PROPERTIES OF STRUCTURES BASED ON NANOCRYSTALS CdS IN GELATIN MATRIX.....	5
<i>O. A. Antoshkina, O. Yu. Khetselius, M. P. Makushkina, A. V. Smirnov</i> THE HYPERFINE STRUCTURE OF HEAVY ELEMENTS ATOMS WITHIN RELATIVISTIC MANY-BODY PERTURBATION THEORY .....	10
<i>Yu. A. Nitsuk, A. S. Leonenko, Yu. F. Vaksman, G. V. Korenkova, V. A. Smyntyna, Ie V. Brytavskiyi</i> PHOTOLUMINESCENCE OF CdSe:Ni NANOPARTICLES OBTAINED BY CHEMICAL METHOD .....	18
<i>V. V. Buyadzhi, T. B. Tkach, A. P. Lavrenko, E. S. Romanenko</i> SPECTROSCOPY OF MULTICHARGED IONS IN PLASMAS: OSCILLATOR STRENGTHS OF Be-LIKE IONS GaXXVIII and GeXXIX.....	24
<i>T. I. Lavrenova, V. A. Borshchak, N. P. Zatovska, M. I. Kutalova</i> SOLDER FOR FORMATION OF CONTACTS TO CONVERTERS OF OPTICAL AND X-RAY IMAGES INTO THE ELECTRICAL SIGNAL.....	30
<i>E. V. Ternovsky, V. V. Buyadzhi, A. V. Tsudik, A. A. Svinarenko</i> RELATIVISTIC CALCULATION OF RYDBERG AUTOIONIZATION STATES PARAMETERS IN SPECTRUM OF BARIUM.....	34
<i>A. V. Glushkov, A. V. Tsudik, D. A. Novak, O. V. Dubrovsky</i> CHAOTIC DYNAMICS OF RELATIVISTIC BACKWARD-WAVE TUBE WITH ACCOUNTING FOR SPACE CHARGE FIELD AND DISSIPATION EFFECTS: NEW EFFECTS.....	44
<i>L. M. Filevska</i> LUMINESCENCE OF NANOSCALE TIN DIOXIDE. REVIEW .....	52
<i>A. V. Ignatenko, A. V. Glushkov, Ya. I. Lepikh, A. S. Kvasikova</i> PHOTOELECTRON SPECTROSCOPY OF DIATOMIC MOLECULES: OPTIMIZED GREEN'S FUNCTIONS AND DENSITY FUNCTIONAL APPROACH .....	60
<i>O. Yu. Khetselius, A. L. Mykhailov, E. A. Efimova, R. E. Serga</i> WAVELENGTHS AND OSCILLATOR STRENGTHS FOR Li-LIKE MULTICHARGED IONS WITHIN RELATIVISTIC MANY-BODY PERTURBATION THEORY.....	69

<i>S. S. Kulikov, Ye. V. Brytavskiy, M. I. Kotalova, N. P. Zatovskaya V. A. Borshchak, N. V. Konopel'skaya, Y. N. Karakis</i> THE STUDY OF CADMIUM SULFIDE HETEROGENEOUSLY SENSITIZED CRYSTALS. RELAXATION CHARACTERISTICS. PART II.....	79
<i>A. A. Kuznetsova, A. A. Buyadzi, M. Yu. Gurskaya, A. O. Makarova</i> SPECTROSCOPY OF MULTIELECTRON ATOM IN A DC ELECTRIC FIELD: MODIFIED OPERATOR PERTURBATION THEORY APPROACH TO STARK RESONANCES .....	94
<i>A. A. Mashkantsev, A. V. Ignatenko, S. V. Kirianov, E. V. Pavlov</i> CHAOTIC DYNAMICS OF DIATOMIC MOLECULES IN AN ELECTROMAGNETIC FIELD .....	103
<i>A. A. Svinarenko, V. B. Ternovsky, I. S. Cherkasova , D. A. Mironenko</i> THEORETICAL STUDYING SPECTRA OF YTTERBIUM ATOM ON THE BASIS OF RELATIVISTIC MANY-BODY PERTURBATION THEORY: DOUBLY EXCITED VALENCE STATES .....	113
<i>V. B. Ternovsky, A.A. Kuznetsova, A.V. Glushkov, E.K. Plysetskaya</i> RELATIVISTIC OPERATOR PERTURBATION THEORY IN SPECTROSCOPY OF MULTIELECTRON ATOM IN AN ELECTROMAGNETIC FIELD.....	121
<i>V. V. Halyan, I. D. Olekseyuk, I. A. Ivashchenko, A. H. Kevshyn, P. V. Tishchenko, M. V. Shevchuk</i> OPTICAL PROPERTIES OF THE $Ag_{28}Ga_{28}Ge_{532}Er_2S_{1123}$ AND $Ag_{12}Ga_{12}Ge_{228}Er_2S_{483}$ GLASSES .....	131
<i>ВАЛЕНТИНУ АНДРІЙОВИЧУ СМІНТИНІ – 70!</i> .....	137
ІНФОРМАЦІЯ ДЛЯ АВТОРІВ НАУКОВОГО ЗБІРНИКА «PHOTOELECTRONICS»..	140
ІНФОРМАЦІЯ ДЛЯ АВТОРОВ НАУЧНОГО СБОРНИКА «PHOTOELECTRONICS» ...	141
INFORMATION FOR CONTRIBUTORS OF «PHOTOELECTRONICS» ARTICLES .....	142

*A. P. Chebanenko, A. V. Polischuk*

Odessa I. I. Mechnikov National University, Dvoryanskaya str.,2, Odessa, 65082, Ukraine,  
e-mail: chebanenko@onu.edu.ua

## **ELECTRICAL PROPERTIES OF STRUCTURES BASED ON NANOCRYSTALS CdS IN GELATIN MATRIX**

The electrical characteristics of composite structures based on nanocrystals of cadmium sulfide in a gelatin matrix are studied. It is shown that in the freshly prepared structures, an electric field is formed, which irreversibly increases the electrical resistance of the structures. A complicated form of the temperature dependence of the current is obtained, which is associated with the participation in the current transport of  $H^+$  and  $OH^-$  ions in the low-temperature region and electrons arising from rupture of  $\pi$ -bonds in the high-temperature region.

### **1. Introduction**

The optical and electronic properties of semiconductor nanocrystals differ significantly from those for macrocrystalline matter and depend on the particle size. Such semiconductors, due to the quantization effect [1], make it possible to control their optical, electrical and structural properties, changing only the particle sizes.

Polycrystalline semiconductor films lose their positions in electrical engineering and they are replaced by polymer films with nanocrystals embedded in them. One of the most suitable for use in creating such structures are semiconductor compounds of the  $A_2B_6$  group and, in particular, cadmium sulfide. This material is promising for use in light-emitting devices, since all colors can be obtained by varying the size of the nanocrystal, which makes such structures universal. The literature contains information on the preparation of structures with CdS nanocrystals in the gelatin matrix, their optical and luminescence characteristics [2-4] are described. However, there is practically no information on the electrical properties of such structures. At the same time, in the excitation of luminescence by an electric field, electronic processes play a decisive role in such structures. In this paper, a probable mechanism of electronic processes that determine the electrical conductivity of composite structures with CdS nanocrystals in a gelatin matrix is considered.

### **2. The film's fabrication methods and experiment**

The structures studied were prepared by chemical synthesis from aqueous solutions of cadmium nitrate (0.025 M) and sodium sulphide (0.25 M). The synthesis of nanocrystals of cadmium sulphide occurred at a temperature of +40 ° C in an aqueous solution of photographic gelatin. Gelatin has all the necessary qualities for its use as matrices for semiconductor nanocrystals. Gelatin molecules consist of three polypeptide spiral chains. These chains are interconnected by a limited number of cross-links (so-called  $\sigma$ -bonds) that support the structure of the molecule [5]. Such a structure does not allow the formation of rigid crystalline blocks and is convenient for creating matrix systems, since it has many cells, where molecules of the most diverse substances can enter under suitable conditions. Thus, gelatin molecules in an aqueous solution form a kind of skeleton that divides the which nucleation of nanocrystals and their subsequent growth takes place. Obviously, the more the volume released (ie the less the gelatin concentration), the more reagents it will be in and the more likely will be the formation of nuclei of nanocrystals followed by their fusion. Therefore, the dimensions of CdS nanocrystals depend on the concentration of the gelatin solution.

At the end of the reaction, a solution of cadmium sulfide nanocrystals was deposited on glass substrates coated with a conductive  $\text{SnO}_2$

layer. After drying of the gelatin with the CdS nanocrystals embedded in their bulk, an upper electrode of the In-Ga alloy was deposited onto the films. Thus, the investigated composite structures located in the interelectrode space were packed chaotically located gelatin molecules, in the space between which CdS nanocrystals are located and also water molecules, ionic products of the chemical synthesis of  $Na^+$ ,  $NO_3^-$ , formed as a result of hydrolysis of polymer molecules ions  $H^+$  and  $OH^-$ . The films had a thickness of 20-50  $\mu m$ . The concentration of CdS nanocrystals in the polymer matrix was about 5 wt%. Measurements of the optical absorption spectra showed that the width of the band gap  $E_g$  of the CdS nanocrystals studied is 2.68 eV, which is much higher than the value for single crystals ( $E_g \approx 2.4$  eV) and is due to the size-quantization effect. The obtained result allowed to calculate [1] the dimensions of nanocrystals of cadmium sulfide, which turned out to be within 12-14 nm.

### 3. Results and discussion

Figure 1 shows the current-voltage characteristics (I-V characteristic) freshly prepared structures measured at constant voltage. Curve 1 is measured in order of increasing applied voltage, and curve 2 is in order of decreasing voltage. When measuring curve 1 on the I-V characteristic, significant instabilities and chaotic oscillations of the current were observed, which disappeared when the voltage applied to the structure was 600-700 V. After this, the I-V characteristic measured in order of decreasing applied voltage (curve 2) was stable and reproducible in subsequent measurements, regardless of whether they were made in order of increasing or decreasing the applied voltage. Thus, in the freshly prepared structure, an electric field is formed, as a result of which the resistance of the composite layer increases by more than an order of magnitude. The mechanism of current flow in similar polymer matrices can be determined both by transport of carriers by means of ions, and by "jumping" electrons through free radical bonds of the molecular skeleton of the matrix element in the direction corresponding to the polarity of the applied voltage [6]. Electric molding in fresh-

ly prepared samples can be caused by a reorientation and a change in the spatial arrangement of gelatin molecules under the action of an electric field. It is possible to polarize gelatin molecules as a result of hydrolytic destruction of some of the weak  $\pi$ -bonds and the formation of polar regions with uncompensated electrons. A necessary condition for rupture of  $\pi$ -bonds is the folding of gelatin molecules in a strong electric field. This reduces the number of current-conducting ion channels by compaction of the gelatin layer and, as a consequence, leads to an increase in the resistance of the matrix element.

A linear section is observed on the current-voltage characteristic of the formed structure at low voltages, which, in the region of stresses exceeding 100 V, is replaced by a section of the power-law dependence of the current on the

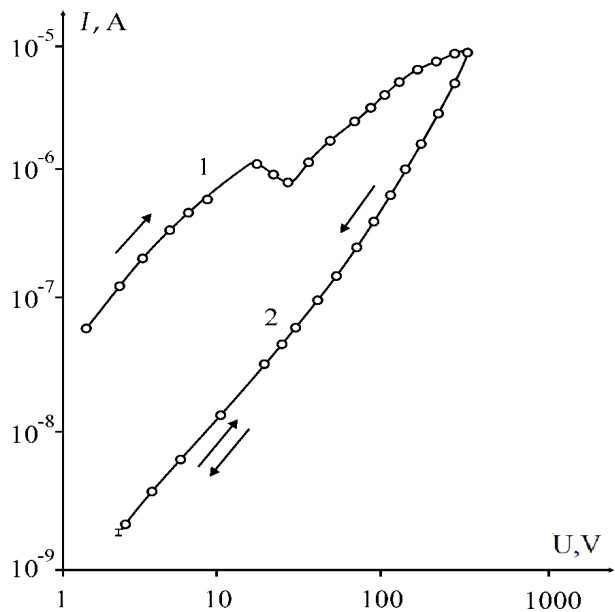
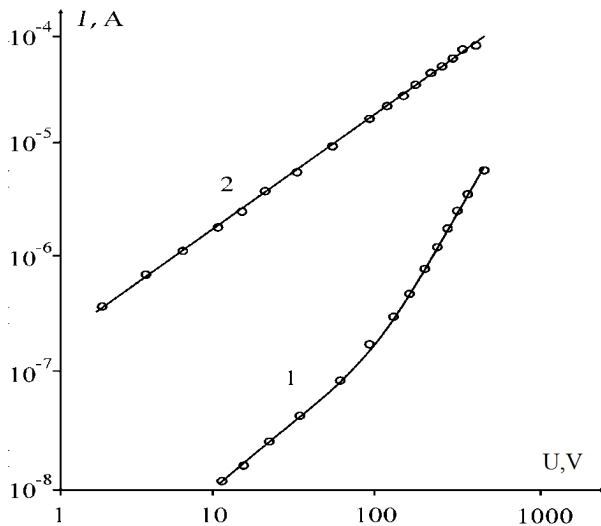


Fig. 1. The current-voltage characteristics of a nanocrystal structure CdS in the gelatin matrix. ( $T = 295$  K).

voltage described by the law  $I = const \cdot V^n$   $I = const \cdot V^n$ , where  $n = 1,8-2$ . Since in the region of these stresses the average electric field strength in the composite layer reaches  $(2 - 5) \cdot 10^4$  V / m, this behavior of the I-V characteristic can be related to the establishment of a current flow regime limited by the space charge [7] in the composite layer, as was

the case in polymer films of polydiphenylene-phthalide, described in [8].

In Fig. 2 shows the current-voltage characteristics of the molded structure measured at a constant (curve 1) and alternating (curve 2) voltage. It can be seen that the current-voltage characteristic measured at alternating voltage remains linear up to voltages of 600 V. This indicates that the quadratic section of the current-voltage characteristic measured at constant voltage is actually due to the flow in the composite of currents limited by the space charge, and is not related to the sample self-heating flowing current [9].



**Fig. 2.** Current-voltage characteristics of a nanocrystal structure CdS, measured at constant (1) and alternating (2) voltages ( $T = 295$  K).

In Fig. 3 shows the temperature dependence of the dark current (TDDC) of the structure under study. You can see that it has a complex view. At low temperatures, the current increases exponentially with an increase in temperature with an activation energy of 0.65 eV. When the temperature reaches about 340 K, a maximum is observed on the TDDC curve. Further, there is a tendency to an insignificant decrease in the current, which, with a further increase in temperature, is again replaced by a segment of its exponential growth with an activation energy of 0.2 eV. When the temperature reaches about 380 K, a second maximum is observed on the TDDC

curve. With further heating of the sample, the current begins to decrease randomly. The TDDC curve, measured in the order of cooling of the sample, shows that the current decrease also takes place exponentially. However, the activation energy of the conductivity turns out to be much larger and amounts to 1.2 eV.

This behavior of TDDC can be explained as follows. In gelatin molecules along polypeptide chains, there are a large number of weak hydrogen bonds ( $\pi$ -bonds), which, in the main, retain  $H^+$  ions and also hydroxyl groups

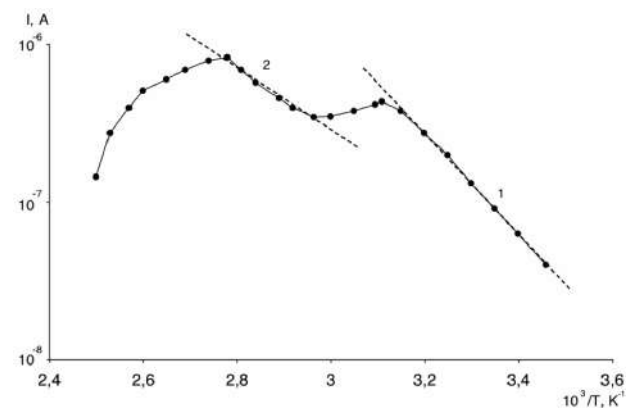


**Fig.3.** The temperature dependence of the dark current of the investigated structure. ( $V = 50$  B).

$OH^-$  [5]. With an increase in temperature due to the energy of thermal motion, these bonds are destroyed, as a result of which the concentration of current carriers, which are  $H^+$  and  $OH^-$  ions, increases. Then the regions on TDDC with activation energies of 0.65 eV and 0.2 eV can be associated with the liberation of  $H^+$  and  $OH^-$  ions, respectively. At a temperature of about 420 K most of the  $\pi$ -bonds are destroyed. However, the broken bonds (as a result of the escape of the  $H^+$  ion) acquire a negative charge, since uncompensated, so-called  $\pi$ -electrons remain on them. Further, in the gelatin, the conjugation effect can be manifested, consisting in the fact that the «clouds» of  $\pi$ -electrons of all atoms that form double bonds on a certain section of the molecular chain are established in one plane and overlap [10]. In this case, the  $\pi$ -electrons are no longer localized, but belong to the entire conjugate system. In the presence of conjugation

tion, the length of the bonds is aligned. Therefore, such systems are characterized by higher stability than non-conjugated systems. With an increase in the length of the conjugation chain, the electrical conductivity of the polymer as a whole increases, since now within the conjugation chain the  $\pi$ -electrons of the macromolecule move both in a single potential well with a periodic potential determined by the structure of the chain. However, the motion of an electron along the conjugation chain is not a sufficient condition for the conductivity of the polymer. It is required that charge carriers can pass from one molecule to another, i.e. from one interface system to another. Such intermolecular transitions are realized by means of activation overcoming of potential barriers between molecules and require energy expenditure. If we assume that during the cooling of the sample from 440 K to room temperature, the predominant current flowing mechanism is the above, then the value of the activation energy of conductivity obtained from TDDC characterizes the height of potential barriers between molecules overcome by  $\pi$ -electrons.

#### 4. Conclusions

The electric molding of freshly prepared structures, leading to an irreversible increase in the resistance of the composite layer, is due to the spatial reorientation of gelatin molecules under the action of an electric field. The electrical conductivity with CdS nanocrystals and its change with increasing temperature are determined by the free  $H^+$  and  $OH^-$  ions, which result from the destruction of  $\pi$ -bonds in gelatin molecules. At high temperatures, conductivity is determined by  $\pi$ -electrons, which freely move along the conjugation chains of gelatin molecules and perform activation transitions between molecules with the overcoming of intermolecular potential barriers.

#### References

1. Ekimov A. I., Efros A. L., Onushchenko A. A. – Quantum size effect in semiconductor microcrystals. // *Solid State Communication*.-1995, Vol.56,

- no.11, P. 921-924.
2. Smyntyna V. A., Skobeeva V. M., Malushin N. V. – The nature of emission centers in CdS nanocrystals. // *Journal of Radiation Measurements*. – 2007, Vol. 42, P. 693-696.
3. Фам Тхи Хаи Мьен, Ключев В. Г., Нгуен Тхи Ким Чунг. – Оптические свойства нанокристаллов сульфида кадмия, полученных золь-гель методом. // *Конденсированные среды и межфазные границы*. – 2011, т. 13, № 4, с. 515-519.
4. Жарков Д. К., Сафиуллин Г. М., Никифоров В. Г., Лобков В. С., Самарцев В. В., Галяметдинов Ю. Г. – Синтез и фотофизические свойства нанокompозитов CdS. // *Учён. зап. Казан. гос. ун-та. Сер. Физ.-матем. науки*. – 2013, т. 155, книга 1, с. 66–73.
5. Михайлов О. В – Желатин как матрица в координационной химии. // *Природа*. – 2000, № 8, с. 12 – 20.
6. Тимонов А. М., Васильева С. В. – Электронная проводимость полимерных соединений. // *Соросовский образовательный журнал*. – 2000, т. 6, № 3, с. 33-39.
7. Ламперт М., Марк П. – Инжекционные токи в твердых телах. – М., Мир, 1975, 340 с.
8. Бунаков А. А., Лачинов А. Н., Салихов Р. Б. – Исследование вольт-амперных характеристик тонких пленок полидифениленфталата. // *ЖТФ* – 2003, т. 73, Вып. 5, с. 104-108.
9. P. V. Kamat P. V. – Interfacial charge transfer processes in colloidal semiconductor systems. // *Reaction Kinetics*. – 1994, № 19, с. 277-316.
10. Измайлова В. Н., Ребиндер П. А. – Структурообразование в белковых системах. – М., Наука, 1974, 268 с.

This article has been received in August 2018

PACS 73.61.LE, 73.63.BD

*A. P. Chebanenko, A. V. Polischuk*

### **ELECTRICAL PROPERTIES OF STRUCTURES BASED ON NANOCRYSTALS CdS IN GELATIN MATRIX**

**Abstract.** The electrical characteristics of composite structures based on nanocrystals of cadmium sulfide in a gelatin matrix are studied. It is shown that in the freshly prepared structures, an electric field is formed, which irreversibly increases the electrical resistance of the structures. A complicated form of the temperature dependence of the current is obtained, which is associated with the participation in the current transport of  $H^+$  and  $OH^-$  ions in the low-temperature region and electrons arising from rupture of  $\pi$ -bonds in the high-temperature region.

**Keywords:** cadmium sulphide, nanocrystals, gelatin films, electrical conductivity.

PACS 73.61.Le, 73.63.Bd

*A. П. Чебаненко, А. В. Полищук*

### **ЭЛЕКТРИЧЕСКИЕ СВОЙСТВА СТРУКТУР НА ОСНОВЕ НАНОКРИСТАЛЛОВ CdS В ЖЕЛАТИНОВОЙ МАТРИЦЕ**

**Резюме.** Исследованы электрические характеристики композитных структур на основе нанокристаллов сульфида кадмия в желатиновой матрице. Показано, что в свежеприготовленных структурах имеет место формовка электрическим полем, которая необратимо повышает электрическое сопротивление структур. Получен сложный вид температурной зависимости тока, который связывается с участием в токопереносе ионов  $H^+$  и  $OH^-$  в области низких температур и электронов, возникающих в результате разрыва  $\pi$ -связей, в области высоких температур.

**Ключевые слова:** сульфид кадмия, нанокристаллы, пленки желатина, электропроводность.

PACS 73.61.Le, 73.63.Bd

*A. П. Чебаненко, А. В. Полищук*

### **ЕЛЕКТРИЧНІ ВЛАСТИВОСТІ СТРУКТУР НА ОСНОВІ НАНОКРИСТАЛІВ CdS В ЖЕЛАТИНОВІЙ МАТРИЦІ**

**Резюме.** Досліджено електричні характеристики композитних структур на основі нанокристалів сульфід кадмію в желатиновій матриці. Показано, що у свіжовиготовлених структурах має місце формовка електричним полем, яка необоротно підвищує електричний опір структур. Отримано складний вигляд температурної залежності струму, який пов'язується з участю у струмопереносі іонів  $H^+$  та  $OH^-$  в області низьких температур і електронів, виникаючих в результаті руйнування  $\pi$ -зв'язків в області високих температур.

**Ключові слова:** сульфід кадмію, нанокристали, плівки желатину, електропровідність.

*O. A. Antoshkina, O. Yu. Khetselius, M. P. Makushkina, A. V. Smirnov*

Odessa State Environmental University, L'vovskaya str.15, Odessa-9, 65016, Ukraine  
E-mail: okhetsel@gmail.com

## THE HYPERFINE STRUCTURE OF HEAVY ELEMENTS ATOMS WITHIN RELATIVISTIC MANY-BODY PERTURBATION THEORY

The hyperfine structure and electric quadrupole moment of the mercury isotope are estimated within the relativistic many-body perturbation theory formalism with a correct and effective taking into account the exchange-correlation, relativistic, nuclear and radiative corrections. Analysis of the data shows that an account of the interelectron correlation effects is crucial in the calculation of the hyperfine structure parameters. The fundamental reason of physically reasonable agreement between theory and experiment is connected with the correct taking into account the interelectron correlation effects, nuclear (due to the finite size of a nucleus), relativistic and radiative corrections. The key difference between the results of the RHF, RMPT methods calculations is explained by using the different schemes of taking into account the inter-electron correlations.

### 1. Introduction

The research on the hyperfine structure characteristics of the heavy neutral and highly ionized atoms is of a great fundamental importance in many fields of atomic physics (spectroscopy, spectral lines theory), astrophysics, plasma physics, laser physics and so on (see, for example, refs. [1-37]). The experiments on the definition of hyperfine splitting also enable to refine the deduction of nuclear magnetic moments of different isotopes and to check an accuracy of the various calculational models employed for the theoretical description of the nuclear effects. The multi-configuration relativistic Hartree-Fock (RHF) and Dirac-Fock (DF) approaches (see, for example, refs. [1,2]) are the most reliable versions of calculation for multi-electron systems with a large nuclear charge. Usually, in these calculations the one- and two-body relativistic effects are taken into account practically precisely. It should be given the special attention to three very general and important computer systems for relativistic and QED calculations of atomic and molecular properties developed in the Oxford and German-Russian groups etc (“GRASP”, “Dirac”, “BERTHA”, “QED”, “Dirac”) (see refs. [1-4] and references there).

In the present paper we present the calculational results for the hyperfine structure and

electric quadrupole moment of the isotope  $^{223}_{88}\text{Ra}$ ,

estimated within the relativistic many-body perturbation theory formalism with a correct and effective taking into account the exchange-correlation, relativistic, nuclear and radiative corrections [3,4,10-20]. Analysis of the data shows that an account of the interelectron correlation effects is crucial in the calculation of the hyperfine structure parameters.

### 2. Relativistic method to computing hyperfine structure parameters of atoms and ions

Let us describe the key moments of the approach (more details can be found in refs. [3,4,10-20]). The electron wave functions (the PT zeroth basis) are found from solution of the relativistic Dirac equation with potential, which includes ab initio mean-field potential, electric, polarization potentials of a nucleus. The charge distribution in the Li-like ion is modelled within the Gauss model. The nuclear model used for the Cs isotope is the independent particle model with the Woods-Saxon and spin-orbit potentials (see refa. [3,4]). Let us consider in details more simple case of the Li-like ion. We set the charge distribution in the Li-like ion nucleus  $\rho(r)$  by the Gaussian function:

$$\rho(r|R) = \left(4\gamma^{3/2}/\sqrt{\pi}\right)\exp(-\gamma r^2) \quad (1)$$

where  $\gamma=4/\pi R^2$  and  $R$  is the effective nucleus radius. The Coulomb potential for the spherically symmetric density  $\rho(r)$  is:

$$V_{nuc}(r|R) = -\left((1/r)\int_0^r dr' r'^2 \rho(r'|R) + \int_r^\infty dr' r' \rho(r'|R)\right) \quad (2)$$

Consider the DF type equations. Formally they fall into one-electron Dirac equations for the orbitals with the potential  $V(r|R)$  which includes the electrical and the polarization potentials of the nucleus; the components of the Hartree potential (in the Coulomb units):

$$V(r|i) = \frac{1}{Z} \int d\vec{r}' \rho(r|i)/|\vec{r} - \vec{r}'| \quad (4)$$

Here  $\rho(r|i)$  is the distribution of the electron density in the state  $|i\rangle$ ,  $V_{ex}$  is the exchange inter-electron interaction. The main exchange and correlation effects will be taken into account in the first two orders of the PT by the total inter-electron interaction [3,4].

A procedure of taking into account the radiative QED corrections is in details given in the refs. [4,44]. Regarding the vacuum polarization effect let us note that this effect is usually taken into consideration in the first PT theory order by means of the Uehling-Serber potential. This potential is usually written as follows:

$$U(r) = -\frac{2\alpha}{3\pi r} \int_1^\infty dt \exp(-2rt/\alpha Z) \left(1 + 1/2t^2\right) \frac{\sqrt{t^2-1}}{t^2} = -\frac{2\alpha}{3\pi r} C(g), \quad (5)$$

where  $g=r/(\alpha Z)$ . In our calculation we use more exact approach [3]. The Uehling potential, determined as a quadrature (6), may be approximated with high precision by a simple analytical function. The use of new approximation of the Uehling potential permits one to decrease the calculation errors for this term down to 0.5 – 1%.

A method for calculation of the self-energy part of the Lamb shift is based on an idea by Ivanov-Ivanova et al [38-41], which generalizes the known hydrogen-like method by Mohr and radiation model potential method by Flambaum-Ginges (look details in Refs. [4,44,45]). The radiative shift and the relativistic part of energy in

an atomic system are, in principle, defined by one and the same physical field [38]. One could suppose that there exists some universal function that connects the self-energy correction and the relativistic energy. Its form and properties are in details analyzed in Refs.[4,45]. Unlike usual purely electronic atoms, the Lamb shift self-energy part in the case of a pionic atom is not significant and much inferior to the main vacuum-polarization effect.

The energies of electric quadruple and magnetic dipole interactions are defined by a standard way with the hyperfine structure constants, usually expressed through the standard radial integrals:

$$A = \{[(4,32587)10^{-4}Z^2 \chi g_I]/(4\chi^2-1)\}(RA)_{-2},$$

$$B = \{7.2878 \cdot 10^{-7} Z^3 Q/(4\chi^2-1)I(I-1)\}(RA)_{-3}, \quad (7)$$

Here  $g_I$  is the Lande factor,  $Q$  is a quadruple momentum of nucleus (in Barn);  $(RA)_{-2}$ ,  $(RA)_{-3}$  are the radial integrals usually defined as follows:

$$(RA)_{-2} = \int dr r F(r)G(r)U(1/r, R)$$

$$(RA)_{-3} = \int dr r \quad (8)$$

The radial parts  $F$  and  $G$  of the Dirac function two components for electron, which moves in the potential  $V(r;R)+U(r;R)$ , are determined by solution of the Dirac equations. To define the hyperfine interaction potentials  $U(1/r^n, R)$ , we use the method by Ivanov et al [11]. The key elements of the optimized relativistic energy approach to computing oscillator strengths are presented in [39,41,42,46-53]. Let us remind that an initial general energy formalism combined with an empirical model potential method has been developed by Ivanov-Ivanova et al [11], further more general ab initio gauge-invariant relativistic approach has been presented in [42], where the calibration of the single model potential parameter  $b$  has been performed on the basis of the special *ab initio* procedure within relativistic energy approach (see also [4,45]). All calculations are performed on the basis of the numeral code Superatom-ISAN (version 93).

### 3. Results and Conclusions

In this subsection we present experimental data and the results of the calculation of the HFS constants and the nuclear quadrupole moment for the radium isotope. In Table 1 we list the experimental and calculational data on the magnetic dipole constant HFS A (MHz) for the  $^{223}_{88}\text{Ra } 7s7p \ ^1P_1, \ ^3P_1, \ ^3P_2$  states. The data are obtained on the basis of calculations in the framework of the standard uncorrelated DF method, MKDF method with taking into account for the Breit and standard QED corrections, the relativistic configuration interaction method with taking into account for the correlation corrections within the random phase approximation (RCI-RPA) [6], as well as our results (Gaussian model for charge distribution in the core) [2,3,6,7].

It is important to note that the key quantitative factor in the agreement of the theory with experiment is associated with a correct allowance for interelectronic correlations, an amendment to the finite size of the nucleus, and Breit and QED radiation effects [3,4].

Table 1

**The experimental and calculational data on the magnetic dipole constant HFS A (MHz) for the  $^{223}_{88}\text{Ra } 7s7p \ ^1P_1, \ ^3P_1, \ ^3P_2$  states (see text)**

Method/ State	$^1P_1$	$^3P_1$	$^3P_2$
DF	-226.59	803.97	567.22
MCDF (Breit+QED)	-330.3	1251.9	737.1
RCI-RPA	-242.4	-	-
Our data	-339.1	1209	704.5
Exp.	-344.5 (0.9)	1201.1 (0.6)	699.6 (3.3)

The analysis shows that the contribution due to the electron – electron correlations to the values of the HFS constants is  $\sim 100\text{--}500$  MHz for various states. This circumstance explains the low degree of consistency in accuracy of the data provided, obtained in the framework of

different versions of the DF method. The key difference between the results of the calculation in the framework of our approach and the MCDF is due to different methods of taking into account the electron-electron correlations. The contributions of higher-order QED TV corrections and corrections for the finite core size can reach 1–2 tens of MHz, and it seems obviously important to consider them more correctly. In addition, it is necessary to take direct account of nuclear polarization contributions, which can be done within the framework of solving the corresponding nuclear problem, for example, using the shell model with Woods-Saxon and spin-orbit potentials. Such an approach is outlined in Refs [3,4].

In Table 2 we present the measured values of the nuclear quadrupole moment Q (in barns) for the isotope, obtained experimentally by the ISOLDE Collaboration group (CERN) based on various methods (see [6]). In addition, this table presents the calculated values of the nuclear quadrupole moment Q (in barns) for the isotope, obtained on the basis of calculations in the framework of the methods of MKDF (including Breit and QED corrections), relativistic many-particle TV (RMBPT) and our data (taken from works [2,3,6,7] and references in them).

Table 2.

**The values of the electric quadrupole moment Q (in barns) for isotope of  $^{223}_{88}\text{Ra}$**

Method	Q (barn)
MCDF (Breit+QED)	1.21 (0.03)
RMBPT	1.28
QED theory	1.22
Our data	1.213
Pykko, Recommend.	1.221 (old) 1.210 (new)
ISOLDE Collaboration fs RaII	1.254 (0.003) {0.066}
Wendt et al, fs RaI	1.19 (0,12)
ISOLDE Collaboration fs RaI	1.190 (0,007) {0,126}
ISOLDE Collaboration B(E2)	1.2

Our final data lie between the latest experimental values of the Wendt group (ISOLDE Collaboration), but have less error definitions.

The fundamental reason of physically reasonable agreement between theory and experiment is connected with the correct taking into account the inter-electron correlation effects, nuclear (due to the finite size of a nucleus), relativistic and radiative corrections.

The key difference between the results of the RHF, RMPT methods calculations is explained by using the different schemes of taking into account the inter-electron correlations. The contribution of the PT high order effects and nuclear contribution may reach the units and even dozens of MHz and should be correctly taken into account. So, it is necessary to take into account more correctly the spatial distribution of the magnetic moment inside a nucleus (the Bohr-Weisskopf effect), the nuclear-polarization corrections etc too. These topics require the separated accurate treatment.

## References

1. Grant I. *Relativistic Quantum Theory of Atoms and Molecules*. Oxford, **2007**.
2. Pyykko, P. Year2008 nuclear quadrupole moments. *Mol. Phys.* **2008**, *106*, Nos. 16–18
3. Khetselius, O.Yu. *Hyperfine structure of atomic spectra*. Astroprint: Odessa, **2008**.
4. Glushkov, A.V. *Relativistic Quantum theory. Quantum mechanics of atomic systems*. Astroprint: Odessa, **2008**.
5. Khetselius, O.Yu.; Gurnitskaya, E.P. Sensing the electric and magnetic moments of a nucleus in the N-like ion of Bi. *Sensor Electr. and Microsyst. Techn.* **2006**, *3*, 35-39.
6. Bieron, J.; Pyykkö, P. Degree of accuracy in determining the nuclear electric quadrupole moment of radium. *Phys.Rev. A*. **2005**, *71*, 032502.
7. Khetselius O.Yu.; Gurnitskaya, E.P. Sensing the hyperfine structure and nuclear quadrupole moment for radium. *Sensor Electr. and Microsyst. Techn.* **2006**, *2*, 25-29.
8. Khetselius, O.Yu. Atomic parity non-conservation effect in heavy atoms and observing P and PT violation using NMR shift in a laser beam: To precise theory. *J. Phys.: Conf. Ser.* **2009**, *194*, 022009
9. Glushkov, A; Khetselius, O; Svinaenko, A.; Buyadzhi, V. *Spectroscopy of autoionization states of heavy atoms and multiply charged ions*. Odessa: TEC, **2015**.
10. Khetselius, O.Yu. Hyperfine structure of radium. *Photoelectronics*. **2005**, *14*, 83-85.
11. Khetselius, O.Yu. Relativistic Hyperfine Structure Spectral Lines and Atomic Parity Non-conservation Effect in Heavy Atomic Systems within QED Theory. *AIP Conf. Proceedings*. **2010**, *1290(1)*, 29-33.
12. Khetselius, O.Yu. Relativistic calculating the spectral lines hyperfine structure parameters for heavy ions. *AIP Conf. Proc.* **2008**, *1058*, 363-365.
13. Khetselius, O.Yu. Relativistic energy approach to cooperative electron- $\gamma$ -nuclear processes: NEET Effect *In Quantum Systems in Chemistry and Physics, Series: Progress in Theoretical Chemistry and Physics*; Nishikawa, K., Maruani, J., Brändas, E., Delgado-Barrio, G., Piecuch, P., Eds.; Springer: Dordrecht, **2012**; Vol. 26, pp 217-229.
14. Khetselius, O.Yu. Relativistic perturbation theory calculation of the hyperfine structure parameters for some heavy-element isotopes. *Int. Journ. Quant.Chem.* **2009**, *109*, 3330-3335.
15. Khetselius, O.Yu. Relativistic calculation of the hyperfine structure parameters for heavy elements and laser detection of the heavy isotopes. *Phys. Scripta*. **2009**, *135*, 014023.
16. Khetselius, O. Optimized Perturbation Theory for Calculating the Hyperfine

- Line Shift and Broadening of Heavy Atoms in a Buffer Gas. *In Frontiers in Quantum Methods and Applications in Chemistry and Physics, Series: Progress in Theoretical Chemistry and Physics*; Nascimento, M., Maruani, J., Brändas, E., Delgado-Barrio, G., Eds.; Springer: Cham, **2015**; Vol. 29, pp. 55-76.
17. Khetselius, O.Yu. *Quantum structure of electroweak interaction in heavy finite Fermi-systems*. Astroprint: Odessa, **2011**.
  18. Buyadzhi, V.V.; Zaichko, P.A.; Antoshkina, O.A.; Kulakli, T.A.; Prepelitsa, G.P.; Ternovsky V.B.; Mansarliysky, V. Computing of radiation parameters for atoms and multicharged ions within relativistic energy approach: Advanced Code. *J. Phys.: Conf. Ser.* **2017**, *905*, 012003.
  19. Svinarenko, A.A. Study of spectra for lanthanides atoms with relativistic many-body perturbation theory: Rydberg resonances. *J. Phys.: Conf. Ser.* **2014**, *548*, 012039.
  20. Svinarenko, A.; Ignatenko, A.; Ternovsky, V.B.; Nikola, L.; Seredenko, S.S.; Tkach, T.B. Advanced relativistic model potential approach to calculation of radiation transition parameters in spectra of multicharged ions. *J. Phys.: Conf. Ser.* **2014**, *548*, 012047.
  21. Buyadzhi, V.; Zaichko, P.; Gurskaya, M.; Kuznetsova, A.; Ponomarenko E.; Ternovsky, V. Relativistic theory of excitation and ionization of Rydberg atomic systems in a Black-body radiation field, *J. Phys.: Conf. Ser.* **2017**, *810*, 012047
  22. Glushkov, A.V.; Malinovskaya, S.V.; Loboda, A.V.; Shpinareva, I.M.; Prepelitsa, G.P. Consistent quantum approach to new laser-electron-nuclear effects in diatomic molecules. *J. Phys.: Conf. Ser.* **2006**, *35*, 420-424.
  23. Glushkov, A.V. Operator Perturbation Theory for Atomic Systems in a Strong DC Electric Field. *In Advances in Quantum Methods and Applications in Chemistry, Physics, and Biology, Series: Progress in Theor. Chem. and Phys.*; Hotokka, M., Brändas, E., Maruani, J., Delgado-Barrio, G., Eds.; Springer: Cham, **2013**; Vol. 27, pp 161–177.
  24. Glushkov, A.V.; Ambrosov, S.V.; Ignatenko, A.V.; Korchevsky, D.A. DC strong field stark effect for nonhydrogenic atoms: Consistent quantum mechanical approach. *Int. Journ. Quant. Chem.* **2004**, *99*, 936-939.
  25. Glushkov, A.V.; Kondratenko, P.A.; Buyadgi V.V.; Kvasikova, A.S.; Sakun, T.N.; Shakhman, A.S. Spectroscopy of cooperative laser electron- $\gamma$ -nuclear processes in polyatomic molecules. *J. Phys.: Conf. Ser.* **2014**, *548*, 012025.
  26. Malinovskaya, S.V.; Dubrovskaya, Yu.V.; Vitavetskaya, L.A. Advanced quantum mechanical calculation of the beta decay probabilities. *AIP Conf. Proc.* **2005**, *796*, 201-205.
  27. Glushkov, A.V.; Malinovskaya, S.V.; Chernyakova Y.G.; Svinarenko, A.A. Cooperative laser-electron-nuclear processes: QED calculation of electron satellites spectra for multi-charged ion in laser field. *Int. Journ. Quant. Chem.* **2004**, *99*, 889-893.
  28. Glushkov, A.V.; Malinovskaya, S.V.; Prepelitsa, G.; Ignatenko, V. Manifestation of the new laser-electron nuclear spectral effects in the thermalized plasma: QED theory of co-operative laser-electron-nuclear processes. *J. Phys.: Conf. Ser.* **2005**, *11*, 199-206.
  29. Glushkov, A.V.; Malinovskaya, S.V.; Loboda, A.V.; Shpinareva, I.M.; Gurnitskaya, E.P.; Korchevsky, D.A. Diagnostics of the collisionally pumped plasma and search of the optimal plasma parameters of x-ray lasing: calculation of electron-collision strengths and rate coefficients for Ne-like plasma. *J. Phys.: Conf. Ser.* **2005**, *11*, 188-198.

30. Glushkov, A.V.; Ambrosov, S.; Loboda, A.; Gurnitskaya, E.; Prepelitsa, G. Consistent QED approach to calculation of electron-collision excitation cross sections and strengths: Ne-like ions. *Int. J. Quantum Chem.* **2005**, *104*, 562-569.
31. Glushkov, A.; Loboda, A.; Gurnitskaya, E.; Svinarenko, A. QED theory of radiation emission and absorption lines for atoms in a strong laser field. *Phys. Scripta.* **2009**, *T135*, 014022.
32. Florko, T.A.; Tkach, T.B.; Ambrosov, S.V.; Svinarenko, A.A. Collisional shift of the heavy atoms hyperfine lines in an atmosphere of the inert gas. *J. Phys.: Conf. Ser.* **2012**, *397*, 012037.
33. Buyadzhi, V.V. Laser multiphoton spectroscopy of atom embedded in Debye plasmas: multiphoton resonances and transitions. *Photoelectronics.* **2015**, *24*, 128-133.
34. Buyadzhi, V.V.; Chernyakova, Yu.G.; Smirnov, A.V.; Tkach, T.B. Electron-collisional spectroscopy of atoms and ions in plasma: Be-like ions. *Photoelectronics.* **2016**, *25*, 97-101.
35. Buyadzhi, V.V.; Chernyakova, Yu.G.; Antoshkina, O.; Tkach, T. Spectroscopy of multicharged ions in plasmas: Oscillator strengths of Be-like ion Fe. *Photoelectronics.* **2017**, *26*, 94-102.
36. Glushkov, A.V.; Malinovskaya S.V. Co-operative laser nuclear processes: border lines effects *In New Projects and New Lines of Research in Nuclear Physics.* Fazio, G., Hanappe, F., Eds.; World Scientific: Singapore, **2003**, 242-250.
37. Glushkov, A.V. Spectroscopy of atom and nucleus in a strong laser field: Stark effect and multiphoton resonances. *J. Phys.: Conf. Ser.* **2014**, *548*, 012020
38. Ivanov, L.N.; Ivanova, E.P. Atomic ion energies for Na-like ions by a model potential method  $Z = 25-80$ . *Atom. Data Nucl. Data Tabl.* **1979**, *24*, 95-109.
39. Ivanov, L.N.; Ivanova, E.P.; Knight, L. Energy approach to consistent QED theory for calculation of electron-collision strengths: Ne-like ions. *Phys. Rev. A.* **1993**, *48*, 4365-4374.
40. Ivanova, E.P.; Ivanov, L.N.; Glushkov, A.V.; Kramida, A.E. High order corrections in the relativistic perturbation theory with the model zeroth approximation, Mg-Like and Ne-Like Ions. *Phys. Scripta* 1985, *32*, 513-522.
41. Glushkov, A.V.; Ivanov, L.N.; Ivanova, E.P. Autoionization Phenomena in Atoms. *Moscow University Press, Moscow*, **1986**, 58-160
42. Glushkov, A.V.; Ivanov, L.N. Radiation decay of atomic states: atomic residue polarization and gauge non-invariant contributions. *Phys. Lett. A* **1992**, *170*, 33-36.
43. Glushkov, A.V. Advanced relativistic energy approach to radiative decay processes in multielectron atoms and multicharged ions. *In Quantum Systems in Chemistry and Physics: Progress in Methods and Applications, Series: Progress in Theoretical Chemistry and Physics*; Nishikawa, K., Maruani, J., Brandas, E., Delgado-Barrio, G., Piecuch, P., Eds.; Springer: Dordrecht, **2012**; Vol. 26, pp 231-252.
44. Flambaum, V.; Ginges J. Radiative potential and calculation of QED radiative corrections to energy levels and electromagnetic amplitudes in many-electron atoms. *Phys.Rev.A.* **2005**, *72*, 052115.
45. Glushkov, A.V. *Relativistic and Correlation Effects in Spectra of Atomic Systems.* Astroprint: Odessa, **2006**.
46. Glushkov, A.V. Negative ions of inert gases. *JETP Lett.* **1992**, *55*, 97-100.
47. Glushkov, A.V. Spectroscopy of cooperative muon-gamma-nuclear processes: Energy and spectral parameters *J. Phys.: Conf. Ser.* **2012**, *397*, 012011
48. Glushkov, A. Multiphoton spectroscopy of atoms and nuclei in a laser

- field: relativistic energy approach and radiation atomic lines moments method// Adv. Quant.Chem. (Elsevier), **2018**, 78, doi.org/10.1016/bs.aiq.2018.06.004
49. Khetselius, O. Optimized relativistic many-body perturbation theory calculation of wavelengths and oscillator strengths for li-like multicharged ions// Adv. Quant. Chem. (Elsevier), **2018**, 78, doi.org/10.1016/bs.aiq.2018.06.001.
50. Ignatenko, A.V. Probabilities of the radiative transitions between Stark sublevels in spectrum of atom in an DC electric field: New approach. *Photoelectronics*, **2007**, 16, 71-74.
51. Glushkov A.V.; Ivanov, L.N. DC strong-field Stark effect: consistent quantum-mechanical approach. *J. Phys. B: At. Mol. Opt. Phys.* **1993**, 26, L379-386.
52. Glushkov, A.V.; Ambrosov, S.V.; Ignatenko, A.V. Non-hydrogenic atoms and Wannier-Mott excitons in a DC electric field: Photoionization, Stark effect, Resonances in ionization continuum and stochasticity. *Photoelectronics*, **2001**, 10, 103-106.
53. Glushkov, A.V.; Gurskaya, M.Yu.; Ignatenko, A.V.; Smirnov, A.V.; Serga, I.N.; Svinarenko, A.A.; Ternovsky, E.V. Computational code in atomic and nuclear quantum optics: Advanced computing multiphoton resonance parameters for atoms in a strong laser field. *J. Phys.: Conf. Ser.* **2017**, 905, 012004.

This article has been received in August 2018

PACS 31.30.Gs

*O. A. Antoshkina, O. Yu. Khetselius, M. P. Makushkina, A. V. Smirnov*

## THE HYPERFINE STRUCTURE OF HEAVY ELEMENTS ATOMS WITHIN RELATIVISTIC MANY-BODY PERTURBATION THEORY

### Summary

The hyperfine structure and electric quadrupole moment of the isotope  $^{223}_{8}\text{R}$  are estimated within the relativistic many-body perturbation theory formalism with a correct and effective taking into account the exchange-correlation, relativistic, nuclear and radiative corrections. Analysis of the data shows that an account of the interelectron correlation effects is crucial in the calculation of the hyperfine structure parameters. The fundamental reason of physically reasonable agreement between theory and experiment is connected with the correct taking into account the inter-electron correlation effects, nuclear (due to the finite size of a nucleus), relativistic and radiative corrections. The key difference between the results of the RHF, RMPT methods calculations is explained by using the different schemes of taking into account the inter-electron correlations.

**Keywords:** Hyperfine structure – Heavy atoms – Relativistic perturbation theory – Correlation, nuclear, radiative corrections

PACS 31.30.Gs

*О. А. Антошкина, О. Ю. Хецелиус, М. П. Макушкина, А. В. Смирнов*

## **СВЕРХТОНКАЯ СТРУКТУРА ТЯЖЕЛЫХ АТОМОВ В РАМКАХ РЕЛЯТИВИСТСКОЙ МНОГОЧАСТИЧНОЙ ТЕОРИИ ВОЗМУЩЕНИЙ**

### **Резюме**

Параметры сверхтонкой структуры и электрический квадрупольный момент изотопа радона рассчитаны на основе релятивистской многочастичной теории возмущений с эффективным аккуратным учетом обменно-корреляционных, релятивистских, ядерных и радиационных поправок. Анализ данных показывает, что учет эффектов межэлектронной корреляции имеет критическое значение при вычислении параметров сверхтонкой структуры. Физически разумное согласие теории и прецизионного эксперимента может быть обеспечено благодаря полному последовательному учету межэлектронных корреляционных эффектов, ядерных, релятивистских и радиационных поправок. Ключевое различие между результатами расчетов в приближениях Дирака-Фока, различных версиях формализма теории возмущений в основном связано с использованием различных схем учета межэлектронных корреляций.

**Ключевые слова:** Сверхтонкая структура - тяжелый атом - релятивистская теория возмущений - корреляционные, ядерные, радиационные поправки

PACS 31.30.Gs

*О. О. Антошкина, О. Ю. Хецелиус, М. П. Макушкина, А. В. Смирнов*

## **НАДТОНКА СТРУКТУРА ВАЖКИХ АТОМІВ В РАМКАХ РЕЛЯТИВІСТСЬКОЇ БАГАТОЧАСТИНКОВОЇ ТЕОРІЇ ЗБУРЕНЬ**

### **Резюме**

Параметри надтонкої структури і електричний квадрупольний момент ізотопу радону розраховані на основі релятивістської багаточастинкової теорії збурень з ефективним акуратним урахуванням обмінно-кореляційних, релятивістських, ядерних і радіаційних поправок. Аналіз даних показує, що урахування ефектів міжелектронної кореляції має критичне значення при обчисленні параметрів надтонкої структури. Фізично розумне узгодження теорії і прецизійного експерименту може бути забезпечено завдяки повному послідовному обліку міжелектронних кореляційних ефектів, ядерних, релятивістських та радіаційних поправок. Ключова відмінність між результатами розрахунків в наближеннях Дірака-Фока, різних версій формалізму теорії збурень в основному пов'язано з використанням різних схем обліку міжелектронних кореляцій.

**Ключові слова:** Надтонка структура – важкий атом - релятивістська теорія збурень – кореляційні, ядерні, радіаційні поправки

*Yu. A. Nitsuk, A. S. Leonenko, Yu. F. Vaksman, G. V. Korenkova, V. A. Smyntyna,  
Ie. V. Brytavskiy*

I. I. Mechnikov Odesa National University  
e-mail: nitsuk@onu.edu.ua

## PHOTOLUMINESCENCE OF CdSe:Ni NANOPARTICLES OBTAINED BY CHEMICAL METHOD

Cadmium selenide nanocrystals doped with nickel were prepared in water phase chemistry technique with gelatin acting as capping agent. Structures were characterized using X-ray diffraction (XRD), scanning electron microscopy (SEM), visible absorption and photoluminescence spectroscopies. Influence of component concentrations and technological parameters on nanocrystals average size and properties was studied.

### I. Introduction

Colloidal CdSe nanocrystals can be used to create structures emitting in the entire visible light range, as a sensitizer for photopolymer cells and in biomedical visualization [1-7]. In comparison with organic fluorophores semiconductor nanocrystals are much more stable to photodegradation. Cadmium selenide nanocrystals exhibit strong quantum confinement and by regulating their size one can obtain emission in almost entire visible range. The wide practical application of this material is restrained by the high dispersion of the obtained particles and their instability. Therefore, the creation of a technology for the synthesis of stable nanoparticles with controlled size is relevant.

The hot-injection method proposed in [5] had instigated activity in the field of metal chalcogenide nanoparticles synthesis. It allowed to obtain highly luminescent crystals with good monodispersity but has certain disadvantages connected with expensive and hazardous pyrophoric reactives being used. Plenty of adaptations of original technology have been developed since then [6,7]. One of the natural choices of medium for QDs preparation might be polar solvents, for example water. Using this aqueous method, the energy level of CdSe QDs can be modified just allowing guest elements (Ag, Mn, Ni, Co etc.) into the CdSe host material and paves the way for discovering the new class luminescent materials with wide range of potential applications.

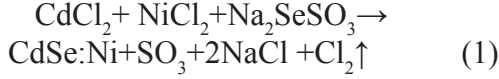
Doping of these ions into the CdSe host material acts as the trap states for electrons and holes and enables the luminescence [8,9]. However, presence of two different kinds of ions simultaneously in a host material produces fluorescence which is totally different from the emission due to a single ion and this property is very useful for white and IR light generation [10].

In this paper, we report the synthesis of high-quality water-soluble CdSe:Ni nanocrystals colloidal method and discuss the influence of important experiment parameters (precursor concentration) on the optical and luminescent properties of prepared QDs. The synthesized CdSe and CdSe:Ni nanocrystals have been characterized absorption and luminescence spectroscopy, X-ray diffraction (XRD), transmission electron microscopy (TEM), electron diffraction spectroscopy (EDS), and their morphology, crystal structure, optical properties, and element composition have been studied with these means. The prepared CdSe nanocrystals meet the requirements for the fluorescence materials in optoelectronics, biological labeling and will surely have promising applications in biochemical detection and biomedical researches.

### II. Experimental

The study used commercially purchased reagents Merck Company. CdCl<sub>2</sub> was the source of cadmium ions. NiCl<sub>2</sub> was the source of cadmium ions in CdSe:Ni. The source of Se<sup>2-</sup> ions

was sodium selenosulfate  $\text{Na}_2\text{SeSO}_3$ , Gelatin was used as the growth stabilizer of nanoparticles. The reaction at room temperature might be described as follows:



The formation of CdSe is confirmed by the presence of diffraction maxima corresponding to the planes (002), (110), (001) in this material (Fig.1). The resulting colloidal solution containing CdSe, CdSe:Ni nanoparticles was deposited on quartz substrates, then the solvent evaporated, forming membranes for measuring optical absorption and photoluminescence. For investigation of structural properties the solvent sprayed on Si substrates.

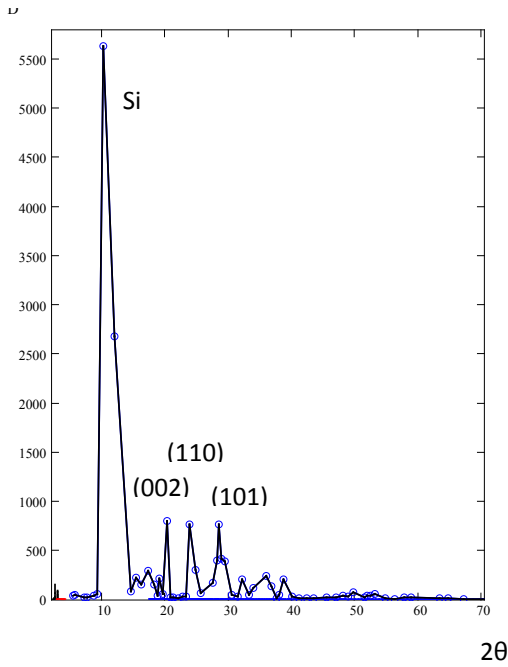


Fig. 1. X-ray diffraction pattern of CdSe nanoparticles

The SEM image was obtained via JEM-2100 (HR) transmission electron microscope (Japan Electron Optics Laboratory CO., Ltd.).

The optical absorption spectra in the visible range were recorded with MDR-6 (LOMO) monochromator with a  $1200 \text{ groove}\cdot\text{mm}^{-1}$ . The photoluminescence spectra were recorded with ISP-51 (LOMO) quartz monochromator using LED (Edison Corporation) excitation on  $\lambda=400 \text{ nm}$ .

The average size of the nanoparticles was estimated from the change in the band gap ( $\Delta E_g$ ) relative to the bulk crystal, using the effective-mass approximation using the equation [5]

$$R = \frac{h}{\sqrt{8\mu\Delta E_g}} \quad (2)$$

There  $h$  is the Planck constant;  $\mu = ((m_{e^*})^{-1} + (m_{h^*})^{-1})^{-1}$ , where  $m_{e^*} = 0.3m_e$ ,  $m_{h^*} = 0.6m_e$  are, respectively, the effective masses of the electron and hole in cadmium selenide,  $m_e$  is the mass of the free electron;  $\Delta E_g$  is the difference between the width of the band gap in the nanoparticle and the bulk crystal of CdSe (1.7 eV).

### III. Experiment and results

Investigations of CdSe:Ni nanocrystals optical absorption were carried out in the range of quanta of incident light 3.5-2 eV. The temperature of explored samples is varied from 77 to 300 K.

All investigated samples are characterized by the presence of a quantum-dimensional effect, which manifests itself in the high-energy shift of the fundamental absorption edge of the samples in comparison with the bulk CdSe absorption edge. Changing of the band gap width is confirmed by a change in solutions color from pale yellow to orange in comparison with the bulk crystals brown color. It is established that the shift magnitude is determined primarily by concentrations of cadmium and selenium precursors (Fig. 1). The highest shift is observed in samples containing 0.3%  $\text{CdCl}_2$  and  $\text{Na}_2\text{SeSO}_3$ .

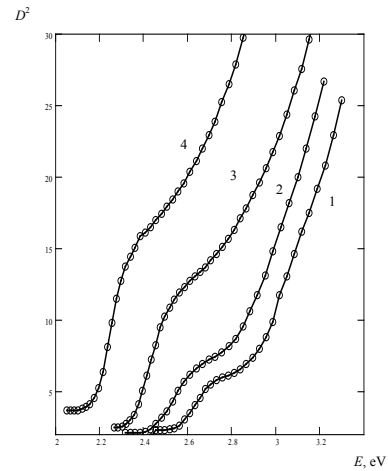


Fig.2. Optical absorption spectra of CdSe nanocrystals stabilized in gelatin matrices. Concentrations of  $\text{CdCl}_2$  and  $\text{Na}_2\text{SeSO}_3$  is equal (1) 0.3%, (2) 0.5%, (3) 1%, (4) 2%.  $T_{\text{meas}} = 300 \text{ K}$ .

By the magnitude of the fundamental absorption edge shift, the formula (2) calculated the size of CdSe nanoparticles. It is shown that when the precursor concentrations varied from 0.3 to 2%, the size of nanoparticles increases from 3 to 6 nm (see TABLE I).

As the nanocrystals temperature decreased from 300 to 77 K, the absorption edge shifted to the high-energy region by 0.14 eV. Such shift corresponds to a temperature change of CdSe band gap edge.

Table 1.  
RESULTS OF CALCULATIONS OF cdse,  
cdse:ni NANOPARTICLES SIZES

No.	$CdCl_2, Na_2SeSO_3$ concentrations	$E_g, eV$	$\Delta E_g, eV$	$R, nm$
1.	2%	2.25	0.55	5.6
2.	1%	2.60	0.9	4.4
3.	0.5%	2.81	1.11	3.8
4.	0.3%	2.93	1.23	3.5
5.	0.3%+NiCl <sub>2</sub> 0.001%	2.86	1.16	3.7
6.	0.3%+NiCl <sub>2</sub> 0.005%	2.77	1.07	3.9
7.	0.3%+NiCl <sub>2</sub> 0.01%	2.7	1	4.2

The doping of nanocrystals with nickel leads to a shift of the absorption edge to a region of lower energies, which is explained both by an increase in the size of nanoparticles and by inter-impurity Coulomb interaction.

The photoluminescence spectra of the investigated CdSe nanocrystals are characterized by emission band localized in the visible spectral region. The half-width of the photoluminescence spectrum varied from 50 to 70 nm, depending on CdCl<sub>2</sub> and Na<sub>2</sub>SeSO<sub>3</sub> concentration (Fig.3).

It is established that the position of these emission lines is determined by the concentration of CdCl<sub>2</sub> and Na<sub>2</sub>SeSO<sub>3</sub> in solution. The position of the emission maxima varied from 2.54 to 2.14 eV with an increase in concentrations of CdCl<sub>2</sub> and Na<sub>2</sub>SeSO<sub>3</sub> from 0.3 to 2%.

The position of the observed emission lines correlates with the second linear region position of the corresponding optical absorption spectrum. The magnitude of the Stokes shift in the samples under study is 20-30 meV.

$I, arb.un.$

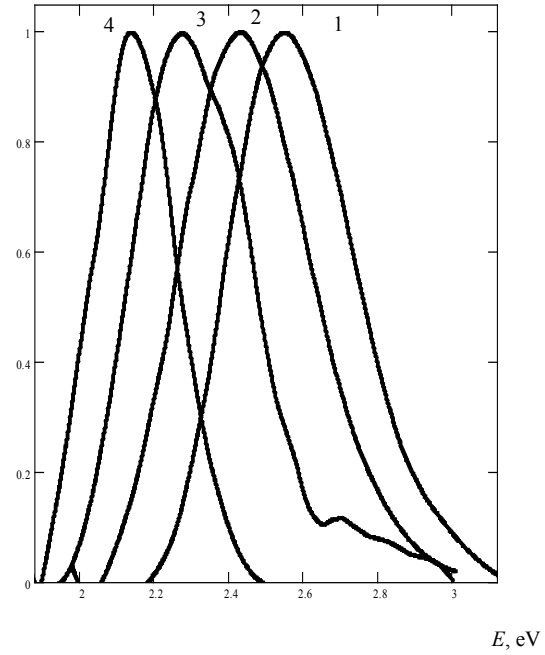


Fig. 3. Photoluminescence spectra of CdSe nanocrystals stabilized in gelatin matrices. Concentrations of CdCl<sub>2</sub> and Na<sub>2</sub>SeSO<sub>3</sub> is equal (1) 0.3%, (2) 0.5%, (3) 1%, (4) 2%. T<sub>meas</sub>=300 K.

When the temperature of nanocrystals changes from 300 to 77 K, the emission lines shift to the high-energy region by 0.14 eV, which corresponds to a temperature change of CdSe band gap. This allows us to assume that transitions involving excitons are responsible for these lines. Lines of a similar nature were observed earlier in [2].

With an increase of precursors concentration, broadening of the emission lines and the appearance of additional high-energy radiation maxima are observed. This is explained by the spread in the sizes of the nanoparticles obtained. SEM images of the investigated nanocrystals (Fig.4) showed that the size of nanoparticles can vary within the limits of 2-6 nm.

The exciton emission spectra of the CdSe:Ni are shifted to the region of lower energies (Fig.5). There is a complete correlation with the

absorption spectra shown in as the nickel concentration increases. At the same time, nickel doping results in a series of emission lines in the visible and near-IR regions.

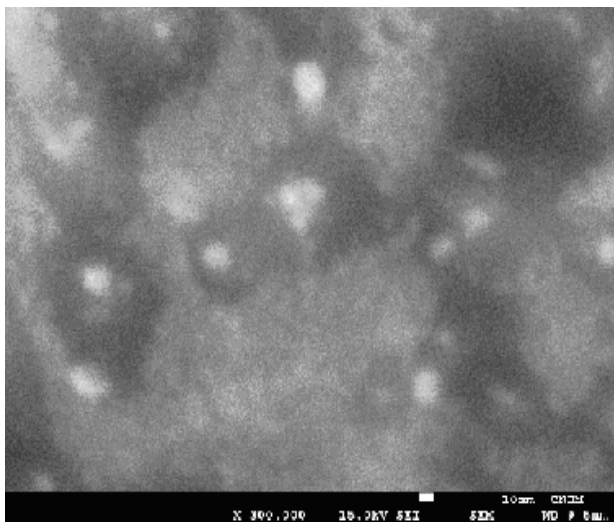


**Fig. 4. SEM image of CdSe nanocrystals with 0.5% precursor concentration.**

The luminescence spectra of nanocrystals in the visible region are characterized by lines localized at 2.47, 2.38, 2.28, and 2.15 eV. In the near-IR region, the photoluminescence spectra of CdSe nanocrystals show three emission lines at 1.86, 1.74, and 1.64 eV. The position of these lines remained unchanged with an increase in the concentration of  $\text{NiCl}_2$ , and their intensity increased. This behavior is characteristic of emission lines due to intracenter radiative transitions.

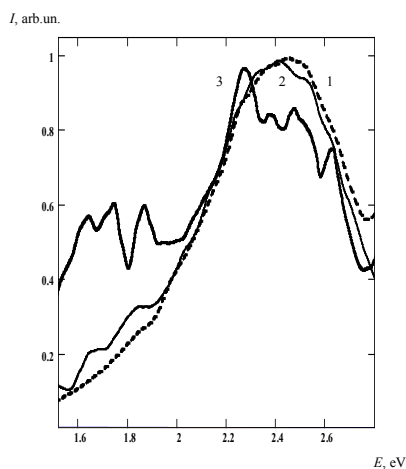


**Fig. 5. Photoluminescence spectra of CdSe:Ni nanocrystals. Concentrations of  $\text{NiCl}_2$  is equal (1) 0.001%, (2) 0.005%, (3) 0.01%,  $T_{\text{meas}}=300$  K.  $\text{CdCl}_2$ ,  $\text{Na}_2\text{SeSO}_3$  concentrations is equal 0.3%.**

The luminescence of bulk crystals of  $\text{ZnSe:Ni}$  was previously investigated [11]. The band gap is varied in the range of 2.8–2.5 eV, depending on the nickel impurity concentration in these crystals. We assume that the visible emission lines are due to the emission transitions from the excited states  $^1E(G)$ ,  $^1T_1(G)$ ,  $^1A_1(G)$ ,  $^1T_2(G)$  to the ground state  $^3T_1(F)$  of the  $\text{Ni}^{2+}$  ion.

The near-IR emission lines are due to transitions from the excited state  $^3T_1(P)$  split by the spin-orbital interaction to the ground state  $^3T_1(F)$  of the  $\text{Ni}^{2+}$  ion.

Thus, the luminescent properties of the  $\text{CdSe:Ni}$  nanocrystals are controlled by the intracenter emission transitions within the  $\text{Ni}^{2+}$  ion.

The obtained results indicate the possibility of controlling the nanoparticles size by different methods. The obtained samples have effective emission in the visible and near-infrared region can be used as the sensitizer for photopolymer cells.

#### Acknowledgment

The authors are grateful to Professor I.R. Yatsunsky from Adam Mickiewicz Poznań University for CEM images and discussion of the results.

#### References

1. D. S. Mazing, L. B. Matyushkin, O. A. Aleksandrova, I. I. Mikhailov, V. A. Moshnikov and S. A. Tarasov “Synthesis of cadmium selenide colloidal quantum dots in aquatic medium”, *Journal of Physics: Conference Series*, vol. 572, pp. 1-4, 2014.
2. C. Wei, J. Li, F. Gao, Sh. Guo, Y. Zhou and D. Zhao “One-Step Synthesis of High-Quality Water-Soluble CdSe Quantum Dots Capped by *N*-Acetyl-L-cysteine via Hydrothermal Method and Their Characterization”, *Journal of Spectroscopy*, vol. 2015, pp.1-7, 2015.
3. F. H. Huang, C. Cheng, and C. Sun, “Synthesis and characterization of water-soluble citrate-capped CdSe quantum dots,” *Chemical Research*, vol. 24, p. 1, 2013.

4. Z. L. Xu, K.Y.Yi, Z. N.Ma, M.Wang, and X.F.Liu, "Synthesis of CdSe quantum dots and their applications for labeling of latent fingerprints," *Synthetic Materials Aging and Application*, vol. 42, p. 15, 2013.
5. Q. Wang, F. Ye, T. Fang et al., "Bovine serum albumin-directed synthesis of biocompatible CdSe quantum dots and bacteria labeling," *Journal of Colloid and Interface Science*, vol. 355, no.1, pp. 9–14, 2011.
6. A. C. A. Silva, S. L. V. D. Deus, M. J. B. Silva, and N. O. Dantas, "Highly stable luminescence of CdSe magic-sized quantum dots in HeLa cells," *Sensors and Actuators B: Chemical*, vol. 191, pp. 108–114, 2014.
6. X. D. Guo, B. B. Ma, L. D. Wang, R. Gao, H. P. Dong, and Y. Qiu, "Electron injection and photovoltaic properties in CdSe/ZnS quantum dot sensitized solar cells," *Acta Physico-Chimica Sinica*, vol. 29, pp. 1240–1246, 2013.
7. L. Z. Du and Y. A. Lei, "Synthesis of high-quality Cl-doped CdSe nanobelts and their application in nanodevices," *Materials Letters*, vol. 106, pp. 100–103, 2013.
8. D.-W. Deng, J.-S. Yu, and Y. Pan, "Water-soluble CdSe and CdSe/CdS nanocrystals: a greener synthetic route," *Journal of Colloid and Interface Science*, vol. 299, no. 1, pp. 225–232, 2006.
9. P. A. Kotin, S. S. Bubenov, N. E. Mordvinova and S. G. Dorofeev, "AgCl-doped CdSe quantum dots with near-IR photoluminescence", *Beilstein J. Nanotechnol.*, 8, 1156, 2017.
10. Ю. А. Ницук "Исследование примесной фотопроводимости и люминесценции в кристаллах ZnSe:Ni в видимой области спектра", *ФТП*, Т.46, В. 10. – С. 1288-1292, 2012

This article has been received in August 2018

UDC 621.315.592

*Yu. A. Nitsuk, A. S. Leonenko, Yu. F. Vaksman, A. V. Korenkova, V. A. Smyntyna,  
Ie. V. Brytavskiy*

I. I. Mechnikov Odesa National University  
e-mail: nitsuk@onu.edu.ua

#### **PHOTOLUMINESCENCE OF CdSe:Ni NANOPARTICLES OBTAINED BY CHEMICAL METHOD**

**Abstract**—Cadmium selenide nanocrystals doped with nickel were prepared in water phase chemistry technique with gelatin acting as capping agent. Structures were characterized using X-ray diffraction (XRD), scanning electron microscopy (SEM), visible absorption and photoluminescence spectroscopies. Influence of component concentrations and technological parameters on nanocrystals average size and properties was studied.

**Key words** – Cadmium Selenide, Nanocrystals, Absorption Edge, Photoluminescence.

УДК 621.315.592

*Ю. А. Ницук, А. С. Леоненко, Ю. Ф. Ваксман, Г. В. Коренкова, В. А. Сминтина,  
С. В. Брита́вський*

Одеський національний університет імені І. І. Мечникова  
e-mail: nitsuk@onu.edu.ua

### **ФОТОЛЮМИНЕСЦЕНЦІЯ НАНОЧАСТИНОК CdSe:Ni ОТРИМАНИХ ХІМІЧНИМ МЕТОДОМ**

**Анотація**–Нанокристали CdSe, леговані нікелем, були отримані в водній фазі з додаванням желатину як зв'язуючого агенту. Структурні властивості були досліджені за допомогою дифракції рентгенівських променів (XRD), скануючої електронної мікроскопії (SEM), видимого поглинання та фотолюмінесцентної спектроскопії. Визначено вплив концентрації компонентів та технологічних параметрів на середній розмір нанокристалів та досліджено їх властивості.

**Ключові слова** – Селенід кадмію, нанокристали, край поглинання, фотолюмінесценція.

УДК 621.315.592

*Ю. А. Ницук, А. С. Леоненко, Ю. Ф. Ваксман, А. В. Коренкова, В. А. Смынтина,  
Е. В. Брита́вский*

Одесский национальный университет имени И. И. Мечникова  
e-mail: nitsuk@onu.edu.ua

### **ФОТОЛЮМИНЕСЦЕНЦІЯ НАНОЧАСТИЦ CdSe:Ni ПОЛУЧЕННЫХ ХИМИЧЕСКИМ МЕТОДОМ**

**Аннотация** – Нанокристаллы CdSe, легированные никелем, были получены в водной фазе с добавлением желатина в качестве связывающего агента. Структурные свойства были исследованы при помощи дифракции рентгеновских лучей (XRD), сканирующей электронной микроскопии (SEM), видимого поглощения та фотолюмінесцентной спектроскопии. Определено влияние компонентов и технологических параметров на средний размер нанокристаллов и их свойства.

**Ключевые слова** – селенид кадмия, нанокристаллы, край поглощения, фотолюмінесценция.

V. V. Buyadzhi, T. B. Tkach, A. P. Lavrenko, E. S. Romanenko

Odessa State Environmental University, 15, Lvovskaya str., Odessa-16, 65016, Ukraine  
E-mail: buyadzhivv@gmail.com

## SPECTROSCOPY OF MULTICHARGED IONS IN PLASMAS: OSCILLATOR STRENGTHS OF BE-LIKE IONS $G_{\text{A}}\text{XXVIII}$ and $G_{\text{E}}\text{XXIX}$

Oscillator strengths  $gf$  for  $2s^2-[2s1/22p3/2]1$  transition in Be-like multicharged ions of  $G_{\text{A}}\text{XXVIII}$  and  $G_{\text{E}}\text{XXIX}$  Fe are computed for different values of the electron density and temperature ( $n_e=10^{22}-10^{24}\text{cm}^{-3}$ ,  $T=0.5-2$  keV) of plasmas are presented and compared with available alternative spectroscopic data. The generalized relativistic energy approach and relativistic many-body perturbation theory with the Debye shielding model as zeroth approximation is used for studying spectral parameters of ions in plasmas. An electronic Hamiltonian for  $N$ -electron ion in a plasma is added by the Yukawa-type electron-electron and nuclear interaction potential.

### 1. Introduction

Spectroscopy of multicharged ions in a plasmas is one of the most fast developing branches of modern atomic spectroscopy. The properties of laboratory and astrophysical plasmas have drawn considerable attention over the last decades [1-14]. It is known that multicharged ions play an important role in the diagnostics of a wide variety of plasmas. Similar interest is also stimulated by importance of this information for correct determination of the characteristics for plasma in thermonuclear (tokamak) reactors, searching new mediums for X-ray range lasers. The electron-ion collisions play a major role in the energy balance of plasmas. ([1-6]). Different theoretical methods were employed along with the Debye screening to study plasma medium. Earlier we have developed a new version of a relativistic energy approach combined with the many-body perturbation theory (RMBPT) for multi-quasiparticle (QP) systems for studying spectra of plasma of the multicharged ions and electron-ion collisional parameters. The method is based on the Debye shielding model and energy approach [3-5]. A new element of this paper is in using the effective optimized Dirac-Kohn-Sham method in general relativistic energy approach to collision processes in the Debye plasmas.

In this paper, which goes on our work [3-5], we present the results of computing energy shifts and oscillator strengths  $gf$  for  $2s^2-[2s_{1/2}2p_{3/2}]_1$  transitions in the Be-like ions of

$G_{\text{A}}\text{XXVIII}$  and  $G_{\text{E}}\text{XXIX}$ , calculated for different values of the electron density and temperature ( $n_e=10^{22}-10^{24}\text{cm}^{-3}$ ,  $T=0.5-2$  keV) of plasmas and compared with available alternative spectroscopic data.

### 2. Generalized energy approach in scattering theory. Debye shielding model

The detailed description of our approach was earlier presented (see, for example, Refs. [3-5]). Therefore, below we are limited only by the key points.

The generalized relativistic energy approach combined with the RMBPT has been in details described in Refs. [7,13-27]. It generalizes earlier developed energy approach. The key idea is in calculating the energy shifts  $\Delta E$  of degenerate states that is connected with the secular matrix  $M$  diagonalization [6,7,13-16]. To construct  $M$ , one should use the Gell-Mann and Low adiabatic formula for  $\Delta E$ . The secular matrix elements are already complex in the PT second order. The whole calculation is reduced to calculation and diagonalization of the complex matrix  $M$  and definition of matrix of the coefficients with eigen state vectors  $B_{e,i}^K$  [5-8]. To calculate all necessary matrix elements one must use the basis's of the 1QP relativistic functions. Within an energy approach the total energy shift of the state is usually presented as [13-15]:

$$\Delta E = \text{Re}\Delta E + i \Gamma/2 \quad (1)$$

where  $\Gamma$  is interpreted as the level width and decay possibility  $P = \Gamma$ . The imaginary part of electron energy of the system, which is defined in the lowest PT order as [3]:

$$\text{Im}\Delta E(B) = -\frac{e^2}{4\pi} \sum_{\substack{\alpha > n > f \\ [\alpha < n \leq f]}} V_{\alpha n \alpha n}^{|\omega_{\alpha n}|}, \quad (2)$$

where  $\sum$  for electron and  $\sum_{\leq}$  for vacancy. The separated terms of the sum in (3) represent the contributions of different channels. It is known that their adequate description requires using the optimized basis's of wave functions. In [6] it has been proposed "ab initio" optimization principle for construction of cited basis's. It uses a minimization of the gauge dependent multielectron contribution of the lowest QED PT corrections to the radiation widths of atomic levels. This contribution describes collective effects and it is dependent upon the electromagnetic potentials gauge (the gauge non-invariant contribution  $\delta E_{\text{nimv}}$ ). The minimization of  $\text{Im}\delta E_{\text{nimv}}$  leads to integral differential equation, that is numerically solved. In result one can get the optimal one-electron basis of the PT [12-16]. It is worth to note that this approach was used under solving of multiple problems of modern atomic, nuclear and molecular physics (see [17-27]). Further let us firstly consider the Debye shielding model according to Refs. [4,5]. It is known in the classical theory of plasmas developed by Debye-Hückel, the interaction potential between two charged particles is modelled by the Yukawa-type potential, which contains the shielding parameter  $\mu$  [2]. The parameter  $\mu$  is connected with the plasma parameters such as the temperature  $T$  and the charge density  $n$  as follows:  $\mu \sim \sqrt{e^2 n / k_B T}$ . Here, as usually,  $e$  is the electron charge and  $k_B$  is the Boltzman constant. The density  $n$  is given as a sum of the electron density  $N_e$  and ion density  $N_k$  of the  $k$ -th ion species having the nuclear charge

$$q_k = \dots \quad (3)$$

It is very useful to remind the simple estimates for the shielding parameter. For example, under typical laser plasmas conditions of  $T \sim$

1keV and  $n \sim 10^{22} \text{ cm}^{-3}$  the parameter  $\mu$  is of the order of 0.1 in atomic units; in the EBIT plasmas  $T \sim 0.05 \text{ keV}$ ,  $n \sim 10^{18} \text{ cm}^{-3}$  and  $\mu \sim 10^{-3}$ . We are interested in studying the spectral parameters of ions in plasmas with the temperature  $T \sim 0.1 \text{ keV}$  ( $10^6 \text{--} 10^7 \text{ K}$ ) and  $n \sim 10^{14} \text{--} 10^{26} \text{ cm}^{-3}$  ( $\mu \sim 10^{-5} \text{--} 10^0$ ). It should be noted that indeed the Debye screening for the atomic electrons in the Coulomb field of nuclear charge is well understood due to the presence of the surrounding plasma electrons with high mobility. On the other hand, the contribution due to the Debye screening between electrons would be of smaller magnitude orders. Majority of the previous works on the spectroscopy study have considered the screening effect only in the electron-nucleus potential where the electron-electron interaction potential is truncated at its first term of the standard exponential expansion for its dominant contribution [3-69]. However, it is also important to take into account the screening in the electron-electron interactions for large plasma strengths to achieve more realistic results in the search for stability of the atomic structure in the plasma environment.

By introducing the Yukawa-type e-N and e-e interaction potentials, an electronic Hamiltonian for N-electron ion in a plasma is in atomic units as follows [4]:

$$H = \sum_i [\alpha c p - \beta m c^2 - Z \exp(-\mu r_i) / r_i] + \sum_{i>j} \frac{(1 - \alpha_i \alpha_j)}{r_{ij}} \exp(-\mu r_{ij}) \quad (4)$$

To generate the wave functions basis we use the optimized Dirac-Kohn-Sham potential with one parameter [8], which calibrated within the special ab initio procedure within the relativistic energy approach [6]. The modified PC numerical code "Superatom" is used in all calculations. Other details can be found in Refs. [3-6].

### 3. Results and conclusion

Firstly, we present our results on energy shifts and oscillator strengths for transitions  $2s^2 \text{--} 2s_{1/2} 2p_{1/2,3/2}$  in spectra of the Be-like Fe. The corresponding plasma parameters are as follows:  $n_e = 10^{22} \text{--} 10^{24} \text{ cm}^{-3}$ ,  $T = 0.5 \text{--} 2 \text{ keV}$  (i.e.  $\mu \sim 0.01 \text{--} 0.3$ ).

We studied a behavior of the energy shifts  $\Delta E$  ( $\text{cm}^{-1}$ ) for  $2s^2-[2s_{1/2}2p_{1/2,3/3}]_1$  transitions and oscillator strengths changes for different plasma parameters (the electron density and temperature). In Table 1 there are listed the oscillator strengths  $gf$  for  $2s^2-[2s_{1/2}2p_{3/2}]_1$  transition in Be-like GaXXVIII for different values of the  $n_e$  ( $\text{cm}^{-3}$ ) and  $T$  (in eV): the alternative theoretical data by Yongqiang Li et al [1] and our data.

Table 1.  
**Oscillator strengths for  $2s^2-[2s_{1/2}2p_{3/2}]_1$  transition in Be-like ion of GaXXVIII different  $n_e$  ( $\text{cm}^{-3}$ ) and  $T$  (eV) ( $gf_0$  –  $gf$  value for free ion)**

$n_e$		$10^{22}$	$10^{24}$
kT	[13]	[13]	[13]
500	0.1416	0.14157	0.14214
1000		0.14157	0.14200
2000		0.14157	0.14190
I-S		0.14157	0.14171
$n_e$		$10^{22}$	$10^{24}$
kT	Our	Our	Our
500	0.1419	0.14185	0.14268
1000		0.14185	0.14255
2000		0.14185	0.14242

There are also listed the available data by Li et al and Saha-Frische: the multiconfiguration Dirac-Fock (DF) calculation results, and ionic sphere (I-S) model simulation data [1, 2] (see refs. therein). In Table 2 we presented our data on the oscillator strengths  $gf$  for  $2s^2-[2s_{1/2}2p_{3/2}]_1$  transition in Be-like ion of GeXXIX for different values of the  $n_e$  ( $\text{cm}^{-3}$ ) and  $T$  (in eV).

Table 2.  
**Oscillator strengths for  $2s^2-[2s_{1/2}2p_{3/2}]_1$  transition in Be-like ion of GeXXIX, for different  $n_e$  ( $\text{cm}^{-3}$ ) and  $T$  (eV) ( $gf_0$  –  $gf$  value for free ion)**

$n_e$	$10^{22}$	$10^{23}$	$10^{24}$
kT	Our	Our	Our
500	0.14052	0.14068	0.14115
1000	0.14052	0.14067	0.14104
2000	0.14052	0.14065	0.14089

The analysis shows that the presented data are in physically reasonable agreement, however, some difference can be explained by using different relativistic orbital bases and different models for accounting of the plasma screening effect. It is important to note that our computing oscillator strengths within an energy approach with different forms of transition operator (this is corresponding to using the photon propagators in the form of Coulomb, Feynman and Babushkin) gives very close results.

## References

1. Yongqiang, Li; Jianhua, Wu; Yong, Hou, Jianmin Yuan. Influence of hot and dense plasmas on energy levels and oscillator strengths of ions: Be-like ions for  $Z = 26-36$ , *J. Phys. B: At. Mol. Opt. Phys.* **2008**, *41*, 145002.
2. Saha B.; Fritzsche S. Influence of dense plasma on the low-lying transitions in Be-like ions: relativistic multi-configuration Dirac-Fock calculation. *J. Phys. B: At. Mol. Opt. Phys.* **2007**, *40*, 259-270.
3. Buyadzhi, V.V. Laser multiphoton spectroscopy of atom embedded in Debye plasmas: multiphoton resonances and transitions. *Photoelectronics*. **2015**, *24*, 128-133.
4. Buyadzhi, V.V.; Chernyakova, Yu.G.; Smirnov, A.V.; Tkach, T.B. Electron-collisional spectroscopy of atoms and ions in plasma: Be-like ions. *Photoelectronics*. **2016**, *25*, 97-101.
5. Buyadzhi, V.V.; Chernyakova, Yu.G.; Antoshkina, O.A.; Tkach, T.B. Spectroscopy of multicharged ions in plasmas: Oscillator strengths of Be-like ion Fe. *Photoelectronics*. **2017**, *26*, 94-102.
6. Ivanova, E.P.; Glushkov, A.V. Theoretical investigation of spectra of multicharged ions of F-like and Ne-like isoelectronic sequences. *J. Quant. Spectr. Rad. Transfer*. 1986, *36*, 127-145.
7. Ivanov, L.N.; Ivanova, E.P.; Knight, L. Energy approach to consistent QED

- theory for calculation of electron-collision strengths: Ne-like ions. *Phys. Rev. A* **1993**, *48*, 4365-4374.
8. Glushkov, A.V.; Malinovskaya, S.V.; Gurnitskaya, E.P.; Khetselius, O.Yu.; Dubrovskaya, Yu.V. Consistent quantum theory of recoil induced excitation and ionization in atoms during capture of neutron. *J. Phys.: Conf. Ser.* **2006**, *35*, 425-430.
  9. Glushkov, A.V.; Malinovskaya, S.V.; Prepelitsa, G.P.; Ignatenko, V. Manifestation of the new laser-electron nuclear spectral effects in the thermalized plasma: QED theory of cooperative laser-electron-nuclear processes. *J. Phys.: Conf. Ser.* **2005**, *11*, 199-206.
  10. Glushkov, A.V.; Malinovskaya, S.V.; Chernyakova Y.G.; Svinarenko, A.A. Cooperative laser-electron-nuclear processes: QED calculation of electron satellites spectra for multi-charged ion in laser field. *Int. Journ. Quant. Chem.* **2004**, *99*, 889-893.
  11. Glushkov, A.V.; Malinovskaya, S.V.; Loboda, A.V.; Shpinareva, I.M.; Gurnitskaya, E.P.; Korchevsky, D.A. Diagnostics of the collisionally pumped plasma and search of the optimal plasma parameters of x-ray lasing: calculation of electron-collision strengths and rate coefficients for Ne-like plasma. *J. Phys.: Conf. Ser.* **2005**, *11*, 188-198.
  12. Glushkov, A.V.; Ambrosov, S.V.; Loboda, A.V.; Gurnitskaya, E.P.; Prepelitsa, G.P. Consistent QED approach to calculation of electron-collision excitation cross sections and strengths: Ne-like ions. *Int. J. Quantum Chem.* **2005**, *104*, 562-569.
  13. Ivanov, L.N.; Ivanova, E.P.; Aglitsky, E.V. Modern trends in the spectroscopy of multicharged ions. *Phys. Rep.* **1988**, *166*, 315-390.
  14. Glushkov, A.V.; Ivanov, L.N.; Ivanova, E.P. Autoionization Phenomena in Atoms. *Moscow University Press, Moscow*, **1986**, 58-160
  15. Glushkov, A.V.; Ivanov, L.N. Radiation decay of atomic states: atomic residue polarization and gauge non-invariant contributions. *Phys. Lett. A* **1992**, *170*, 33-36.
  16. Glushkov, A.V. *Relativistic Quantum theory. Quantum mechanics of atomic systems*; Astroprint: Odessa, **2008**.
  17. Glushkov, A.V. Spectroscopy of atom and nucleus in a strong laser field: Stark effect and multiphoton resonances. *J. Phys.: Conf. Ser.* **2014**, *548*, 012020
  18. Khetselius, O.Yu. Spectroscopy of cooperative electron-gamma-nuclear processes in heavy atoms: NEET effect. *J. Phys.: Conf. Ser.* **2012**, *397*, 012012.
  19. Khetselius, O.Yu. *Hyperfine structure of atomic spectra*. Astroprint: Odessa, **2008**.
  20. Glushkov A.V.; Ivanov, L.N. DC strong-field Stark effect: consistent quantum-mechanical approach. *J. Phys. B: At. Mol. Opt. Phys.* **1993**, *26*, L379-386.
  21. Glushkov, A.V. Negative ions of inert gases. *JETP Lett.* **1992**, *55*, 97-100.
  22. Glushkov, A.V.; Khetselius, O.Yu.; Malinovskaya, S.V. Optics and spectroscopy of cooperative laser-electron nuclear processes in atomic and molecular systems – new trend in quantum optics. *Europ. Phys. Journ. ST* **2008**, *160*, 195-204.
  23. Glushkov, A.V.; Khetselius, O.Yu.; Malinovskaya, S.V. Spectroscopy of cooperative laser–electron nuclear effects in multiatomic molecules. *Molec. Phys.* **2008**, *106*, 1257-1260.
  24. Ignatenko, A.V. Probabilities of the radiative transitions between Stark sub-levels in spectrum of atom in an DC electric field: New approach. *Photoelectronics*, **2007**, *16*, 71-74.
  25. Glushkov, A.V.; Ambrosov, S.V.; Ignatenko, A.V. Non-hydrogenic atoms and Wannier-Mott excitons in a DC electric field: Photoionization, Stark effect, Resonances in ionization con-

- tinuum and stochasticity. *Photoelectronics*, **2001**, *10*, 103-106.
26. Khetselius, O.Yu. Relativistic perturbation theory calculation of the hyperfine structure parameters for some heavy-element isotopes. *Int. Journ.*

- Quant.Chem.* **2009**, *109*, 3330-3335.
27. Khetselius, O.Yu. Hyperfine structure of radium. *Photoelectronics*. **2005**, *14*, 83-85.

This article has been received in August 2018

PACS 31.15.-p

*V. V. Buyadzhi, T. B. Tkach, A. P. Lavrenko, E. S. Romanenko*

### **SPECTROSCOPY OF MULTICHARGED IONS IN PLASMAS: OSCILLATOR STRENGTHS OF Be-LIKE IONS GaXXVIII and GeXXIX**

#### **Summary**

Oscillator strengths  $gf$  for  $2s^2-[2s_{1/2}2p_{3/2}]_1$  transition in Be-like multicharged ions of GaXXVIII and GeXXIX are computed for different values of the electron density and temperature ( $n_e=10^{22}-10^{24}\text{cm}^{-3}$ ,  $T=0.5-2\text{ keV}$ ) of plasmas are presented and compared with available alternative spectroscopic data. The generalized relativistic energy approach and relativistic many-body perturbation theory with the Debye shielding model as zeroth approximation is used for studying spectral parameters of ions in plasmas. An electronic Hamiltonian for  $N$ -electron ion in a plasma is added by the Yukawa-type electron-electron and nuclear interaction potential.

**Key words:** spectroscopy of ions in plasmas, relativistic energy approach, oscillator strengths

PACS 31.15.-p

*В. В. Буйаджи, Т. Б. Ткач, А. П. Лавренко, Э. С. Романенко*

### **СПЕКТРОСКОПИЯ МНОГОЗАРЯДНЫХ ИОНОВ В ПЛАЗМЕ: СИЛЫ ОСЦИЛЛЯТОРОВ ДЛЯ Be-ПОДОБНЫХ ИОНОВ GaXXVIII и GeXXIX**

#### **Резюме**

Силы осцилляторов  $2s^2-[2s_{1/2}2p_{3/2}]_1$  переходов в Be-подобных многозарядных ионах GaXXVIII, GeXXIX рассчитаны для различных значений электронной плотности и температуры ( $n_e=10^{22}-10^{24}\text{cm}^{-3}$ ,  $T=0.5-2\text{ keV}$ ) плазмы и сравниваются с имеющимися альтернативными спектроскопическими данными. Изучение спектральных параметров ионов в плазме выполнено на основе обобщенного релятивистского энергетического подхода и релятивистской многочастичной теории возмущений с использованием экранировочной модели Дебая. Электронный гамильтониан для  $N$ -электронного иона в плазме дополнен потенциалом электрон-электронного и ядерного взаимодействия типа Юкавы.

**Ключевые слова:** спектроскопия ионов в плазме, энергетический подход, силы осцилляторов

## **СПЕКТРОСКОПІЯ БАГАТОЗАРЯДНИХ ІОНІВ В ПЛАЗМІ: СИЛИ ОСЦИЛЯТОРІВ ДЛЯ Ве-ПОДІБНИХ ІОНІВ GaXXVIII і GeXXIX**

### **Резюме**

Сили осциляторів  $2s^2-[2s_{1/2}2p_{3/2}]_1$  переходів в Ве-подібних багатозарядних іонах GaXXVIII, GeXXIX розраховані для різних значень електронної густини і температури ( $n_e=10^{22}-10^{24}\text{cm}^{-3}$ ,  $T=0.5-2\text{ keV}$ ) плазми та порівнюються з наявними альтернативними спектроскопічними даними. Вивчення спектральних параметрів іонів в плазмі виконано на основі узагальненого релятивістського енергетичного підходу і релятивістської багаточастинкової теорії збурень з використанням екраніровочної моделі Дебая. Електронний гамільтоніан для N-електронного іона в плазмі доповнений потенціалом електрон-електронної та ядерного взаємодії типу Юкави.

**Ключові слова:** спектроскопія іонів в плазмі, енергетичний підхід, сили осциляторів

*T. I. Lavrenova, V. A. Borshchak, N. P. Zatovska, M. I. Kutalova*

Odessa I. I. Mechnikov National University, 2 Dvorianskaya str., Odessa 65026, Ukraine,  
Tel. +38 048 7233461, E-mail: borschak1957@gmail.com

## **SOLDER FOR FORMATION OF CONTACTS TO CONVERTERS OF OPTICAL AND X-RAY IMAGES INTO THE ELECTRICAL SIGNAL**

The pasty solder is used in the technology of the installation of electro-radio elements. Such elements can be microcircuits and optical and X-ray images microelectronic sensors with a hard raster [1]. Tinning of such sensor contact surfaces and printed circuit boards, where such sensors are mounted and soldering of the sensors to the plate is a considerable problem due to the need to remove corrosive active paste radical. The advantage of the developed solder is low corrosion activity and high fluxing ability. After soldering, there is no need to clean the surface of the printed circuit board and the contact sensor from paste radicals and chemical reaction products.

Because of the high printing density of the optical and X-ray images sensors with a rigid raster, when the distance between the current circles, the width and thickness of the tracks can be less than 10 microns, the solder paste should have high fluxing activity and not cause corrosion, while providing satisfactory soldering.

The main disadvantages of known pasty solders:

1. Insufficient fluxing activity. The paste radicals after soldering are corrosively active.

2. When soldering due to the presence of rosin (up to 22%), there is the formation of a large number of resinification products on a surface that is soldered. Removal of these substances needs thorough washing with mixtures of various organic solvents, and in some cases, additional mechanical cleaning. This is associated with the significant technological difficulties, especially with the high compactness of the printed assembly and the presence on the printed circuit boards without hull and hinged elements.

3. High rosin corrosion activity (acid number 170-180) leads to the maturation and dissolution of the metal, which is soldered, especially when soldered by the technology of mounting on the surface, when the contact plane (CP) thickness is 10-20 microns.

4. During the soldering process, compounds are formed which, in conditions of high humidity, can cause corrosion and reduce insulation

resistance of printed circuit boards, especially with high density of printed assembly (distance between conductive tracks is 10 - 30 microns). Maleic acid has a very large fluxing activity, but at its content of  $\approx 0.5 - 3.0\%$ , the insulation resistance after soldering is reduced by 1-2 orders of magnitude, which is in accordance with the requirements of the STD, but is not acceptable for special purpose radioelectronic equipment (REE).

5. High activity of fluxing components (diethylamine hydrochloric acid and maleic acid (or maleic anhydride) leads to the maturation and dissolution of soldered metal, especially when soldered using surface mount technology, when the CP thickness is of 10-20  $\mu\text{m}$  (Fig. 1).

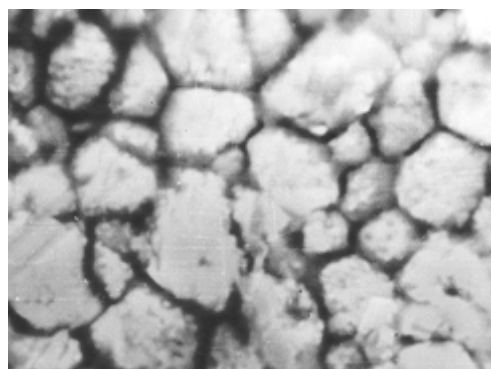


**Fig. 1 Solder seam surface destruction. Raster electron microscope. Mode of the secondary electrons. Increase 2000 $\times$ .**

6. The paste fluxing activity reducing during its storage. Because of the high corrosion activity of the fluxing components (diethylamine hydrochloric acid and maleic acid (or maleic anhydride)) with the paste prolonged storage (warranty period of 3 months or more) due to the developed surface of the solder powder, its oxidation occurs, which significantly reduces the technological characteristics of the paste: fluxing activity, wettability, spread ratio.

These factors reduce the reliability of the contact of the optical and X-ray image sensor to the board on which it is mounted. Their removing leads to the reduction of material costs, time and funds for soldering technology.

Due to the fact that the distance between the current paths may be less than 10 microns, the solder paste should have high fluxing activity and should not cause corrosion while providing satisfactory soldering. For this purpose, as an active fluxing component, rosin and extra relatively inactive succinic acid and glycerin, which have the properties of a reducing agent and greatly enhance the fluxing effect of the rosin, are selected. The introduction of the solvent paste of succinic acid and glycerine reduces the content of the rosin, which significantly reduces the amount of product of the resinification and simplifies the operation of laundering after soldering.

In the proposed composition, the optimal quantitative ratios of active reagents - rosin, succinic acid, glycerol are selected in such way as to provide sufficient fluxing activity (required for wetting and spreading) without increasing the corrosion activity of the paste solder.

The proposed composition is prepared in this way [2].

Amber acid is thoroughly rubbed in a mortar to a fine powder, then add glycerol and dissolve in alcohol at a temperature of 70-80 ° C. In the resulting solution, add a solder powder and mix. Rosin is thoroughly rubbed in a mortar to a fine powder then adds castor oil and dibutylphthalate. The resulting mixture is heated to 90-120°C and, when stirred, dissolved to obtain a homogeneous mass. Both solutions are combined and also thoroughly mixed.

The trial of the proposed paste solder and the known paste were performed by soldering the prototype of optical and X-ray image sensor samples to the printed circuit boards. The paste remnants after soldering were not removed. Further, accelerated tests of printed circuit boards in a climate chamber at a temperature of 40°C and a relative humidity of 98% were carried out. After soldering and after performed accelerated tests, the insulation resistance of printed circuit boards was measured, which depends on the corrosion activity of the compositions. Fluxing activity was determined by the coefficient of diffusion (for copper, silver). Results of comparative tests are given in tables 1, 2.

Table 1

Technical characteristics	Paste flux, which is offered	Prototype solder paste
Residual corrosive activity after soldering.	Resistance to PCB insulation after soldering does not change. After accelerated tests, the resistance does not change.	Resistance to PCB insulation after soldering does not change. After accelerated tests, the resistance decreases by 5-10 times.

Table 2

Paste rheological characteristics	Paste flux, which is offered	Prototype solder paste
Dispersion coefficient (after manufacturing)	1.4	1.4
Dispersion coefficient (after 1 month of storage)	1.4	1.3
Dispersion coefficient (after 2 months of storage)	1.4	1.25
Dispersion coefficient (after 3 months of storage)	1.4	1.0

The advantage of the proposed paste solder is low corrosion activity and high fluxing ability when soldered, which does not decrease with prolonged storage (the warranty period is 3 months or more). The resistance of PCB insulation after soldering and accelerated testing is not changed. After soldering, no cleaning of the PCBs surface and contact nodes from paste residues or chemical reactions is required. The introduction into the composition of the paste solder of succinic acid and glycerol allows to reduce the content of rosin, which significantly reduces the resinification products amount. The economic efficiency at the invention implementing is that, when practically the same cost of chemical components (ingredients) as the proto-

type paste, the soldering quality is significantly increased and the reliability and operating (time) of the equipment as a whole increases.

1. Smyntyna V. A. Image sensor on the basis of nonideal heterojunction with rigid raster/ Smyntyna V.A., Borschak V.A., Kutalova M.I., Zatovskaya N.P., Balaban A.P.// Photoelectronics.- 2006.- №15.- P.21-23.
2. Patent of Ukraine № 70407. «Paste form» / Lepich Ya.I., Sh.D.Kurmashev, T.I.Lavrenova, T.M. Bugayova. Public 11.06 2012, bul. No. 11

This article has been received in August 2018

UDC 621.315.592

*T. I. Lavrenova, V. A. Borshchak, N. P. Zatovska, M. I. Kutalova*

## **SOLDER FOR FORMATION OF CONTACTS TO CONVERTERS OF OPTICAL AND X-RAY IMAGES INTO THE ELECTRICAL SIGNAL**

The pasty solder is used in the technology of the installation of electro-radio elements. Such elements can be microcircuits and optical and X-ray images microelectronic sensors with a hard raster [1]. Tinning of such sensor contact surfaces and printed circuit boards, where such sensors are mounted and soldering of the sensors to the plate is a considerable problem due to the need to remove corrosive active paste radical. The advantage of the developed solder is low corrosion activity and high fluxing ability. After soldering, there is no need to clean the surface of the printed circuit board and the contact sensor from paste redicals and chemical reaction products.

**Keywords:** solder, sensor, contact

УДК 621.315.592

*Т. И. Лавренова, В. А. Борщак, Н. П. Затовская, М. И. Куталова*

## **ПРИПОЙ ДЛЯ СОЗДАНИЯ КОНТАКТА К ПРЕОБРАЗОВАТЕЛЯМ ОПТИЧЕСКОГО И РЕНТГЕНОВСКОГО ИЗОБРАЖЕНИЙ В ЭЛЕКТРИЧЕСКИЙ СИГНАЛ**

Пастообразный припой используется в технологии монтажа электрорадиоэлементов. Такие элементы могут быть микросхемами и микроэлектронными датчиками оптических и

рентгеновского изображений с твердым растром [1]. Лужение контактных площадок контакта сенсора и печатной платы на которую такие сенсоры монтируются есть важной проблемой из-за необходимости удаления коррозионно активных остатков пасты. Преимуществом разработанного припоя является низкая коррозионная активность и высокая флюсующая способность. После пайки, нет необходимости очищать поверхность печатной платы и контактов датчика от остатков пасты и продуктов химических реакций.

**Ключевые слова:** припой, сенсор, контакт

УДК 621.315.592

*Т. І. Лавренова, В. А. Борщак, Н. П. Затовська, М. І. Куталова*

### **ПРИПОЙ ДЛЯ СТВОРЕННЯ КОНТАКТУ ДО ПЕРЕТВОРЮВАЧА ОПТИЧНОГО ТА РЕНТГЕНІВСЬКОГО ЗОБРАЖЕНЬ В ЕЛЕКТРИЧНИЙ СИГНАЛ**

Пастоподібний припій використовується в технології монтажу електрорадіоелементів. Такими елементами можуть бути мікросхеми і мікроелектронні сенсори оптичного та рентгеновського зображень з жорстким растром [1]. Лудіння контактних площадок таких сенсорів та друкованих плат, на яких такі сенсори монтується і паяння сенсорів є чималою проблемою через необхідність видалення корозійно активних залишків пасты. Перевагою розробленого припою є низька корозійна активність та висока флюсуюча здатність. Після паяння не потрібне очищення поверхні друкованих плат та контактних сенсору від залишків пасты та продуктів хімічних реакцій.

**Ключові слова:** припой, сенсор, контакт

*E. V. Ternovsky, V. V. Buyadzhi, A. V. Tsudik, A. A. Svinarenko*

Odessa State Environmental University, L'vovskaya str.15, Odessa-16, 65016, Ukraine

E-mail: svinarenkoa@gmail.com

## RELATIVISTIC CALCULATION OF RYDBERG AUTOIONIZATION STATES PARAMETERS IN SPECTRUM OF BARIUM

The combined relativistic energy approach and relativistic many-body perturbation theory with the zeroth order Dirac-Kohn-Sham one-particle approximation are used for estimating the energies the in Rydberg autoionization  $4f_{5/2,7/2}n^f$   $J=6,5,4$  states, excited from the initial state  $5d_{3/2}15f$   $J=5$  in spectrum of the barium atom. The comparison with available theoretical and experimental (compillated) data is performed. The important point is linked with an accurate accounting for the complex exchange-correlation (polarization) effect contributions and using the optimized one-quasiparticle representation in the relativistic many-body perturbation theory zeroth order that significantly provides a physically reasonable agreement between theory and precise experiment.

### 1. Introduction

The research in many fields of modern atomic physics (spectroscopy, spectral lines theory, theory of atomic collisions etc), astrophysics, plasma physics, laser physics and quantum and photo-electronics requires an availability of sets of correct data on the energetic, spectroscopic and structural properties of atoms, especially in the high excited, Rydberg states. Naturally, the correct corresponding data about radiative decay widths, probabilities and oscillator strengths of atomic transitions are needed in building adequate astrophysical models, realizing regular astrophysical, laboratory, thermonuclear plasma diagnostics and in fusion research. Besides, a great interest to studying Rydberg atomic states parameters can be easily explained by a powerful development of such new fields as quantum computing, and quantum cryptography, construction of new type Rydberg atomic lasers etc. The knowledge of the Rydberg autoionization states parameters for many of atomic systems is of a great importance note for many applications in atomic and molecular physics, plasma chemistry and physics, laser physics and quantum electronics etc. [1-62]. However, studying spectral characteristics of heavy atoms and ions in the Rydberg states has to be more complicated as it requires a necessary accounting the relativistic, exchange-correlations effects and possibly the QED corrections for superheavy atomic sys-

tems. There have been sufficiently many reports of calculations and compilation of energies and oscillator strengths, autoionization states energies and widths for the barium and even Ba-like ions (see, for example, [1–3] and refs. therein), however, an accuracy of these data call for further serious analysis and calculation. In many papers the Dirac-Fock method, model potential approach, quantum defect (QD) approximation (different versions such as QD, MCQD etc) different realizations have been used for calculating the energy and spectral properties of barium and it has been shown that an account of the polarization interelectron corrections is of a great quantitative importance. The consistent relativistic MCQD calculations of the transitions energies and oscillator strengths for some chosen transitions between the Rydberg states are performed in Refs. [1,63,64]. However, it should be stated that for majority of the barium Rydberg states and there is not enough precise information available in literatures [1-3]. In our paper The combined relativistic energy approach and relativistic many-body perturbation theory with the zeroth order Dirac-Kohn-Sham one-particle approximation are used for estimating the energies the in Rydberg autoionization  $4f_{5/2,7/2}n^f$   $J=6,5,4$  states, excited from the initial state  $5d_{3/2}15f$   $J=5$  in spectrum of the barium atom.

## 2. The theoretical method

In refs. [8-170] the fundamentals of the relativistic many-body PT formalism have been in details presented, so further we are limited only by the novel elements. Let us remind that the majority of complex atomic systems possess a dense energy spectrum of interacting states. In refs. [3-65, 17-20] it is realized a field procedure for calculating the energy shifts DE of degenerate states, which is connected with the secular matrix  $M$  diagonalization. The whole calculation of the energies and decay probabilities of a non-degenerate excited state is reduced to the calculation and diagonalization of the  $M$ . The complex secular matrix  $M$  is represented in the form [9,10]:

$$M = M^{(0)} + M^{(1)} + M^{(2)} + M^{(3)}. \quad (1)$$

where  $M^{(0)}$  is the contribution of the vacuum diagrams of all order of PT, and  $M^{(1)}$ ,  $M^{(2)}$ ,  $M^{(3)}$  those of the one-, two- and three-QP diagrams respectively. The diagonal matrix  $M^{(1)}$  can be presented as a sum of the independent 1QP contributions. The optimized 1-QP representation is the best one to determine the zeroth approximation. In the relativistic energy approach [4-9], which has received a great applications during solving numerous problems of atomic, molecular and nuclear physics (e.g., see Refs. [10-59]), the imaginary part of electron energy shift of an atom is directly connected with the radiation decay possibility (transition probability). An approach, using the Gell-Mann and Low formula with the QED scattering matrix, is used in treating the relativistic atom. The total energy shift of the state is usually presented in the form:

$$\text{DE} = \text{ReDE} + i G/2 \quad (2)$$

where  $G$  is interpreted as the level width, and the decay possibility  $P = G$ . The imaginary part of electron energy of the system, which is defined in the lowest order of perturbation theory as [4]:

$$\text{Im } \Delta E(B) = -\frac{e^2}{4\pi} \sum_{\substack{\alpha > n > f \\ \alpha < n \leq f}} V_{\alpha n \alpha n}^{\omega \alpha n}, \quad (3)$$

where ( $\alpha > n > f$ ) for electron and ( $\alpha < n < f$ ) for vacancy. Under calculating the matrix elements (3) one should use the angle symmetry of the task and write the expansion for potential  $\sin|w|r_{12}/r_{12}$  on spherical functions as follows [4]:

$$\frac{\sin|\omega|r_2}{r_2} = \frac{\pi}{2\sqrt{r_1 r_2}} \sum_{\lambda=0}^{\infty} (\lambda) J_{\lambda+1/2}(\omega r_1) J_{\lambda+1/2}(\omega r_2) P_{\lambda}(\cos r_1 r_2). \quad (4)$$

$$\frac{\sin|\omega|r_2}{r_2} = \frac{\pi}{2\sqrt{r_1 r_2}} \sum_{\lambda=0}^{\infty} (\lambda) J_{\lambda+1/2}(\omega r_1) J_{\lambda+1/2}(\omega r_2) P_{\lambda}(\cos r_1 r_2)$$

where  $J$  is the Bessel function of first kind and  $(l) = 2l + 1$ . This expansion is corresponding to usual multipole one for probability of radiative decay. Substitution of the expansion (5) to matrix element of interaction gives as follows [5-8]:

$$V_{\beta_1 \beta_2; \beta_4 \beta_3} = \sqrt{(2j_1+1)(2j_2+1)(2j_3+1)(2j_4+1)} \times$$

$$\times \begin{matrix} j & j & j & j & m & m \\ \times & & & & & \times \end{matrix}$$

$$\times \sum_{a\mu} (-1)^\mu \begin{pmatrix} j_1 & j_3 & a \\ m_1 & -m_3 & \mu \end{pmatrix} \begin{pmatrix} j_2 & j_4 & a \\ m_2 & -m_4 & \mu \end{pmatrix} \times$$

$$\times \sum_{a\mu} (-1)^\mu \begin{pmatrix} j_1 & j_3 & a \\ m_1 & -m_3 & \mu \end{pmatrix} \begin{pmatrix} j_2 & j_4 & a \\ m_2 & -m_4 & -\mu \end{pmatrix} \quad (5)$$

$$Q_a(n_1 j_1 l_1 n_2 j_2 l_2; n_4 j_4 l_4 n_3 j_3 l_3)$$

$$= Q_a^{\text{Cul}} + Q_a^{\text{B}}. \quad (6)$$

where  $j_i$  is the total single electron momentums,  $m_i$  – the projections;  $Q^{\text{Cul}}$  is the Coulomb part of interaction,  $Q^{\text{Br}}$  – the Breit part. The detailed expressions for the Coulomb and Breit parts and the corresponding radial  $R_i$  and angular  $S_i$  integrals can be found in Refs. [22-32].

The calculating of all matrix elements, wave functions, Bessel functions etc is reduced to solving the system of differential equations. The formulas for the autoionization (Auger) decay probability include the radial integrals  $R_a(akgb)$ , where one of the functions describes electron in the continuum state. When calculating this integral, the correct normalization of the wave functions is very important, namely, they should have the following asymptotic at  $r \rightarrow \infty$ :

$$\left. \begin{matrix} f \\ g \end{matrix} \right\} \rightarrow (\lambda\omega)^{-1/2} \begin{cases} [\omega + (\alpha Z)^{-2}]^{-1/2} \sin(kr + \delta), \\ [\omega - (\alpha Z)^{-2}]^{-1/2} \cos(kr + \delta). \end{cases} \quad (7)$$

The important aspect of the whole procedure is an accurate accounting for the exchange-correlation effects. We have used the generalized relativistic Kohn-Sham density functional [8-17] in the zeroth approximation of relativistic PT; naturally, the perturbation operator contains the operator (3) minus the cited Kohn-Sham density functional. Further the wave functions are corrected by accounting of the first order PT contribution. Besides, we realize the procedure of optimization of relativistic orbitals base. The main idea is based on using ab initio optimization procedure, which is reduced to minimization of the gauge dependent multielectron contribution  $ImDE_{ninv}$  of the lowest QED PT corrections to the radiation widths of atomic levels.

According to [6,8], “in the fourth order of QED PT (the second order of the atomic PT) there appear the diagrams, whose contribution to the  $ImDE_{ninv}$  accounts for correlation effects and this contribution is determined by the electromagnetic potential gauge (the gauge dependent contribution)”. The accurate procedure for minimization of the functional  $ImDE_{ninv}$  leads to the Dirac-Kohn-Sham-like equations for the electron density that are numerically solved by the Runge-Cutts standard method It is very important to know that the regular realization of the total scheme allow to get an optimal set of the 1QP functions and more correct results in comparison with so called simplified one, which

has been used in Refs. [6-8] and reduced to the functional minimization using the variation of the correlation potential parameter  $b$ . Other details can be found in refs.[8-17, 22-40]. All calculations are performed on the basis of the modified numeral code Superatom (version 93).

### 3. Results and conclusion

As an important application of the theory we study the Rydberg autoionization states, which are corresponding to transitions into 4fnf, states, in particular,  $4f_{5/2,7/2}n^1f$  J=6,5,4 states, excited from the initial state  $5d_{3/2}15f$  J=5 (Figure 1).

In Table 1 we present the values of Energies ( $cm^{-1}$ ) of autoionization states 4fnf, n = 15: Exp.- experiment; Теория: (1)-data, obtained within the quantum defect method MCQD with empirical fitting by de Graaf et al; (2) –our theory).

Physically reasonable agreement between theory and precise experiment can be reached under condition of an accurate accounting of the complex exchange-correlation effects and using the optimized relativistic orbitals basis sets (the optimal one-quasiparticle representation).

Table 1.  
**Energies ( $cm^{-1}$ ) of autoionization states  $4f_{5/2,7/2}n^1f$  J=6,5,4, n = 15: Exp.- experiment; Theory: (1)-quantum defect method MCQD with empirical fitting; (2) –our theory**

AC	J	Exp.	(1)	(2)
$4f_{5/2}15f_{7/2}$	6	89 758.4±0.5	89759.1	89758.8
$4f_{7/2}15f_{5/2}$	6	89 993.6±0.5	89992.4	89993.6
$4f_{7/2}15f_{7/2}$	6	89 926.6±5.0	89937.1	89926.8
$4f_{5/2}15f_{7/2}$	5	89 726.3±1.0	89718.7	89726.9
$4f_{5/2}15f_{5/2}$	5	89 951.0±0.5	89952.9	89951.6
$4f_{7/2}15f_{5/2}$	5	-	89943.6	89942.3
$4f_{5/2}15f_{5/2}$	4	89 705.6±0.5	89706.8	89705.4
$4f_{5/2}15f_{7/2}$	4	-	89720.0	89718.5
$4f_{7/2}15f_{5/2}$	4	-	89937.2	89937.6
$4f_{7/2}15f_{7/2}$	3	-	-	89953.4
$4f_{5/2}15f_{7/2}$	2	-	-	89767.8

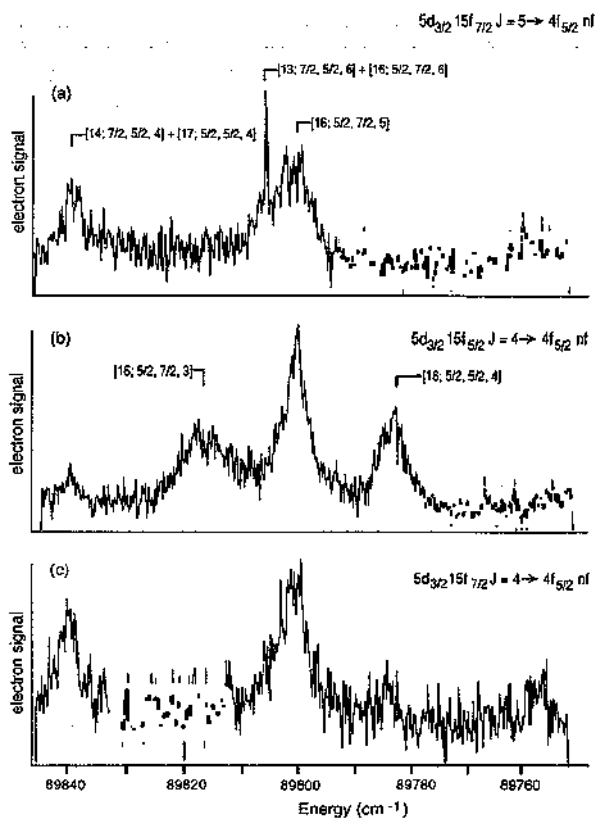


**Figure 1.** The experimental spectrum of the Ba  $4f_{5/2} n'f$   $J=6,5,4$  autoionization states, excited from initial state:  $5d_{3/2} 15f_{7/2} J=5$

## References

1. Luc Koenig E., Aymar M., Van Leeuwen R., Ubachs W., Hogervorst W., The  $5d5g$  states in Ba//Phys. Rev.A-1995.-Vol.52.-P.208-215
2. Klose J., Fuhr J., Wiese W., Critically evaluated atomic transition probabilities for BaI, BaII// J. Phys. Ch. Ref. Dat.-2002.-Vol. 31.-P.217-230.
3. Ivanova E.P., Grant I., Oscillator strength anomalies in Ne isoelectronic sequence with applications to X-ray laser modeling// J. Phys. B:At.Mol. Phys.-1998-Vol.31.-P.2871.
4. Ivanov L.N., Ivanova E.P., Extrapolation of atomic ion energies by model potential method: Na-like spectra// Atom.Data Nucl Data Tab.-1979.-Vol.24.-P.95-121.
5. Ivanov L.N., Ivanova E.P., Knight L.,

Energy Approach to consistent QED theory for calculation of electron-collision strengths// Phys.Rev.A.-1993.-Vol.48.-P.4365-4374.

6. Glushkov A.V., Ivanov L.N., Radiation decay of atomic states: atomic residue polarization and gauge noninvariant contributions// Phys.Lett.A.-1992.-Vol. 170, N1.-P.33-36.
7. Glushkov A.V., Ivanov L.N., DC Strong-Field Stark-Effect: consistent quantum-mechanical approach// J. Phys.B: At. Mol. Opt. Phys.-1993.-Vol.26.-P.L379-386.
8. Glushkov A.V., Relativistic Quantum Theory. Quantum, mechanics of Atomic Systems.-Odessa: Astroprint, 2008.-700P.
9. Glushkov A.V., Khetselius O.Y., Malinovskaya S.V., New laser-electron nuclear effects in the nuclear  $\gamma$  transition spectra in atomic and molecular systems// Frontiers in Quantum Systems in Chemistry and Physics. Series: Progress in Theoretical Chemistry and Physics Eds. S.Wilson, P.J.Grout, J. Maruani, G. Delgado-Barrio, P. Piecuch (Springer).-2008.-Vol.18.-525-541.
10. Glushkov A.V., Khetselius O.Yu., Svinarenko A.A., Prepelitsa G.P., Energy approach to atoms in a laser field and quantum dynamics with laser pulses of different shape// In: Coherence and Ultrashort Pulse Laser Emission, Ed. by Dr. F. Duarte (InTech).-2010.-P.159-186.
11. Glushkov A.V., Khetselius O., Svinarenko A, Relativistic theory of cooperative muon-g gamma-nuclear processes: Negative muon capture and metastable nucleus discharge// Advances in the Theory of Quantum Systems in Chemistry and Physics. Ser.: Progress in Theor. Chem. and Phys., Eds. P.Hoggan, E.Brandas, J.Maruani, G. Delgado-Barrio, P.Piecuch (Springer).-2012.-Vol.22.-P.51.

12. Glushkov A.V., Svinarenko A.A., Nuclear quantum optics: Energy approach to multi-photon resonances in nuclei // *Sensor Electr. and Microsyst. Techn.*-2010.-N2.-P.5-10.
13. Glushkov A.V., Energy approach to resonance states of compound super-heavy nucleus and EPPP in heavy nuclei collisions// *Low Energy Antiproton Phys. AIP Conference Proceedings.*-2005.-Vol. 796.-P.206-210.
14. Malinovskaya S.V., Glushkov A.V., Khetselius O.Yu., Lopatkin Yu., Loboda A.V., Svinarenko A., Nikola L., Perelygina T., Generalized energy approach to calculating electron collision cross-sections for multicharged ions in a plasma: Debye shielding model// *Int. Journ. Quant. Chem.*-2011.-Vol.111,N2.-P.288-296.
15. Malinovskaya S., Glushkov A.V., Khetselius O.Yu., Svinarenko A.A., Mischenko E., Florko T., Optimized perturbation theory scheme for calculating the interatomic potentials and hyperfine lines shift for heavy atoms in the buffer inert gas//*Int. J. Quant.Chem.*-2009.-Vol.109.-P. 3325-3329.
16. Glushkov A., Malinovskaya S., Prepelitsa G., Ignatenko V., Manifestation of the new laser-electron nuclear spectral effects in thermalized plasma: QED theory of cooperative laser-electron- nuclear processes // *J. Phys.: Conf. Ser.*-2005.-Vol.11.-P.199.
17. Glushkov A.V., Khetselius O.Yu., Lovett L., Electron- $\beta$ -Nuclear Spectroscopy of Atoms and Molecules and Chemical Environment Effect on the  $\beta$ -Decay parameters// *Advances in the Theory of Atomic and Molecular Systems Dynamics, Spectroscopy, Clusters, and Nanostructures. Series: Progress in Theor. Chem. and Phys.*, Eds. Piecuch P., Maruani J., Delgado-Barrio G., Wilson S. (Springer).-2009.-Vol.20.-P.125-152.
18. Glushkov A.V., Malinovskaya S.V., Ambrosov S., Shpinareva I.M., Troitskaya O.V., Resonances in quantum systems in strong external fields consistent quantum approach// *J. of Techn.Phys.*-1997.-Vol.38, Iss.2.-P.215-218.
19. Glushkov A., Malinovskaya S., Loboda A., Shpinareva I., Gurnitskaya E., Korchevsky D., Diagnostics of the collisionally pumped plasma and search of the optimal plasma parameters of x-ray lasing: Calculation of electron-collision strengths and rate coefficients for Ne-like plasma// *J. Phys.: Conf.Ser.*-2005.-Vol.11.-P.188-198.
20. Glushkov A.V., Khetselius O.Yu., Loboda A., Ignatenko A., Svinarenko A., Korchevsky D., Lovett L., QED approach to modeling spectra of the multicharged ions in a plasma: Oscillator and electron-ion collision strengths//*Spectral Line Shapes. AIP Conf.Proc.*-2008.-Vol.1058.-P.175-177
21. Malinovskaya S.V., Dubrovskaya Yu.V., Vitavetskaya L.A., Advanced quantum mechanical calculation of the beta decay probabilities// *Low Energy Antiproton Phys. AIP Conference Proceedings.*-2005.-Vol. 796.-P.201-205.
22. Glushkov A.V., Ambrosov S.V., Loboda A., Gurnitskaya E.P., Prepelitsa G.P., Consistent QED approach to calculation of electron-collision excitation cross-sections and strengths: Ne-like ions//*Int. Journ. Quant. Chem.*-2005.-Vol.104, N4 .-P. 562-569.
23. Glushkov A.V., Ambrosov S., Ignatenko A., Korchevsky D., DC Strong Field Stark effect for non-hydrogenic atoms: Consistent quantum mechanical approach// *Int.Journ. Quant. Chem.*-2004.-

- Vol.99,N6.-P.936-939.
24. Glushkov A.V., Malinovskaya S.V., Chernyakova Y.G., Svinarenko A.A., Cooperative laser-electron-nuclear processes: QED calculation of electron satellites spectra for multi-charged ion in laser field// *Int. J. Quant. Chem.*-2004.-Vol.99.-P.889-893.
  25. Glushkov A.V., Khetselius O.Yu., Malinovskaya S.V., Optics and spectroscopy of cooperative laser-electron nuclear processes in atomic and molecular systems - new trend in quantum optics// *Europ. Phys. Journ. ST.*-2008.-Vol.160,N1.-P.195-204.
  26. Malinovskaya S., Glushkov A., Dubrovskaya Yu., Vitavetskaya L., Quantum calculation of cooperative muon-nuclear processes: discharge of metastable nuclei during negative muon capture// *Recent Advances in Theory of Chemical and Physical Systems (Springer)*.-2006.-Vol.15.-P.301-307.
  27. Glushkov A.V., Khetselius O.Yu., Loboda A., Svinarenko A., QED approach to atoms in a laser field: Multi-photon resonances and above threshold ionization// *Frontiers in Quantum Systems in Chemistry and Physics, Ser.: Progress in Theor. Chem.and Phys.;* Eds. S.Wilson, P.Grout, J. Maruani et al, (Springer), 2008.-Vol.18.-P.543-560.
  28. Glushkov A.V., Dan'kov S., Prepelitsa G., Polischuk V., Efimov A., Qed theory of nonlinear interaction of the complex atomic systems with laser field multi-photon resonances// *Journal of Tech. Phys.*-1997.-Vol.38.-P.219-222
  29. Glushkov A.V., Ambrosov S.V., Loboda A.V., Gurnitskaya E.P., Khetselius O.Yu., QED calculation of heavy multicharged ions with account for the correlation, radiative and nuclear effects// *Recent Advances in Theor. Phys. and Chem. Systems.*-2006.-Vol.15.-P.285-300.
  30. Glushkov A.V., Calculation of parameters of the interaction potential between excited alkali atoms and mercury atoms-the Cs-, Fr-Hg interaction// *Optika i Spekt.*-1994.-Vol.77 (1).-P.5-10.
  31. Glushkov A.V., Khetselius O.Yu., Gurnitskaya E.P., Korchevsky D.A., Loboda A.V., Prepelitsa G.P., Sensing the electron-collision excitation cross-sections for Ne-like ions of Fe in a plasma in the Debye shielding approximation// *Sensor Electr. and Microsyst. Techn.*-2007.-N2.-P.9-13
  32. Svinarenko A.A., Ignatenko A.V., Ternovsky V.B., Nikola V.V., Seredenko S.S., Tkach T.B., Advanced relativistic model potential approach to calculation of radiation transition parameters in spectra of multicharged ions// *J.Phys.:Conf. Ser.*-2014.-Vol.548.-P. 012047
  33. Svinarenko A.A., Khetselius O.Yu., Buyadzhi V.V., Floriko T.A., Zaichko P.A., Ponomarenko E.L., Spectroscopy of Rydberg atoms in a Black-body radiation field: Relativistic theory of excitation and ionization// *J. Phys.: Conf. Ser.*-2014.-Vol. 548.-P. 012048.
  34. Glushkov A., Khetselius O., Bunyakova Y., Buyadzhi V., Brusentseva S., Zaichko P., Sensing interaction dynamics of chaotic systems within chaos theory and micro-system technology Geomath with application to neurophysiological systems// *Sensor Electr.Microsyst. Techn.*-2014-Vol. 11.-P.62
  35. Prepelitsa G.P., Glushkov A.V., Lepikh Ya.I., Buyadzhi V.V., Ternovsky V.B., Zaichko P.A., Chaotic dynamics of non-linear processes in atomic and molecular systems in electromagnetic field and semiconductor and fiber laser devices: new approaches, uniformity and charm of chaos// *Sensor Electr. and Microsyst. Techn.*-2014.-Vol.11,N4.-P.43-57.

36. Glushkov A.V., Relativistic and correlation effects in spectra of atomic systems.-Odessa: Astroprint.-2006.-400P.
37. Glushkov A.V., Atom in electromagnetic field.-Kiev: KNT, 2005.
38. Khetselius O.Yu., Hyperfine structure of atomic spectra.-Odessa: Astroprint, 2008.
39. Khetselius O.Yu., Hyperfine structure of radium//Photoelectronics.-2005-N14-P.83-85
40. Khetselius O., Spectroscopy of cooperative electron-gamma-nuclear processes in heavy atoms: NEET effect// J. Phys.: Conf. Ser.-2012.-Vol.397.-P.012012
41. Glushkov A., Malinovskaya S., Gurnitskaya E., Khetselius O.Yu.,Dubrovskaya Yu., Consistent quantum theory of the recoil induced excitation and ionization in atoms during capture of neutron// Journal of Physics: Conf. Series (IOP).-2006.-Vol.35.-P.425-430.
42. Khetselius O.Yu., Quantum Geometry: New approach to quantization of the quasistationary states of Dirac equation for super heavy ion and calculating hyperfine structure parameters// Proc. Int.Geometry Center.-2012.-Vol.5,№ 3-4.-P.39-45.
43. Glushkov A., Khetselius O., Svinarenko A., Theoretical spectroscopy of autoionization resonances in spectra of lanthanide atoms// Physica Scripta.-2013.-Vol. T153.-P.014029.
44. Glushkov A., Khetselius O., Gurnitskaya E., Loboda A., Sukharev D., Relativistic quantum chemistry of heavy ions and hadronic atomic systems: spectra and energy shifts//Theory and Applications of Computational Chemistry. AIP Conf.Proceedings.-2009.-Vol.1102.-P.168-171.
45. Khetselius O.Yu., Relativistic calculating the spectral lines hyperfine structure parameters for heavy ions// Spectral Line Shapes, AIP Conf. Proc.-2008.-Vol.1058.-P.363-365.
46. Khetselius O., Glushkov A., Gurnitskaya E., Loboda A., Mischenko E., Florko T., Sukharev D., Collisional Shift of the Tl hyperfine lines in atmosphere of inert gases// Spectral Line Shapes, AIP Conf. Proc.-2008.-Vol.1058.-P.231-233.
47. Khetselius O.Yu., Hyperfine structure of energy levels for isotopes  $^{73}\text{Ge}$ ,  $^{75}\text{As}$ ,  $^{201}\text{Hg}$ // Photoelectronics.-2007.-N16.-P.129-132.
48. Khetselius O.Y., Gurnitskaya E.P., Sensing electric and magnetic moments of a nucleus in the N-like ion of Bi// Sensor Electr. and Microsyst. Techn.-2006.-N3.-P.35-39.
49. Khetselius O.Y., Gurnitskaya E.P., Sensing the hyperfine structure and nuclear quadrupole moment for Ra// Sensor Electr. and Microsyst. Techn.-2006.-N2.-P.25-29.
50. Florko T.A., Loboda A.V., Svinarenko A.A., Sensing forbidden transitions in spectra of some heavy atoms and multicharged ions: New theoretical scheme// Sensor Electr. and Microsyst. Techn.-2009.-N3.-P.10-15.
51. Khetselius O.Yu., Florko T.A., Svinarenko A.A., Tkach T.B., Radiative and collisional spectroscopy of hyperfine lines of the Li-like heavy ions and Tl atom in atmosphere of inert gas//Phys.Scripta.-2013.-Vol. T153-P. 014037.
52. Khetselius O.Yu., Turin A.V., Sukharev D.E., Florko T.A., Estimating of X-ray spectra for kaonic atoms as tool for sensing the nuclear structure// Sensor Electr. and Microsyst. Techn.-2009.-N1.-P.30-35.
53. Khetselius O., On possibility of sensing nuclei of rare isotopes by means of laser spectroscopy of hyperfine

- structure//Sensor Electr. Microsyst. Techn.-2008.-Vol.3.-P.28.
54. Svinarenko A.A., Glushkov A.V., Loboda A.V., Sukharev D.E., Dubrovskaya Yu.V., Mudraya N.V., Serga I.N., Green's function of the Dirac equation with complex energy and non-singular central nuclear potential//Quantum Theory: Reconsideration of Foundations. AIP Conf. Proceedings.-2010.-Vol.1232.-P.259-266.
  55. Buyadzhi V., Chernyakova Yu., Smirnov A., Tkach T., Electron-collisional spectroscopy of atoms and ions in plasma: Be-like ions// Photoelectronics.-2016.-Vol.25.-P.97-101.
  56. Sukharev D.E., Khetselius O.Yu., Dubrovskaya Yu.V., Sensing strong interaction effects in spectroscopy of hadronic atoms// Sensor Electr. and Microsyst. Techn.-2009.-N3.-P.16-21.
  57. Glushkov A.V., Khetselius O.Yu., Kuzakon V., Prepelitsa G.P., Solyanikova E.P., Svinarenko A., Modeling of interaction of the non-linear vibrational systems on the basis of temporal series analyses (application to semiconductor quantum generators)// Dynamical Systems- Theory and Applications.-2011.-BIF110.
  58. Glushkov A., Khetselius O.Y., Brusentseva S., Zaichko P., Ternovsky V., Studying interaction dynamics of chaotic systems within a non-linear prediction method: application to neurophysiology// Advances in Neural Networks, Fuzzy Systems and Artificial Intelligence, Ser: Recent Adv. in Computer Engineering, Ed. J.Balicki.-2014.-Vol.21.-P.69-75.
  59. Glushkov A.V., Operator Perturbation Theory for Atomic Systems in a Strong DC Electric Field//Advances in Quantum Methods and Applications in Chemistry, Physics, and Biology. Series: Frontiers in Theoretical Physics and Chemistry, Eds. M.Hotokka, J.Marvani, E. Brändas, G.Delgado-Barrio (Springer).-2013.-Vol. 27.-P.161-178.
  60. Glushkov A., Khetselius O., Prepelitsa G., Svinarenko A., Geometry of Chaos: Theoretical basis's of a consistent combined approach to treating chaotic dynamical systems and their parameters determination // Proc. Int. Geometry Center".-2013.-Vol.6, N1.-P.43-48.
  61. Svinarenko A., Nikola L., Prepelitsa G., Tkach T., Mischenko E., Auger (autoionization) decay of excited states in spectra of multicharged ions: Relativistic theory//AIP Conf. Proc.-2010.-Vol.1290, N1 P.94-98.
  62. Florko T.A., Ignatenko A.V., Svinarenko A.A., Tkach T.B., Ternovsky V.B, Advanced relativistic model potential approach to calculation of the radiation transition and ionization characteristics for Rydberg atoms// Photoelectronics.-2014.-Vol.23.-P.91-95.
  63. Van Leuwen R., Ubachs W., Hogervorst W., Autoionization of low-lying 5dng states in barium//J. Phys.B.: Atom.Mol.Opt.Phys.-1994.-Vol.27.-P.3891-3904.
  64. Glushkov A V, Khetselius O Yu, Svinarenko A A and Buyadzhi V V, Spectroscopy of autoionization states of heavy atoms and multiply charged ions (Odessa: TEC) -2015.

This article has been received in August 2018

PACS 31.15.A-; 32.30.-r

*E. V. Ternovsky, V. V. Buyadzhi, A. V. Tsudik, A. A. Svinarenko*

## RELATIVISTIC CALCULATION OF RYDBERG AUTOIONIZATION STATES PARAMETERS IN SPECTRUM OF BARIUM

### Summary

The combined relativistic energy approach and relativistic many-body perturbation theory with the zeroth order Dirac-Kohn-Sham one-particle approximation are used for estimating the energies in the Rydberg autoionization  $4f_{5/2,7/2}n^{\prime}f$   $J=6,5,4$  states, excited from the initial state  $5d_{3/2}15f$   $J=5$  in the spectrum of the barium atom. The comparison with available theoretical and experimental (compiled) data is performed. The important point is linked with an accurate accounting for the complex exchange-correlation (polarization) effect contributions and using the optimized one-quasiparticle representation in the relativistic many-body perturbation theory zeroth order that significantly provides a physically reasonable agreement between theory and precise experiment.

**Key words:** relativistic theory, Rydberg autoionization states, barium

PACS 31.15.A-; 32.30.-r

*Е. В. Терновский, В. В. Бюаджи, А. В. Цудик, А. А. Свиноренко*

## РЕЛЯТИВИСТСКИЙ РАСЧЕТ ПАРАМЕТРОВ РИДБЕРГОВСКИХ АВТОИОНИЗАЦИОННЫХ СОСТОЯНИЙ В СПЕКТРЕ БАРИЯ

### Резюме

Комбинированный релятивистский энергетический подход и релятивистская многочастичная теория возмущений с дирак-кон-шэмовским одночастичным нулевым приближением используются для вычисления энергий ридберговских автоионизационных состояний  $4f_{5/2,7/2}n^{\prime}f$   $J=6,5,4$ , возбуждаемых из начального состояния  $5d_{3/2}15f$ ,  $J=5$  в спектре атома бария. Проведено сравнение с имеющимися теоретическими и экспериментальными (скопированными) данными. Важный момент связан с аккуратным учетом вкладов сложных многочастичных обменных корреляционных (поляризационных) эффектов и с использованием оптимизированного одноквазичастичного представления в нулевом приближении релятивистской многочастичной теории возмущений, что существенно определяет физически разумное согласие между теорией и точным экспериментом.

**Ключевые слова:** релятивистская теория, ридберговские автоионизационные состояния, барий

*Є. В. Терновський, В. В. Буяджи, А. В. Цудік, А. А. Свинаренко*

## **РЕЛЯТИВІСТСЬКИЙ РОЗРАХУНОК ПАРАМЕТРІВ РІДБЕРГІВСЬКИХ АВТОІОНІЗАЦІЙНИХ СТАНІВ В СПЕКТРІ БАРІЯ**

### **Резюме**

Комбінований релятивістський енергетичний підхід і релятивістська багаточастинкова теорія збурень з дірак-кон-шемівським одночастинковим наближенням нульового порядку використовуються для енергій рідбергівських автоіонізаційних станів  $4f_{5/2,7/2}n^{\prime}f$   $J=6,5,4$ , збуджених з початкового стану  $5d_{3/2}15f$ ,  $J=5$  в спектрі атома барію. Проведено порівняння з наявними теоретичними і експериментальними (скопійованими) даними. Важливий момент пов'язаний з акуратним урахуванням вкладів складних багаточасткових обмінних кореляційних (поляризаційних) ефектів із використанням оптимізованого одноквазічастічного уявлення в нульовому наближенні релятивістської багаточастинкової теорії збурень, що істотно визначає фізично розумне згоду між теорією і точним експериментом..

**Ключові слова:** релятивістська теорія, рідбергівські автоіонізаційні стани, барій

*A. V. Glushkov, A. V. Tsudik, D. A. Novak, O. V. Dubrovsky*

<sup>1</sup>Odessa State Environmental University, L'vovskaya str.15, Odessa-16, 65016, Ukraine  
E-mail: glushkovav@gmail.com

## **CHAOTIC DYNAMICS OF RELATIVISTIC BACKWARD-WAVE TUBE WITH ACCOUNTING FOR SPACE CHARGE FIELD AND DISSIPATION EFFECTS: NEW EFFECTS**

We have performed an advanced modelling nonlinear dynamics elements for relativistic backward-wave tube (RBWT) with accounting for dissipation and space charge field effects etc. The temporal dependences of the normalized field amplitude (power) in a wide range of variation of the controlling parameters (electric length of an interaction space  $N$ , bifurcation parameter  $L$  and relativistic factor  $\gamma_0$ ) are computed. The dynamic and topological invariants of the RBWT dynamics in auto-modulation and chaotic regimes such as correlation dimensions values, embedding, Kaplan-York dimensions, Lyapunov's exponents, Kolmogorov entropy etc are calculated. It has been discovered the "beak" effect on the plane of parameters: bifurcation Piers-like parameter  $L$  – relativistic factor  $\gamma_0$ .

### **1. Introduction**

Powerful generators of chaotic oscillations of microwave range of interest for radar, plasma heating in fusion devices, modern systems of information transmission using dynamic chaos and other applications. Among the most studied of vacuum electronic devices with complex dynamics are backward-wave tubes (BWT), for which the possibility of generating chaotic oscillations has been theoretically and experimentally found [1-12]. The BWT is an electronic device for generating electromagnetic vibrations of the superhigh frequencies range. Authors [7] formally considered the possible chaos scenario in a single relativistic BWT. Authors [4,6] have studied dynamics of a non-relativistic BWT, in particular, phase portraits, statistical quantifiers for a weak chaos arising via period-doubling cascade of self-modulation and the same characteristics of two non-relativistic backward-wave tubes. The authors of [4,6] have solved the equations of nonstationary nonlinear theory for the O-type BWT without account of the spatial charge, relativistic effects, energy losses etc. It has been shown that the finite-dimension strange attractor is responsible for chaotic regimes in

the BWT. The multiple studies [1-12], increasing the beam current in the system implemented complex pattern of alternation of regular and chaotic regimes of generation, completes the transition to a highly irregular wideband chaotic oscillations with sufficiently uniform continuous spectrum.

In this work we have performed an advanced modelling emission spectrum and nonlinear dynamics elements for relativistic backward-wave tube (RBWT) with accounting for dissipation and space charge effects etc. The temporal dependences of the normalized field amplitude (power) in a wide range of variation of the controlling parameters (electric length of an interaction space  $N$ , bifurcation parameter  $L$  and relativistic factor  $\gamma_0$ ) are computed. The dynamic and topological invariants of the RBWT dynamics in automodulation and chaotic regimes such as correlation dimensions values, embedding, Kaplan-York dimensions, Lyapunov's exponents, Kolmogorov entropy etc are calculated. WE discovered discovered the «beak» effect on the plane  $L - \gamma_0$ .

## 2. Relativistic model and some results

As the key ideas of our technique for nonlinear analysis of chaotic systems have been in details presented in refs. [13-28], here we are limited only by a short representation. We use the standard non-stationary theory [3-7], however, despite the above cited papers we take into account a number of effects, namely, influence of space charge, dissipation, the waves reflections at the ends of the system and others (a modification of model of Refs. [12,13]).

The relativistic dynamics is described system of equations for unidimensional relativistic electron phase  $\theta(\zeta, \tau, \theta_0)$  (which moves in the interaction space with phase  $\theta_0$  ( $\theta_0 \in [0; 2\pi]$ ) and has a coordinate  $\zeta$  at time moment  $\tau$ ) and field unidimensional complex amplitude

$$\begin{aligned} \partial^2 \theta / \partial \zeta^2 &= -L^2 \gamma_0^3 \left[ \left( 1 + \frac{1}{2\pi N} \partial \theta / \partial \zeta \right)^2 - \beta_0^2 \right]^{3/2} \\ \text{Re}[F \exp(i\theta) + \frac{4QC}{ik} \sum_{k=1}^M I_k \exp(ik\theta)] \\ \partial F / \partial \tau - \partial F / \partial \zeta + dF &= -L\tilde{I}, \\ I_k &= -\frac{1}{\pi} \int_0^{2\pi} e^{-ik\theta} d\theta_0 \end{aligned} \quad (1)$$

with the corresponding boundary and initial conditions. The dynamical system studied has several controlling parameters which are characteristic for distributed relativistic electron-waved self-vibrational systems: i) electric length of an interaction space  $N$ ; ii) bifurcation parameter  $L = 2\pi CN / \gamma_0$  (here  $C$ - is the known Piers parameter) ; iii) relativistic factor, which is determined as:

(2)

As input parameters there were taken following initial values: relativistic factor  $\gamma_0=1.5$  (further we will increase  $\gamma_0$  in 2 and 4 times), electrical length of the interaction space  $N = k_0 l$  ( $\pi = 10$ , electrons speed  $v_0=0.75c$ ,  $v_{ip}=0.25c$ , dissipation parameter  $D = 5\text{Db}$ , starting reflection parameters:  $s = 0.5$ ,  $\rho=0.7$ ,  $0 < \theta_0 < 2\pi$  . A choice

of  $\varphi$  due to the fact that the dependence upon it is periodic. The influence of reflections leads to the fact that bifurcational parameter  $L$  begins to be dependent on the phase  $\varphi$  of the reflection parameter (see discussion regarding it in [7,8]).

The basic idea of the construction of our approach to prediction of chaotic properties of complex systems is in the use of the traditional concept of a compact geometric att (CGA) in which evolves the measurement data, plus the neural networks (NNW) algorithm implementation [10-16]. Let us consider some scalar measurements  $s(n) = s(t_0 + n\Delta t) = s(n)$ , where  $t_0$  is the start time,  $\Delta t$  is the time step, and  $n$  is the number of the measurements. The main task is to reconstruct phase space using as well as possible information contained in  $s(n)$ . To do it, the method of using time-delay coordinates by Packard et al [17] can be used. The direct using lagged variables  $s(n+\tau)$  (here  $\tau$  is some integer to be defined) results in a coordinate system where a structure of orbits in phase space can be captured. A set of time lags is used to create a vector in  $d$  dimensions,  $\mathbf{y}(n) = [s(n), s(n + \tau), s(n + 2\tau), \dots, s(n + (d-1)\tau)]$ , the required coordinates are provided. Here the dimension  $d$  is the embedding dimension,  $d_E$ . To determine the proper time lag at the beginning one should use the known method of the linear autocorrelation function (ACF)  $C_L(\delta)$  and look for that time lag where  $C_L(\delta)$  first passes through 0 [4]. The alternative additional approach is provided by the average mutual information (AMI) method as an approach with so called nonlinear concept of independence. The further next step is to determine the embedding dimension,  $d_E$ , and correspondingly to reconstruct a Euclidean space  $R^d$  large enough so that the set of points  $d_A$  can be unfolded without ambiguity. The dimension,  $d_E$ , must be greater, or at least equal, than a dimension of attractor,  $d_A$ , i.e.  $d_E > d_A$ . To reconstruct the attractor dimension and to study the signatures of chaos in a time series, one could use such methods as the correlation integral algorithm (CIA) by Grassberger and Procaccia [21] or the false nearest neighbours (FNN) method by Kennel et al [18]. The principal question of

studying any complex chaotic system is to build the corresponding prediction model and define how predictable is a chaotic system. The new element of our approach is using the NNW algorithm in forecasting nonlinear dynamics of chaotic systems [9,10]. In terms of the neuro-informatics and neural networks theory the process of modelling the evolution of the system can be generalized to describe some evolutionary dynamic neuro-equations. Imitating the further evolution of a system within NNW simulation with the corresponding elements of the self-study, self-adaptation, etc., it becomes possible to significantly improve the prediction of its evolutionary dynamics. The fundamental parameters to be computed are the Kolmogorov entropy (and correspondingly the predictability measure as it can be estimated by the Kolmogorov entropy), the Lyapunov's exponents (LE), the Kaplan-Yorke dimension (KYD) etc. The LE are usually defined as asymptotic average rates and they are related to the eigenvalues of the linearized dynamics across the attractor. Naturally, the knowledge of the whole LE allows to determine other important invariants such as the Kolmogorov entropy and the attractor's dimension. The Kolmogorov entropy is determined by the sum of the positive LE. The estimate of the dimension of the attractor is provided by the Kaplan and Yorke conjecture

$$\sum_{j=1}^{\infty} \lambda_j^+, \text{ where } j \text{ is such that } \sum_{j=1}^j \lambda_j^+ > 0$$

and  $\sum_{j=1}^j \lambda_j^+ < 0$ , and the LE are taken in descending order. In Figure 1 we present the flowchart of the our combined chaos-geometric and NNW computational approach to nonlinear analysis and prediction of dynamics of any complex system [10-30].

In figure 2 we list the data on the temporal dependence of normalized field amplitude  $F(\alpha \delta) = \tilde{E} / (2\hat{a}_0 UC^2)$  (our data subject dissipation, the influence of space charge, the effect of reflections waves) at the values of the bifurcation parameter  $L$ : (a) – 3.5, (b) – 3.9 (other parameters:  $\gamma_0=1.5$ ,  $\omega=10$ ,  $s=0.5$ ,  $\rho=0.7$ ,  $\theta=1.3\pi$ ).

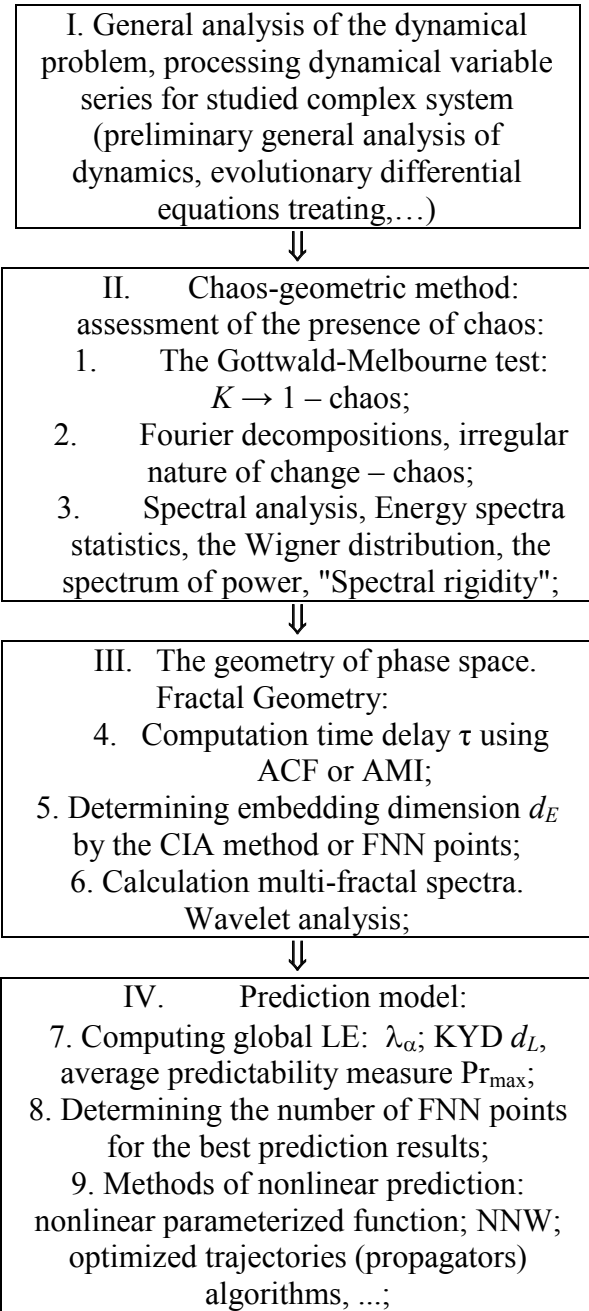


**Figure 1. Flowchart of the combined chaos-geometric approach and NNW to nonlinear analysis and prediction of chaotic dynamics of the complex systems (devices)**

Figures 1a,b are corresponding to the regimes of periodical automodulation (a) and hyper chaotic regime (b). It is worth to note that our results obtained without accounting for the reflection effect are very well correlated with the data by Ryskin-Titov in Ref. [7], where it has been in details studied the RBWT dynamics with.

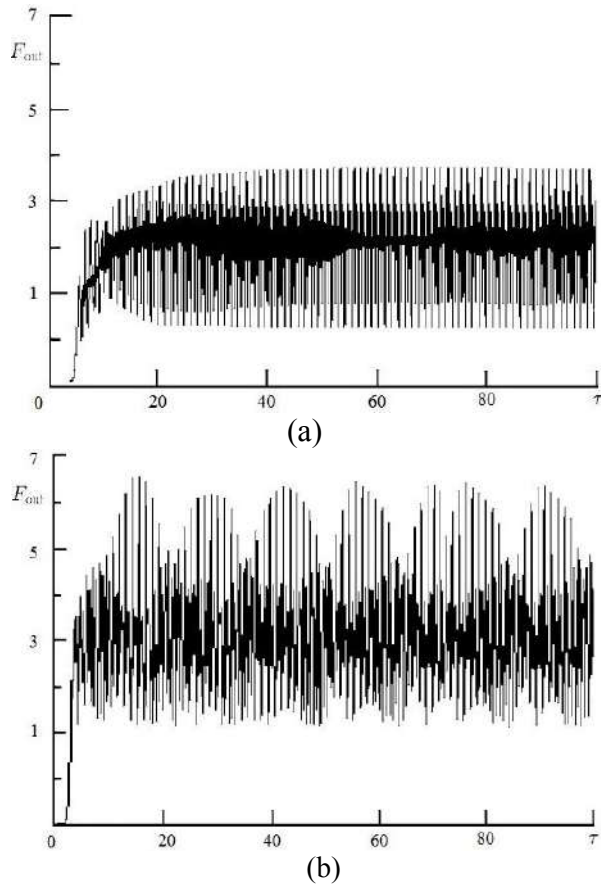


**Figure 2.** Data on the time dependence of normalized field amplitude  $F(\zeta, \tau)$  (our data with accounting dissipation, the influence of space charge and an effect of wave reflections) at the values of the bifurcation parameter  $L$ : (a) 3.0 (b) 4.0 (other parameters:  $\gamma_0=1.5$ ,  $10$ ,  $s=0.5$ ,  $\rho=0.7$ ,  $=1.3\pi$ ).

In table 1 we list our data on the correlation dimension  $d_2$ , embedding dimension, determined on the basis of false nearest neighbours algorithm ( $d_N$ ) with percentage of false neighbours (%). calculated for different values of lag  $\tau$  (data on fig1b, regime of a chaos).

In Table 2 we list our computing data on the Lyapunov exponents (LE), the dimension of the Kaplan-York attractor, the Kolmogorov entropy  $K_{entr}$ .

Table 1.

**Correlation dimension  $d_2$ , embedding dimension, determined on the basis of false nearest neighbours algorithm ( $d_N$ ) with percentage of false neighbours (%) calculated for different values of lag  $\tau$**

$\tau$	$d_2$	( $d_N$ )
60	8.2	10 (12)
8	6.5	8 (2.1)
10	6.5	8 (2.1)

Table 2.

**The Lyapunov exponents (LE), the dimension of the Kaplan-York attractor, the Kolmogorov entropy  $K_{entr}$ . (our data)**

$\lambda_1$	$\lambda_2$	$\lambda_3$	$\lambda_4$	$K$
0.508	0.196	-0.0001	-0.0003	0.704

For studied series there are the positive and negative LE values. The resulting KYD in both cases are very similar to the correlation dimension (calculated by the algorithm by Grassberger-Procachia). More important is the analysis of the RBWT nonlinear dynamics in the plane “relativistic factor – bifurcation parameter.”

The numerical solution has shown that under the realistic values of the dissipation parameter, the effect is reduced to the shift of the value of the bifurcation parameter  $L$  towards the increase. The most interesting, in our opinion, is the results of the analysis of the change of the nonlinear dynamics of the considered RBWT in the plane “relativistic factor - bifurcation parameter”. In this aspect, in fact, the three parametric nonlinear dynamics of the RBWT are fundamentally different from the dynamics of processes in the non-relativistic BWT. In Figure 3 we refer to our calculated diagram which quantitatively shows the limits of automodulation (line I) on the plane of parameters:  $L-\gamma_0$ . Note that line II limits the region where the particle rotation takes place, that is, the used theoretical model (1) works. A characteristic feature

of Figure 3 is the presence of the “beak” effect, which, depending on the relativistic factor, goes far into the domain of automodulation.

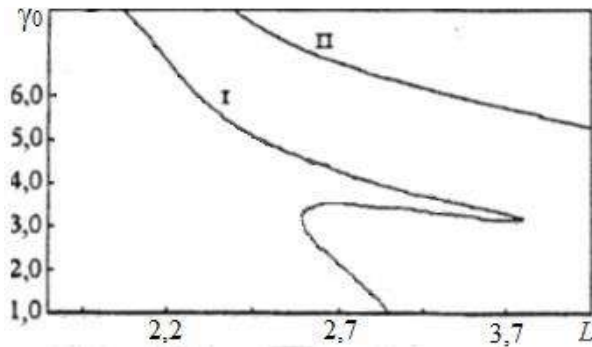


Figure 3. The boundaries of automodulation (line I) on the plane of parameters:  $L-g_0$ .

### 3. Conclusions

In this work we have performed an advanced modelling and for the first time forecasting an emission spectrum and nonlinear dynamics elements for relativistic backward-wave tube (RBWT) with accounting for dissipation and space charge effects etc. The temporal dependences of the normalized field amplitude (power) in a wide range of variation of the controlling parameters (electric length of an interaction space  $N$ , bifurcation parameter  $L$  and relativistic factor  $\gamma_0$ ) are computed. The dynamic and topological invariants of the RBWT dynamics in auto-modulation and chaotic regimes such as correlation dimensions values, embedding, Kaplan-York dimensions, Lyapunov's exponents, Kolmogorov entropy etc are calculated. diagram which quantitatively shows the limits of self-modulation (line I) on the plane of parameters:  $L-\gamma_0$ . is calculated. It has been discovered the “beak” effect (on the plane of parameters  $L, \gamma_0$ ), which, depending on the relativistic factor, goes far into the domain of automodulation for the RBWT studied.

### References

1. Glushkov, A.V.; Prepelitsa, G.P.; Svinarenko, A.A.; Zaichko, P.A. Studying interaction dynamics of the nonlinear vibrational systems within non-linear prediction method (application to quantum autogenerators) *In Dynamical Systems Theory*; Awrejcewicz, J., Kazmierczak, M., Olejnik, P., Mrozowski, J., Eds.; Wyd. Politech. Łódź.: Łódź, **2013**; Vol T1, pp 467-477.
2. Ignatenko, A.V.; Buyadzhi, A.; Buyadzhi, V.; Kuznetsova, A.; Mashkantsev, A.; Ternovsky, E. Nonlinear chaotic dynamics of quantum systems: molecules in an electromagnetic field// *Adv. Quant. Chem.* **2018**, 78 doi.org/10.1016/bs.aiq.2018.06.006.
3. Ginsburg, H. S.; Kuznetsov, S.P.; Fedoseyev, T.N. Theory of transients in relativistic BWO. *Izv. Vuzov. Ser. Radiophys.* **1978**, 21, 1037-1052.
4. Ginzburg, N.S.; Zaitsev, N.A.; Ilyakov, E.; Kulagin, V.I.; Novozhilov, Yu. Rosenthal P., Sergeev V., Chaotic generation in backward wave tube of the megawatt power level. *Journ. of Techn.Phys.* **2001**, 71, 73-80.
5. Glushkov, A.V.; Buyadzhi, V.V.; Ternovsky V.B. Geometry of Chaos: Consistent combined approach to treating of chaotic self-oscillations in backward-wave tube. *Proc. Intern. Geometry Center.* **2013**, 6(2), 6-12.
6. Levush, B.; Antonsen, T.M.; Bromborsky, A.; Lou, W.R.; Carmel, Y. Theory of relativistic backward wave oscillator with end reflections. *IEEE Trans. on Plasma Sci.* **1992**, 20, 263-280.
7. Ryskin, N.M.; Titov, V.N. Self-modulation and chaotic regimes of generation in a relativistic backward-wave oscillator with end reflections. *Radiophys. and Quant.Electr.* **2001**, 44, 793-806.
8. Glushkov, A.V.; Khetselius, O.Yu.; Svinarenko, A.A.; Prepelitsa, G.P. Energy approach to atoms in a laser field and quantum dynamics with laser pulses of different shape. *In Coherence and Ultrashort Pulsed Laser Emission*. Duarte, F.J., Ed.; InTech:

- Rijeka, **2010**, 159-186.
9. Levush, B.; Antonsen, T.; Bromborsky, A.; Lou, W. Relativistic backward wave oscillator: theory and experiment. *Phys.Fluid.* **1992**, *B4*, 2293-2299.
  10. Glushkov, A.V. *Methods of a Chaos Theory*. OSENU: Odessa, **2012**.
  11. Glushkov, A.V.; Khetselius, O.Yu.; Brusentseva, S.V.; Zaichko, P.A.; Ternovsky, V.B. Studying interaction dynamics of chaotic systems within a non-linear prediction method: Application to neurophysiology *In Advances in Neural Networks, Fuzzy Systems and Artificial Intelligence, Series: Recent Advances in Computer Engineering*; Balicki, J., Ed.; WSEAS Press: Gdansk, **2014**; Vol 21, pp 69-75.
  12. Khetselius, O.Yu. Forecasting evolutionary dynamics of chaotic systems using advanced non-linear prediction method *In Dynamical Systems Applications*; Awrejcewicz, J., Kazmierczak, M., Olejnik, P., Mrozowski, J., Eds.; Wyd. Politech. Łódź.: Łódź, **2013**; Vol T2, pp 145-152..
  13. Glushkov, A.V.; Malinovskaya, S.V.; Gurnitskaya, E.P.; Khetselius, O.Yu.; Dubrovskaya, Yu.V. Consistent quantum theory of recoil induced excitation and ionization in atoms during capture of neutron. *J. Phys.: Conf. Ser.* **2006**, *35*, 425-430.
  14. Khetselius, O.Yu. *Hyperfine structure of atomic spectra*. Astroprint: Odessa, **2008**.
  15. Glushkov, A.V.; Prepelitsa, G.P.; Svinarenko, A.A. ; Zaichko, P.A. Studying interaction dynamics of the non-linear vibrational systems within non-linear prediction method (application to quantum autogenerators) *In Dynamical Systems Theory*; Awrejcewicz, J., Kazmierczak, M., Olejnik, P., Mrozowski, J., Eds.; Wyd. Politech. Łódź.: Łódź, **2013**; Vol T1, pp 467-477.
  16. Abarbanel, H.; Brown, R.; Sidorowich, J; Tsimring, L. The analysis of observed chaotic data in physical systems. *Rev. Mod. Phys.* **1993**, *65*, 1331- 1392.
  17. Packard, N.; Crutchfield, J; Farmer, J.; Shaw, R. Geometry from a time series *Phys. Rev. Lett.* **1988**, *45*, 712-716.
  18. Kennel, M.; Brown, R.; Abarbanel, H. Determining embedding dimension for phase-space reconstruction using a geometrical construction. *Phys. Rev. A.* **1992**, *45*, 3403-3412.
  19. Packard N., Crutchfield J., Farmer J., Shaw R., Geometry from a time series//Phys Rev Lett.-1988.-Vol.45.-P.712–716.
  20. Gallager, R. *Information theory and reliable communication*. Wiley: N.-Y., **1986**.
  21. Grassberger, P. ; Procaccia, I. Measuring the strangeness of strange attractors. *Physica D.* **1983**, *9*, 189-208.
  22. Theiler, J.; Eubank, S.; Longtin, A.; Galdrikian, B.; Farmer, J. Testing for nonlinearity in time series: The method of surrogate data. *Physica D.* **1992**, *58*, 77-94.
  23. Glushkov, A.V.; Malinovskaya, S.V.; Loboda, A.V.; Shpinareva, I.M.; Gurnitskaya, E.P.; Korchevsky, D.A. Diagnostics of the collisionally pumped plasma and search of the optimal plasma parameters of x-ray lasing: calculation of electron-collision strengths and rate coefficients for Ne-like plasma. *J. Phys.: Conf. Ser.* **2005**, *11*, 188-198.
  24. Taken, F. Detecting strange attractors in turbulence. *Lecture notes in mathematics (Springer)* **1981**, *898*, 366–381.
  25. Glushkov, A.V.; Buyadzhi, V.V.; Ponomarenko, E.L. Geometry of Chaos: Advanced approach to treating chaotic dynamics in some nature systems// Proc. Intern. Geom. Center. 2014 *7(1)*,24-30.
  26. Sano, M.; Y. Sawada, Y. Measurement of the Lyapunov spectrum from cha-

- otic time series. *Phys Rev.Lett.* **1995**, 55, 1082-1085
27. Glushkov, A.V.; Malinovskaya S.V. Co-operative laser nuclear processes: border lines effects *In New Projects and New Lines of Research in Nuclear Physics*. Fazio, G., Hanappe, F., Eds.; World Scientific: Singapore, **2003**, 242-250.
28. Glushkov, A.; Khetselius, O.; Svinarenko, A.; Buyadzhi, V. *Spectroscopy of autoionization states of heavy atoms and multiply charged ions*. Odessa: TEC, **2015**.
29. Glushkov, A.V.; Malinovskaya, S.V.; Prepelitsa, G.P.; Ignatenko, V. Manifestation of the new laser-electron nuclear spectral effects in the thermalized plasma: QED theory of co-operative laser-electron-nuclear processes. *J. Phys.: Conf. Ser.* **2005**, 11, 199-206.
30. Prepelitsa, G.; Glushkov, A.V.; Lepikh, Ya.; Buyadzhi, V.; Ternovsky, V.; Zaichko, P. Chaotic dynamics of non-linear processes in atomic and molecular systems in electromagnetic field and semiconductor and fiber laser devices: new approaches, uniformity and charm of chaos. *Sensor Electr. and Microsyst. Techn.* **2014**, 11, 43-57.
- This article has been received in August 2018

PACS 42.55.-f

*A. V. Glushkov, A. V. Tsudik, D. A. Novak, O. V. Dubrovsky*

## **CHAOTIC DYNAMICS OF RELATIVISTIC BACKWARD-WAVE TUBE WITH ACCOUNTING FOR SPACE CHARGE FIELD AND DISSIPATION EFFECTS: NEW EFFECTS**

### **Summary.**

We have performed an advanced modelling and for the first time forecasting an emission spectrum and nonlinear dynamics elements for relativistic backward-wave tube (RBWT) with accounting for dissipation and space charge effects etc. The temporal dependences of the normalized field amplitude (power) in a wide range of variation of the controlling parameters (electric length of an interaction space  $N$ , bifurcation parameter  $L$  and relativistic factor  $\gamma_0$ ) are computed. The dynamic and topological invariants of the RBWT dynamics in auto-modulation and chaotic regimes such as correlation dimensions values, embedding, Kaplan-York dimensions, Lyapunov's exponents, Kolmogorov entropy etc are calculated. It has been discovered the «beak» effect on the plane of parameters: bifurcation Piers-like parameter  $L$  – relativistic factor  $\gamma_0$ , which, depending on the relativistic factor, goes far into the domain of automodulation.

**Key words:** relativistic backward-wave tube, chaos, non-linear methods

PACS 42.55.-f

*А. В. Глушков, А. В. Цудик, Д. А. Новак, О. В. Дубровский*

## **ХАОТИЧЕСКАЯ ДИНАМИКА РЕЛЯТИВИСТСКОЙ ЛАМПЫ ОБРАТНОЙ ВОЛНЫ С УЧЕТОМ ВЛИЯНИЯ ПОЛЯ ПРОСТРАНСТВЕННОГО ЗАРЯДА И ДИССИПАЦИИ: НОВЫЕ ЭФФЕКТЫ**

### **Резюме.**

Представлены результаты моделирования элементов нелинейной динамики для релятивистской обратной волны (РЛОВ) с учетом эффектов диссипации и поля пространственного заряда и др. Временные зависимости нормированной амплитуды поля (мощности) вычислены в широком диапазоне вариаций управляющих параметров (электрическая длина пространства взаимодействия  $N$ , параметр бифуркации  $L$  и релятивистский фактор  $\gamma_0$ ). Рассчитаны динамические и топологические инварианты динамики РЛОВ в автомодуляционном и хаотичном режимах, в частности, значения корреляционной размерности, размерности вложения, Каплана-Йорка, показатели Ляпунова, энтропия Колмогорова и др. Обнаружен эффект «клюва» на плоскости параметров: бифуркационный параметр  $L$  - релятивистский фактор  $\gamma_0$ .

**Ключевые слова:** релятивистская лампы обратной волны, хаос, нелинейные методы

PACS 42.55.-f

*О. В. Глушков, А. В. Цудік, Д. А. Новак, О. В. Дубровський*

## **ХАОТИЧНА ДИНАМІКА РЕЛЯТИВІСТСЬКОЇ ЛАМПИ ЗВЕРНЕНОЇ ХВИЛІ З УРАХУВАННЯМ ВПЛИВУ ПОЛЯ ПРОСТОРИВОВОГО ЗАРЯДУ ТА ДИСПАЦІЇ: НОВІ ЕФЕКТИ**

### **Резюме.**

Представлені результати моделювання спектру випромінювання та елементів нелінійної динаміки для релятивістської зворотної хвилі (РЛЗХ) з урахуванням ефектів дисипації та поля просторового заряду тощо. Часові залежності нормированної амплітуди поля (потужності) обчислені в широкому діапазоні варіацій керуючих параметрів (електрична довжина простору взаємодії  $N$ , параметр біфуркації  $L$  і релятивістський фактор  $\gamma_0$ ). Розраховані динамічні та топологічні інваріанти динаміки РЛЗХ в автомодуляційному та хаотичному режимах, зокрема, значення кореляційної розмірності, розмірності вкладення, Каплана-Йорка, показники Ляпунова, ентропія Колмогорова тощо. Виявлено ефект «дзьоба» на площині параметрів: біфуркаційний параметр  $L$  - релятивістський фактор  $\gamma_0$ .

**Ключові слова:** релятивістська лампы зворотної хвилі, хаос, нелінійні методи

*L. M. Filevska*

Odessa I. I. Mechnikov National University, Dvorianskaya str., 2, Odessa 65082, Ukraine,  
lfilevska@gmail.com

## LUMINESCENCE OF NANOSCALE TIN DIOXIDE. REVIEW

The article presents a brief review of luminescence in nanoscale tin dioxide. The luminescence caused by its intrinsic defects, the luminescence associated with impurities, the mechanisms of luminescence in tin dioxide are considered. The results of research by various authors presented in this review show the promising use of tin dioxide in optoelectronics and LED technology.

### Introduction

Requirements for modern electronic display devices stimulate the search for new luminescent materials. Nanoscale forms of compounds that are not classical phosphors help in solving new electronics' problems. One of these compounds is tin dioxide. In recent years, studies of the luminescence of various nanoscale forms of pure and doped  $\text{SnO}_2$ , as well as composite compounds and heterojunctions using it, have been activated. This interest is due to the promising use of such materials as phosphors [1], in LED applications [2], in solid-state optical amplifiers and tunable lasers [3], etc. Thermoluminescence of tin dioxide doped by Europium [4] is used as a detection phenomenon for dosimetry purposes. Stannates of calcium, barium and strontium with a perovskite-like structure have attracted the attention of researchers to create IR phosphors as an alternative to expensive phosphors. [5].

Low-temperature luminescence of crystalline tin dioxide was described in 1979 [6]. In the ultraviolet spectrum region ( $\sim 350\text{-}355\text{ nm}$ ), the intrinsic luminescence band of  $\text{SnO}_2$  is located. In the visible range, at low temperatures, wide photoluminescence (PL) bands in the range of 2 and 2.5 eV [7, 8] are observed in bulk samples of tin dioxide, which are associated with electron transitions in the interstitial tin/oxygen vacancy. With increasing temperature, the intensity of such a PL decreases, the PL becomes almost invisible at room temperature. The PL

spectra of nanoscale samples of tin dioxide differ from the spectra of the bulk material, which was shown by a number of researchers [9]. Photoluminescence in nanoscale  $\text{SnO}_2$  is increasingly observed at higher temperatures [10-12].

A brief review of luminescence in nanoscale tin dioxide will be presented in this paper.

### Luminescence in nanoscale forms of tin dioxide

***Glow due to its intrinsic defects.*** The edge luminescence of tin dioxide nanoscale forms was recorded by researchers in the ultraviolet region of the spectrum. For example, in [13] it was observed in transparent conductive thin films at 4.18 eV ( $\sim 300\text{ nm}$ ), and in [14] - at 333 nm. The differences in values are explained by the difference in the sizes of the nanocrystallites that form the film – the smaller it is, the greater is the energy of the peak of the edge luminescence.

In addition to the main UV peak of its intrinsic luminescence, the researchers report a whole set of radiation peaks in the visible region. As a rule, researchers observe bands in the blue-violet and orange-red regions of the spectrum. For example, Meier and colleagues [9] observed a PL peak at a wavelength of 625 nm ( $E = 2\text{ eV}$ ) in  $\text{SnO}_x$  nanoparticles at liquid nitrogen temperature. Korean researchers [11] observed in thin films of  $\text{SnO}_2$  PL in the region of 2.5 eV, Bonu and colleagues [12] observed at 2.54 eV and 2.42 eV and about 1.96 eV in  $\text{SnO}_2$  nanoparticles. In

[15], photoluminescence measurements in thin  $\text{SnO}_2$  films at room temperature with excitation at 280 nm show two broad emission peaks (400 and 430 nm). In thin undoped tin dioxide films on silicon substrates in [3], a broad emission peak at 395 nm was observed. The behavior of the peak at 590 nm depending on the diameter of tin dioxide nanowires was investigated in [16]. In addition to the edge luminescence at 333 nm, the authors of [14] observed a band of 480 nm at 13 K in thin  $\text{SnO}_2$  films deposited by the MOCVD method on  $\alpha\text{-Al}_2\text{O}_3$  substrates. In [17], luminescence in the visible region (577 nm and 642 nm) of nanosized tin dioxide films was detected at room temperature. Violet (371-382) nm and blue (400-415 and 430-470 nm) luminescence bands in nanorods and tin dioxide nanocrystals were studied in [18].

#### *Luminescence associated with impurities.*

The luminescence was often observed by researchers in tin dioxide with various additives, as well as in complex compounds, ceramics and heterojunctions with its use. For example, [19] found a violet photoluminescence band of about  $\sim 404$  nm and weak red emission of about 700 nm in fluorine-doped films of tin dioxide deposited by spray pyrolysis on glass substrates. The  $\text{SnO}_2$  quantum dots doped by Mn obtained using the solution combustion synthesis show the emission of orange radiation at about 590 nm [20]. The effect of doping by Mn and Ce on the luminescence associated with oxygen vacancies (400 nm) was studied in [21]. The properties of the intense peak of ultraviolet luminescence about 392 nm observed in  $\text{SnO}_2\text{:Sb}$  films at room temperature were studied in detail [22]. The use of nanoscale tin dioxide as a doping luminescent material used to enhance radiation in conjunction with other additives in glass or other similar structures has been reported in the literature. In [23], strontium phosphate glasses were doped with  $\text{SnO}_2$  and  $\text{Gd}_2\text{O}_3$ , and they detected enhanced blue emission at 421 nm. The authors of [24] used tin dioxide nanocrystals to enhance the fluorescence of  $\text{Eu}^{3+}$  in  $\text{SiO}_2$  glass by more than 150 times. The luminescence of  $\text{SnO}_2$  was modified in [25] by doping with Cr.

The normalized emission spectra from [25] are shown in Fig. 1. In the doped Cr nanostructures, a new emission with a center of 1.5 eV was detected; Cr doping also contributes to the enhancement of luminescence associated with oxygen vacancies (1.94 eV).

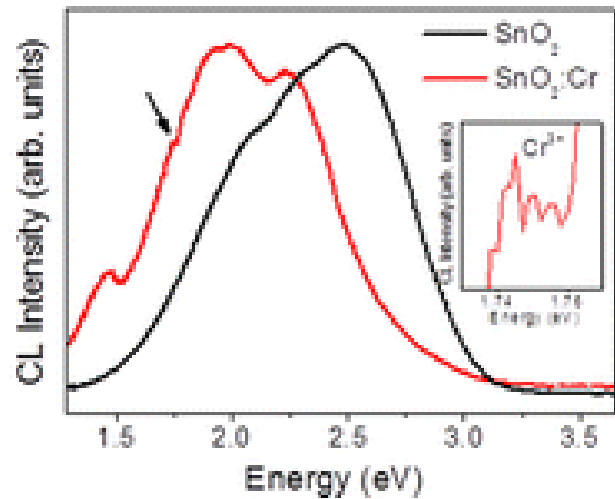


Fig 1. The normalized emission spectra  $\text{SnO}_2$  and  $\text{SnO}_2\text{:Cr}$ . [25]

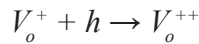
#### *Luminescence mechanisms in tin dioxide.*

The variety of radiation centers provides the possibility of widespread use of the material, but it causes difficulties in unambiguous associating of bands with specific defects and luminescence mechanisms.

The authors of [26] attributed the PL peak to approximately 3.307 eV (at 10 K) to the donor – acceptor transition in high quality tin oxide nanowires. The observed by Chen and colleagues phonon replicas of this band indicated a high crystallinity of the samples. With an increase of temperature, donor energy of 32 meV was observed and the nature of the luminescence changed to recombination of a free electron on an acceptor with a shift in the emission maximum towards lower energies. They also observed an emission band with a maximum of 3.355 eV, the nature of which the authors attributed to radiative recombination on neutral donors. The relative intensity of this band decreases faster and disappears completely at about 70 K, which is the characteristic behavior of excitons associ-

ated with neutral donors and their transition to a free state with increasing temperature. At room temperature (300 K) all PL bands form a broad emission band at 3.18 eV. Unfortunately, the authors did not associate the observed luminescence with specific defects — interstitial tin, dangling bonds, or oxygen vacancies.

Radiation in the region of about 400 nm has several explanations in the literature. Thus, in [27], a broad peak of about 396 nm ( $\sim 3.14$  eV) was reported in thin SnO<sub>2</sub> films, the origin of which was associated with the nanodimension of crystallites and defects in the film. The radiation at 400 nm [28] was explained by an electron transition to the levels of defects in the band gap, such as oxygen vacancies. At the same time, they considered three different charge states of oxygen vacancies in the oxide:  $V_o^0$ ,  $V_o^+$  and  $V_o^{++}$ . The model of visible radiation at 400 nm thin SnO<sub>2</sub> films included the formation of an exciton upon photoexcitation. After tunneling deep into the film previously trapped on the surface or on the center of  $V_o^+$  hole, recombination occurs with an electron in a deep trap with the formation of center  $V_o^{++}$ :



Thereafter, the visible emission at 400 nm can appear due to the recombination of a conduction band electron with the  $V_o^{++}$  center:



A decrease in the peak intensity of 400 nm with the annealing temperature increase is in favor of this mechanism, since it increases the size of the films' crystallites. As a result, the ratio of surface to volume, and the number of surface defects and the number of oxygen vacancies decreases as a result of their recombination with oxygen diffusing into the film volume. In another paper, these authors [21] successfully proposed to introduce Ce<sup>3+</sup> and Mn<sup>2+</sup> ions into particles of tin dioxide to increase the number of oxygen vacancies and to increase the luminescence intensity.

In [29], in the photoluminescence spectra of cubic SnO<sub>2</sub> nanocrystals, a double peak was observed in the violet region between 360 and 400 nm. The energy separation between the two

sub-peaks increased with the size of the nanocrystals. According to the authors, this is due to the edge recombination of the strip caused by different depths of oxygen vacancies. The conducted Density functional theory calculations showed that changes in the depth of oxygen vacancies lead to splitting of the peak of the valence band, which leads to the observed splitting and shift of the double peak[29].

In [30], the photoluminescence of the 417 nm band of a SnO<sub>2</sub> nanocrystalline powder obtained by direct chemical deposition was studied. The emission was associated with the recombination of electrons on oxygen vacancies with photoexcited holes of the valence band. With an increase in the annealing temperature, red mixing and a decrease in the luminescence intensity were observed, due to a decrease in the number of oxygen vacancies with an increase in the crystallite size from 9 to 43 nm. As we see, in this case, and in the case of 400 nm luminescence in thin nanoscale films of tin dioxide [28], the reason for the decrease in intensity is the same – a decrease in the number of oxygen vacancies in the samples.

Meier and colleagues [9] detected the PL peak of nanosized tin dioxide particles at liquid nitrogen temperature at a wavelength of 625 nm ( $E = 2$  eV). The radiation wavelength did not depend on the particle size, which indicates the group defect responsible for it, according to the authors, associated with oxygen vacancies. Interestingly, the PL intensity increased with an increase in the size of nanoparticles from 5 to 20 nm and as the samples approached stoichiometry from SnO<sub>1.5</sub> to SnO<sub>1.7</sub> (Fig. 2).

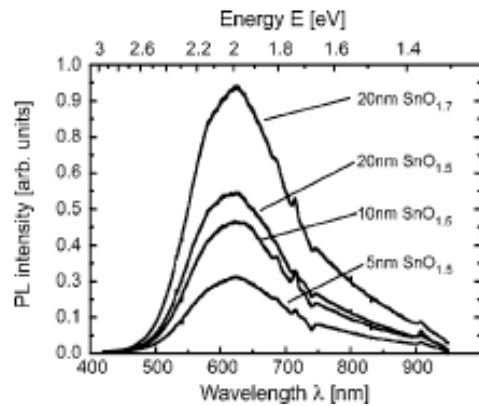
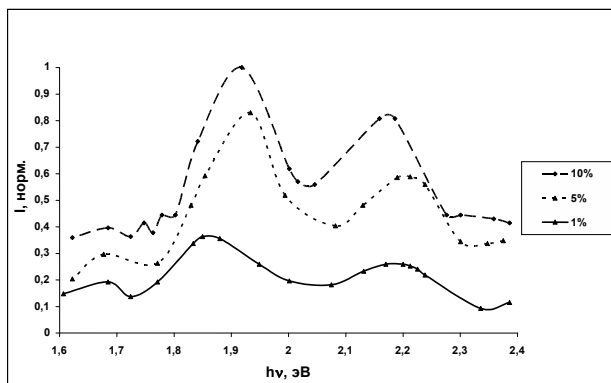


Fig. 2. The results of PL measurements for particles of various sizes and degrees of oxidation [9].

This fact correlated with the observation of a high density of electronic states inside the band gap from absorption measurements presented by the researchers there. The authors of this work associate this increase in intensity with a low rate of nonradiative recombination in  $\text{SnO}_{1.7}$  due to the low total density of defects. Obviously, ideally, in a defect-free  $\text{SnO}_2$  crystal, there are no defects providing PL. If the number of oxygen vacancies increases, the PL intensity will increase until nonradiative recombination processes dominate, as in the case of  $\text{SnO}_{1.5}$ .

The PL observed in nanostructured tin dioxide films obtained using polymers [31] was detected at room temperature. The authors also associated a peak at 647 nm (1.9 eV) with oxygen vacancies in samples whose PL results are shown in Fig. 3.



**Fig. 3.** The photoluminescence spectrum of  $\text{SnO}_2$  films with different concentrations of the precursor (0.05% PVA) at room temperature.

The difference in the energy values of the luminescence peaks in the films obtained by the authors [9] and [31] may be due to both different temperatures during the experiments and differences in the structure of the samples studied by different authors. The authors of [31] also made the assumption that the band groups 2.17-2.2 eV in the films correspond to the luminescence centers representing interstitial tin atoms or clusters of these atoms, since it is known from reference data [32] that the free singly charged Sn atom has the spectrum band is 579 nm (2.15 eV). The presence of metal clusters in  $\text{SnO}_2$  films was previously established by the authors of [33],

and their significant contribution to the electrical conductivity and adsorption activity of  $\text{SnO}_2$  layers was noted. In addition, it was shown in [34] that, at  $T = 723$  K, at least 3 substances exist in films of tin dioxide: Sn, SnO,  $\text{SnO}_2$ .

The authors from Korea [11] also associated their observed peaks in thin  $\text{SnO}_2$  films deposited by using CVD techniques in the 2.5-eV region with oxygen vacancies. Bonu and colleagues [12] also explained their observed luminescence at 2.54 eV and 2.42 eV with oxygen defects, namely in-plane and bridging ‘O’ vacancies. The authors observed a broad luminescence peak at about 1.96 eV in  $\text{SnO}_2$  nanoparticles, the authors associate with  $\text{OH}^-$  hydroxyl groups on the surface of the particles. In work [35], the wide luminescence bands observed in the region of 350–550 nm were associated with defect states on the surface of  $\text{SnO}_2$  nanoparticles. As we see, surface states play an important role in the luminescence of tin dioxide nanoforms.

Radiation at 421 nm was explained by the authors [23] as the Sn band. Moreover, the addition of  $\text{Gd}_2\text{O}_3$  to the strontium phosphate glasses doped with tin dioxide they studied increases the  $\text{Sn}^{2+}/\text{Sn}^{4+}$  ratio, which contributes to enhanced blue emission of  $\text{SnO}_2$ -such doped glasses. The band at 430 nm in [28] was explained by the contribution of interstitial tin.

Based on experimental results, Indian researchers [18] proposed a schematic model for various relaxation processes in  $\text{SnO}_2$  nanocrystals during photoexcitation (Fig.4). Visible radiation of  $\text{SnO}_2$  nanocrystals was attributed by the authors to the transition of an electron from a level close to the edge of the conduction band to a deeply trapped hole in the volume ( $V_o^{++}$ ) of  $\text{SnO}_2$  nanocrystals. It was also shown that surface defects are more noticeable in smaller nanocrystals than in nanorods. It was found that the PL emission time and the decay time strongly depend on the shape of the nanocrystals.

Studying the cathode luminescence of tin dioxide nanowires, [36] found that the CL bands centered at 1.90 and 2.20 eV belong to the surface oxygen vacancies coordinated with tin atoms at an angle of  $100^\circ$ , and the CL bands centered at 2.37 and 2.75 eV, are associated with

vacancies on the surface of oxygen, coordinated at 130°. The model of radiative transitions in the tin dioxide nanosized forms studied in [37] also takes into account the participation of coordinated oxygen vacancies in photoluminescence (Fig. 5).

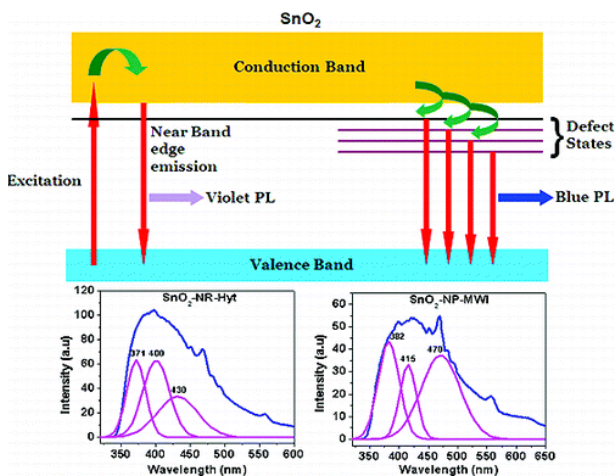


Fig. 4. A schematic model for various relaxation processes in SnO<sub>2</sub> nanocrystals upon photoexcitation [18].

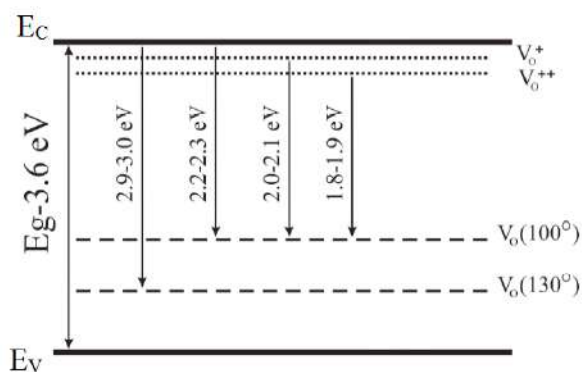


Fig. 5. Generalized scheme of levels and radiative transitions in photoluminescence of SnO<sub>2</sub> [37].

The results of research by various authors, presented in this review, allow us to consider tin dioxide not only one of the most popular and promising materials in sensorics, but also having wide applications in optoelectronics and LED technology.

## References

1. Arai T., Adachi S. Simple wet chemical synthesis and photoluminescence characterization of SnO<sub>2</sub>:Eu<sup>3+</sup> reddish-orange phosphor// *J. Luminescence*.-2014.- Vol.153, №9.- P.46-53
2. Yang Y., Li S., Liu F., Zhang N., Fang G. Bidirectional electroluminescence from p-SnO<sub>2</sub>/i-MgZnO/n-ZnO heterojunction light-emitting diodes// *J. Luminescence*.- 2017.-Vol.186,№6.- P.223-228
3. Bouzidi C., Elhouichet H., Moadhen A.. Yb<sup>3+</sup> effect on the spectroscopic properties of Er–Yb codoped SnO<sub>2</sub> thin films// *J. Luminescence*. - 2011. - Vol.131, Iss.12.- P.2630-2635.
4. Bajpai N., Khan S.A., Kher R.S., Bramhe N., Tiwari A. Thermoluminescence investigation of sol-gel derived and  $\gamma$ -irradiated SnO<sub>2</sub>:Eu<sup>3+</sup> nanoparticles// *J. Luminescence*.- 2014.- Vol.145, N1.- P. 940-943
5. Марыина У.А. Разработка технологии синтеза и исследование люминофоров на основе CaSnO<sub>3</sub>, BaSnO<sub>3</sub>, SrSnO<sub>3</sub>, активированных редкоземельными ионами. Дисс.... канд. техн. наук. Ставрополь. 2017
6. Агекян В.Т. Сложный спектр экситонно-примесных комплексов в дефектных кристаллах двуокиси олова. Письма в ЖЭТФ.-1979.- 29,№8.-С.475-479.
7. Рябцев С.В. Электрофизические и оптические свойства различных наночастиц оксида олова, Автореф. дисс. ... докт. физ.-мат. наук, Воронеж, 2011. 46 с.
8. Агекян В.Ф., Серов А.Ю., Филоффов Н.Г. Излучение света кристаллами двуокиси олова// *ФТП*.- 2014.-Т.48,№4.-С.458-461
9. Meier C., Luttjohann S., Kravets V. G., Nienhaus H., Lorke A., Ifeacho P., Wiggers H., Schulz Ch., Kennedy M. K. and Kruis F. E. Vibrational and defect states in SnO<sub>x</sub> nanoparticles// *J. of*

- Appl. Phys.-2006.- Vol.99.-113108.
10. Gu F., Wang Sh.F., Song Ch.F., Lü M.K., Qi Y.X., Zhou G.J., Xu D., Yuan D.R.. Synthesis and luminescence properties of SnO<sub>2</sub> nanoparticles// Chem. Phys. Lett.-2003.-Vol.372,Iss.3-4, P.451-454.
  11. Jeong J., Choi S. P. and Hong K. J., Song H. J., Park J. S.. Structural and Optical Properties of SnO<sub>2</sub> Thin Films Deposited by Using CVD Techniques// J. Korean Phys. Soc.-2006.-Vol.48,No.5.-P.960-963.
  12. Bonu V., Das A., Amirthapandian S., Dhara S., Tyagi A.K. Photoluminescence of oxygen vacancies and hydroxyl group surface functionalized SnO<sub>2</sub> nanoparticles// Phys. Chem. Chem. Phys.- 2015.- 17.-P. 9794-9801.
  13. Alhuthali A., El-Nahass M. M., Atta A. A., Abd El-Raheem M. M., Hassanien A. M. Study of topological morphology and optical properties of SnO<sub>2</sub> thin films deposited by RF sputtering technique// J. Luminescence.-2015.- Vol.158, No2.- P. 165-171.
  14. Zhu Z., Ma J., Luan C., Kong L., Q. Yu. Structure and photoluminescence properties of epitaxial SnO<sub>2</sub> films grown on  $\alpha$ -Al<sub>2</sub>O<sub>3</sub> (012) by MOCVD// J. Luminescence.-2011.- Vol.131,Iss.1.-P.88-91
  15. Gu F., Wang Sh.F., Song Ch.F., Lü M.K., Cheng X.F., Liu S.W., Zhou G.J., Xu D., Yuan D.R.. Luminescence of SnO<sub>2</sub> thin films prepared by spin-coating methods// J Cryst Growth.-2004.-Vol.262.-P. 182-185.
  16. Lee S.Y., Shin Y.H., Kim Y., Kim S., Ju S.. Emission characteristics of diameter controlled SnO<sub>2</sub> nanowires. J. Luminescence.- 2011.- Vol.131, Iss.12.-P. 2565-2568
  17. Grinevich V.S., Smyntyna V.A., Filivska L.M.. Photoluminescence of tin dioxide thin films obtained with the use of polymers// Photoelectron-ics.- 2005. -No 14, P. 42-44.
  18. Kar A., Kundu S., and Patra A. Surface Defect-Related Luminescence Properties of SnO<sub>2</sub> Nanorods and Nanoparticles// J. Phys. Chem. C.-2011.- Vol.115 (1).- P. 118-124.
  19. Shewale P.S., Sim K.U., Kim Y.-b., Kim J.H. Moholkar A.V., Uplane M.D. Structural and photoluminescence characterization of SnO<sub>2</sub>:F thin films deposited by advanced spray pyrolysis technique at low substrate temperature J. Luminescence.- 2013.- Vol.139,No7.-P. 113-118.
  20. Babu B., Kadam A. N., Rao G.T., Lee S.-W., J. Shim. Enhancement of visible-light-driven photoresponse of Mn-doped SnO<sub>2</sub> quantum dots obtained by rapid and energy efficient synthesis// J. Luminescence.- 2018.-Vol.195, No3.- P. 283-289.
  21. Gu F., Wang S.F., Lü M.K., Zhou G.J., Xu D., and Yuan D.R.. Photoluminescence Properties of SnO<sub>2</sub> Nanoparticles Synthesized by Sol-Gel Method// J. Phys.Chem. B.- 2004.- Vol.108(24).- P.8119-8123.
  22. Wang Y., Ma J., Ji F., Yu X., Ma H. Structural and photoluminescence characters of SnO<sub>2</sub>:Sb films deposited by RF magnetron sputtering// J. Luminescence.- 2005.-Vol.114, Iss 1.- P. 71-76.
  23. Tong Y., Yan Zh., Zeng H., Chen G. Enhanced blue emission of SnO<sub>2</sub> doped phosphate glasses by Gd<sub>2</sub>O<sub>3</sub> co-doping J. Luminescence.- 2014.- Vol.145, No1, P.438-442.
  24. Nogami M., Enomoto T., Hayakawa T. Enhanced fluorescence of Eu<sup>3+</sup> induced by energy transfer from nano-sized SnO<sub>2</sub> crystals in glass// J. Luminescence, 2002.-Vol. 97, Iss.3-4.-P. 147-152.
  25. García-Tecedor M., Maestre D., Cremades A., and Piqueras J.. Influence of Cr Doping on the Morphology and Luminescence of SnO<sub>2</sub> Nanostructures J.

- Phys. Chem. C.-2016.-Vol.120 (38).- P.22028–22034
26. Chen R., Xing G. Z., Gao J., Zhang Z., Wu T. and Sun H.D.. Characteristics of ultraviolet photoluminescence from high quality tin oxide nanowires// *Appl. Phys. Lett.*- 2009.-Vol.95.- 061908.
  27. Kim T.W., Lee D.U., Yoon Y.S., Microstructural, electrical, and optical properties of SnO<sub>2</sub> nanocrystalline thin films grown on InP (100) substrates for applications as gas sensor devices. *J. Appl. Phys.* 2000.-Vol.88.- P. 3759-3761.
  28. Gu F., Wang Sh.F., Song Ch.F., Lü M.K., Cheng X. F., Liu S.W., Zhou G.J., Xu D., Yuan D.R.. Luminescence of SnO<sub>2</sub> thin films prepared by spin-coating methods. *J Cryst. Growth.*-2004.-Vol.262.-P.182-185.
  29. Liu L.Z., Wu X.L., Xu J.Q., Li T. H., Shen J.C., and Chu P.K.. Oxygen-vacancy and depth-dependent violet double-peak photoluminescence from ultrathin cuboid SnO<sub>2</sub> nanocrystals// *Appl. Phys. Lett.*- 2012. Vol.100.- 121903.
  30. Nehru L. C., Swaminathan V., Sanjeeviraja C. Photoluminescence Studies on Nanocrystalline Tin Oxide Powder for Optoelectronic Devices, *American J Mater. Science.*- 2012.- Vol.2(2).- P.6-10.
  31. Filevskaya L.N., Smyntyna V.A., Grinevich V.S. Surface and optical properties of nano SnO<sub>2</sub> films for sensor electronics. *International Meeting EVROSENSORS XX*, September 2006 Goteborg, Sweden. – p.96-97.
  32. Зейдель А.Н., Прокофьев В.К., Райский С.М., Славный В.А., Шрейдер Е.Я. Таблицы спектральных линий. М., изд-во “Наука”.- 1977.- С. 679.
  33. Витер Р.В., Сминтына В.А., Евтушенко Н.Г., Филевская Л.Н., Курков В.В., Исследование адсорбционно-кинетических характеристик тонких плёнок SnO<sub>2</sub>. *Фотоэлектроника.* – 2002. – Вып. 11. – С.109-113.
  34. Ховив А.М., Логачева В.А., Новикова О.В.. Особенности оксидирования пленок олова в условиях пониженного и атмосферного давления кислорода при воздействии ИК-излучения. *ВЕСТНИК ВГУ. Серия: Химия. Биология. Фармация.*- 2004. – № 1. – С. – 101-106.
  35. Lin T, Wan N, Xu J, Xu L, Chen KJ. Size-dependent optical properties of SnO<sub>2</sub> nanoparticles prepared by soft chemical technique. *J Nanosci Nanotechnol.* – 2010. – Vol.10, No7. – P.4357-4362.
  36. Prades J.D., Arbiol J., Cirera A., Morante J.R., Avella M., Zanotti L., Comini E., Faglia G., Sberveglieri G. Defect study of SnO<sub>2</sub> nanostructures by cathodo-luminescence analysis: Application to nanowires. *Sens and Actuat B.*- 2007/- Vol.126.-P.6–12.
  37. Хадия Н.М.А. Получение и исследование оптических свойств нитевидных полупроводниковых оксидов SnO<sub>2</sub> и In<sub>2</sub>O<sub>3</sub> Автореф. дисс.... канд. физ.– мат. Наук. Воронеж.– 2011. – 16 стр.

This article has been received in September 2018

PACS 73.61.Le, 73.63.Bd

*L. M. Filevska*

## LUMINESCENCE OF NANOSCALE TIN DIOXIDE. REVIEW

### Summary

The article presents a brief review of luminescence in nanoscale tin dioxide. The luminescence caused by its own defects, the luminescence associated with impurities, the mechanisms of luminescence in tin dioxide are considered. The results of research by various authors presented in this review show the promising use of tin dioxide in optoelectronics and LED technology.

**Key words:** tin dioxide, nanoscale, luminescence.

PACS 73.61.Le, 73.63.Bd

*Л. М. Філевська*

## ЛЮМІНЕСЦЕНЦІЯ НАНОРОЗМІРНОГО ДІОКСИДУ ОЛОВА. ОГЛЯД

### Резюме

У статті подано короткий огляд люмінесценції в нанорозмірному діоксиді олова. Розглядається світіння, обумовлене його власними дефектами, люмінесценція, пов'язана з домішками, механізми люмінесценції в діоксиді олова. Результати досліджень різних авторів, представлені в цьому огляді, показують перспективність застосування двоокису олова для широке застосування в оптоелектроніці і світлодіодним техніці.

**Ключові слова:** діоксид олова, нанорозмір, люмінесценція

PACS 73.61.Le, 73.63.Bd

*Л. Н. Филевская*

## ЛЮМИНЕСЦЕНЦИЯ НАНОРАЗМЕРНОГО ДИОКСИДА ОЛОВА. ОБЗОР

### Резюме

В статье представлен краткий обзор люминесценции в наноразмерном диоксиде олова. Рассматривается свечение, обусловленное его собственными дефектами, люминесценция, связанная с примесями, механизмы люминесценции в диоксиде олова. Результаты исследований различных авторов, представленные в этом обзоре, показывают перспективность применения двуокиси олова в оптоэлектронике и светодиодной технике.

**Ключевые слова:** диоксид олова, наноразмер, люминесценция

*A. V. Ignatenko<sup>1</sup>, A. V. Glushkov<sup>1</sup>, Ya. I. Lepikh<sup>2</sup>, A. S. Kvasikova<sup>1</sup>*

<sup>1</sup>Odessa State Environmental University, 15, Lvovskaya str., Odessa, 65016

<sup>2</sup>I. I. Mechnikov's Odessa National University, Dvoryanskaya str., 2, Odessa, 65028

E-mail: ignatenkoav13@gmail.com

## PHOTOELECTRON SPECTROSCOPY OF DIATOMIC MOLECULES: OPTIMIZED GREEN'S FUNCTIONS AND DENSITY FUNCTIONAL APPROACH

We present the optimized version of the hybrid combined density functional theory (DFT) and the Green's-functions (GF) approach to quantitative treating the diatomic photoelectron spectra. The Fermi-liquid quasiparticle version of the density functional theory is used. The density of states, which describe the vibrational structure in photoelectron spectra, is defined with the use of combined DFT-GF approach and is well approximated by using only the first order coupling constants in the optimized one-quasiparticle approximation. Using the combined DFT-GF approach leads to significant simplification of the calculation and increasing an accuracy of theoretical prediction.

### Introduction

In this paper we present the optimized version of the hybrid combined density functional theory (DFT) and the Green's-functions (GF) approach to quantitative treating the diatomic photoelectron spectra.

The approach is based on the Green's function method (Cederbaum-Domske version) [11,12], Fermi-liquid DFT formalism [1-8] and use of the novel effective density functionals (see also [13-16]). The density of states is well approximated by using only the first order coupling constants in the one-particle approximation. It is important that the calculational procedure is significantly simplified with using the quasiparticle DFT formalism. Thus quite simple method becomes a powerful tool in interpreting the vibrational structure of photoelectron spectra for different molecular systems.

As usually (see details in refs. [1-12]), the quantity which contains the information about the ionization potentials (I.P.) and molecular vibrational structure due to quick ionization is the density of occupied states:

$$N_k(\epsilon) = (1/2\pi\hbar) \int dt e^{i\hbar^{-1}\epsilon t} \langle \Psi_0 | a_k^\dagger(0) a_k(t) | \Psi_0 \rangle, \quad (1)$$

where  $|\Psi_0\rangle$  is the exact ground state wave

function of the reference molecule and is an electron destruction operator, both in the Heisenberg picture. Usually in order to calculate the value (1) states for photon absorption one should express the Hamiltonian of the molecule in the second quantization formalism.

### 2. Theory: Density of states in one-body and many-body solution

As usually, introducing a field operator

$$\sum$$

with the

Hartree-Fock (HF) one-particle functions

$\phi_i$  ( $\epsilon_i$  are the one-particle HF energies and

$f$  denotes the set of orbitals occupied in the HF

ground state;  $R_0$  is the equilibrium geometry on

the HF level) and dimensionless normal coordi-

nates  $Q_s$  one can write the standard Hamiltonian

as follows [2,11]:

$$H = H_E + H_N + H_{EN}^{(1)} + H_{EN}^{(2)}, \quad (3)$$

$$H_E = \sum_i \epsilon_i(R_0) a_i^\dagger a_i + \frac{1}{2} \sum_{ijkl} V_{ijkl}(R_0) a_i^\dagger a_j^\dagger a_l a_k -$$

$$- \sum_{i,j} \sum_{k \in f} [V_{ikjk}(R_0) - V_{ikkj}(R_0)] a_i^\dagger a_j$$

$$H_N = \hbar \sum_{s=1}^M \omega_s (b_s^\dagger b_s + \frac{1}{2}),$$

$$\begin{aligned}
H_{EN}^{(1)} &= 2^{-1/2} \sum_{s=1}^M \left( \frac{\partial \epsilon_i}{\partial Q_s} \right)_0 (b_s + b'_s) [a_i' a_i - n_i] + \\
&+ \frac{1}{4} \sum_i \sum_{s,s'=1}^M \left( \frac{\partial^2 \epsilon_i}{\partial Q_s \partial Q_{s'}} \right)_0 (b_s + b'_s)(b_{s'} + b'_{s'}) [a_i' a_i \\
H_{EN}^{(2)} &= 2^{-3/2} \sum_{s=1}^M \sum_{s'=1}^M \left( \frac{\partial V_{ijkl}}{\partial Q_s} \right)_0 (b_s + b'_s) [\delta v_1 a_i' a_j' a_k' a_l' \\
&+ \delta v_2 a_i a_k a_i' a_j' + 2\delta v_3 a_i' a_k a_i a_j'] + \\
&+ \frac{1}{8} \sum_{s,s'=1}^M \left( \frac{\partial^2 V_{ijkl}}{\partial Q_s \partial Q_{s'}} \right)_0 (b_s + b'_s)(b_{s'} + b'_{s'}) \cdot \\
&[\delta v_1 a_i' a_j' a_k + \delta v_2 a_i a_k a_i' a_j' + 2\delta v_3 a_i' a_k a_i a_j']
\end{aligned}$$

with  $n_i=1$  (0),  $i \in f$  ( $i \notin f$ ),  $\delta \sigma_j=1$  (0),  $(ijkl) \in \sigma_j$  where the index set  $v_1$  means that at least  $i$  and  $j$  or  $i$  and  $k$  are unoccupied,  $v_2$  that at most one of the orbitals is unoccupied, and  $v_3$  that  $i$  and  $j$  or  $i$  and  $k$  are unoccupied. The  $\omega_i$  are the HF frequencies;  $a_i$ ,  $a_i'$  are destruction and creation operators for vibrational quanta as

$$\begin{aligned}
Q_s &= (1/\sqrt{2})(b_s + b'_s), \\
\partial/\partial Q_s &= (1/\sqrt{2})(b_s - b'_s).
\end{aligned} \quad (4)$$

The interpretation of the above Hamiltonian and an exact solution of the one-body HF problem is given in refs. [1,2,11,12]. The usual way is to define the HF-single-particle component of the Hamiltonian (4) is as in Refs. [11,12]. Correspondingly in the one-particle picture the density of occupied states is given by

$$N_k^0(\epsilon) = \frac{1}{2\pi\hbar} \int_{-\infty}^{\infty} dt e^{i\hbar^{-1}(\epsilon - \epsilon_k)t} \langle 0 | e^{\pm i\hbar^{-1}\tilde{H}_0 t} | 0 \rangle, \quad (5)$$

$$\begin{aligned}
\tilde{H}_0 &= \sum_{s=1}^M \hbar\omega_s b'_s b_s + \sum_{s=1}^M g_s^k (b_s + b'_s) + \\
&+ \sum_{s,s'=1}^M \gamma_s^k (b_s + b'_s)(b_{s'} + b'_{s'})
\end{aligned} \quad (6)$$

$$g_s^i = \pm \frac{1}{\sqrt{2}} \left( \frac{\partial \epsilon_i^0}{\partial Q_s} \right), \quad \gamma_s^i = \pm \frac{1}{4} \left( \frac{\partial^2 \epsilon_i^0}{\partial Q_s \partial Q_{s'}} \right). \quad (7)$$

In a diagrammatic method to get function  $G_k(\epsilon)$  one should calculate the GF  $G_k(\epsilon)$  first [1,2,11,12]:

$$G_k(\epsilon) = -i\hbar^{-1} \int_{-\infty}^{\infty} dt e^{i\hbar^{-1}\epsilon t} \langle \psi_0 | \hat{O} \{ a_k(t) a_k'(0) \} | \psi_0 \rangle \quad (8)$$

and the function  $G_k(\epsilon)$  can be found from the relation

$$\pi N_k(\epsilon) = a \ln G_k(\epsilon) - \hat{a} \eta, \quad a = -\text{sign} \epsilon. \quad (9)$$

Choosing the unperturbed Hamiltonian

to be  $H_0$  one could define the GF as follows:

$$\begin{aligned}
G_{kk'}^{\theta}(t) &= \pm \delta_{kk'} i \exp[-i\hbar^{-1}(\epsilon_k \mp \Delta\epsilon)t] \cdot \\
&\cdot \sum_n \left| \langle \hat{n}_k | U_k | 0 \rangle \right|^2 \exp(\pm i\hbar^{-1} \hat{n}_k \cdot \hat{\omega}_k t)
\end{aligned} \quad (10)$$

The direct method for calculation of  $N_k(\epsilon)$  as the imaginary part of the GF includes a definition of the vertical I.P. (V.I.P.s) of the reference molecule and then of  $N_k(\epsilon)$ . The zeros of the functions

$$D_k(\epsilon) = \epsilon - [\epsilon^p + \Sigma(\epsilon)]_k, \quad (11)$$

where  $(\epsilon^p + \Sigma)_k$  denotes the  $k$ -th eigenvalue of the diagonal matrix of the one-particle energies added to matrix of the self-energy part, are the negative V. I. P. 's for a given geometry. One can write [2,11,12]:

$$(V.I.P.)_k = -(\epsilon_k + F_k),$$

$$F_k = \Sigma_k (-(V.I.P.)_k) \approx \frac{1}{1 - \partial \Sigma_k(\epsilon_k) / \partial \epsilon} \Sigma_k(\epsilon_k) \quad (12)$$

Expanding the ionic energy  $\epsilon_k$  about the equilibrium geometry of the reference molecule in a power series of the normal coordinates of this molecule leads to a set of linear equations in the unknown normal coordinate shifts  $\delta Q_{s'}$  and new coupling constants are then:

$$g_1 = \pm (1/\sqrt{2}) [\partial(\epsilon_k + F_k) / \partial Q_{s'}]_0 \quad (13)$$

$$\gamma_{ll'} = \pm \left( \frac{1}{4} \right) \left[ \partial^2 (\epsilon_k + F_k) / \partial Q_l / \partial Q_{l'} \right]$$

The coupling constants  $\gamma_{ll'}$  and  $\rho_k$  are calculated by the well-known perturbation expansion of the self-energy part. In second order one obtains:

$$\sum_{\mathbf{k}}^{(2)}(\epsilon) = \sum_{\substack{i,j \\ s \neq F}} \frac{(V_{ksij} - V_{ksji})V_{ksij}}{\epsilon + \epsilon_s - \epsilon_i - \epsilon_j} + \sum_{\substack{i,j \\ s \neq F}} \frac{(V_{ksij} - V_{ksji})V_{ksij}}{\epsilon + \epsilon_s - \epsilon_i - \epsilon_j} \quad (14)$$

and the coupling constant  $g_p$  are written as [17]:

$$g_l \approx \pm \frac{1}{\sqrt{2}} \frac{\partial \epsilon_k}{\partial Q_l} \frac{1 + q_k (\partial / \partial \epsilon) \sum_{\mathbf{k}} [-(V.I.P.)_{\mathbf{k}}]}{1 - (\partial / \partial \epsilon) \sum_{\mathbf{k}} [-(V.I.P.)_{\mathbf{k}}]} \quad (15)$$

The pole strength of the corresponding GF:

$$\rho_k = \left\{ 1 - \frac{\partial}{\partial \epsilon} \sum_{\mathbf{k}} [-(V.I.P.)_{\mathbf{k}}] \right\}^{-1}; 1 \geq \rho_k \geq 0, \\ g_l \approx g_l^0 [\rho_k + q_k (\rho_k - 1)] \pm \frac{\partial \epsilon_k}{\partial Q_l} \quad (16)$$

Below we give another the definition of the pole strength corresponding to V. I. P.'s.

### 3. Fermi-liquid quasiparticle density functional theory

The quasiparticle Fermi-liquid version of the DFT [1-3,8,17] is used to determine the coupling constants etc. The master equations can be obtained on the basis of variational principle, if we start from a Lagrangian of a molecule  $L_q$ . It should be defined as a functional of quasiparticle densities:

$$\Sigma \\ \sum \nabla \\ \rho_2(r) \sum_n [ * * ] \quad (17)$$

The densities  $v_0$  and  $v_1$  are similar to the HF electron density and kinetical energy density correspondingly; the density  $v_2$  has no an analog in the HF or DFT theory and appears as result of account for the energy dependence of the mass

operator  $\Sigma$ . A Lagrangian  $L_q$  can be written as a sum of a free Lagrangian and Lagrangian of interaction:  $L_q = L_q^0 + L_q^{int}$ , where the interaction Lagrangian is defined in the form, which is characteristic for a standard DFT (as a sum of the Coulomb and exchange-correlation terms), however, it takes into account for the energy dependence of a mass operator  $\Sigma$  :

$$L_q^{int} = L_K - \frac{1}{2} \sum_{i,k=0}^2 \int \beta_k F(r_1, r_2) v_i(r_1) v_k(r_2) d\mathbf{r}_1 d\mathbf{r}_2 \quad (18)$$

where F is an effective potential of the exchange-correlation interaction. The constants  $\beta_{ik}$  are defined in Ref. [8,17]. The single used constant  $\beta_{02}$  can be calculated by analytical way, but it is very useful to remember its connection with a spectroscopic factor  $F_{sp}$  of the system [18]:

$$F_{sp} = \left\{ 1 - \frac{\partial}{\partial \epsilon} \sum_{\mathbf{k}} [-(V.I.P.)_{\mathbf{k}}] \right\} \quad (19)$$

The terms  $\partial \Sigma / \partial \epsilon$  and  $\Sigma$  is directly linked [2,17]. In the terms of the Green function method expression (7) is in fact corresponding to the pole strength of the Green's function [2]. The new element of an approach is connected with using the DFT correlation functional of the Gunnarsson-Lundqvist, Lee-Yang-Parr (look details in ref. [13-16]).

### 3. Results and conclusions

In further calculation as potential  $V_{\mathcal{K}}$  we use the exchange-correlation pseudo-potential which contains the correlation (Gunnarsson-Lundqvist) potential and relativistic exchanger Kohn-Sham one [40-42]. As example in table 1 we present our calculational data for spectroscopic factors of some atoms together with available experimental data and results, obtained in the Hartree-Fock theory plus random phase approximation. As an object of studying we choose the diatomic molecule of  $N_2$  for application of the combined Green's function method and quasiparticle DFT approach. The nitrogen molecule has been naturally discussed in many papers. The valence V. I. P. of  $N_2$  have been calculated [1,13,14,24] by the method of Green's functions and therefore the pole strengths  $p_k$  are known and the mean values

$q_k$  can be estimated. It should be reminded that the  $N_2$  molecule is the classical example where the known Koopmans' theorem (KT) even fails in reproducing the sequence of the V. I. P. 's in the PE spectrum. From the HF calculation of Cade *et al.*[24] one finds that including reorganization the V. I. P. 's assigned by and improve while for  $\pi$  V. I. P. the good agreement between the Koopmans value and the experimental one is lost, leading to the same sequence as given by Koopmans' theorem. In Table 1 the experimental V. I. P. 's (a), the one-particle HF energies (b), the V. I. P. 's calculated by Koopmans' theorem plus the contribution of reorganization (c), the V. I. P. 's calculated with Green's functions method (d), the combined Green functions and DFT approach (e), the similar our results (f).

Table 1.  
**The experimental and calculated V. I. P. (in eV) of  $N_2$  ( $R_k$  is the contribution of reorganization (see text))**

	Exp	KT $-\epsilon_k^b$	EKT $-\epsilon_k^b$	GF $-\epsilon_k^b$	MCEP $-\epsilon_k^b$
$3\sigma_g$	15.6	17.24	16.37 16.13 16.84 15.66	15.31	15.52
$1\pi_u$	16.98	16.73	16.73	16.80	17.24
$2\sigma_u$	18.78	21.13	21.13	19.01	18.56
	Exp	GF+ Reorg.	GF- All corr	GF- DFT	This work
$3\sigma_g$	15.6	16.0	15.50	15.52	15.58
$1\pi_u$	16.98	15.7	16.83	16.85	16.93
$2\sigma_u$	18.78	19.9	18.59	18.63	18.71

Besides, the comparisons are made in Table 1 with the multiconfigurational electron propagator method (MCEP) and extended KT (EKT) theory (the extended KT has been implemented using multiconfigurational self-consistent field wave functions within different basis sets (I-IV) [52], calculated with the GAMESS, HONDO,

and SIRIUS programs. The EKT ionization energies for the  $3\sigma_g$  and  $1\pi_u$  are comparable to the MCEP values. Note that our data are in physically reasonable agreement with the best theoretical values and experimental data. But the most important point of all consideration is connected the principal possibility to reproduce diatomic spectra by applying a one-particle theory with accounting for the correlation and reorganization effects. The combined DFT-GF theoretical approach can be prospectively used for quantitative treating photoelectron spectra of more complicated diatomic molecules.

## References

1. Glushkov A.V., New approach to theoretical definition of ionization potentials for molecules on the basis of Green's function method// Journ.of Phys.Chem.-1992.-Vol.66.-P.2671-2677.
2. Glushkov A.V., Relativistic quantum theory. Quantum mechanics of atomic systems.-Odessa: Astroprint, 2008.-700P.
3. Glushkov A.V., The Green's functions and density functional approach to vibrational structure in the photoelectron spectra of molecules: Review of method// Photoelectronics.-2014.-Vol.23.-P.54-72.
4. Glushkov A.V., Lepikh Ya.I., Fedchuk A.P., Loboda A.V., The Green's functions and density functional approach to vibrational structure in the photoelectron spectra of molecules//Photoelectronics.-2009.-N18.-P.119-127.
5. Svinarenko A.A., Fedchuk A.P., Glushkov A.V., Lepikh Ya.I., Loboda A.V., Lopatkin Yu.M., The Green's functions and density functional approach to vibrational structure in the photoelectron spectra of carbon oxide molecule//Photoelectronics.-2010.-N19.-P.115-120.
6. Glushkov A.V., Fedchuk A.P., Kon-

- dratenko P.A., Lepikh Ya.I., Lopatkin Yu.M., Svinarenko A.A., The Green's functions and density functional approach to vibrational structure in the photoelectron spectra: Molecules of CH, HF//Photoelectronics.-2011.-Vol.20.-P.58-62.
7. Glushkov A., Koltzova N., Effective account of polarization effects in calculation of oscillator strengths and energies for atoms and molecules by method of equations of motion// Opt. Spectr. -1994.- Vol. 76,№6.-P.885-890.
  8. Glushkov A.V., Quasiparticle approach in the density functional theory under finite temperatures and dynamics of effective Bose -condensate // Ukr. Phys. Journ.- 1993.-Vol. 38, №8.-P.152-157.
  9. Ponomarenko E.L., Kuznetsova A.A., Dubrovskaya Yu.V., Bakunina (Mischenko) E.V., Energy and spectroscopic parameters of diatomics within generalized equation of motion method// Photoelectronics.-2016.-Vol.25.-P.114-118.
  10. Mischenko E.V., An effective account of correlation in calculation of excited states energies for molecules by equation of motion method: O<sub>3</sub>//Photoelectronics.-2007.-N16.-P.123-125.
  11. Köppel H., Domcke W., Cederbaum L.S., Green's function method in quantum chemistry// Adv. Chem. Phys.-1984.-Vol.57.-P.59-132.
  12. Cederbaum L.S., Domcke W., On vibrational structure of photoelectron spectra by the Green's functions method// J.Chem. Phys.-1984.-Vol.60.-P.2878-2896.
  13. Zangwill A., Soven P.J. Density-functional approach to local field effects in finite systems. Photo-absorption in rare gases // Phys.Rev.A.-1980.-Vol.21,N5-P.1561-1572.
  14. Kobayashi K., Kurita N., Kumahora H., Kuzatami T. Bond-energy calculations of Cu, Ag, CuAg with the generalized gradient approximation// Phys. Rev.A.-1991.-Vol.43.-P.5810-5813.
  15. Lagowski J.B., Vosko S.H. Analysis of local and gradient- correction correlation energy functionals using electron removal energies// J. Phys.B: At. Mol. Opt. Phys.-1988.-Vol.21,N1-P.203-208.
  16. Guo Y., Whitehead M.A. Effect of the correlation correction on the ionization potential and electron affinity in atoms// Phys.Rev.A-1989.-Vol.39,N1.-P.28-34.
  17. Glushkov A.V., An universal quasiparticle energy functional in a density functional theory for relativistic atom// Optics and Spectr.-1989.-Vol.66,N1-P.31-36.
  18. Glushkov A.V., Relativistic and correlation effects in spectra of atomic systems.-Odessa: Astroprint.-2006.-400P.
  19. Glushkov A.V., Atom in electromagnetic field.-Kiev: KNT, 2005.-450P.
  20. Khetselius O.Yu., Hyperfine structure of atomic spectra.-Odessa: Astroprint, 2008.-210P.
  21. Glushkov A.V., Khetselius O.Y., Malinovskaya S.V., Spectroscopy of cooperative laser-electron nuclear effects in multiatomic molecules// Molec. Phys.-2008. -Vol.106.-N9-10.-P.1257-1260.
  22. Glushkov A.V., Khetselius O.Y., Malinovskaya S.V., New laser-electron nuclear effects in the nuclear  $\gamma$  transition spectra in atomic and molecular systems// Frontiers in Quantum Systems in Chemistry and Physics. Series: Progress in Theoretical Chemistry and Physics, Eds. S.Wilson, P.J.Grout, J. Maruani, G. Delgado-Barrio, P. Piecuch (Springer).-2008.-Vol.18.-525-541.
  23. Glushkov A.V., Khetselius O.Yu., Svinarenko A.A., Prepelitsa G.P., Shakhman A., Spectroscopy of co-

- operative laser-electron nuclear processes in diatomic and multiatomic molecules//Spectral Lines Shape (AIP, USA).-2010.-Vol.16.-P.269-273.
24. Glushkov A.V., Kondratenko P.A., Buyadzhi V., Kvasikova A.S., Shakhman A., Sakun T., Spectroscopy of cooperative laser electron- $\gamma$ -nuclear processes in polyatomic molecules// Journal of Physics: C Series (IOP, London, UK).-2014.-Vol.548.-P. 012025 (5p.).
  25. Glushkov A.V., Kondratenko P.A., Lopatkin Yu., Buyadzhi V., Kvasikova A., Spectroscopy of cooperative laser electron-  $\gamma$  -nuclear processes in diatomics and multiatomic molecules // Photoelectronics.-2014.-Vol.23.-P.142-146.
  26. Khetselius O.Yu., Optimized perturbation theory to calculating the hyperfine line shift and broadening for heavy atoms in the buffer gas// Frontiers in Quantum Methods and Applications in Chemistry and Physics. Ser.: Progress in Theor. Chem. and Phys., Eds. M.Nascimento, J.Maruardi, E.Brändas, G.Delgado-Barrio (Springer).-2015-Vol.29.-P.54-76.
  27. Khetselius O.Yu., Relativistic energy approach to cooperative electron- $\gamma$ -nuclear processes: NEET Effect// Quantum Systems in Chemistry and Physics: Progress in Methods and Applications. Ser.: Progress in Theor. Chem. and Phys., Eds. K.Nishikawa, J. Maruardi, E.Brandas, G. Delgado-Barrio, P.Piecuch (Springer).-2012-Vol.26.-P.217-229.
  28. Buyadzhi V.V., Glushkov A.V., Lovett L., Spectroscopy of atoms and nuclei in a strong laser field: AC Stark effect and multiphoton resonances// Photoelectronics.-2014.-Vol.23.-P. 38-43.
  29. Khetselius O., Spectroscopy of cooperative electron-gamma-nuclear processes in heavy atoms: NEET effect// J. Phys.: Conf. Ser.-2012.- Vol.397.-P.012012
  30. Glushkov A.V., Khetselius O.Yu., Loboda A.V., Svinarenko A.A., QED approach to atoms in a laser field: Multi-photon resonances and above threshold ionization// Frontiers in Quantum Systems in Chemistry and Physics, Ser.: Progress in Theoretical Chemistry and Physics; Eds. S.Wilson, P.J.Grout, J. Maruardi, G. Delgado-Barrio, P. Piecuch (Springer), 2008.-Vol.18.-P.541-558.
  31. Glushkov A.V., Khetselius O.Yu., Svinarenko A.A., Prepelitsa G.P., Energy approach to atoms in a laser field and quantum dynamics with laser pulses of different shape//In: Coherence and Ultrashort Pulse Laser Emission, Ed. by Dr. F. Duarte (InTech).-2010.-P.159-186.
  32. Glushkov A.V., Khetselius O., Svinarenko A., Relativistic theory of cooperative muon-g gamma-nuclear processes: Negative muon capture and metastable nucleus discharge// Advances in the Theory of Quantum Systems in Chemistry and Physics. Ser.: Progress in Theor. Chem. and Phys., Eds. P.Hoggan, E.Brandas, J.Maruardi, G. Delgado-Barrio, P.Piecuch (Springer).-2012.-Vol.22.-P.51-68.
  33. Glushkov A.V., Khetselius O.Yu., Prepelitsa G., Svinarenko A.A., Geometry of Chaos: Theoretical basis's of a consistent combined approach to treating chaotic dynamical systems and their parameters determination //Proc. of International Geometry Center".-2013.-Vol.6, N1.-P.43-48.
  34. Malinovskaya S.V., Glushkov A.V., Dubrovskaya Yu.V., Vitavetskaya L.A., Quantum calculation of cooperative muon-nuclear processes: discharge of metastable nuclei during negative muon capture// Recent Advances in the Theory of Chemical and Physical Systems (Springer).-2006.-

- Vol.15.-P.301-307.
35. Malinovskaya S.V., Glushkov A.V., Khetselius O.Yu., Lopatkin Yu., Loboda A., Svinarenko A., Nikola L., Perelygina T., Generalized energy approach to calculating electron collision cross-sections for multicharged ions in a plasma: Debye shielding model// *Int. Journ. Quant. Chem.*-2011.-Vol.111,N2.-P.288-296.
  36. Malinovskaya S.V., Glushkov A.V., Khetselius O.Yu., Svinarenko A.A., Mischenko E.V., Florko T.A., Optimized perturbation theory scheme for calculating the interatomic potentials and hyperfine lines shift for heavy atoms in the buffer inert gas//*Int. Journ. Quant.Chem.*-2009.-Vol.109,N14.-P.3325-3329.
  37. Glushkov A.V., Khetselius O.Yu., Svinarenko A., Prepelitsa G., Mischenko E., The Green's functions and density functional approach to vibrational structure in the photoelectron spectra for molecules// *AIP Conf. Proceedings.*-2010.-Vol.1290.-P. 263-268.
  38. Khetselius O.Yu., Florko T.A., Svinarenko A.A., Tkach T.B., Radiative and collisional spectroscopy of hyperfine lines of the Li-like heavy ions and Tl atom in an atmosphere of inert gas//*Phys.Scripta.*-2013.-Vol.T153-P.014037.
  39. Khetselius O.Yu., Hyperfine structure of radium// *Photoelectronics.*-2005.-N14.-P.83-85.
  40. Glushkov A.V, Malinovskaya S.,Cooperative laser nuclear processes: border lines effects// In: *New projects and new lines of research in nuclear physics.* Eds. G.Fazio, F.Hanappe, Singapore: World Scientific.-2003.-P.242-250.
  41. Glushkov A.V., Lovett L., Khetselius O., Gurnitskaya E., Dubrovskaya Yu., Loboda A., Generalized multiconfiguration model of decay of multipole giant resonances applied to analysis of reaction (m-n) on the nucleus  $^{40}\text{Ca}$ // *Internat. Journ. Modern Physics A.*-2009.- Vol. 24, N.2-3.-P.611-615.
  42. Glushkov A., Malinovskaya S., Sukharev D., Khetselius O.Yu., Loboda A., Lovett L., Green's function method in quantum chemistry: New numerical algorithm for the Dirac equation with complex energy and Fermi-model nuclear potential//*Int.J. Quant. Chem.*-2009.- Vol. 109.-N8.-P.1717-1727.
  43. Glushkov A.V., Malinovskaya S.V, Gurnitskaya E.P., Khetselius O.Yu., Dubrovskaya Yu.V., Consistent quantum theory of the recoil induced excitation and ionization in atoms during capture of neutron// *Journal of Physics: Conf. Series (IOP).*-2006.-Vol.35.-P.425-430.
  44. Glushkov A V, Khetselius O Yu, Svinarenko A A and Buyadzhi V V, Spectroscopy of autoionization states of heavy atoms and multiply charged ions (Odessa: TEC), 2015
  45. Khetselius O.Yu., Turin A.V., Sukharev D.E., Florko T.A., Estimating of X-ray spectra for kaonic atoms as tool for sensing the nuclear structure// *Sensor Electr. and Microsyst. Techn.*-2009.-N1.-P.30-35.
  46. Glushkov A.V., Effective quasi-particle valence hamiltonian of molecules in the comprehensive semi-empirical theory// *Sov. J. Struct. Chem.*-1988.-Vol.29,N4.-P.3-9.
  47. Khetselius O.Yu., Quantum Geometry: New approach to quantization of the quasistationary states of Dirac equation for super heavy ion and calculating hyper fine structure parameters// *Proc. Int.Geometry Center.*-2012.-Vol.5,№ 3-4.-P.39-45.
  48. Glushkov A.V., Khetselius O.Yu., Svinarenko A.A., Theoretical spectroscopy of autoionization resonances in spectra of lanthanide atoms//

- Physica Scripta.-2013.-Vol.T153.-P.014029.
49. Gedasimov V N, Zelenkov A G, Kulakov V M et al 1984 *JETP*. **86** 1169; Soldatov A A 1983 Preprint of I.V.Kurchatov Institute for Atomic Energy IAE-3916, Moscow
50. Glushkov A.V., Operator Perturbation Theory for Atomic Systems in a Strong DC Electric Field//Advances in Quantum Methods and Applications in Chemistry, Physics, and Biology. Series: Frontiers in Theoretical Physics and Chemistry, Eds. M.Hotokka, J.Marvani, E. Brändas, G.Delgado-Barrio (Springer).-2013.-Vol. 27.-P.161-177.
51. Glushkov A.V., Kondratenko P.A., Lepikh Ya., Fedchuk A.P., Svinarenko A.A., Lovett L., Electrodynamical and quantum - chemical approaches to modelling the electrochemical and catalytic processes on metals, metal alloys and semiconductors// Int. J. Quantum Chem.-2009.-Vol.109, N14.-P.3473-3481.
52. Robert C. Morrison R., Liu G., Extended Koopmans' Theorem: Approximate Ionization Energies from MCSCF Wave Functions// J. Comput. Chem.-1992.-Vol. 13.-P.1004-1010.

This article has been received in August 2018

PACS 33.20.-t

*A. V. Ignatenko, A. V. Glushkov, Ya. I. Lepikh, A. S. Kvasikova*

## **ADVANCED GREEN'S FUNCTIONS AND DENSITY FUNCTIONAL APPROACH TO VIBRATIONAL STRUCTURE IN THE PHOTOELECTRON SPECTRA OF DIATOMIC MOLECULE**

### **Summary**

We present the optimized version of the hybrid combined density functional theory (DFT) and the Green's-functions (GF) approach to quantitative treating the diatomic photoelectron spectra. The Fermi-liquid quasiparticle version of the density functional theory is used. The density of states, which describe the vibrational structure in photoelectron spectra, is defined with the use of combined DFT-GF approach and is well approximated by using only the first order coupling constants in the optimized one-quasiparticle approximation. Using the combined DFT-GF approach leads to significant simplification of the calculation and increasing an accuracy of theoretical prediction.

**Key words:** photoelectron spectra of molecules, Green's functions, density functional theory

PACS 33.20.-t

*А. В. Игнатенко, А. В. Глушков, Я. И. Лепих, А. С. Квасикова*

## **ОБОБЩЕННЫЙ МЕТОД ФУНКЦИЙ ГРИНА И ФУНКЦИОНАЛА ПЛОТНОСТИ В ОПРЕДЕЛЕНИИ КОЛЕБАТЕЛЬНОЙ СТРУКТУРЫ ФОТОЭЛЕКТРОННОГО СПЕКТРА ДВУХАТОМНЫХ МОЛЕКУЛ**

### **Резюме**

Мы представляем оптимизированную версию гибридной комбинированной теории функционала плотности (DFT) и метода функций Грина (GF) для количественного описания фотоэлектронных спектров двухатомных молекул. Используется модель ферми-жидкостная квазичастичная версия теории функционала плотности. Плотность состояний, которые описывают колебательную структуру в фотоэлектронных спектрах, определяется с использованием комбинированного DFT-GF подхода и физически разумно аппроксимируется с использованием только первого порядка констант связи в одноквазичастичном приближении. Использование комбинированного DFT-GF подхода приводит к значительному упрощению молекулярных расчетов и увеличению точности теоретического предсказания.

**Ключевые слова:** фотоэлектронный спектр молекул, метод функций Грина, теория функционала плотности

PACS 33.20.-t

*Г. В. Игнатенко, О. В. Глушков, Я. И. Лепих, Г. С. Квасикова*

## **УДОСКОНАЛЕНИЙ МЕТОД ФУНКЦІЙ ГРИНА І ФУНКЦІОНАЛУ ГУСТИНИ У ВИЗНАЧЕННІ ВІБРАЦІЙНОЇ СТРУКТУРИ ФОТОЕЛЕКТРОННОГО СПЕКТРУ ДВОАТОМНИХ МОЛЕКУЛ**

### **Резюме**

Ми представляємо оптимізовану версію гібридної комбінованої теорії функціоналу густини (DFT) і методу функцій Грина (ГФ) для кількісного опису фотоелектронних спектрів двоатомних молекул. Використовується фермі-рідинна квазічастична версія теорії функціоналу густини. Густина стану, яка описує коливальну структуру в фотоелектронних спектрах, визначається з використанням комбінованого DFT-GF підходу та фізично розумно апроксимується за допомогою тільки першого порядку констант зв'язку в одноквазічастинковому наближенні. Використання комбінованого DFT-GF підходу призводить до значного спрощення молекулярних обчислень та збільшення точності теоретичного прогнозування.

**Ключові слова:** фотоелектронний спектр молекул, метод функцій Грина, теорія функціонала густини

*O. Yu. Khetselius, A. L. Mykhailov, E. A. Efimova, R. E. Serga*

Odessa State Environmental University, L'vovskaya str.15, Odessa-9, 65016, Ukraine  
E-mail: okhetsel@gmail.com

## WAVELENGTHS AND OSCILLATOR STRENGTHS FOR LI-LIKE MULTICHARGED IONS WITHIN RELATIVISTIC MANY-BODY PERTURBATION THEORY

The relativistic many-body perturbation theory with the optimized Dirac-Kohn-Sham zeroth approximation is applied to calculation of the radiative transitions wavelengths and oscillator strengths for some Li-like multicharged ions. The relativistic, exchange-correlation and other corrections are accurately taken into account. The optimized relativistic orbital basis set is generated in the optimal many-body perturbation theory approximation with fulfilment of the gauge invariance principle. An accurate treatment of the QED perturbation theory fourth order (a second order of the atomic perturbation theory) Feynman diagrams (whose contribution into the energy shift imaginary part (radiation width) for the multi-electron atoms accounts for multi-body correlation effects) is performed. The obtained data on the radiative transition wavelengths and oscillator strengths for some transition in spectra of the Li-like multicharged ions are analyzed and compared with alternative theoretical and experimental results.

### 1. Introduction

The levels energies, transitions probabilities, oscillator strengths and so on are very important in atomic physics (spectroscopy, spectral lines theory), astrophysics, plasma physics, laser physics, quantum electronics. They are very much needed in research of thermonuclear reactions, where the ionic radiation is one of the primary loss mechanisms and so on. The spectral lines belonging to the radiation of many multicharged ions have been identified in both solar flares and nonflaring solar active regions, observed in high-temperature plasmas, such as pinches and laser-produced plasmas, and in beam-foil spectra [1-30].

There have been sufficiently many reports of theoretical and experimental studies of energies and oscillator strengths for the Li-like ions and other alkali-like ions (see, for example, [7-15]). Banglin Deng et al [12] presented the calculated wavelengths, oscillator strengths, transition probabilities, and line strengths for Li-like ions ( $Z = 7-30$ ) in the framework of the relativistic configuration-interaction formalism using MCDF wave functions and considering the Breit interaction, QED and nuclear mass

corrections. A critical evaluation and compilation of the spectroscopic parameters for Li-like ions ( $Z=3-28$ ) was undertaken by Martin and Wiese [153-156]. Bièmont [30] applied fully variational nonrelativistic HF wave functions in computing  $1s2n2L$  ( $n<8=s,p,d,f$ ;  $3<Z<22$ ) Li-like states]. Aglitskii et al [121] experimentally observed the  $L\alpha$  wavelengths of Li-like ions ( $Z = 19-26$ ) in laser-produced plasmas. Theoretical approach to studying the spectroscopic characteristics of the heavy multicharged ions (Li-like ions) within the RMBPT with the model potential zeroth approximation is developed by Ivanov-Ivanova [119-125]. Fully relativistic computing the wavelengths and oscillator strengths from excitation of Li-like ions ( $Z = 8-92$ ) have been given by Zhang et al. [53]. Nahar [54] applied the Breit-Pauli R-matrix method to calculations of the wavelengths, transition probabilities, and oscillator strengths for a number of the Li-like ions with the nuclear charge  $Z=6-68$ . The relativistic quantum defect method has been used by Martin et al [55] to calculate the oscillator strengths for a number of radiative transitions between low-lying states in the Li-like ions for  $Z < 45$ . The energy levels and hy-

perfine constants of neutral lithium were studied by Lindgren[9] within a nonrelativistic coupled-cluster method, by Guan-Wang [47] within the effective operator form of MBPT etc. Relativistic all-order MBPT calculations of energies and matrix elements for Li and Be+ were reported in Ref. [44]. Wu Xiao-Li et al [50] have performed the relativistic MBPT calculation for lithium-like isoelectronic sequence ( $Z=3-9$ ) within the DF method with using the finite basis sets of the Dirac-Fock equations, constructed by B splines.

Chen Chao and Wang Zhi-Wen [48] applied a full core plus correlation method with using multiconfiguration interaction wave functions to computing the nonrelativistic values of the oscillator strengths for a number of transitions into the Rydbers states along the LiI isoelectronic sequence. The Hylleraas-type variational method and the  $1/Z$  expansion method have been used also to obtain the non-relativistic calculations data on the energies and oscillator strengths of  $1s2s, 1s2p$  for Li-like systems up to  $Z = 50$  [41-51].

In this paper the relativistic many-body perturbation theory with the optimized Dirac-Kohn-Sham zeroth approximation is applied to calculation of the radiative transitions wavelengths and oscillator strengths for some Li-like multicharged ions. The relativistic, exchange-correlation and other corrections are accurately taken into account.

## 2. Relativistic many-body perturbation theory with optimized zeroth approximation and energy approach

The theoretical basis of the RMBPT with the Dirac-Kohn-Sham zeroth approximation was widely discussed [26,27,93-102], and here we will only present the essential features.

As usually, we use the charge distribution in atomic (ionic) nucleus  $\rho(r)$  in the Gaussian approximation:

$$\rho(r|R) = \left(4\gamma^{3/2}/\sqrt{\pi}\right)\exp(-\gamma r^2) \quad (1)$$

where  $\gamma=4/\pi R^2$  and  $R$  is the effective nucleus radius. The Coulomb potential for the spherically symmetric density  $\rho(r)$  is:

$$V_{nuc}(r|R) = -\left(\frac{1}{r}\right)\int_0^r dr' r'^2 \rho(r'|R) + \int_r^\infty dr' r' \rho(r'|R) \quad (2)$$

Further consider the Dirac-like type equations for the radial functions  $F$  and  $G$  (components of the Dirac spinor) for a three-electron system  $1s^2nlj$ . Formally a potential  $V(r|R)$  in these equations includes electric and polarization potentials of the nucleus,  $V_x$  is the exchange inter-electron interaction (in the zeroth approximation). The standard Kohn-Sham (KS) exchange potential is [13]:

$$V_x^{KS}(r) = -(1/\pi)[3\pi^2\rho(r)]^{1/3}. \quad (3)$$

In the local density approximation the relativistic potential is [33]:

$$V_x[\rho(r), r] = \frac{\delta E_x[\rho(r)]}{\delta\rho(r)}, \quad (4)$$

where  $E_x[\rho(r)]$  is the exchange energy of the multielectron system corresponding to the homogeneous density  $\rho(r)$ , which is obtained from a Hamiltonian having a transverse vector potential describing the photons. In this theory the exchange potential is [33]:

$$V_x[\rho(r), r] = V_x^{KS}(r) \cdot \left\{ \frac{3}{2} \ln \frac{[\beta + (\beta^2 + 1)^{1/2}]}{\beta(\beta^2 + 1)^{1/2}} - \frac{1}{2} \right\}, \quad (5)$$

where  $\beta = [3\pi^2\rho(r)]^{1/3}/c$ ,  $c$  is the velocity of light. The corresponding one-quasiparticle correlation potential

$$V_c[\rho(r), r] = -0.0333 \cdot b \cdot \ln[1 + 18.3768 \cdot \rho(r)^{1/3}], \quad (6)$$

(here  $b$  is the optimization parameter; see below).

The perturbation operator contains the relativistic potential of the interelectron interaction of the form:

$$V_{e-e}^{rel}(r_i, r_j) = \frac{(1 - \alpha_i \alpha_j)}{r_{ij}} \exp(i\omega_{ij} r_{ij}), \quad (7)$$

(here  $\alpha_i, \alpha_j$  are the Dirac matrices,  $\omega_{ij}$  is the transition frequency) with the subsequent subtraction of the exchange and correlation potentials. The rest of the exchange and correlation effects will be taken into account in the first two orders of the PT [93-102].

In Ref. [127,128] it has been proposed “ab initio” optimization principle for construction of the optimal relativistic orbital basis set. The minimization condition of the gauge dependent multielectron contribution of the lowest QED PT corrections to the radiation widths of the atomic levels is used. The details of procedure can be found in Ref. [126-134]. As in Ref. [127, 134], let us examine the multi-electron atomic ion with one quasiparticle in the first excited state, connected with the ground state by the electric dipole radiation transition. In the QED PT zeroth order we use the one-electron bare potential  $V_N(r)+V_X(r)+V_C(r)$ . As usual, the perturbation operator is as follows:

$$-V_{xc}(r)-J_\mu(x)A^\mu(x) \quad (8)$$

where  $A$  – vector-potential of the electromagnetic field,  $J$  – current operator.

Further one may treat the lowest order multi-electron effects, in particular, the gauge dependent radiative contribution for a certain class of the photon propagator calibration. The contribution of the QED PT fourth order diagrams  $A$  into the  $\text{Im}\delta E$  accounts for the exchange-polarization effects. In fact it describes the collective effects and is dependent upon the electromagnetic potentials gauge (the gauge non-invariant contribution). This value is considered to the typical electron correlation effect, whose minimization is a reasonable criterion in searching the optimal one-electron basis of PT. All the gauge non-invariant terms are multi-electron by their nature (the particular case of the gauge non-invariance manifestation is the non-coincidence of the oscillator strengths values, obtained in the approximate calculations with the “length” and “velocity” transition operator forms). Quite complicated calculation of contribution of the QED PT fourth order polarization diagrams into  $\text{Im}\delta E$  gives the following result [127]:

Here,  $f$  is the boundary of the closed shells;  $n \geq f$  indicates the unoccupied bound and the upper continuum electron states;  $m \leq f$  indicates the finite number of states in the core and the states of the negative continuum (accounting for the electron vacuum polarization).

$$\begin{aligned} \text{Im}\delta E_{nmv}(\alpha-s;b) = & -C \int \int \int \int dr_1 dr_2 dr_3 dr_4 \\ & \sum_{\substack{n \geq f \\ m \leq f}} \left( \frac{1}{\omega_{mn} + \omega_{\alpha s}} + \frac{1}{\omega_{mn} - \omega_{\alpha s}} \right) \cdot \\ & \cdot \psi_\alpha^+(r_1) \psi_m^+(r_2) \psi_s^+(r_4) \psi_n^+(r_3) \frac{1 - \alpha_1 \alpha_2}{r_{12}} \quad (9) \\ & \{[(\alpha_3 \alpha_4 - \alpha_3 n_{34} \alpha_4 n_{34}) / r_{14}]\cdot \\ & \cdot \sin[\omega_{\alpha n}(r_{12} + r_{34})] + \omega_{\alpha n} \cos[\omega_{\alpha n}(r_{12} + r_{34})] \\ & (1 + \alpha_3 n_{34} \alpha_4 n_{34})\} \cdot \psi_m(r_3) \psi_\alpha(r_4) \psi_n(r_2) \psi_s(r_1). \end{aligned}$$

The expression (9) can be represented in the form of terms:

$$\sum_{\substack{n \geq f \\ m \leq f}} \langle \alpha m | W_1 | ns \rangle \langle sn | W_2 | m \alpha \rangle / (\omega_{mn} \pm \omega_{\alpha s}) \quad (10)$$

with four different combinations of operators and (see details in Refs. [127-129]). The sum over  $n$  can be calculated by the method of differential equations. The minimization of the density functional  $\text{Im}\delta E$  leads to the integral differential equation for the  $\rho_c$ , that can be numerically solved. This step allows to determine the optimization parameter  $b$ . In Ref. [127] the authors elaborated a simplified computational procedure. We have used more sophisticated method, presented in Ref. [131-133]. It presents for first time the full consistent realization of the optimization approach within our version of the RMBPT.

The key elements of the relativistic energy approach to computing radiation widths and oscillator strengths for atomic systems are presented in Refs. [13-13]. Let us remind that an initial general energy formalism combined with an empirical model potential method in a theory of atoms and multicharged ions has been developed by Ivanov-Ivanova et al [119-125], further more general ab initio gauge-invariant relativistic approach has been presented in [127,128]. We use the optimized version of this formalism with our construction of one-quasiparticle representation. In the energy approach [124-126] the imaginary part of electron energy shift of an atom is connected with the radiation decay pos-

sibility (transition probability). An approach, based on the Gell-Mann and Low formula with the QED scattering matrix, is used in treatment of the relativistic atom. The total energy shift of the state is usually presented in the form:

$$\delta E = \text{Re}\delta E + i\Gamma / 2 \quad (11)$$

where  $\Gamma$  is interpreted as the level width, and the decay probability  $P = \Gamma$ . For the  $\alpha$ -s radiation transition the imaginary part of electron energy in the lowest order of perturbation theory is determined as [124]:

$$\text{Im}\delta E = -\frac{1}{4\pi} \sum_{\substack{\alpha > n > f \\ [\alpha < n \leq f]}} V_{\alpha n \alpha n}^{|\omega_{\alpha n}|}, \quad (12)$$

where  $\omega_{\alpha n}$  is a frequency of the  $\alpha$ -n radiation, ( $\alpha > n > f$ ) for electron and ( $\alpha < n < f$ )

for vacancy. The matrix element  $V$  is determined as follows:

$$V_{ijkl}^{|\omega|} = \iint dr_1 dr_2 \Psi_i^*(r_1) \Psi_j^*(r_2) \frac{\sin|\omega|r_{12}}{r_{12}} (1 - \alpha_1 \alpha_2) \Psi_k^*(r_2) \Psi_l^*(r_1) \quad (13)$$

The separated terms of the sum in (34) represent the contributions of different channels and a probability of the dipole transition is:

$$\Gamma_{\alpha n} = \frac{1}{4\pi} V_{\alpha n \alpha n}^{|\omega_{\alpha n}|}. \quad (36)$$

The corresponding oscillator strength:  $gf = \lambda^2 \Gamma_{\alpha n} / 6.67 \times 10^{15}$ , where  $g$  is the degeneracy degree,  $\lambda$  is a wavelength in angstroms ( $\text{\AA}$ ). All calculations are performed on the basis of the numeral code Superatom-ISAN (version 93). The details of the used method can be found in the references [1,11,14,21-24].

### 3. Results and Conclusions

In table 1 we list our computational results on the wavelengths and oscillator strengths  $gf$  (upper number in the line ‘‘Our work’’: data, obtained without using the optimized basis set and accounting for the exchange-polarization corrections; lower number in the line ‘‘Our work’’ – with using the optimized basis set and accounting for the exchange-polarization corrections) for  $1s^2 2s$  ( $^2S_{1/2}$ )  $\rightarrow$   $1s^2 3p$  ( $^2P_{1/2}$ ) transitions in the Li-like ions with  $Z=21,22$ . In Table 1 the data on the wavelengths, oscillator strengths, calculated by Banglin Deng et al [52] (in the framework

of the relativistic configuration-interaction formalism using multiconfiguration DF wave functions and considering the Breit interaction, QED and nuclear mass corrections), Zhang et al (the Dirac-Fock-Slater method and disturbed wave approximation), Martin et al (the relativistic quantum defect method), Nahar (ab initio calculations including relativistic effects employing the Breit-Pauli R-matrix method) and the NIST data [10-14] are listed too. The data by Banglin Deng et al [12] are obtained in the length gauge, and the ratios (V/L; in %) of the velocity and length gauges data to check the accuracy of calculations are listed. We also present our values of the gauge non-invariant contribution (Ninv; in %). Comparison of the presented data shows that the agreement between the theoretical data and experimental results is more or less satisfactory.

Table 1.

**The calculated wavelengths, oscillator strengths for  $1s^2 2s$  ( $^2S_{1/2}$ )  $\rightarrow$   $1s^2 3p$  ( $^2P_{1/2}$ ) transitions in the Li-like ions with  $Z=21-30$ ; V/L is the ratios of the velocity and length gauges values by Banglin Deng et al [12]; Ninv (in %) is the gauge non-invariant contribution (this work);**

Z	Ref.	Wavelength (A)	Oscillator strength (gf, 10 <sup>-1</sup> )	V/L; Ninv (%)
21	Banglin Deng et al	16.862	1.2392	V/L= 0.117
	NIST	16.861	1.2404	
	Zhang et al	16.856	1.250	
	Martin et al	-	1.24	
	This work	16.860	1.2835 1.2401	Ninv= 0.10
22	Banglin Deng et al	15.254	1.2484	V/L= 0.128
	NIST	15.253	1.2489	
	Zhang et al	15.249	1.259	
	Nahar	15.3	1.281	
	Martin et al		1.24	
	This work	15.252	1.2967 1.2492	Ninv= 0.11

The approach presented (with using the optimized relativistic PT) can provide sufficiently high accuracy and physically reasonable description of the corresponding wavelengths and oscillator strengths. It should be noted that an estimate of the gauge-non-invariant contributions (the difference between the oscillator strengths values calculated with using the transition operator in the form of “length” and “velocity”) is about 0.15%, i.e., the results for oscillator strengths obtained with using different photon propagator gauges (Coulomb, Babushkin, Landau) are practically equal. This is the evidence of a successful choice of the one-quasiparticle representation.

### References

1. Davidson E.R., Natural Orbitals. *Adv. Quant. Chem.* **1972**, *6*, 235-266.
2. Kohn, J.W.; Sham, L.J. Self-Consistent Equations Including Exchange and Correlation Effects. *Phys. Rev. A* **1964**, *140*, 1133.
3. Froelich, P.; Davidson, E.R.; Brändas, E. Error estimates for complex eigenvalues of dilated Schrödinger operators. *Phys. Rev. A* **1983**, *28*, 2641.
4. Wang, Y.A.; Yung, Y.C.; Chen, Y.K.; Chen, G.H. Communication: Linear-expansion shooting techniques for accelerating self-consistent field convergence. *J. Chem. Phys.* **2011**, *134*, 241103.
5. Thakkar, A.J.; Koga, T.; Tanabe, F.; Teruya, H. Compact Hylleraas-type wave functions for the lithium isoelectronic sequence. *Chem. Phys. Lett.* **2002**, *366*, 95-99.
6. Khetselius, O.Yu. *Hyperfine structure of atomic spectra*. Astroprint: Odessa, **2008**.
7. Glushkov, A.V. *Relativistic Quantum theory. Quantum mechanics of atomic systems*. Astroprint: Odessa, **2008**.
8. Svinarenko, A.A. Study of spectra for lanthanides atoms with relativistic many-body perturbation theory: Rydberg resonances. *J. Phys.: Conf. Ser.* **2014**, *548*, 012039.
9. Svinarenko, A.A.; Ignatenko, A.V.; Ternovsky, V.B.; Nikola, L.V.; Serechenko, S.S.; Tkach, T.B. Advanced relativistic model potential approach to calculation of radiation transition parameters in spectra of multicharged ions. *J. Phys.: Conf. Ser.* **2014**, *548*, 012047.
10. Zhang, H.L.; Sampson, D.H.; Fontes, C.J. Relativistic distorted-wave collision strengths and oscillator strengths for the 85 Li-like ions with  $8 < Z < 92$ . *Atom. Dat. Nucl. Dat. Tabl.* **1990**, *44*, 31-77.
11. Nahar, S. N. Relativistic fine structure oscillator strengths for Li-like ions: C IV - Si XII, SXIV, ArXVI, CaXVIII, Ti XX, Cr XXII, Ni XXVI. *Astr. and Astrophys.* **2002**, *389*, 716-728.
12. Banglin, Deng.; Gang, Jiang; Chuan-yu Zhang. Relativistic configuration-interaction calculations of electric dipole  $n = 2 - n = 3$  transitions for medium-charge Li-like ions. *Atom. Dat. and Nucl. Dat. Tabl.* **2014**, *100*, 1337-1355.
13. Buyadzhi, V.V.; Zaichko, P.A.; Gurskaya, M.Y.; Kuznetsova, A.A.; Ponomarenko E.L.; Ternovsky, V.B.; Relativistic theory of excitation and ionization of Rydberg atomic systems in a Black-body radiation field, *J. Phys.: Conf. Ser.* **2017**, *810*, 012047
14. Buyadzhi, V.V.; Zaichko, P.A.; Antoshkina, O.A.; Kulakli, T.A.; Prepelitsa, G.P.; Ternovsky V.B.; Mansarliysky, V. Computing of radiation parameters for atoms and multicharged ions within relativistic energy approach: Advanced Code. *J. Phys.: Conf. Ser.* **2017**, *905*, 012003.
15. Glushkov, A.V.; Malinovskaya, S.V.; Loboda, A.V.; Shpinareva, I.M.; Prepelitsa, G.P. Consistent quantum approach to new laser-electron-nuclear effects in diatomic molecules. *J. Phys.: Conf. Ser.* **2006**, *35*, 420-424.

16. Glushkov, A.V. Operator Perturbation Theory for Atomic Systems in a Strong DC Electric Field. *In Advances in Quantum Methods and Applications in Chemistry, Physics, and Biology, Series: Progress in Theoretical Chemistry and Physics*; Hotokka, M., Brändas, E., Maruani, J., Delgado-Barrio, G., Eds.; Springer: Cham, **2013**; Vol. 27, pp 161–177.
17. Glushkov, A.V.; Ambrosov, S.V.; Ignatenko, A.V.; Korchevsky, D.A. DC strong field stark effect for nonhydrogenic atoms: Consistent quantum mechanical approach. *Int. Journ. Quant. Chem.* **2004**, *99*, 936-939.
18. Glushkov, A.V.; Kondratenko, P.A.; Buyadgi V.V.; Kvasikova, A.S.; Sakun, T.N.; Shakhman, A.S. Spectroscopy of cooperative laser electron- $\gamma$ -nuclear processes in polyatomic molecules. *J. Phys.: Conf. Ser.* **2014**, *548*, 012025.
19. Malinovskaya, S.V.; Dubrovskaya, Yu.V.; Vitavetskaya, L.A. Advanced quantum mechanical calculation of the beta decay probabilities. *AIP Conf. Proc.* **2005**, *796*, 201-205.
20. Filatov, M.; Cremer, D. A gauge-independent zeroth-order regular approximation to the exact relativistic Hamiltonian—Formulation and applications. *J. Chem. Phys.* **2005**, *122*, 044104.
21. Glushkov, A.V.; Malinovskaya, S.V.; Chernyakova Y.G.; Svinarenko, A.A. Cooperative laser-electron-nuclear processes: QED calculation of electron satellites spectra for multi-charged ion in laser field. *Int. Journ. Quant. Chem.* **2004**, *99*, 889-893.
22. Glushkov, A.V.; Malinovskaya, S.V.; Prepelitsa, G.; Ignatenko, V. Manifestation of the new laser-electron nuclear spectral effects in the thermalized plasma: QED theory of co-operative laser-electron-nuclear processes. *J. Phys.: Conf. Ser.* **2005**, *11*, 199-206.
23. Glushkov, A.V.; Malinovskaya, S.V.; Loboda, A.V.; Shpinareva, I.M.; Gurnitskaya, E.P.; Korchevsky, D.A. Diagnostics of the collisionally pumped plasma and search of the optimal plasma parameters of x-ray lasing: calculation of electron-collision strengths and rate coefficients for Ne-like plasma. *J. Phys.: Conf. Ser.* **2005**, *11*, 188-198.
24. Glushkov, A.V.; Ambrosov, S.; Loboda, A.; Gurnitskaya, E.; Prepelitsa, G. Consistent QED approach to calculation of electron-collision excitation cross sections and strengths: Ne-like ions. *Int. J. Quantum Chem.* **2005**, *104*, 562-569.
25. Glushkov, A.; Loboda, A.; Gurnitskaya, E.; Svinarenko, A. QED theory of radiation emission and absorption lines for atoms in a strong laser field. *Phys. Scripta.* **2009**, *T135*, 014022.
26. Florko, T.A.; Tkach, T.B.; Ambrosov, S.V.; Svinarenko, A.A. Collisional shift of the heavy atoms hyperfine lines in an atmosphere of the inert gas. *J. Phys.: Conf. Ser.* **2012**, *397*, 012037.
27. Buyadzhi, V.V. Laser multiphoton spectroscopy of atom embedded in Debye plasmas: multiphoton resonances and transitions. *Photoelectronics.* **2015**, *24*, 128-133.
28. Buyadzhi, V.V.; Chernyakova, Yu.G.; Smirnov, A.V.; Tkach, T.B. Electron-collisional spectroscopy of atoms and ions in plasma: Be-like ions. *Photoelectronics.* **2016**, *25*, 97-101.
29. Buyadzhi, V.V.; Chernyakova, Yu.G.; Antoshkina, O.; Tkach, T. Spectroscopy of multicharged ions in plasmas: Oscillator strengths of Be-like ion Fe. *Photoelectronics.* **2017**, *26*, 94-102.
30. Khetselius, O.Yu. Relativistic Energy Approach to Cooperative Electron- $\gamma$ -Nuclear Processes: NEET Effect *In Quantum Systems in Chemistry and Physics, Series: Progress in Theoretical Chemistry and Physics*; Nishikawa, K., Maruani, J., Brändas, E.,

- Delgado-Barrio, G., Piecuch, P., Eds.; Springer: Dordrecht, **2012**; Vol. 26, pp 217-229.
31. Khetselius, O.Yu. Relativistic perturbation theory calculation of the hyperfine structure parameters for some heavy-element isotopes. *Int. Journ. Quant.Chem.* **2009**, *109*, 3330-3335.
  32. Khetselius, O.Yu. Relativistic calculation of the hyperfine structure parameters for heavy elements and laser detection of the heavy isotopes. *Phys. Scripta.* **2009**, *135*, 014023.
  33. Khetselius, O.Yu. Optimized Perturbation Theory for Calculating the Hyperfine Line Shift and Broadening of Heavy Atoms in a Buffer Gas. In *Frontiers in Quantum Methods and Applications in Chemistry and Physics, Series: Progress in Theoretical Chemistry and Physics*; Nascimento, M., Maruani, J., Brändas, E., Delgado-Barrio, G., Eds.; Springer: Cham, **2015**; Vol. 29, pp. 55-76.
  34. Khetselius, O.Yu. *Quantum structure of electroweak interaction in heavy finite Fermi-systems*. Astroprint: Odessa, **2011**.
  35. Glushkov, A.V.; Malinovskaya S.V. Co-operative laser nuclear processes: border lines effects *In New Projects and New Lines of Research in Nuclear Physics*. Fazio, G., Hanappe, F., Eds.; World Scientific: Singapore, **2003**, 242-250.
  36. Glushkov, A.V. Spectroscopy of atom and nucleus in a strong laser field: Stark effect and multiphoton resonances. *J. Phys.: Conf. Ser.* **2014**, *548*, 012020
  37. Ivanov, L.N.; Ivanova, E.P. Atomic ion energies for Na-like ions by a model potential method  $Z = 25-80$ . *Atom. Data Nucl. Data Tabl.* **1979**, *24*, 95-109.
  38. Driker, M.N.; Ivanova, E.P.; Ivanov, L.N.; Shestakov, A.F. Relativistic calculation of spectra of 2-2 transitions in O-and F-like atomic ions. *J. Quant. Spectr. Rad. Transf.* **1982**, *28*, 531-535.
  39. Ivanova, E.P.; Ivanov, L.N.; Glushkov, A.V.; Kramida, A.E. High order corrections in the relativistic perturbation theory with the model zeroth approximation, Mg-Like and Ne-Like Ions. *Phys. Scripta* 1985, *32*, 513-522.
  40. Ivanov, L.N.; Ivanova, E.P.; Knight, L. Energy approach to consistent QED theory for calculation of electron-collision strengths: Ne-like ions. *Phys. Rev. A.* **1993**, *48*, 4365-4374.
  41. Glushkov, A.V.; Ivanov, L.N.; Ivanova, E.P. Autoionization Phenomena in Atoms. *Moscow University Press*, Moscow, **1986**, 58-160
  42. Glushkov, A.V.; Ivanov, L.N. Radiation decay of atomic states: atomic residue polarization and gauge non-invariant contributions. *Phys. Lett. A* **1992**, *170*, 33-36.
  43. Glushkov A.V.; Ivanov, L.N. DC strong-field Stark effect: consistent quantum-mechanical approach. *J. Phys. B: At. Mol. Opt. Phys.* **1993**, *26*, L379-386.
  44. Glushkov, A.V. *Relativistic and Correlation Effects in Spectra of Atomic Systems*. Astroprint: Odessa, **2006**.
  45. Glushkov, A.V. Relativistic polarization potential of a many-electron atom. *Sov. Phys. Journal.* **1990**, *33(1)*, 1-4.
  46. Glushkov, A.V. Negative ions of inert gases. *JETP Lett.* **1992**, *55*, 97-100.
  47. Glushkov, A.V. Energy approach to resonance states of compound superheavy nucleus and EPPP in heavy nuclei collisions *In Low Energy Antiproton Physics*; Grzonka, D., Czyzykiewicz, R., Oelert, W., Rozek, T., Winter, P., Eds.; AIP: New York, *AIP Conf. Proc.* **2005**, *796*, 206-210.
  48. Glushkov, A.V. Spectroscopy of cooperative muon-gamma-nuclear processes: Energy and spectral parameters *J. Phys.: Conf. Ser.* **2012**, *397*, 012011

49. Glushkov, A.V. Advanced Relativistic Energy Approach to Radiative Decay Processes in Multielectron Atoms and Multicharged Ions. In *Quantum Systems in Chemistry and Physics: Progress in Methods and Applications, Series: Progress in Theoretical Chemistry and Physics*; Nishikawa, K., Maruani, J., Brandas, E., Delgado-Barrio, G., Piecuch, P., Eds.; Springer: Dordrecht, **2012**; Vol. 26, pp 231–252.
50. Glushkov, A. Multiphoton spectroscopy of atoms and nuclei in a laser field: relativistic energy approach and radiation atomic lines moments method// *Adv. Quant.Chem.* (Elsevier), **2018**, 78, doi.org/10.1016/bs.aiq.2018.06.004
51. Khetselius, O. Optimized relativistic many-body perturbation theory calculation of wavelengths and oscillator strengths for Li-like multicharged ions// *Adv. Quant. Chem.* (Elsevier), **2018**, 78, doi.org/10.1016/bs.aiq.2018.06.001.
52. Khetselius, O.Yu. Relativistic Hyperfine Structure Spectral Lines and Atomic Parity Non-conservation Effect in Heavy Atomic Systems within QED Theory. *AIP Conf. Proceedings*. **2010**, 1290(1), 29-33.
53. Khetselius, O.Yu. Relativistic Calculating the Spectral Lines Hyperfine Structure Parameters for Heavy Ions. *AIP Conf. Proc.* **2008**, 1058, 363-365.
54. Khetselius, O.Yu. Hyperfine structure of radium. *Photoelectronics*. **2005**, 14, 83-85.
55. Khetselius, O.Yu.; Gurnitskaya, E.P. Sensing the electric and magnetic moments of a nucleus in the N-like ion of Bi. *Sensor Electr. and Microsyst. Techn.* **2006**, 3, 35-39.
56. Khetselius O.Yu.; Gurnitskaya, E.P. Sensing the hyperfine structure and nuclear quadrupole moment for radium. *Sensor Electr. and Microsyst. Techn.* **2006**, 2, 25-29.
57. Khetselius, O.Yu. Atomic parity non-conservation effect in heavy atoms and observing P and PT violation using NMR shift in a laser beam: To precise theory. *J. Phys.: Conf. Ser.* **2009**, 194, 022009
58. Ignatenko, A.V. Probabilities of the radiative transitions between Stark sublevels in spectrum of atom in an DC electric field: New approach. *Photoelectronics*, **2007**, 16, 71-74.
59. Glushkov, A.V.; Ambrosov, S.V.; Ignatenko, A.V. Non-hydrogenic atoms and Wannier-Mott excitons in a DC electric field: Photoionization, Stark effect, Resonances in ionization continuum and stochasticity. *Photoelectronics*, **2001**, 10, 103-106.
60. Glushkov, A.V.; Gurskaya, M.Yu.; Ignatenko, A.V.; Smirnov, A.V.; Serga, I.N.; Svinarenko, A.A.; Ternovsky, E.V. Computational code in atomic and nuclear quantum optics: Advanced computing multiphoton resonance parameters for atoms in a strong laser field. *J. Phys.: Conf. Ser.* **2017**, 905, 012004.
61. Glushkov, A.; Khetselius, O.; Svinarenko, A.; Buyadzhi, V. *Spectroscopy of autoionization states of heavy atoms and multiply charged ions*. Odessa: TEC, **2015**.

This article has been received in August 2018

PACS 31.15.A-;32.30.-r

*O. Yu. Khetselius, A. L. Mykhailov, E. A. Efimova, R. E. Serga*

## THE HYPERFINE STRUCTURE OF HEAVY ELEMENTS ATOMS WITHIN RELATIVISTIC MANY-BODY PERTURBATION THEORY

### Summary

The relativistic many-body perturbation theory with the optimized Dirac-Kohn-Sham zeroth approximation is applied to calculation of the radiative transitions wavelengths and oscillator strengths for some Li-like multicharged ions. The relativistic, exchange-correlation and other corrections are accurately taken into account. The optimized relativistic orbital basis set is generated in the optimal many-body perturbation theory approximation with fulfilment of the gauge invariance principle. An accurate treatment of the QED perturbation theory fourth order (a second order of the atomic perturbation theory) Feynman diagrams (whose contribution into the energy shift imaginary part (radiation width) for the multi-electron atoms accounts for multi-body correlation effects) is performed. The obtained data on the radiative transition wavelengths and oscillator strengths for some transition in spectra of the Li-like multicharged ions are analyzed and compared with alternative theoretical and experimental results.

**Keywords:** Relativistic many-body perturbation theory – Optimal one-quasiparticle representation – Oscillator strengths – Energy approach – Correlation corrections

PACS 31.15.A-;32.30.-r

*О. Ю. Хецелиус, А. Л. Михайлов, Э. А. Ефимова, Р. Э. Серга*

## СВЕРХТОНКАЯ СТРУКТУРА ТЯЖЕЛЫХ АТОМОВ В РАМКАХ РЕЛЯТИВИСТСКОЙ МНОГОЧАСТИЧНОЙ ТЕОРИИ ВОЗМУЩЕНИЙ

### Резюме

Релятивистская многочастичная теория возмущений с оптимизированным нулевым приближением Дирака-Кона-Шэма применена для расчета длин волн радиационных переходов и сил осцилляторов для некоторых Li-подобных многозарядных ионов. Релятивистские, обменно-корреляционные и другие поправки учитываются в рамках последовательных процедур. Оптимизированный базис релятивистских орбиталей генерируется в последовательном нулевом приближении релятивистской многочастичной теории возмущений, исходя из условия выполнения принципа калибровочной инвариантности. Предложена процедура аккуратного учета вкладов, описываемых диаграммами Фейнмана четвертого порядка КЭД теории возмущений (второй порядок атомной теории возмущений), в мнимую часть энергетического сдвига атомных уровней (радиационные ширины) многоэлектронных атомов с целью учета многочастичных корреляционных эффектов. Полученные данные о длинах волн радиационного перехода и силах осциллятора для некоторого перехода в спектрах Li-подобных многозарядных ионов анализируются и сравниваются с альтернативными теоретическими и экспериментальными результатами.

**Ключевые слова:** Релятивистская многочастичная теория возмущений – оптимальное одноквазичастичное представление – Силы осцилляторов – Энергетический подход – Корреляционные поправки

PACS 31.15.A-;32.30.-r

*О. Ю. Хецелиус, О. Л. Михайлов, Е. О. Ефимова, Р. Е. Серга*

## **НАДТОНКА СТРУКТУРА ВАЖКИХ АТОМІВ В РАМКАХ РЕЛЯТИВІСТСЬКОЇ БАГАТОЧАСТИНКОВОЇ ТЕОРІЇ ЗБУРЕНЬ**

### **Резюме**

Релятивістська багаточастинова теорія збурень з оптимізованим нульовим наближенням Дірака-Кона-Шема застосована для розрахунку довжин хвиль радіаційних переходів і сил осциляторів для деяких Li-подібних багатозарядних іонів. Релятивістські, обмінно-кореляційні та інші поправки враховуються в рамках послідовних процедур. Оптимізований базис релятивістських орбіталей генерується в послідовному нульовому наближенні релятивістської багаточастинової теорії збурень, виходячи з умови виконання принципу калібрувальної інваріантності. Запропоновано процедуру акуратного урахування вкладів, описуваних діаграмами Фейнмана четвертого порядку КЕД теорії збурень (другий порядок атомної теорії збурень), в уявну частину енергетичного зсуву атомних рівнів (радіаційні ширини) багатоелектронних атомів з метою врахування багаточастинових кореляційних ефектів. Отримані дані по довжинам хвиль радіаційних переходів та силам осциляторів для деяких переходів у спектрах Li-подібних багатозарядних іонів, які порівнюються з альтернативними теоретичними і експериментальними результатами.

**Ключові слова:** Релятивістська багаточастинова теорія збурень – Оптимальне одноквазичастичное представлення – Силы осциляторов – Энергетичний підхід – Кореляційні поправки

*S. S. Kulikov, Ye. V. Brytavskiy, M. I. Kutalova, N. P. Zatovskaya,  
V. A. Borshchak, N. V. Konopel'skaya, Y. N. Karakis*

Odessa I. I. Mechnikov National University, 2, Dvoryanskaya str,  
ph. 723-34-61, e-mail: photoelectronics@onu.edu.ua

## THE STUDY OF CADMIUM SULFIDE HETEROGENEOUSLY SENSITIZED CRYSTALS. PART II. RELAXATION CHARACTERISTICS

The photoelectric properties of CdS crystals with combined doping has been considered. The relaxation of the photocurrent determined by the long-term (months) redistribution of the sensitive impurity has been found. The possibility of creating of a new type of light sensors with super long memory has been shown. The medium-time (minutes) and fast (seconds) relaxation of the photocurrent under excitation by intrinsic and infrared light has been studied.

This article is a continuation of the review [1]. For the sake of maintaining wholeness the numbering of sections were selected transparent. References in each article are given individually.

The term «Heterogenic» is understood in two senses.

Firstly, the process of tactile sensing Bube-Rose you must have at least two classes of centers – R (slow recombination) and S (fast recombination). Moreover, each of these groups may consist of several physically different types. The condition of predominance of concentration of one of the classes  $N_R > N_S$  or  $N_R < N_S$  creates some features considered in Part I.

Secondly, under the influence of external factors (electric field, light, temperature), spatial redistribution of the sensitive centers is possible. This creates a number of specific effects, discussed below, which are impossible in samples with uniform doping.

### 3.1. Long-term (hours) migration-dependent relaxation of photocurrent

After pre-lightings of the samples with our own light and long (2-3 months) stay in the dark, we observed almost complete absence of photosensitivity [2,3,4,5]. Then the photosensitivity was restored for several days, while the crystals were exposed to monochromatic light

with a wavelength of 515 nm [6]. The process passed independently of the duration or the number of lightings and remained the same even under lighting for 20 minutes once a day [7,8]. The rate of recovery of photosensitivity turned out to be the maximum at first, then the increase decreased. After about 100 hours, the photocells stabilized and no longer responded to daily lightings.

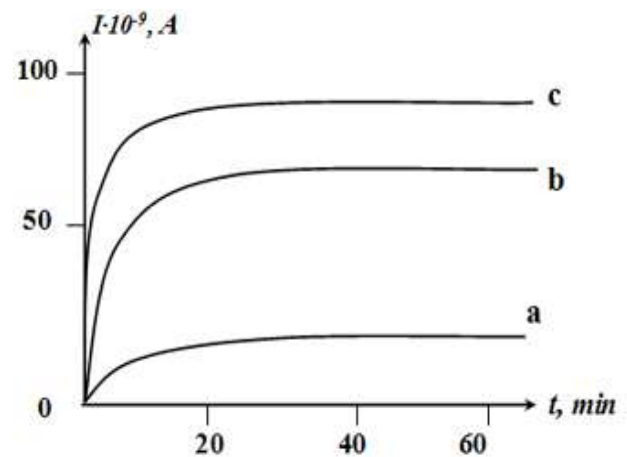


Fig. 3.1 Relaxation of the photocurrent after exposure in the dark for 3 months (curve "a"), then five days ("b") and two days ("c").

At the same time, there was a certain limit level of sensitivity, which could not be exceeded, regardless of the time of illumination, both one-time and total.

The type of relaxation curve depended on the applied field strength. Moreover, if a simple decrease in the applied voltage did not make fundamental changes in the shape of the curve, only reducing the corresponding currents, then an increase in the distance between the contacts to 2 mm at a displacement on the sample was still 50 V led to a modification of the initial stage of changes-at small times of less than 10 min, a section of relatively slow current increase appeared and the relaxation curve as a whole acquired an S – shaped form. Characteristically, in this case, although the strength applied field is decreased approximately four times, the value of flowing current decreases disproportionately, accounting for roughly half of the original value on the plot of saturation after relaxation in 35 – 40 minutes.

The samples had a strong effect of infrared quenching of photocurrent. Even with not very large values of the ratio of the intensity of the quenching light to the intensity of the exciting, the value of the IR quenching coefficient  $Q$  easily reached 100 %. The spectral distribution curve  $Q(\lambda)$  was typical with two maxima at 1080 and 1400 nm (0.9 and 1.1 eV, respectively).

At temperatures of large 40 – 50 °C for the excitation intensities used, the effect of temperature quenching of the photocurrent with standard characteristics was observed.

The presence of both types of quenching indicates the presence of S – and R – centers of comparable concentrations in the crystal, and the absolute value of the number of centers of each class should be significant.

Since the described situation is close to the existing model with moving S-centers, we have put a special selective experiment. After completion of the relaxation process is already in a sensual state (curve "b,, Fig. 3.1) the polarity of the applied field was reversed.

If the observed phenomena are associated with the migration in the sample of light-charged defects, which play the role of centers of rapid recombination and their gradual accumulation in the anode, then such processes should be expected:

When changing the sign of the pulling field (the light continues to operate and, therefore, the centers retain the charging state), the defects

must migrate in the opposite direction. During the time comparable with the time of the previous relaxation, they first dissipate over the crystal (due to the spread of mobility and fluctuations of the diffusion jumps of  $V_{Ca}^-$  vacancies). The sample returns to the pre-relaxation state with low sensitivity. And then, even for the same period of time, there is a spatial repolarization of S-centers with their accumulation at the opposite contact.

Instead, we observed a slight change in the photocurrent within 20-25 minutes no more than 10 – 20 % of the initial value. Given the inefficient process of moving S-centers through the crystal grate as already noted, such time intervals are completely inadequate diffusion of defects of this type.

Thus, the features of the time dependence of the current require to exclude from consideration in our case the movement of S-centers. The difference between this model and the situation under study is the state of contacts to the sample. The study of the light current-voltage characteristics both at different moments of relaxation (instantaneous or almost instantaneous values) and in a stationary, sensitive state, indicates the presence of locking barriers in the entire temperature range and the light intensities used. The curves of the current-voltage characteristic had the form typical for the reverse branches of the diodes. Moreover, we are talking about both contacts, since there were no fundamental differences in the applied voltage at opposite polarities.

The non-ohmic contact with the crystal is also reflected in the volt-farad dependencies. During the measurement times excluding the diffusion of impurities, in the case of anti-lock contacts, the sample capacity should not change at all with the applied voltage. Instead, we observed a volt-farad dependence, although not straightening in standard coordinates  $C^{-2}(U)$ .

With the increase in temperature, the relaxation process was revived. However, it seems anomaly practically no differences in the graphs in the temperature range from slightly increased to 80 °C.

Contrariwise, temperature rise has proved to be an effective way of returning cadmium sulfide crystals to photosensitivity. Even after long exposure in the dark (situation of “a” Fig. 3.1) as a result of subsequent heating (without photoexcitation and voltage) at a temperature of 40 °C for 4 to 6 hours, the crystal passed to the state characteristic of the dependence “b” Fig. 3.1. At the same time, no accumulation from the photo effect was observed. However, even in this case, we could not achieve an improvement in the transfer of the sample to a state with increased photosensitivity by simply increasing the temperature. The effect of infrared light on our crystals also increased their photo response to their own excitation after a long stay in the dark. The combination of a small heating and IR – effect almost completely removed the relaxation of the photocurrent.

Since the investigated chronological dependence of the current in the samples occurred under the conditions of photoexcitation with the simultaneous presence in the electric field, it was of interest to study the effect of each of these effects individually.

Curve “a” in fig. 3.2 measured under the same conditions as the curve “a” in fig. 3.1 and transferred here as a reference. Curves “b” and “c” in Fig. 3.2 is obtained according to the scenario based on “c” Fig. 3.1 however, an additional stage has been introduced. The sample was kept for one hour either in a light without a field or in the dark but under voltage.

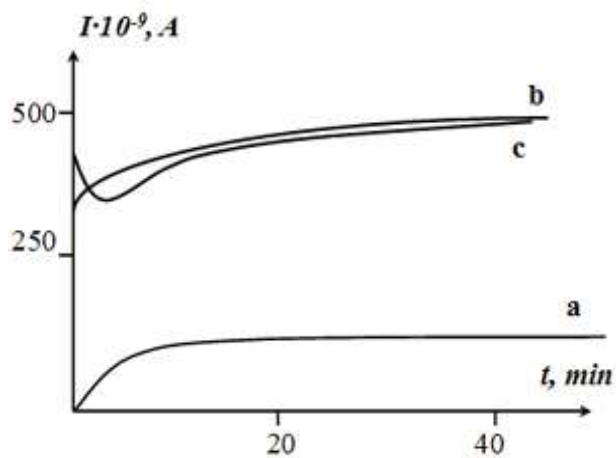


Fig. 3.2 Discrete process impact.

As can be seen from the figure, the introduction of such an additional effect significantly modifies the relaxation graph. In both situations, an initial conduction spike appears, the causes of which are discussed below.

The totality of the data obtained was interpreted as follows.

Direct experiments have proved the presence of S – and R-centers in the studied crystals. The observed duration of current relaxation excludes purely electronic interpretations. At the same time, these intervals are too small, as shown earlier, to participate in the processes of rapid recombination centers. Therefore, in consideration of the concentration changes are introduced for R – centers.

When the external voltage is turned on, the role of the pelotons from the R-centers at the contacts is different. Let the field be directed in such a way that it causes the charged R-centers to move from right to left. Then the left contact centers are compacted and would have to lower the height of this barrier. But at the same time, since its intensity coincides with the external field, it must increase. Because of this competition, the changes taking place here practically do not affect the relaxation of the current of photo excited carriers.

The right peloton has a significant impact. The external field pulls out of it the sensitive centers from a potential hole in the middle part of the crystal, significantly increasing the life time of the main carriers. From the outside, this is manifested in the form of current relaxation. While remaining small due to shut-off contacts, it nevertheless increases from  $10^{-10} - 10^{-9}$  A to  $10^{-7}$  A (Fig. 3.1). It is obvious that the barriers are approximately symmetrical, the effect is insensitive to the sign of the applied voltage. When the polarity changes, the left and right barriers change roles.

This also explains the indifference to the sign of the field after the relaxation. A small decline here may be due to the fact that some of the free R-centers of the middle band of the crystal (see Fig. 3.4) goes faster to your contact that they are replaced with the held field R-centers of the opposite potential well. It is clear that the

longer the Central part, the less influence the field injection of the sensitive centers has on it.

It is clear that the longer the Central part, the less influence the field injection of the sensitive centers has on it. Especially in the initial periods of time, while the concentration of additional agents here is small.

Especially in the initial periods of time, while the concentration of additional agents here is small. Having a depth of about 1 eV, R-centers are capable of holding captured non-equilibrium holes at room temperature for a long time. This, obviously, determines the processes of redistribution of the concentration of the sensitive centers after the light is turned off (Fig. 3.1), if the time spent in the dark was not too long. We see this as a “remembering” the previous crystal effects.

The developed concept easily explains why the increase in stationary current decreases with increasing lighting cycles. At first, when there are many centers in the SCR, their transition to the central part is massive. In descending order of their concentration in the SCR for the subsequent cycles of illumination, the intensity of all the considered processes decreases. The photocurrent is higher due to the sensitive action of R-centers, while the subsequent relaxation is more lively (curves “b” and “c” Fig. 3.1). Limit relaxed sensitivity to external influence in this case is limited to the total concentration of R-centers. No combination of effects on the crystal can increase its conductivity in our model, if all the sensitive centers from the contact area are already involved, which could take part in these processes (curve “c” Fig. 3.1).

Obviously, heating increases the mobility of the centers and accelerates relaxation. However, with increasing temperature there is a competing process – due to the thermal emptying of traps, part of the R-centers, losing charge, ceases to respond to the external field.

The same action produces IR radiation. This explains its ability to return to crystals sensitivity in combination with a small heating. R-centers in those conditions is a Central part of the crystal, sensing it due to the usual mechanisms of diffusion due to concentration gradients from the contacts to the center. Current surges at the

initial moments of time in Fig. 3.2 (curves “b” and “c”) have different nature. With the preliminary influence on the crystal field in the dark, we lower the height of the barrier, the intensity of which is opposite to the external. He is no longer able to hold R-centers in a potential pit and there is a perception of the crystal (curve “b” Fig. 3.2). On the contrary, if the crystal was exposed to illumination without a field, in both contact SCR appear R-centers, captured no equilibrium holes. Because of their charge they lower retaining their intensity of the internal fields, the injection of excess with the appropriate sensitizing. Because both areas at the same time participate in sensitizing, the magnitude of the emission is somewhat larger (Fig. 3.2, curve “c”).

In conclusion, we indicate several ways of recycling the discovered patterns [10]. The relaxation process itself allows the use of CdS samples with locking contacts as timers for tens of minutes. The process of returning to balance, which has lasted for dozens of days, allows for the implementation of long-term devices. In turn, since both processes-increasing relaxation in their own light and their dark aging depend from temperature and IR effects, it is possible to create appropriate sensors with memory. In addition, the relaxation process itself is dependent on the previous exposure to white light, which allows the use of such samples as photoreceptors for illumination.

### **3.2. Average time (minutes) relaxation of the photocurrent in crystals with inhomogeneous focus**

Because the barriers in contacts play an important role in the implementation of long-term relaxation of the photocurrent, it was of interest to strengthen this effect. To do this, the contacts were shifted to 0,1-0,2 mm. In this case, the interelectrode distance is comparable in magnitude to the SCR width. Thus, the contact barriers and the processes taking place there become current controlling. An unusual form of photocurrent relaxation was found on crystals with a small distance between the contacts after staying in equilibrium conditions [5,11].

With a small level of its own lighting (1-3 lx), the photocurrent was installed in a few minutes. For large illuminances (10-15 lx) the photocurrents first also increased during 3-4 min (1 stage); then during the time up to 15 minutes ~ 30 % (2 stage) decreased; and later returned to the same value and stabilized during the period of 45-50 minutes.

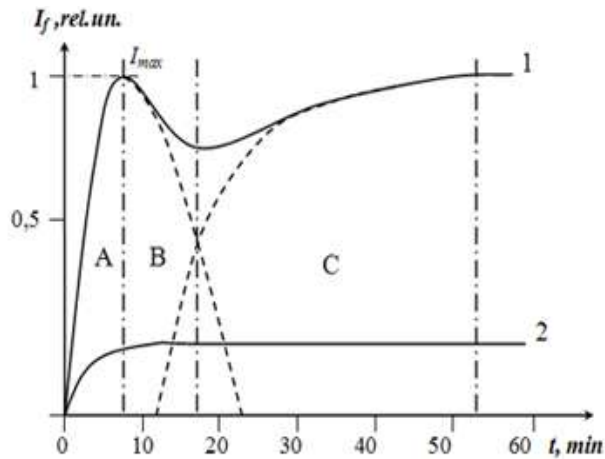


Fig. 3.3. Relaxation of own photocurrent at the level of illumination: (1) – 10-15 lx and (2) – 1-3 lx.

When illuminated with its own light (515 nm) in the sensitive samples CdS have been long time relaxation of the photocurrent in the range of 50-60 min (Fig. 3.3).

Typically, that at low light the photocurrent stabilized within 10 minutes. When the light flux was increasing, a disproportionate increase in the photocurrent occurred. With the increase in the order of the level of illumination, the magnitude of the photocurrent increased only several times. This indicates the flow of several competing processes in the crystal.

In addition, for some crystals, relaxation was accompanied by a decrease of the photocurrent for 10 to 15 minutes. And then the restoration of its value for the period of about 40-50 minutes.

Times like these flowing processes exclude purely electronic interpretation and are typical for migration-ionic phenomena. It was also shown that in the fields  $10^4 - 10^5$  V/sm it is possible to move the impurity ions along the crystal grate. When the barrier height is about 1 eV and the width is  $\sim 1 \mu\text{m}$ , it is possible to reaching such fields in the contact areas of crystals.

At the same time, the fields of the barriers are directed in such a way that they contribute to the outflow of the negatively charged impurity to the Central part and the extraction of the positively charged impurity to the SCR contacts.

In the first approximation for the present consideration it is assumed that in the electric field used the distribution of S-centers remains uniform. They cannot have any noticeable mobility to move around the crystal grate. On the contrary, the R-center is copper in the cadmium sublattice, which is able to move relatively easily through the crystal.

According to the Baby-Rose model, R-centers create levels in the forbidden zone with a depth of 0,9-1,1 eV. It is obvious that in equilibrium conditions, capturing their own holes, these centers are able to hold them for a long time. At the same time, as shown in chapter 2.1 (part I), they charge positively. Under these conditions, under the action of Schottky barrier fields, they are extracted from the crystal areas of the width of the order of diffusion length from the inner boundary of the barriers and the accumulation of this impurity in the SCR contacts.

In General, the distribution of the concentration of R-centers takes the form, as shown in Fig. 3.4. As a result of sluggish recombination processes, some of these centers lose their charge. Therefore, under equilibrium conditions, the concentration of charged  $N_2^+$  centers in the contact areas is much less than their total concentration of  $N_2$ .

When exposed at the same time its own light and external voltage to the crystal (Fig. 3.3) the situation in the crystal changes. Let's first consider the initial state of the contacts.

In the dark, in conditions  $N^+ < N$ , the charge in the SCR is concentrated on ionized donors. Since the barrier is locking, the influence of free electric charge is neglected. Then

The potential distribution in the SCR is found from the Poisson equation

$$\frac{d^2 \varphi}{dx^2} = \frac{4\pi e^2}{\varepsilon} N_d, \quad (3.1)$$

the standard solution is:

$$\varphi(x) = \frac{2\pi e^2}{\varepsilon} N_d (L-x)^2. \quad (3.2)$$

The value  $L$  in (3.2) sets the width of the SCR at the equilibrium height of the barrier  $\varphi_0$ :

$$L_{dark} = \sqrt{\frac{\varepsilon}{2\pi e^2} \frac{1}{N_d} \varphi_0}. \quad (3.3)$$

When the light intensity is high, the condition  $N^+ < N$  is violated. R-centers, already located in the SCR and distributed there evenly, capture appeared in a large number of no equilibrium holes and are completely ionized. We used high-resistance crystals. Consequently, the concentration of donors is low. At the same time, a bright effect of infrared extinction indicates the presence of a large concentration of second-class centers. As a result  $N_2^+ = N_2 \gg N_d$ .

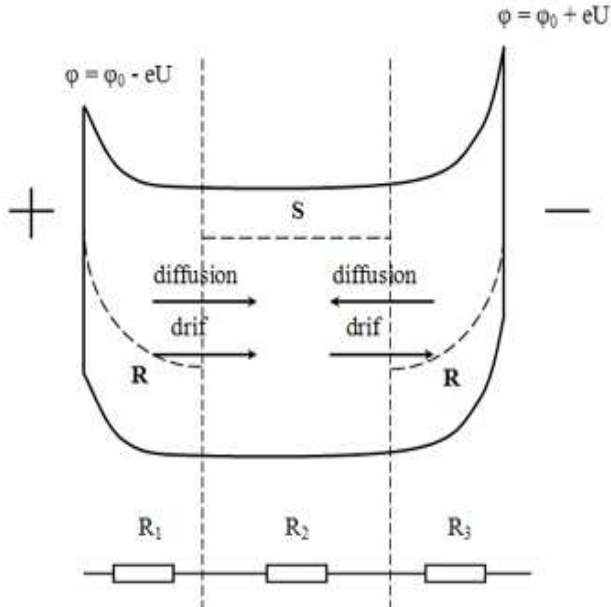


**Fig. 3.4. Migration processes in the crystal in the light under the influence of the field.**

Positive charge in the SCR is now fixed on R-centers and formulas (3.2) – (3.3) are modified:

$$\varphi_{big}^{illum}(x) = \frac{2\pi e^2}{\varepsilon} N_2 (L-x)^2; \quad (3.4)$$

$$L_{big}^{illum} = \sqrt{\frac{\varepsilon}{2\pi e^2} \frac{1}{N_2} (\varphi_0 - eU)}. \quad (3.5)$$

Here it is taken into account that under the influence of external voltage the height of the barrier has decreased to a value  $\varphi(0) = \varphi_0 - eU$ . It will be shown below that the changes on the second barrier increasing in the same field are insignificant.

Formulas (3.3),(3.5) allow to explain the increase in the photocurrent in the region “a” Fig. 3.3.

It is seen that the light width of the barrier (3.5) because of the conditions decreased in comparison with the black values (3.3). At the same time it became lower.

Resistance  $R_1$  (Fig. 3.4) this part of the crystal decreases. The current grows. Because processes are limited only by the time the traps are captured, changes occur quickly.

However, the processes that occur with the barrier (in Fig. 3.4-left), more harder. If light quanta are small, then a small concentration of non-equilibrium holes is created. In SCR of the contact they distributed according to the law:

$$\Delta p(x) = \Delta p \exp\left[\frac{\varphi(x)}{kT}\right], \quad (3.6)$$

Where  $\Delta p$  – is the concentration of holes at the bottom of the barrier;  $\varphi(x)$  - potential distribution. As a criterion of low light we choose

$$\Delta p \exp\left[\frac{\varphi(x)}{kT}\right] < N_2. \quad (3.7)$$

That is, at any point in the barrier holes are not enough to fill all the R-centers. Under these conditions, a fixed positive charge is the holes, according to (3.7) captured on the R-centers

$$\rho = eN_2^+(x) = e\Delta p \exp\left[\frac{\varphi(x)}{kT}\right]. \quad (3.8)$$

Then the Poisson equation has the form:

$$\frac{d^2\varphi}{dx^2} = \frac{4\pi e^2}{\varepsilon} \Delta p \exp\left[\frac{\varphi(x)}{kT}\right]. \quad (3.9)$$

or:

$$\frac{d^2z}{dx^2} = A \exp(z), \quad (3.10)$$

where

$$z = a\varphi; \quad A = \left(\frac{4\pi e^2}{\varepsilon} \Delta p\right) \frac{1}{kT}; \quad a = \frac{1}{kT}. \quad (3.11)$$

Integration (3.10) gives:

$$\left(\frac{dz}{dx}\right)^2 = 2A[\exp(z) - 1]. \quad (3.12)$$

The equation (3.12) requires numerical integration. However, it can be simplified. The condition (3.7) assumes a small number of holes at the sole of the barrier and, accordingly, a small charge at the centers of the sensitivity. In other words, the far edge of the barrier again depends on ionized donors:

$$\Delta p(L) \exp\left[\frac{\varphi(L)}{kT}\right] < N_d^+. \quad (3.13)$$

Here, small levels of illumination and a small barrier potential are taken into account

$\varphi(L) \rightarrow 0$ . Thus, the barrier now consists of two parts, most of which are subject to (3.12), and the edge is defined similarly (3.2). To estimate the width of the SCR of such a barrier is sufficient to use (3.12) in the conditions

$\gg$

Then

$$\frac{dz}{dx} = \pm \sqrt{2A} \exp\left(\frac{z}{2}\right). \quad (3.14)$$

In all of the SCR with the increasing coordinate value, and hence  $z$ , is decreasing (see Fig. 3.4, left barrier). Then, in (3.14), the “+” sign should be discarded as having no physical meaning. We have in view (3.11)

$$\exp\left(-\frac{\varphi}{2kT}\right) = \sqrt{\frac{2\pi e^2 \Delta p}{\varepsilon kT}} (x - L_1) + 1. \quad (3.15)$$

It is not difficult to obtain an explicit form of potential distribution

$$\varphi = 2kT \ln \left[ \frac{1}{1 - \sqrt{\frac{2\pi e^2 \Delta p}{\varepsilon kT}} (L_1 - x)} \right], \quad (3.16)$$

moreover, because of the conditions (3.7), equation (3.16) still need to sew with (3.2). However, (3.15) is sufficient to estimate the width of the

SCR. On the left border, at

$$\exp\left(\frac{\varphi_0 - eU}{2kT}\right) = 1 - \sqrt{\frac{2\pi e^2 \Delta p}{\varepsilon kT}} L_1. \quad (3.17)$$

It is taken into account that voltage is applied together with the light (as shown in Fig. 3.4), which lowers the height of the barrier. And

- is only part of the barrier, although large, which is determined by the charge captured on the R-centers:

$$L_1 = \frac{1 - \exp\left(-\frac{\varphi_0 - eU}{2kT}\right)}{\sqrt{\frac{2\pi e^2}{\varepsilon} \Delta p} \frac{1}{kT}}. \quad (3.18)$$

Calculate, taking into account (3.5) for large levels of illumination, the ratio

$$\frac{L_1}{L_{big}^{illum}} = \frac{1 - \exp\left(-\frac{\varphi_0 - eU}{2kT}\right)}{\sqrt{\frac{\varphi_0 - eU}{kT}}} \cdot \sqrt{\frac{N_2}{\Delta p}} \quad (3.19)$$

Or applying (3.13),

$$\frac{L_1}{L_{big}^{illum}} > \frac{\exp\left(\frac{\varphi_0 - eU}{2kT}\right) - 1}{\sqrt{\frac{\varphi_0 - eU}{kT}}}. \quad (3.20)$$

And the equation for  $\varphi(x)$  solved, due to the condition  $\exp\left[\frac{\varphi(x)}{kT}\right] \gg 1$  for large barriers.

Therefore, the unit in the numerator (3.20) can be discarded. It is obvious that any exponent with an exponent greater than one is greater than its degree. Therefore, finally,

$$\frac{L_1}{L_{big}^{illum}} > \sqrt{\frac{\exp\left(\frac{\varphi_0 - eU}{kT}\right)}{\frac{\varphi_0 - eU}{kT}}} \gg 1.$$

Here  $L_1$  – only part of the barrier in low light conditions. Finally

$$\frac{L_{small}^{illum}}{L_{big}^{illum}} \gg 1. \quad (3.21)$$

That is, at low light conditions the barrier, having the same height, is considerably broadened. And this is the second reason that the current on the curve 2 in the “A” region of Fig. 3.3 much less.

Note also that the  $N_2^+ = N_2 \gg N_d$  comparison of (3.3) and (3.5) follows  $L^{dark} > L_{big}^{illum}$ . At the same time, any appearance of a positive charge in the SCR in the light should reduce its width. Therefore, the logical chain of (3.3), (3.5) and (3.21) is built as  $L^{dark} > L_{small}^{illum} > L_{big}^{illum}$ . When lighting SCR width is reduced, and the more, the higher the light intensity. This is also consistent with (3.18) (  $L$  in the denominator) and (3.5).

Now let’s consider the influence of  $N_2^+$  on the formation of ion-coordination mechanisms.

For times of about tens of minutes (area “B” Fig. 3.3) the charged  $N_2^+$ -impurity can already be moved in the applied electric field. The fate of SCR at both ends of the crystal is different.

Let the polarity of the applied field be as shown in Fig. 3.4. Then it should cause outflow

$N_2^+$ -centers from the left barrier and increase

their concentration due to the drift component in the right. At the same time, since  $N_2^+$ -centers in the light are charged there and there, a diffusion outflow of the  $N_2^+$  centers from both contacts is formed. The figure shows that for the left barrier both reasons are formed, and for the right – compete with each other. As a result, the applied field and light cause much greater extraction of R-centers from the left contact to the Central part. In this case, its height is reduced by an external field. In the right contact, the outer field would have to raise the height. However, a much greater concentration of the residual

charge  $N_2^+$  - it lowers. Thus, the parameters of the right SCR are controlled by a set of mutually competing causes. In the first approximation, it can be considered stable and changes in Fig. 3.3 bind to the left contact only. The dominant mechanism for it is the broadening, as shown above. The height of this barrier can also be considered to be slightly changing, since the external field reduces it, and the departure of a positive charge  $N_2^+$  – increases it.

Thus, area "B" Fig. 3.3 controlled by only one process: the left SCR expands, its resistance increases, the current drops. This process will be the stronger the greater the light intensity. First, then there is more concentration of charged centers. And secondly, as can be seen from (3.21), the twilight lighting barrier and so wide. Its relative changes are much smaller. That is why we have not recorded a long-term decrease in the current on the curve 2 Fig.3.3.

Note that the change of polarity of the applied voltage does not change the picture. Just the barriers are reversed and their roles.

Extracting of contact of the SCR, the centers of tactile sensing include two other mechanisms beyond. Depending on the intensity of the light, as shown above, in the near-surface layer is more or less increased concentration captured on the centers of the positive charge. Accordingly, they leave this area under the influence of diffusion and drift. This should be accompanied by its expansion. This changes the length of the Central part of the crystal.

Since the total length of the crystal-the central part plus two contact areas-remains unchanged, the broadening of one of the contacts should inevitably lead to a narrowing of the central part. At the same time its electrical resistance ( at Fig. 3.4) decreases due to simple length reduction. The resistance of the entire tandem increases as part of the inter-electrode space has to be replaced by the high resistance region of the barrier.

This would have to lead to further stimulation to reduce the photocurrent. However, this process is superimposed on another.

Getting into the central part, R-centers are sensitive to it. At the same time, the life time of the main carriers can increase to five orders of magnitude. We were able to show (Chapter 2.1 Part I) that this will be when the concentrations of S - and R - centers are roughly compared:  $N_2 \sim N_1$ .

In turn, the increase in life time causes an increase in conductivity

$$\sigma = en\mu = e(f\tau)\mu . \quad (3.22)$$

Since the decrease in conductivity with the broadening of the barrier is approximately linear and even sublinear, and (3.22) accompanied by an avalanche increase, the current in the “C” figure. 3.3 increase as shown by dotted line. However, this process is longer. First, unlike area “B “and the more area” A” Fig. 3.3 it is called by several competing mechanisms. And secondly, a simple increase in the concentration of sensory centers in the sole of the SCR does not cause additional changes. It takes time for the resorption of the peloton of the R-centers on the crystal. This is what causes the asymmetry of the pit walls in relaxation in Fig. 3.3.

It is also obvious that in low light conditions these processes are absent (curve 2 Fig. 3.3). - centers are much smaller, and their addition in the Central part of the crystal is insignificant. In addition, the barrier is initially much wider [see (3.21)]. For relatively short samples, the SCR contacts in General can be gathered. Sensitive centers extract nowhere. It is with this that we connect the experimentally observed absence of an increase in the current in the area “C” of the curve 2 Fig. 3.3.

Note in conclusion that at the end of all the redistribution processes for the curve 1 Fig. 3.3 as expected, the current stabilizes again at the same level in the “C” area as in the maximum after the capture processes in the area “A”. This is not difficult to explain, given that just as many of the sensory centers have left the SCR, exactly the same amount eventually caused changes in the Central part of the crystal.

### 3.3. Experimental confirmation of mobile R-centers model

Thus, we link the peculiarities of relaxation processes of the own photocurrent in samples with two types of recombination centers with the redistribution of charged R-centers from the regions of the space charge in the contact parts of the crystals. To test this model, a special experiment was carried out to artificially change the concentration of such centers. Of course, it is quite difficult to model the physical amount of 1 ligand in the element under study.

However, in our case we are talking about the charged admixture after the capture of non-primary carriers. The number of holes located on the R-levels and providing a change of state [12], is easily regulated by infrared radiation in accordance with the model of the Bube-Rose. Long-wave photons, knocking holes from R-centers, return them to a neutral state, which completely excludes them from drift processes under the influence of an external field.

In addition, since the concentration of the ligand is, of course, much less than the number of basic atoms of the substance, the distance between the neighboring R-centers exceeds several translations of the crystal lattice. This means that the uncharged impurity practically does not interact with each other, which completely excludes the formation of diffusion flows. Thus, the use of IR radiation is a good modulating means for virtual change of the concentration of R-centers, turning them off from the ongoing processes (see also chapter 2.2 Part I).

Figure 3.5 shows the change in the relaxation curve when the crystal is exposed to additional infrared illumination. The curves were normalized to the maximum of the curve 1 photocur-

rent in the region of 10 minutes. It is seen that the additional effect of IR photons, and thus reducing the effective number of R-centers, completely eliminates the feature of the relaxation process with the formation of a cavity (area "B" Fig. 3.3). The photocurrent curve 2 Fig. 3.5 smoothly went to saturation for much longer times several times longer than the time to reach the maximum on curve 1.

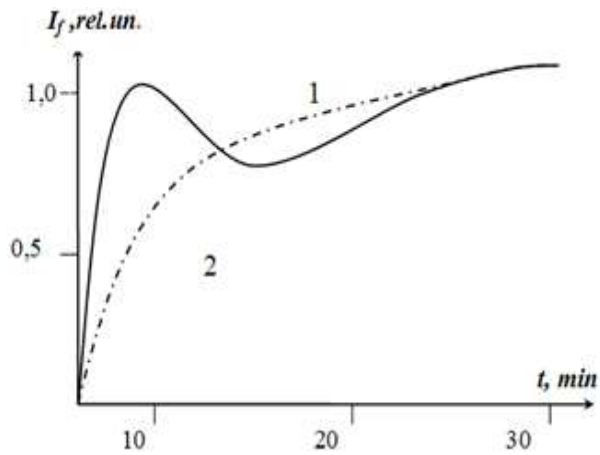


Fig. 3.5. Change of photocurrent with time under the action of only self-illuminating (1) and using IR illumination (2).

The absolute value of the photocurrent was almost an order of magnitude less than in the initial state without IR radiation. This is the expected result, given that under the action of IR radiation from SCR contact areas disappears fixed positive charge. In accordance with the conclusion of chapter 3.2, both barriers become higher and wider, the resistance  $R_1$  and  $R_3$  in the equivalent circuit Fig. 3.4 increases, the current drops.

### 3.4. Fast (seconds) relaxation of the photocurrent at excitation by own and infrared light

Long-term processes of spatial redistribution of impurities in the sensitive crystals described in sections 2.1 – 2.2 of Part I camouflage fast electronic relaxation. In this regard, it is of interest to study the changes of the photocurrent for the times excluding the influence of ion processes –  $10^1$ - $10^2$  sec, (tens of seconds, up to several minutes). For its observation, the samples were kept for a long time in their own light. The situ-

ations considered in this section occur [8] under already established conditions of dynamic equilibrium and correspond to the ends of the graphs Fig. 3.1 and 3.3.

The sample was illuminated with its own light of different intensity. The luminous flux was regulated stepwise by varying the annular diaphragms in the region of the focusing lens. Usually, the relaxation of the photocurrent is measured from the initial state, i.e. darkness, to a fully steady state, i.e. saturation on the  $I_f(t)$  chart. At the same time, they are limited to someone fixed light intensity. Note that the proposed method for the first time to study the comparative changes in the relaxation of the photocurrent with a step change in the intensity of light has a number of advantages over the traditional excitation of "dark  $\rightarrow$  full light" or "light  $\rightarrow$  dark". This is especially noticeable for complex capture centers, such as R-centers, with the possibility of internal transitions to excited  $R'$  states.

In the traditional method, a large number of photons with a wavelength from the self-absorption band appear at once and at the same time a huge number of non-basic carriers are formed, which are able to fill both the main and excited States of the R-centers from the V-zone. Redistribution processes between them are simply not included.

If the photoexcitation and disappears immediately to zero, the effective S-centers of a large concentration of free carriers take to recombine. Against the background of this intensive process, weak amendments related to changes in the population of the R and  $R'$ , and even more so, its redistribution between them, are not noticeable.

And of course, apply low light, when the concentration of non-equilibrium charge will be less than the number of free places on the impurity levels. However, since both the concentration of recombination S-centers and the concentration of capture traps for holes are not known in advance, groping for this ratio will lead to the same stepwise method.

The process of changing the flowing current consists of at least two fundamentally differ-

ent phases. At the initial stage, the photo excitation of free media is carried out (area I Fig. 3.6), most of which go to fill existing traps and recombination centers. In the studied sensitive crystals, there are definitely at least effective R-centers for this. The usual mechanisms of perception due to redistribution of carriers between the centers of the first and second classes, and even more so, the center-to-center distribution between R and R' centers have not yet been included. Especially for small light intensities, when the number of photons absorbed is less than the concentration of traps, the non-equilibrium charge capture process dominates. The conditions for the formation of the photocurrent are unfavorable.

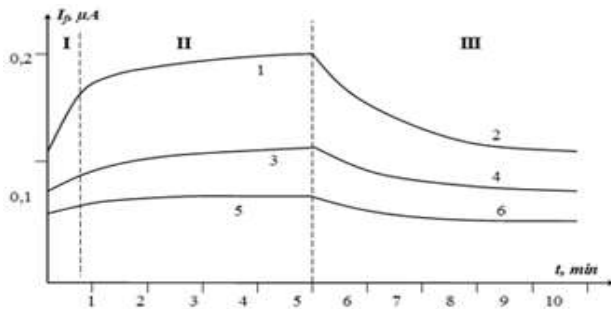


Fig. 3.6. The kinetics of infrared quenching of photocurrent in the high quenches at wavelengths of 1100 nm (1) and 1380 nm (2).

1. – from 4,25 to 9,8 lx;
2. – from 9,8 to 4,25 lx;
3. – from 1,35 to 4,25 lx;
4. – from 4,25 to 1,35 lx;
5. – from 0,6 to 1,35 lx;
6. – from 1,35 to 0,6 lx.

On the contrary, the final stages of relaxation take place in the conditions of quasi-steady equilibrium between the capture-release processes. For our samples, this is done for at least four channels: in addition to the always present adhesion centers, recombination at the S-centers, captures and emissions from the ground and excited States of the R-centers and intra-center transitions between them.

It is this complex ensemble of interactions that mainly represented the subject of research. Therefore, the measurements were carried out under conditions of the existing intensity of the

natural light and the steady-state photocurrent in the transition to higher illumination [13]. For the moment  $t=0$  inclusion of additional light was accepted (Fig. 3.6).

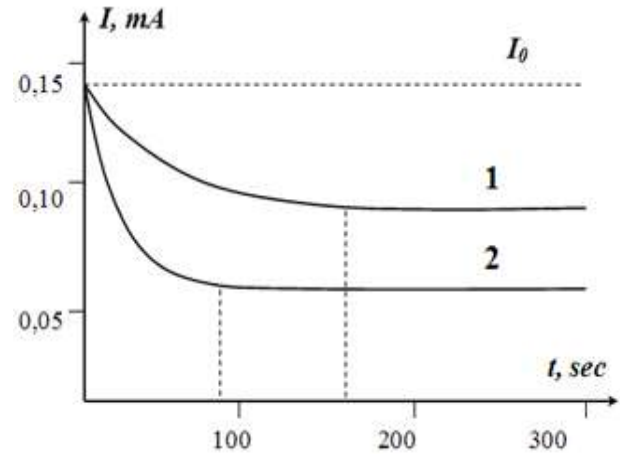


Fig. 3.7. The kinetics of infrared quenching of photocurrent in the high quenches at wavelengths of 1100 nm (1) and 1380 nm (2).

The measurement results were compared with the reverse process, when the illumination returned to its original value. In this case, the determining process becomes a competing-the centers are emptied.

Indeed, the measurements under low illumination, we observed a relatively tight region of the exit to the plateau of the graph  $I_f(t)$ . At the same time, the decreasing relaxation was faster.

For transitions from smaller to larger illumination at large light fluxes, in addition to the natural increase in the absolute values of the photocurrent, the increasing part increased slightly in time. This is because it is not determined by the parameters of light, and the presence of empty spaces on the traps. The decaying part of the  $I_f(t)$  dependence was delayed to a greater extent because it was determined by the large charge accumulated on the traps.

Finally, for relatively high light intensities, as seen in Fig. 3.6, the magnitude of the photocurrent itself depended on the intensity of the light used. The kinetics of its change-both increasing and decreasing, since the time of about two minutes, became more and more identical. With visual superposition of graphs at light intensities

of more than 10 Lux, these parts of the curves coincided.

In addition, it is characteristic that the value of the relaxation interval for the recession (Fig. 3.6 area III) also increased with increasing light intensity.

Short-term plot, less than 2 minutes, was dependent on the temperature at which the measurement was made. The absolute values of the current with increasing temperature decreased both in the saturation region and the current value. In order to exclude the collapse reduction of currents associated with the effect of temperature quenching, not considered in this work, the temperature change region was used below 50-60 °C, characteristic for the beginning of T-quenching. The increase in temperature led to a noticeable recovery of relaxation by 2-3 times. Given the seconds of the duration of the evolutions of the current, we connected the observed variation exclusively with electronic processes. In contact with own light on the sample there is a release of no equilibrium charge carriers. A number of them take part in the formation of the photocurrent. And a significant part, especially in the initial moments of time, goes to fill deep traps. It is obvious that the number of such captured carriers on the traps is large at first, because the traps were empty. But over time it is reduced as the traps are filled. This ensures an increase in the proportion of carriers remaining in the free state with a corresponding relaxation increase in the photocurrent.

At the same time, it is superimposed by a competing process – as the traps are filled under the influence of temperature, the number of thermally ejected carriers increases. In General, the presence of equilibrium is characterized by the approximate equality of the flows of captured and discarded carriers from the traps. As the temperature increases with the same capture intensity, the number of thermal emissions increases. This provides a more rapid achievement of the saturation current.

As noted, when excited by its own light, the formation of the photocurrent is controlled by the recombination processes at the S-centers. The role of R-centers can be made decisive, if you do otherwise-without changing the current

intensity of this light, turn on the infrared. The relaxation curves of the effect of infrared quenching of the photocurrent, not studied earlier, are shown in Fig. 3.7. To observe the relaxation of the photocurrent under the influence of radiation from the long – wave part of the spectrum, the wavelengths corresponding to the damping maxima of 1100 and 1380 nm were used. Optimal values of the Eigen frequency and quenching light intensities were chosen in accordance with [14] – [17] (see chapter 1.1. Part I).

With an ongoing and exciting light, when the photocurrent  $I_0$  achieved relaxation, including infrared light, pre-set to the wavelength of the corresponding maximum damping and started time dependence of the photocurrent.

Both curves start from a single point corresponding to the value of the self-excitation. When the infrared illumination is switched on, the photocurrent is quenched and its value decreases-and the curve 1 corresponding to the wavelength of the short-wave maximum (see Fig. 1.1. Part I) is above the curve 2 for the wavelength maximum and relaxes to the steady-state value longer.

This is explained as follows. Since there is a thermal transition from level R to level R', the probability of transition from this level is greater due to the greater population of the excited States. This determines that the curve 2 corresponding to the transition from levels R' is lower than the curve 1 corresponding to the transition from levels R.

As you can see from figure 3.7, curve 2 relaxes to steady value faster. This is due to only one process, namely-transitions from the levels R'. At the same time, the curve 1 is due to transitions from the levels R and R', plus thermal transitions within the centers of sensitivity from the ground to the excited States. In addition, there is a possibility of reverse capture of the hole from the valence band to the R-centers. In General, the existence of such a complex combination of processes and causes a more protracted front of the observed curve.

Thus, the considered model assumes a large population of R' level holes due to thermal transitions to them from the main state of R-centers.

## References

1. Simanovych N.S., Brytavskiy Ye.V., Kutalova M.I., Borshchak V.A., Karakis Y.N.  
The study of heterogeneous sensitized crystals of cadmium sulfide. Part I. About charge state of the centers recombination. // *Photoelectronics* – 2017. – n. 26. – s. 121–135.
2. Каракис К.Ю. Релаксационные характеристики полупроводниковых кристаллов с ИК-гашением фототока. // Одесса, Работа – лауреат Областного конкурса (3 место) Малой академии наук, Областное территориальное отделение, Секция “Физика”. Одесса – 2001. с. 1–37.
3. Ю.Н. Каракис, Н.П. Затовская, В. В. Зотов, М. И. Куталова Особенности релаксации фототока в кристаллах сульфида кадмия с запорными контактами // 1-а Українська наукова конференція з фізики напівпровідників. – Одеса, 10-14 вересня 2002. Тези доповідей. Т.2. – с. 138.
4. К.Ю. Каракис, В.А. Борщак, В.В. Зотов, М.И. Куталова Релаксационные характеристики кристаллов сульфида кадмия с ИК- гашением. // *Фотоэлектроника* 2002. – вып.11. – с.51 – 55.
5. Melnik A.S., Karakis Y.N., Kutalova M.I., Chemeresjuk G.G. Features of thermo-optical transitions from the recombination centers excited states. // *Photoelectronics* –2011. – n. 20. – s. 23–28.
6. Каракис Ю.Н., Борщак В.А. Затовская Н.П., Зотов В.В., Куталова М.И., Балабан А.П. Исследование релаксации фототока в полупроводниковом устройстве. // *Фотоэлектроника* – 2003. – №12 – с. 132 – 135.
7. Кочергіна А.А., Каракіс Ю.М. Деградація фоточутливості напівпровідників, зумовлена міграцією домішок. // Всеукраїнська конференція молодих вчених “Фізика і хімія твердого тіла. Стан, досягнення і перспективи”. 20 – 21 жовтня 2010 р. Волинський національний технічний університет. Тези доповідей. Секція 2. “Сучасні фізико-технічні аспекти напівпровідникових пристроїв”. Луцьк. – с. 212 – 217.
8. Софія Зіміна, Юрій Каракіс, Вікторія Федоренко Релаксаційні властивості фотоструму в монокристалах CdS // International Conference of Students and Young Scientists in Theoretical and Experimental Physics HEUREKA -2012. Book of abstracts. April 19-22– Lviv, Ukraine. – 2012 – s. D 19.
9. G.G.Chemeresyuk, Ye. V. Brytavskiy, Yu. N. Karakis (Ukraine) Infrared radiation sensor with selective controlled sensitiviti // The Ninth International Conference “Correlation Optics 2009” – Chernivtsi National University Chernivtsi, Ukraine. September 20 – 24. – 2009. Poster Session. Session 2 – D-2.
10. Кочергіна А.А., Каракіс Ю.Н., Ницук Ю.А. Датчики инфракрасного света на основе чувствлённых полупроводников // 4 nd International Scientific and Technical Conference “Sensors Electronics and Microsystems Technology” (СЕМСТ-4). Book of abstracts Секция VI “Радіаційні, оптичні, та оптоелектричні сенсори”. – Україна, Одеса, 28 червня – 2 липня 2010 р. ”– s. 100.
11. A.A. Dragoev, A.V. Muntjanu, Yu. N. Karakis, M. I. Kutalova Calculation for migration-dependent changes in near-contact space-charge regions of sensitized crystals. // *Photoelectronics*. – 2010. – n. 19. – s. 74 – 78.
12. Ye.V.Britavsky, Y.N.Karakis, M.I.Kutalova, G.G.Chemeresyuk On the charge state of rapid and slow re-

- combination centers in semiconductors // Photoelectronics. – 2008. – n. 17. – 2009. – n. 18 – s. 65 – 69.
13. Dragoev A.A., Ilyashenko A.S., Babinchuk V.S., Karakis Yu. N., Kutalova M.I. Features of photocurrent relaxation in sensor-based CdS crystals or features or features of photocurrent relaxation in crystals with fast and slow recombination centres // Photoelectronics. – 2012. – n. 21. – s. 110 – 115.
  14. Новикова М.А. (под научным руководством Ю.Н.Каракис) Особливості інфрачервоного гасіння фотоструму у напівпровідниках CdS. // Работа – лауреат Областного конкурса (1 место) Малой академии наук, Областное территориальное отделение, Секция “Физика”. Одесса, 2005 г., с. 1 – 37.
  15. M. A. Novikova Change of Photoelectric Properties of Semiconductors as a Tool for the Control of Environmental Pollution by Extraneous Admixtures and IR-illumination. // Section of Environmental Science. Finalist of Intel International Science and Engineering Fair. USA, AZ, Phoenix, May 8 – 18. 2005.
  16. Драгоев А.А., Затовская Н.П., Каракис Ю.Н., Куталова М.И. Управляемые электрическим полем датчики инфракрасного излучения. // Материалы 2 nd International Scientific and Technical Conference “Sensors Electronics and Microsystems Technology” Book of abstracts s. 115. Секция IV “Радіаційні, оптичні, та оптоелектричні сенсори”. Україна, Одеса, 26–30 червня 2006 р. “Астропринт”. 2006.
  17. M.A.Novikova, Yu.N.Karakis, M.I. Kutalova Particularities of current transfer in the crystals with two types of Recombination centers. // Photoelectronics- 2005. – n.14. – s. 58–61.

This article has been received in August 2018

UDC 621.315.592

*S. S. Kulikov, Ye. V. Brytavskiy, M. I. Kutalova, N. P. Zatovskaya, V. A. Borshchak,  
N. V. Konopel'skaya, Y. N. Karakis*

## **THE STUDY OF CADMIUM SULFIDE HETEROGENEOUSLY SENSITIZED CRYSTALS. PART II. RELAXATION CHARACTERISTICS**

The photoelectric properties of CdS crystals with combined doping are considered.

The relaxation of the photocurrent determined by the long-term (months) redistribution of the sensitive impurity is found. The possibility of creating a new type of light sensors with super long memory.

The medium-time (minutes) and fast (seconds) relaxation of the photocurrent under excitation by natural and infrared light are studied.

УДК 621.315.592

*С. С. Куликов, Е. Д. Бритавский, М. И. Куталова, Н. П. Затовская, В. А. Борщак,  
Н. В. Конопельская, Ю. Н. Каракис*

### **ИССЛЕДОВАНИЕ НЕОДНОРОДНО ОЧУВСТВЛЁННЫХ КРИСТАЛЛОВ СУЛЬФИДА КАДМИЯ. ЧАСТЬ II. РЕЛАКСАЦИОННЫЕ ХАРАКТЕРИСТИКИ.**

Рассмотрены фотоэлектрические свойства кристаллов CdS с комбинированным легированием.

Обнаружена релаксация фототока, определяемая долговременным (месяцы) перераспределением очувствляющей примеси. Указана возможность создания световых датчиков нового типа со сверхдолгой памятью.

Исследованы средневременная (минуты) и быстрая (секунды) релаксация фототока при возбуждении собственным и инфракрасным светом.

УДК 621.315.592

*С. С. Куліков, Є. Д. Бритавський, М. І. Куталова, Н. П. Затовська, В. А. Борщак,  
Н. В. Конопельська, Ю. М. Каракіс*

### **ДОСЛІДЖЕННЯ НЕОДНОРІДНО ЗЧУВСТВЛЕННИХ КРИСТАЛІВ СУЛЬФІДУ КАДМІЮ. ЧАСТИНА II. РЕЛАКСАЦІЙНІ ХАРАКТЕРИСТИКИ.**

Розглянуті фотоелектричні властивості кристалів CdS з комбінованим легуванням.

Виявлена релаксація фотоструму, що пов'язана з довготривалим (місяці) перерасподілом зчувствляючої домішки. Вказана можливість створення світлових датчиків нового типу з сверхдовгою памятью.

Досліджена середньотривала (хвилини) і швидка (секунди) релаксація фотоструму при збудженні власним і інфрачервоним світлом.

*A. A. Kuznetsova<sup>1</sup>, A. A. Buyadzhi<sup>2</sup>, M. Yu. Gurskaya<sup>2</sup>, A. O. Makarova<sup>2</sup>*

<sup>1</sup> National University “Odessa Maritime Academy”, Didrikhson str. 8, Odessa, Ukraine

<sup>2</sup> Odessa State Environmental University, L’vovskaya str. 15, Odessa, 65016, Ukraine

E-mail: kuznetsovaa232@gmail.com

## SPECTROSCOPY OF MULTIELECTRON ATOM IN A DC ELECTRIC FIELD: MODIFIED OPERATOR PERTURBATION THEORY APPROACH TO STARK RESONANCES

It is presented a new modified method to calculation of the Stark resonances energies characteristics (energies and widths) for the multielectron atomic systems in a DC electric field. The method is based on the modified operator perturbation theory. The latter allows an accurate, consistent treatment of a strong field DC Stark effect and includes the physically reasonable distorted-waves approximation in the frame of the formally exact quantum-mechanical procedure. As illustration, some test data for the Stark resonances energies and widths in the lithium atom spectrum are presented and compared with results of calculations within the alternative consistent sophisticated methods.

### 1. Introduction

At last years it attracts a great interest especially in the multielectron atoms that is stimulated by a whole range of interesting phenomena to be studied (such as quasi-discrete state mixing, a zoo of Landau-Zener anticrossings, autoionization in the multielectron atoms, the effects of potential barriers (shape resonances), new kinds of resonances above threshold etc) and by many applications on atomic, laser and plasmas physics [1-54].

An external electric field shifts and broadens the bound state atomic levels. The standard quantum-mechanical approach relates the complex eigenenergies (EE) and complex eigenfunctions (EF) to the shape resonances. The field effects drastically increase upon going from one excited level to another. The highest levels overlap forming a “new continuum” with lowered boundary.

The calculation difficulties inherent to the standard quantum mechanical approach are well known. Here one should mention the well-known Dyson phenomenon. The Wentzel-Kramers-Brillouin (WKB) approximation overcomes these difficulties for the states lying far

from the “new continuum” boundary. Some modifications of the WKB method (see review in Ref. [1]) are introduced by Stebbings and Dunning, Kondratovich and Ostrovsky, Popov et al. Ivanov-Letokhov [5] have fulfilled the first estimations of the effectiveness of the selective ionization of the Rydberg atom using a DC electric and laser fields within the quasiclassical model. Different calculational procedures are used in the Pade and then Borel summation of the divergent Rayleigh-Schrödinger perturbation theory (PT) series (Franceschini et al 1985, Popov et al 1990) and in the sufficiently exact numerical solution of the difference equations following from expansion of the wave function over finite basis (Benassi and Grecchi 1980, Maquet et al 1983, Kolosov 1987, Telnov 1989, Anokhin-Ivanov 1994), complex-coordinate method, quantum defect approximation etc (see review in Ref. [1]).

Hehenberger, McIntosh and E. Brändas [10] have applied the Weyl’s theory to the Stark effect in the hydrogen atom.

Themelis and Nicolaides [42] adopted an *ab initio* theory to compute the complex energy

of multielectron atomic states. Their approach is based on the state-specific construction of a non-Hermitian matrix according to the form of the decaying-state EF which emerges from the complex eigenvalue Schrodinger equation (CESE) theory. Sahoo and Ho [45] carried out the calculation the Stark resonances energies and widths in the lithium atom on the basis of the complex absorbing potential (CAP) formalism. Jianguo Rao et al and Hui-Yan Meng et al [40] have presented the B-spline-based coordinate rotation method plus the model potential approach and applied it to investigate the complex energies of low-lying resonances of the hydrogen and lithium atoms in an electric field.

In Refs.[5,16] it has been presented a consistent uniform quantum approach to the solution of the non-stationary state problems including the DC (Direct Current) strong-field Stark effect and also scattering problem It is based on the operator form of the perturbation theory (OPT) for the Schrödinger equation of an atom in a strong DC electric field.  $\ddot{\mathbf{e}}$

In this work we present a new modified version of the OPT method for the non-H atomic systems and test it by studying the Stark resonances parameters for some lithium atom states in a DC electric field. Besides, a relativistic generalization is presented too. The Stark resonances parameters energies and widths are calculated and compared with the data of calculations on the basis of the alternative sophisticated complex eigenvalue approaches [40,42,45].

## 2.Modified operator perturbation theory to Stark resonances for atoms in a DC electric field

As usually [16,47], the Schrödinger equation for the electron function taking into account the uniform electric field and field of the nucleus (Coulomb units are used: for length, 1 unit is  $\hbar^2/Ze^2m$ ; for energy 1 unit is  $mZ^2e^4/\hbar^2$ ) is:

$$[-(1 - N/Z) / r + V_m(r) + \varepsilon z - 1/2\Delta - E] \psi = 0, \quad (1)$$

where  $E$  is the electron energy,  $Z$  is the nucleus charge,  $N$  is the number of electrons in the atom-

ic core (for the hydrogen atom:  $Z=1, N=0$ ),  $V_m$  is a model potential that describes interaction with the electron shells for multi-electron atom (for the hydrogen atom  $V_m=0$ ). Firstly, we only deal with the Coulomb part of the electron-atomic residue interaction. The non-Coulomb part, as well as relativistic effects, can be approximately accounted for next step. The separation of variables in the parabolic coordinates:

$$\psi(\zeta, \eta, \varphi) = f(\zeta) g(\eta) (\zeta \cdot \eta)^{|m|/2} \exp(im\varphi) / (2\pi)^{1/2} \quad (2)$$

transforms it to the system of two equations for the functions  $f, g$ :

$$f'' + \frac{|m|+1}{t} f' + [1/2E + (\beta_1 - N/Z) / t - 1/4\varepsilon(t)] f = 0 \quad (3)$$

$$g'' + \frac{|m|+1}{t} g' + [1/2E + \beta_2 / t + 1/4\varepsilon(t)] g = 0, \quad (4)$$

coupled through the constraint on the separation constants:

$$(5)$$

Here and below variable  $t$  denotes the argument common for the whole differential equations system (4). For the uniform electric field  $\varepsilon(t) = \varepsilon$ . Potential energy in equation (4) has the barrier. Two turning points for the classical motion along the axis, and , at a given energy  $E$  are the solutions of the quadratic equation ( ):

$$t_2 = \{ [E^2_0 - 4\varepsilon(1-\beta)]^{1/2} - E_0 \} / \varepsilon, \quad (6)$$

$$t_1 = \{ -[E^2_0 - 4\varepsilon(1-\beta)]^{1/2} - E_0 \} / \varepsilon, \quad t_1 < t_2 \quad (7)$$

To simplify the calculational procedure, the uniform electric field in (3) and (4) should be substituted by the function [16]:

$$e(t) = \frac{1}{t} e \left[ (t - \tau) \frac{\tau^4}{\tau^4 + t^4} + \tau \right] \quad (8)$$

with sufficiently large  $t$  ( $t=1.5t_2$ ). The motivation of a choice of the  $\varepsilon(t)$  and some physical features of electron motion along the  $h$ -axis are

presented in Refs. [1,2,16]. Here we only underline that the function  $\varepsilon(t)$  practically coincides with the constant  $\varepsilon$  in the inner barrier motion region, i.e.  $t < t_0$  and disappears at  $t > t_0$ . It is important that the final results do not depend on the parameter  $t$ . It is carefully checked in the numerical calculation. The scattering states energy spectrum now spreads over the range  $(-\varepsilon/2, +\infty)$ , compared with  $(-\infty, +\infty)$  in the uniform field. In contrast to the case of a free atom in scattering states in the presence of the uniform electric field remain quantified at any energy  $E$ , i.e. only definite values of  $\beta$  are possible. The latter are determined by the confinement condition for the motion along the  $h$ -axis. The same is true in our case, but only for  $E \in \left(-\frac{1}{2}\varepsilon, +\frac{1}{2}\varepsilon\right)$ . Ultimately, such a procedure provides construction of realistic functions of the bound and scattering states. In a certain sense, this completely corresponds to the advantages of the distorted-wave approximation known in scattering theory [2].

The total Hamiltonian  $H(\zeta, \nu, \varphi)$  does not possess the bound stationary states. According to OPT [16]), one has to define the zero order Hamiltonian  $H_0$ , so that its spectrum reproduces qualitatively that of the initial one. To calculate the width  $G$  of the concrete quasistationary state in the lowest PT order one needs only two zeroth-order EF of  $H_0$ : bound state function  $\Psi_E(\varepsilon, \eta, \varphi)$  and scattering state function  $\Psi_E(\varepsilon, \eta, \varphi)$  with the same EE. It can be solved a more general problem: a construction of the bound state function along with its complete orthogonal complementary of scattering functions with  $E \in \left(-\frac{1}{2}\varepsilon, +\infty\right)$ . First, one has to define the EE of the expected bound state. It is the well-known problem of states quantification in the case of the penetrable barrier [16]. The system (3) and (4) with the total Hamiltonian is solved under the conditions:

$$f(t) \rightarrow 0 \text{ at } t \Rightarrow \infty, \quad (9)$$

$$\partial x(\beta, E) / \partial E = 0 \text{ with}$$

$$x(\beta, E) = \lim_{t \Rightarrow \infty} [g^2(t) + \{g'(t)/k\}^2] t^{|m|+1}. \quad (10)$$

These two conditions quantify the bound energy  $E$  and separation constant  $\beta$ . Further one should solve the system of the ordinary differential equations (3) and (4) with probe pairs of  $E, \beta$ . The corresponding EF:

$$\psi_{Eb}(\zeta, \eta, \varphi) = f_{Eb}(\zeta) g_{Eb}(\eta) (\zeta \eta)^{|m|/2} \exp(im\varphi) (2\pi)^{-1/2}, \quad (11)$$

where  $f_b(t)$  is the solution of (3) (with the just determined  $E, \beta$ ) at  $t \in (0, \infty)$  and  $g_b(t)$  is the solution of (4) (with the same  $E, \beta$ ) at (inside barrier) and  $g(t) = 0$  otherwise.

These bound state EE, eigenvalue  $E$  and EF for the zero-order Hamiltonian  $H_0$  coincide with those for the total Hamiltonian  $H$  at  $\varepsilon \Rightarrow 0$ , where all the states can be classified due to the quantum numbers  $(n, l, m)$  (principal, parabolic, azimuthal) connected with  $E, \beta, m$  by the well-known expressions. The scattering state functions:

$$\psi_{E's}(\zeta, \eta, \varphi) = f_{E's}(\zeta) g_{E's}(\eta) (\zeta \eta)^{|m|/2} \exp(im\varphi) (2\pi)^{-1/2} \quad (12)$$

is orthogonal to the above defined bound state function and to each other. In addition, these functions must describe the motion of the ejected electron, i.e.  $\beta$  must satisfy the equation (4) asymptotically. Following the OPT ideology [16], we choose the next form of  $\beta$ :

$$g_{E's}(t) = g_1(t) - z_2' g_2(t) \quad (13)$$

with  $g_1(t)$  and  $g_2(t)$  satisfying the differential equations (3) and (4). The function  $g_2(t)$  satisfies the non-homogeneous differential equation, which differs from (4) only by the right-hand term, disappearing at  $t \Rightarrow \infty$ . The total equation system, determining the scattering function, reads

$$\begin{aligned} f'_{E's} + \frac{|m|+1}{t} f_{E's} + [1/2E' + (\beta_1' - N/Z)/t - 1/4 \varepsilon(t)t] f_{E's} &= 0, \\ g_1'' + \frac{|m|+1}{t} g_1' + [1/2E' + \beta_2'/t + 1/4 \varepsilon(t)t] g_1 &= 0, \\ g_2'' + \frac{|m|+1}{t} g_2' + [1/2E + \beta_2'/t + 1/4 \varepsilon(t)t] g_2 &= 2g_{Eb}, \end{aligned} \quad (14)$$

( ' ' ). At the given ' , the only quantum parameter ' is determined by the natural boundary condition:  $f_{E's} \rightarrow 0$  at  $t \rightarrow \infty$ . Of course: ' ,  $f_{E's} = f_{E'}^*$  at ' ; only this case is needed in the particular problem we deal with here. The coefficient ' ensures the orthogonality condition:

$$\langle \Psi_{E'} | \Psi_{E's} \rangle = 0. \quad (15)$$

The imaginary part of state energy in the lowest PT order is as follows:

$$\text{Im}E = \Gamma/2 = p | \langle Y_{E'b} | H | Y_{E's} \rangle |^2 \quad (16)$$

with the total Hamiltonian . The state functions  $\Psi_{E'}$  and  $\Psi_{E's}$  are assumed to be normalized to 1 and by the  $\delta(k-k')$  condition, accordingly. The matrix elements  $\langle \Psi_{E'} | H | \Psi_{E's} \rangle$  entering the high-order PT corrections can be determined in the same way. They can be expressed through the set of one-dimensional integrals, described in details in Refs. [1,16].

In contrast to the hydrogen atom, the non-relativistic Schrödinger equation for an electron moving in the field of the atomic core in many-electron atom (in particular, an alkali element) and a uniform external electric field does not allow separation of variables in the parabolic coordinates  $x, y, z$  [2]. One of the ways this problem could be related to the use of effective potentials, chosen in such a way (for example, in the Miller-Green approximation; look review in ref [2]) that to achieve the separation of variables in the Schrödinger equation. Here the model potential approach [2] is used. One may introduce the ion core charge  $Z$  for the multielectron atom. According to standard quantum defect theory, the relation between quantum defect value  $\mu_l$ , electron energy  $E$  and principal quantum number  $n$  is:  $\mu_l = \delta - z^* (-2E)^{-1/2}$ . The quantum defect in the parabolic coordinates  $\delta(n_1, n_2, m)$  is connected to the quantum defect value of the free ( $\varepsilon = 0$ ) atom by the following relation [25,47]:

$$\delta(n_1, n_2, m) = (1/n) \sum_{l=m}^{n-1} (2l+1) (C_{J,M-mlm}^{JM})^2 \mu_l, \quad (17)$$

Using the quantum defect approximation allows to modify the OPT method for the non-H atoms. All calculations are performed on the basis of the numeral code Superatom-ISAN (version 93). The details of the used method can be found in the references [1,2,16,25,47].

### 3. Results and Conclusions

We have applied the developed computational approach to calculating the complex energy eigenvalues representing the shifted and broadened 2s state of lithium atom as a function of electric field strength. Sahoo and Ho [45] performed the calculation on the basis of a complex absorbing potential (CAP) method. Themelis and Nicolaides [42] adopted *ab initio* theory to compute the complex energy of multielectron atomic states. Their approach is based on the state-specific construction of a non-Hermitian matrix according to the form of the decaying-state eigenfunction which emerges from the complex eigenvalue Schrödinger equation (CESE) theory. Meng et al [40] has elaborated the B-spline based coordinate rotation (B-CR) approach. In Table 1 we present our data on the eigenvalues  $E \pm i\Gamma/2$  (in atomic units: a.u.) representing the shifted and broadened 2s state of lithium atom as a function of electric field strength (in a.u.).

Table 1.  
**Complex eigenvalues for the shifted and broadened 2s state of lithium atom as a function of the field strength, calculated by different methods (see text)**

Li 2s	B-CR [40]	B-CR [40]	CAP [45]	CAP [45]
$\varepsilon$ (a.u.)	$E_r$ (a.u.)	$\Gamma/2$ (a.u.)	$E_r$ (a.u.)	$\Gamma/2$ (a.u.)
0.0050	-0.20009	-	-0.20019	7.20[-9]
0.0100	-0.20642	4.50[-5]	-0.20651	4.77[-5]
0.0125	-0.21147	4.76[-4]	-0.21155	4.68[-4]
0.0175	-0.22393	4.03[-3]	-0.22397	4.06[-3]
Li 2s	CESE [42]	WKB [42]	This work	This work
$\varepsilon$ (a.u.)	$\Gamma/2$ (a.u.)	$\Gamma/2$ (a.u.)	$E_r$ (a.u.)	$\Gamma/2$ (a.u.)
0.0050	-	4.6[-11]	-0.20012	7.80[-9]
0.0100	5.50[-5]	1.72[-4]	-0.20645	4.81[-5]
0.0125	5.46[-4]	2.95[-3]	-0.21149	4.96[-4]
0.0175	4.35[-3]	6.35[-2]	-0.22394	4.24[-3]

For comparison the analogous results, obtained on the basis of the CAP, CESE, B-CR methods [40,42,45] are presented. Analysis of the data shows that the positions (energies) of the Stark resonances in the present calculation are in a physically reasonable agreement with theoretical data obtained by other, in particular, CESE and B-CR methods. However, the results for the width of resonance differ more significantly from each other. For example, the CAP calculation for the width of the 2s state at strength  $F < 0.0060$  a.u. gives systematically larger values than obtained by the CESE, B-CR and our methods. The resonance width values are higher than the corresponding B-CR data and correspondingly a little less than the values, obtained within the CESE method for all strengths of the electric field under consideration. Concerning the widths of resonances it should be paid attention on convergence aspect for the CAP and CESE method. As it has been underlined in [40], in the case of a weak electric field (naturally the widths of resonances became very small), the methods have difficulties in obtaining a stable value of a width. In order to obtain the well-converged results, it is necessary to use larger basis size. Naturally, in a limit of a weak electric field the well-known quasiclassical WKB approximation and standard PT [1,2] calculation will be more appropriate. One of the advantages of the B-CR method is possibility to apply in the case of increasing field strengths without a significant computational effort growth, however, the convergence of the width  $\Gamma$  to obtain reliable complex eigenvalues should be carefully carried out. In the CAP method, there is no systematic way of choosing a scaling factor in an quite artificial complex potential, which is added to the original atomic Hamiltonian. One of the serious advantages of the modified OPT method is that an increasing a field strength does not lead to an increase of computational effort and there is no a convergence problem.

## References

1. Glushkov, A.V. *Atom in an electromagnetic field*. KNT: Kiev, **2005**.
2. Glushkov, A.V. *Relativistic Quantum theory. Quantum mechanics of atomic systems*. Astroprint: Odessa, **2008**.
3. Lisitsa, V.S. New results on the Stark and Zeeman effects in the hydrogen atom. *Sov. Phys. Usp.* **1987**, *30*, 927-960.
4. Ivanov, L.N.; Letokhov, V.S. Selective ionization of atoms by a light and electric field. *Quant. Electr.*(in Russian) **1975**, *2*, 585-590.
5. Glushkov, A.V. Operator Perturbation Theory for Atomic Systems in a Strong DC Electric Field. *In Advances in Quantum Methods and Applications in Chemistry, Physics, and Biology, Series: Progress in Theoretical Chemistry and Physics*; Hotokka, M., Brändas, E., Maruani, J., Delgado-Barrio, G., Eds.; Springer: Cham, **2013**; Vol. 27, pp 161–177.
6. Glushkov, A.V. Advanced Relativistic Energy Approach to Radiative Decay Processes in Multielectron Atoms and Multicharged Ions. *In Quantum Systems in Chemistry and Physics: Progress in Methods and Applications, Series: Progress in Theoretical Chemistry and Physics*; Nishikawa, K., Maruani, J., Brandas, E., Delgado-Barrio, G., Piecuch, P., Eds.; Springer: Dordrecht, **2012**; Vol. 26, pp 231–252.
7. Moiseyev, N. Quantum theory of resonances: calculating energies, widths and cross-sections by complex scaling *Phys. Rep.* **1998**, *302*, 211-293
8. Rao, J.; Liu, W.; Li, B. Theoretical complex Stark energies of hydrogen by a complex-scaling plus B-spline approach. *Phys. Rev. A.* **1994**, *50*, 1916-1919 (1994).
9. Rao, J.; Li, B. Resonances of the hydrogen atom in strong parallel magnetic and electric fields. *Phys. Rev. A.* **1995**, *51*, 4526-4530.
10. Hehenberger, M.; McIntosh, H.V.; Brändas, E. Weyl's theory applied to the Stark effect in the hydrogen atom. *Phys. Rev. A* **1974**, *10* (5), 1494-1506.

11. Glushkov, A.; Khetselius, O.; Svinarenko, A.; Buyadzhi, V. *Spectroscopy of autoionization states of heavy atoms and multiply charged ions*. Odessa: TEC, **2015**.
12. Buyadzhi, V.V. Laser multiphoton spectroscopy of atom embedded in Debye plasmas: multiphoton resonances and transitions. *Photoelectronics*. **2015**, *24*, 128-133.
13. Khetselius, O.Yu. *Quantum structure of electroweak interaction in heavy finite Fermi-systems*. Astroprint: Odessa, **2011**.
14. Khetselius, O.Yu. Spectroscopy of cooperative electron-gamma-nuclear processes in heavy atoms: NEET effect. *J. Phys.: Conf. Ser.* **2012**, *397*, 012012
15. Glushkov, A.V. Spectroscopy of cooperative muon-gamma-nuclear processes: Energy and spectral parameters *J. Phys.: Conf. Ser.* **2012**, *397*, 012011
16. Glushkov A.V.; Ivanov, L.N. DC strong-field Stark effect: consistent quantum-mechanical approach. *J. Phys. B: At. Mol. Opt. Phys.* **1993**, *26*, L379-386.
17. Glushkov, A.V. Spectroscopy of atom and nucleus in a strong laser field: Stark effect and multiphoton resonances. *J. Phys.: Conf. Ser.* **2014**, *548*, 012020
18. Buyadzhi, V.V.; Glushkov, A.V.; Lovett, L. Spectroscopy of atom and nucleus in a strong laser field: Stark effect and multiphoton resonances. *Photoelectronics*. **2014**, *23*, 38-43.
19. Glushkov, A.V.; Dan'kov, S.V.; Prepelitsa, G.P.; Polischuk, V.N.; Efimov, A.E. Qed theory of nonlinear interaction of the complex atomic systems with laser field multi-photon resonances. *J. Techn. Phys.* **1997**, *38(2)*, 219-222.
20. Ignatenko, A.V. Probabilities of the radiative transitions between Stark sublevels in spectrum of atom in an DC electric field: New approach. *Photoelectronics*, **2007**, *16*, 71-74.
21. Glushkov, A.V.; Ambrosov, S.V.; Ignatenko, A.V. Non-hydrogenic atoms and Wannier-Mott excitons in a DC electric field: Photoionization, Stark effect, Resonances in ionization continuum and stochasticity. *Photoelectronics*, **2001**, *10*, 103-106.
22. Glushkov, A.V.; Malinovskaya S.V. Co-operative laser nuclear processes: border lines effects *In New Projects and New Lines of Research in Nuclear Physics*. Fazio, G., Hanappe, F., Eds.; World Scientific: Singapore, **2003**, 242-250.
23. Stambulchik, E.; Maron, Y. Stark effect of high-n hydrogen-like transitions: quasi-contiguous approximation. *J. Phys. B: At. Mol. Opt. Phys.* **2008**, *41*, 095703.
24. Dunning, F.B.; Mestayer, J.J.; Reinhold, C.O.; Yoshida S.; Burgdörfer, J. Engineering atomic Rydberg states with pulsed electric fields. *J. Phys. B: At. Mol. Opt. Phys.* **2009**, *42*, 022001.
25. Glushkov, A.V.; Ambrosov, S.V.; Ignatenko, A.V.; Korchevsky, D.A. DC strong field stark effect for nonhydrogenic atoms: Consistent quantum mechanical approach. *Int. Journ. Quant. Chem.* **2004**, *99*, 936-939.
26. Ivanov, L.N.; Ivanova, E.P. Atomic ion energies for Na-like ions by a model potential method  $Z = 25-80$ . *Atom. Data Nucl. Data Tabl.* **1979**, *24*, 95-109
27. Glushkov, A.V.; Gurskaya, M.Yu.; Ignatenko, A.V.; Smirnov, A.V.; Serga, I.N.; Svinarenko, A.A.; Ternovsky, E.V. Computational code in atomic and nuclear quantum optics: Advanced computing multiphoton resonance parameters for atoms in a strong laser field. *J. Phys.: Conf. Ser.* **2017**, *905*, 012004.
28. Glushkov, A. Multiphoton spectroscopy of atoms and nuclei in a laser

- field: relativistic energy approach and radiation atomic lines moments method// *Adv. Quant.Chem.* (Elsevier), **2018**, 78, doi.org/10.1016/bs.aiq.2018.06.004
29. Khetselius, O. Optimized relativistic many-body perturbation theory calculation of wavelengths and oscillator strengths for li-like multicharged ions// *Adv. Quant. Chem.* (Elsevier) , **2018**, 78, doi.org/10.1016/bs.aiq.2018.06.001.
  30. Glushkov, A.V.; Ivanov, L.N. Radiation decay of atomic states: atomic residue polarization and gauge non-invariant contributions. *Phys. Lett. A* **1992**, 170, 33-36.
  31. Ivanova, E.P.; Glushkov, A.V. Theoretical investigation of spectra of multicharged ions of F-like and Ne-like isoelectronic sequences. *J. Quant. Spectr. Rad. Transfer.* 1986, 36, 127-145.
  32. Glushkov, A.V.; Ivanov, L.N.; Ivanova, E.P. Autoionization Phenomena in Atoms. *Moscow University Press*, Moscow, **1986**, 58-160
  33. Khetselius, O.Yu. Relativistic perturbation theory calculation of the hyperfine structure parameters for some heavy-element isotopes. *Int. Journ. Quant.Chem.* **2009**, 109, 3330-3335.
  34. Glushkov, A.V. Negative ions of inert gases. *JETP Lett.* **1992**, 55, 97-100.
  35. Glushkov, A.V. *Relativistic and Correlation Effects in Spectra of Atomic Systems*; Astroprint: Odessa, **2006**.
  36. Khetselius, O.Yu. Hyperfine structure of radium. *Photoelectronics.* **2005**, 14, 83-85.
  37. Glushkov, A.V.; Malinovskaya, S.V.; Loboda, A.V.; Shpinareva, I.M.; Prepelitsa, G.P. Consistent quantum approach to new laser-electron-nuclear effects in diatomic molecules. *J.Phys.: Conf. Ser.* **2006**, 35, 420-424.
  38. Glushkov, A.V.; Malinovskaya, S.V.; Loboda, A.V.; Shpinareva, I.M.; Gurnitskaya, E.P.; Korchevsky, D.A. Diagnostics of the collisionally pumped plasma and search of the optimal plasma parameters of x-ray lasing: calculation of electron-collision strengths and rate coefficients for Ne-like plasma. *J. Phys.: Conf. Ser.* **2005**, 11, 188-198.
  39. Glushkov, A.V. Energy approach to resonance states of compound superheavy nucleus and EPPP in heavy nuclei collisions *In Low Energy Antiproton Physics*; Grzonka, D., Czyzykiewicz, R., Oelert, W., Rozek, T., Winter, P., Eds.; AIP: New York, *AIP Conf. Proc.* **2005**, 796, 206-210.
  40. Meng, H.-Y.; Zhang, Y.-X.; Kang, S.; Shi, T.-Y.; Zhan, M.-S. Theoretical complex Stark energies of lithium by a complex scaling plus the B-spline approach. *J. Phys. B: At. Mol. Opt. Phys.* **2008**, 41, 155003.
  41. Glushkov, A.V.; Malinovskaya, S.V.; Prepelitsa, G.P.; Ignatenko, V. Manifestation of the new laser-electron nuclear spectral effects in the thermalized plasma: QED theory of co-operative laser-electron-nuclear processes. *J. Phys.: Conf. Ser.* **2005**, 11, 199-206.
  42. Themelis, S.I.; Nicolaides, C.A. Complex energies and the polyelectronic Stark problem: II. The Li  $n = 4$  levels for weak and strong fields 2001 *J. Phys. B: At. Mol. Opt. Phys.* **2001**, 34, 2905-2926.
  43. Glushkov, A.V.; Ambrosov, S.V.; Ignatenko, A.V.; Korchevsky, D.A. DC strong field stark effect for nonhydrogenic atoms: Consistent quantum mechanical approach. *Int. Journ. Quant. Chem.* **2004**, 99, 936-939.
  44. Khetselius, O.Yu. Relativistic Energy Approach to Cooperative Electron- $\gamma$ -Nuclear Processes: NEET Effect *In Quantum Systems in Chemistry and Physics, Series: Progress in Theoretical Chemistry and Physics*; Nishikawa, K., Maruani, J., Brändas, E., Delgado-Barrio, G., Piecuch, P., Eds.;

- Springer: Dordrecht, **2012**; Vol. 26, pp 217-229.
45. Sahoo, S.; Ho, Y. K. Stark effect on the low-lying excited states of the hydrogen and the lithium atoms. *J. Phys. B: At. Mol. Opt. Phys.* **2000**, *33*, 5151.
  46. Glushkov, A.V.; Ternovsky, V.B.; Buyadzhi, V.V.; Prepelitsa, G.P. Geometry of a Relativistic Quantum Chaos: New approach to dynamics of quantum systems in electromagnetic field and uniformity and charm of a chaos. *Proc. Intern. Geom. Center.* **2014**, *7(4)*, 60-71.
  47. Kuznetsova, A.A.; Glushkov, A.V.; Ignatenko, A.V.; Svinarenko, A.A.; Ternovsky V.B. Spectroscopy of multielectron atomic systems in a DC electric field. *Adv. Quant. Chem.* (Elsevier) **2018**, *78*,
  2. doi.org/10.1016/bs.aiq.2018.06.005
  48. Khetselius, O.Yu. Optimized Perturbation Theory for Calculating the Hyperfine Line Shift and Broadening of Heavy Atoms in a Buffer Gas. *In Frontiers in Quantum Methods and Applications in Chemistry and Physics, Series: Progress in Theoretical Chemistry and Physics*; Nascimento, M., Maruani, J., Brändas, E., Delgado-Barrio, G., Eds.; Springer: Cham, **2015**; Vol. 29, pp. 55-76.
  49. Khetselius, O.Yu. Atomic parity non-conservation effect in heavy atoms and observing P and PT violation using NMR shift in a laser beam: To precise theory. *J. Phys.: Conf. Ser.* **2009**, *194*, 022009.
  50. Buyadzhi, V.V.; Chernyakova, Yu.G.; Smirnov, A.V.; Tkach, T.B. Electron-collisional spectroscopy of atoms and ions in plasma: Be-like ions. *Photoelectronics.* **2016**, *25*, 97-101.
  51. Buyadzhi, V.V.; Chernyakova, Yu.G.; Antoshkina, O.A.; Tkach, T.B. Spectroscopy of multicharged ions in plasmas: Oscillator strengths of Be-like ion Fe. *Photoelectronics.* **2017**, *26*, 94-102.
  52. Glushkov, A.V.; Kondratenko, P.A.; Buyadgi, V.V.; Kvasikova, A.S.; Sakun T.N.; Shakhman, A.S. Spectroscopy of cooperative laser electron- $\gamma$ -nuclear processes in polyatomic molecules. *J. Phys.: Conf. Ser.* **2014**, *548*, 012025.
  53. Svinarenko, A.A. Study of spectra for lanthanides atoms with relativistic many-body perturbation theory: Rydberg resonances. *J. Phys.: Conf. Ser.* **2014**, *548*, 012039.
  54. Khetselius, O.Yu. *Hyperfine structure of atomic spectra.* Astroprint: Odessa, **2008**.

This article has been received in August 2018

PACS 31.15.A-

*A. A. Kuznetsova, A. A. Buyadzhi, M. Yu. Gurskaya, A. O. Makarova*

## **SPECTROSCOPY OF MULTIELECTRON ATOM IN A DC ELECTRIC FIELD: MODIFIED OPERATOR PERTURBATION THEORY APPROACH TO STARK RESONANCES**

### **Summary**

It is presented a new modified method to calculation of the Stark resonances energies characteristics (energies and widths) for the multielectron atomic systems in a DC electric field. The method is based on the modified operator perturbation theory. The latter allows an accurate, consistent treatment of a strong field DC Stark effect and includes the physically reasonable distorted-waves approximation in the frame of the formally exact quantum-mechanical procedure. As illustration,

some test data for the Stark resonances energies and widths in the lithium atom spectrum are presented and compared with results of calculations within the alternative consistent sophisticated methods.

**Keywords:** multielectron atom in a dc electric field – modified operator perturbation theory – Stark resonances

PACS 31.15.A-

*A. A. Кузнецова, А. А. Буяджи, М. Ю. Гурская, А. О. Макарова*

## **СПЕКТРОСКОПИЯ МНОГОЭЛЕКТРОННОГО АТОМА В DC ЭЛЕКТРИЧЕСКОМ ПОЛЕ: МОДИФИЦИРОВАННЫЙ МЕТОД ОПЕРАТОРНОЙ ТЕОРИИ ВОЗМУЩЕНИЙ ДЛЯ ОПИСАНИЯ ШТАРКОВСКИХ РЕЗОНАНСОВ**

### **Резюме**

Представлен новый модифицированный метод расчета характеристик энергий штарковских резонансов (энергии и ширины) для многоэлектронных атомных систем в электрическом поле. Метод основан на модифицированной операторной теории возмущений, которая обеспечивает последовательное, корректное описание эффекта Штарка в сильном поле для многоэлектронных атомов и базируется на использовании физически обоснованного приближения искаженных волн в рамках формально точной квантово-механической процедуры. В качестве иллюстрации представлены некоторые тестовые данные для энергий и ширин резонансов Штарка в спектре атомов лития, которые сравниваются с результатами расчетов в рамках альтернативных последовательных теоретических методов.

**Ключевые слова:** Многоэлектронный атом в электрическом поле – модифицированная операторная теория возмущений – штарковские резонансы

PACS 31.15.A-

*Г. О. Кузнецова, Г. А. Буяджи, М. Ю. Гурська, О. О. Макарова*

## **СПЕКТРОСКОПИЯ БАГАТОЕЛЕКТРОННОГО АТОМА В DC ЕЛЕКТРИЧНОМУ ПОЛІ: МОДИФІКОВАНИЙ МЕТОД ОПЕРАТОРНОЇ ТЕОРІЇ ЗБУРЕНЬ ДЛЯ ОПИСУ ШТАРКІВСЬКИХ РЕЗОНАНСІВ**

### **Резюме**

Представлений новий модифікований метод розрахунку характеристик енергій штарківських резонансів (енергії і ширини) для багатоелектронних атомних систем в електричному полі. Метод заснований на модифікованій операторній теорії збурень, яка забезпечує послідовний, коректний опис ефекту Штарка в сильному полі для багатоелектронних атомів і базується на використанні фізично обґрунтованого наближення перекручених хвиль в рамках формально точної квантово-механічної процедури. В якості ілюстрації представлені деякі тестові дані для енергій і ширин резонансів Штарка в спектрі атомів літію, які порівнюються з результатами розрахунків в рамках альтернативних послідовних теоретичних методів.

**Ключові слова:** багатоелектронний атом у електричному полі – модифікована операторна теорія збурень – штарківські резонанси

*A. A. Mashkantsev, A. V. Ignatenko, S. V. Kirianov, E. V. Pavlov*

<sup>1</sup>Odessa State Environmental University, 15, Lvovskaya str., Odessa, 65016  
E-mail: ignatenkoav13@gmail.com

## CHAOTIC DYNAMICS OF DIATOMIC MOLECULES IN AN ELECTROMAGNETIC FIELD

Nonlinear chaotic dynamics of the diatomic molecules interacting with a resonant linearly polarized electromagnetic field is computationally modelled. It is presented an effective quantum-mechanical model for diatomic molecule in an electromagnetic field, based on the Schrödinger equation and model potential method. To detect the elements of a chaotic dynamics, we used the known chaos theory and non-linear analysis methods such as a correlation integral algorithm, the Lyapunov's exponents and Kolmogorov entropy analysis, prediction model etc. There are listed the data of computing dynamical and topological invariants such as the correlation, embedding and Kaplan-Yorke dimensions, Lyapunov's exponents, Kolmogorov entropy etc, for polarization time series of the ZrO molecule interacting with a linearly polarized electromagnetic field. The results obtained are in a physically reasonable agreement with the conclusions by Berman, Kolovskii, Zaslavsky, Zganh et al, Glushkov et al.

### Introduction

Theoretical and experimental studying regular and chaotic dynamics of nonlinear processes in the different classes of quantum systems (in particular, atomic and molecular systems in an external electromagnetic field) attracts a great interest that is of a significant importance for multiple scientific and technical applications etc [1-70]. Some of the beauty of quantum chaos is that it has developed a set of tools which have found applications in a large variety of different physical contexts, ranging from atomic, molecular and nuclear physics (Chirijov, 1979, Delande-Gay 1986, Wintgen-Friedrich 1986, Wintgen 1987, Zaslavsky, Berman, Kolovsky, 1988, 1992, Meredith et al, 1988, Chelkowski et al, 1991, Delande et al 1991, Zhang, Katsouleas, Joshi, 1993, Cassati et al 1994, Glushkov et al 1993, 1997, 2014, Bohigas and Leboeuf 2002, Olofsson et al 2006, López, Mercado, 2015 et al), optical (Nockel-Stone 1997, Gmachl et al 1998) or microwave (Stockmann and Stein 1990, Sridhar 1991, Alt et al 1995, Kudrolli et al 1995, Pradhan and Sridhar 2000) resonators and mesoscopic physics (Richter et al 1996b, Richter 2000, Alhassid 2000, Glushkov et al, 2005-

2007) and others (see review [11]). New field of investigations of the quantum and other systems has been provided by the known progress in a development of a nonlinear analysis and chaos theory methods [1-12,17-30]. In Refs. [11,27-33] the authors applied different approaches to quantitative studying regular and chaotic dynamics of atomic and molecular systems interacting with a strong electromagnetic field and laser systems. The most popular approach includes the combined using the advanced nonlinear analysis and a chaos theory methods such as the autocorrelation function method, multifractal formalism, mutual information approach, correlation integral analysis, false nearest neighbour algorithm, Lyapunov exponent's analysis, surrogate data method, stochastic propagators method, memory and Green's functions approaches etc (see details in Refs. [17-33]).

In this paper we present the results of computing chaotic dynamics of the concrete molecular systems (diatomic molecules) interacting with a linearly polarized resonant electromagnetic field. The quantum-dynamic approach to diatomic molecule in an electromagnetic field

is used and based on the solution of the time-dependent Schrödinger equation, optimized operator perturbation theory and realistic model potential method.

## 2. Quantum-dynamical and chaos-geometric modeling dynamics of diatomic molecule in a field

Below we briefly consider a quantum dynamical approach to studying a regular and chaotic dynamics of diatomic molecules in a resonant electromagnetic field [11]. It is based on the numerical solution of the time-dependent Schrödinger equation and realistic Simons-Parr-Finlan model for the diatomic molecule potential  $U(x)$ . The Simons-Parr-Finlan formulae for the molecular potential is:

$$U(x) = \sum_{i=1}^n \frac{b_i}{(x - r_0)^2} \quad (1a)$$

or introducing  $x = r - r_0$ :

$$U(x) = \sum_{i=1}^n \frac{b_i}{(x - r_0)^2} \quad (1b)$$

where the coefficients  $b_i$  are linked with corresponding molecular constants.

The problem of dynamics of diatomic molecules in an infrared field is reduced to solving the Schrödinger equation:

$$i\partial\Psi/\partial t = [H_0 + U(x) - d(x)E_M \varepsilon(t) \cos(\omega_L t)]\Psi \quad (2)$$

where  $E_M$  - the maximum field strength,  $\varepsilon(t) = E_0 \cos(\nu t)$  corresponds the pulse envelope (chosen equal to one at the maximum value of electric field). A molecule in the field gets the induced polarization and its high-frequency component can be defined as:

$$P_x(t) = p_c^{(x)}(t) \cos \omega t + p_s^{(x)}(t) \sin \omega t, \quad (3a)$$

$$P_y(t) = p_c^{(y)}(t) \cos \omega t + p_s^{(y)}(t) \sin \omega t, \quad (3b)$$

$$p_c^{(x,y)}(t) = \left(\frac{1}{T}\right) \oint (\psi(t) | \hat{d}_{x,y} | \psi(t) \cos \omega t dt), \quad (3c)$$

where  $T$  — period of the external field,  $d$  — dipole moment. As usually, the power spectrum can be further determined as follows:

$$S(\omega) = |F[p(t)]|^2. \quad (4)$$

To avoid the numerical noise during the Fourier transformation, the attenuation technique used, i.e. at  $t > t_p$ ,  $p(t)$  is replaced by

$$p(t) \cos^2\{\pi(t - t_p)/[2(T - t_p)]\}, \quad (t_p < t < T) \quad (5)$$

with  $T = 1.5t_p$ .

It is understood that in the regular case of molecular dynamics, a spectrum will consist of a small number of the well resolved lines. In the case of chaotic dynamics of molecule in a field situation changes essentially. The corresponding energy of interaction with the field is much higher than anharmonicity constant  $W > xh\Omega$ . It is obvious that a spectrum in this case become more complicated [7-12].

The theoretical foundations of the universal approach to analysis of chaotic dynamics of the quantum systems in an electromagnetic field have been presented earlier (see, c.g., [11, 17-33]). Here we are limited only by the key moments. Generally speaking, the approach includes a set of such non-linear analysis and a chaos theory methods as the correlation integral approach, multi-fractal and wavelet analysis, average mutual information, surrogate data, Lyapunov's exponents and Kolmogorov entropy approach, spectral methods, nonlinear prediction (predicted trajectories, neural network etc) algorithms.

The goal of the embedding dimension determination is to reconstruct a Euclidean space  $R^d$  large enough so that the set of points  $d_A$  can be unfolded without ambiguity. In accordance with the embedding theorem, the embedding dimension,  $d_E$ , must be greater, or at least equal, than a dimension of attractor,  $d_A$ , i.e.  $d_E > d_A$ . There are several standard approaches to reconstruction of the attractor dimension (see, e.g., [17-33]). The correlation integral analysis is one of the widely used techniques to investigate the signatures of

chaos in a time series. The analysis uses the correlation integral,  $C(r)$ , to distinguish between chaotic and stochastic systems.

To compute the correlation integral, the algorithm of Grassberger and Procaccia [24] is the most commonly used approach. According to this algorithm, the correlation integral is

$$C(r) = \lim_{N \rightarrow \infty} \frac{2}{N(n-1)} \sum_{\substack{i,j \\ (1 \leq i < j \leq N)}} H(r - |y_i - y_j|) \quad (6)$$

where  $H$  is the Heaviside step function with  $H(u) = 1$  for  $u > 0$  and  $H(u) = 0$  for  $u \leq 0$ ,  $r$  is the radius of sphere centered on  $y_i$  or  $y_j$ , and  $N$  is the number of data measurements. To verify the results obtained by the correlation integral analysis, one could use the surrogate data method. This approach makes use of the substitute data generated in accordance to the probabilistic structure underlying the original data.

The important dynamical invariants of a chaotic system are the Lyapunov's exponents (see, e.g., [11,25-30]). They are usually defined as asymptotic average rates, they are independent of the initial conditions, and therefore they do comprise an invariant measure of attractor. Saying simply, the Lyapunov's exponents are a parameter to detect whether the system is chaotic or not.

The Kolmogorov entropy  $K_{ent}$  measures the average rate at which information about the state is lost with time. An estimate of this measure is the sum of the positive Lyapunov's exponents. The estimate of the dimension of the attractor is provided by the Kaplan and York conjecture:

$$d_L = j + \frac{\sum_{\alpha=1}^j \lambda_{\alpha}}{|\lambda_{j+1}|}, \quad (7)$$

where  $j$  is such that  $\sum_{\alpha=1}^j \lambda_{\alpha} > 0$  and  $\sum_{\alpha=1}^{j+1} \lambda_{\alpha} \leq 0$ , and the Lyapunov's exponents  $\lambda_{\alpha}$  are taken in descending order.

There are a few approaches to computing the Lyapunov's exponents. One of them computes the whole spectrum and is based on the Jacobi matrix of system. In our work we use the method with the linear fitted map proposed by Sano and Sawada [58], although the maps with higher order polynomials can be also used.

### 3. Some results and conclusions

Here we present the results of numerical simulation of the time dynamics for diatomic molecule ZrO in the electromagnetic field. An electromagnetic field is characterized by the parameter:  $S = cE / 8\pi$ , where  $c$  is the velocity of light and  $E$  is a field strength. The parameter  $W$  of interaction of an electromagnetic radiation with a molecule is as follows:

$$W[\text{cm}^{-1}] = 120.3(d_0 / r_0)(S / M\omega_e)^{1/2} \quad (8)$$

where an interatomic distance  $r_0$  in Å, dipole moment  $d_0$  in D,  $\omega_e$  in  $\text{cm}^{-1}$ ,  $M$  in a.u.m., and the field parameter  $S$  in  $\text{GW}/\text{cm}^2$ . In Table 1 we list a set of the ZrO molecules and field parameters [68-70].

The corresponding Chirikov<sub>1</sub> parameter [10] in this case is as:  $\delta n = 2(Ed/B)^2 \gg 1$ . The typical theoretical time dependence of polarization for ZrO molecule in the field in a chaotic regime is presented in Ref. [11]. The concrete step is an analysis of the corresponding time series with the  $n=7.6 \times 10^3$  and  $\Delta t=5 \times 10^{-14}$ s.

In Table 3 we list the computed values of the correlation dimension  $d_2$ , the Kaplan-York attractor dimension ( $d_L$ ), the Lyapunov's exponents ( $\lambda_i$ ,  $i=1-3$ ), the Kolmogorov entropy ( $K_{ent}$ ), and the Gottwald-Melbourne parameter

Table 1.  
Set of the ZrO molecular constants and electromagnetic field parameters

Parameters	ZrO
$\omega_e =$ ( $\text{cm}^{-1}$ )	969.7
$\omega_e x_e =$ ( $\text{cm}^{-1}$ )	4.90
$B_e$ ( $\text{cm}^{-1}$ )	0.423
$D_e$ ( $\text{cm}^{-1}$ )	$3.19 \times 10^{-7}$
$d_0$ (D)	2.55
$r_0$ (Å)	1.72
$M$ (a.u.m)	13.58
$W$ ( $\text{cm}^{-1}$ )	15.5-49.1

Table 2.

The correlation dimension  $d_2$ , Lyapunov's exponents ( $\lambda_i$ ,  $i=1,2$ ), Kaplan-York attractor dimension ( $d_L$ ), Kolmogorov entropy ( $K_{entr}$ ), the Gottwald-Melbourne parameter  $K_{GW}$

$d_2$	$\lambda_1$	$\lambda_2$	$d_L$	$K_{entr}$	$K_{GW}$
2.76	0.147	0.018	2.53	0.165	0.73

Analysis of the presented data allows to make conclusions that the dynamics of the ZrO molecule in a resonant linearly polarized electromagnetic field has the elements of a deterministic chaos (the strange attractor) and this conclusion is entirely agreed with the results of modelling for other diatomic molecules [3,7-11].

### References

- Lichtenberg, A. J. ; Lieberman, M. A. *Regular and Stochastic Motion*; Springer-Verlag: City, **1983**.
- Martin C.; Gutzwiller, G. *Chaos in Classical and Quantum Mechanics*; Springer-Verlag: New York, **1990**.
- Chirikov, B.V. A universal instability of many-dimensional oscillator systems. *Phys. Rep.* 1979, *52(5)*, 263-379.
- Aurich, R.; Steiner, F. Statistical properties of highly excited quantum eigenstates of a strongly chaotic system. *Physica D.* **1993**, *64*, 185
- Benvenuto, F.; Casati, G.; Shepelyansky, D.L. Rydberg Stabilization of atoms in strong fields: "magic" mountain in chaotic sea. *Z.Phys.B.* **1994**, *94*, 481-486.
- Glushkov, A.V. Spectroscopy of atom and nucleus in a strong laser field: Stark effect and multiphoton resonances. *J. Phys.: Conf. Ser.* **2014**, *548*, 012020.
- Berman, G.P.; Bulgakov, E.N.; Holm, D.D. Nonlinear resonance and dynamical chaos in a diatomic molecule driven by a resonant IR field. *Phys. Rev. A* **1995**, *52*, 3074-3080.
- Zhang, C.; Katsouleas, T.; Joshi, C. Harmonic frequency generation and chaos in laser driven molecular vibrations. In *Proc. of Shortwavelength Physics with Intense Laser Pulses*, San-Diego, CA, March 29-31, 1993; Bederson, B., Walther, H., Eds.; Acad. Press: San Diego, 1993, pp 21-28.
- López, G. V.; Mercado, A. P. Classical Chaos on Double Nonlinear Resonances in Diatomic Molecules. *J. Mod. Phys.* 2015, *6*, 496-509.
- Arango, C.A.; Kennerly, W.W.; Ezra, G.S. Classical and quantum mechanics of diatomic molecules in tilted fields. *J. Chem. Phys.* **2005**, *122*, 184303.
- Ignatenko, A.V.; Buyadzhi, A.; Buyadzhi, V.; Kuznetsova, A.; Mashkantsev, A.; Ternovsky, E. Non-linear chaotic dynamics of quantum systems: molecules in an electromagnetic field// *Adv. Quant. Chem.* **2018**, *78* <https://doi.org/10.1016/bs.aiq.2018.06.006>.
- Glushkov, A.V. True effective molecular valency Hamiltonian in a logical semiempirical theory. *Journal of Structural Chem.* **1988**, *29(4)*, 495-501.
- Glushkov, A.V. Operator Perturbation Theory for Atomic Systems in a Strong DC Electric Field. In *Advances in Quantum Methods and Applications in Chemistry, Physics, and Biology, Series: Progress in Theoretical Chemistry and Physics*; Hotokka, M., Brändas, E., Maruani, J., Delgado-Barrio, G., Eds.; Springer: Cham, **2013**; Vol. 27, pp 161–177.
- Malinovskaya, S.V.; Glushkov, A.V.; Khetselius, O.Yu.; Svinarenko, A.A.; Mischenko, E.V.; Florko, T.A. Optimized perturbation theory scheme for calculating the interatomic potentials and hyperfine lines shift for heavy atoms in the buffer inert gas. *Int. J. Quant. Chem.* **2009**, *109(4)*, 3325-3329.

15. Glushkov, A.V.; Khetselius, O.Yu.; Malinovskaya, S.V. Optics and spectroscopy of cooperative laser-electron nuclear processes in atomic and molecular systems – new trend in quantum optics. *Europ. Phys. Journ. ST* **2008**, *160*, 195-204.
16. Glushkov, A.V.; Khetselius, O.Yu.; Malinovskaya, S.V. Spectroscopy of cooperative laser–electron nuclear effects in multiatomic molecules. *Molec. Phys.* **2008**, *106*, 1257-1260.
17. Glushkov, A.V.; Khetselius, O.Yu.; Svinarenko, A.A.; Serbov, N.G. The sea and ocean 3D acoustic waveguide: rays dynamics and chaos phenomena, *J. Acoust. Soc. Amer.* **2008**, *123*(5), 3625.
18. Bunyakova, Yu.Ya.; Glushkov, A.V.; Fedchuk, A.P.; Serbov, N.G.; Svinarenko, A.A.; Tsenenko, I.A. Sensing non-linear chaotic features in dynamics of system of coupled autogenerators: multifractal analysis, *Sensor Electr. and Microsyst. Techn.* **2007**, *Issue 1*, 14-17.
19. Gottwald, G.A. ; Melbourne, I. Testing for chaos in deterministic systems with noise. *Physica D.* **2005**, *212*, 100-110.
20. Abarbanel, H.; Brown, R.; Sidorowich, J; Tsimring, L. The analysis of observed chaotic data in physical systems. *Rev. Mod. Phys.* **1993**, *65*, 1331-1392.
21. Packard, N.; Crutchfield, J; Farmer, J.; Shaw, R. Geometry from a time series *Phys. Rev. Lett.* **1988**, *45*, 712-716.
22. Kennel, M.; Brown, R.; Abarbanel, H. Determining embedding dimension for phase-space reconstruction using a geometrical construction. *Phys. Rev. A.* **1992**, *45*, 3403-3412.
23. Gallager, R. *Information theory and reliable communication*. Wiley: N.-Y., **1986**.
24. Grassberger, P. ; Procaccia, I. Measuring the strangeness of strange attractors. *Physica D.* **1983**, *9*, 189-208.
25. Theiler, J.; Eubank, S.; Longtin, A.; Galdrikian, B.; Farmer, J. Testing for nonlinearity in time series: The method of surrogate data. *Physica D.* **1992**, *58*, 77-94.
26. Sano, M.; Y. Sawada, Y. Measurement of the Lyapunov spectrum from chaotic time series. *Phys Rev.Lett.* **1995**, *55*, 1082-1085.
27. Glushkov, A.V. *Methods of a Chaos Theory*. OSENU: Odessa, **2012**.
28. Glushkov, A.V.; Khetselius, O.Yu.; Brusentseva, S.V.; Zaichko, P.A.; Ternovsky, V.B. Studying interaction dynamics of chaotic systems within a non-linear prediction method: Application to neurophysiology *In Advances in Neural Networks, Fuzzy Systems and Artificial Intelligence, Series: Recent Advances in Computer Engineering*; Balicki, J., Ed.; WSEAS Press: Gdansk, **2014**; Vol 21, pp 69-75.
29. Glushkov, A.V.; Prepelitsa, G.P.; Svinarenko, A.A. ; Zaichko, P.A. Studying interaction dynamics of the non-linear vibrational systems within non-linear prediction method (application to quantum autogenerators) *In Dynamical Systems Theory*; Awrejcewicz, J., Kazmierczak, M., Olejnik, P., Mrozowski, J., Eds.; Wyd. Politech. Łódź.: Łódź, **2013**; Vol T1, pp 467-477.
30. Khetselius, O.Yu. Forecasting evolutionary dynamics of chaotic systems using advanced non-linear prediction method *In Dynamical Systems Applications*; Awrejcewicz, J., Kazmierczak, M., Olejnik, P., Mrozowski, J., Eds.; Wyd. Politech. Łódź.: Łódź, **2013**; Vol T2, pp 145-152.
31. Khetselius, O.Yu.; Brusentseva, S.; Tkach, T.B. Studying interaction dynamics of chaotic systems within non-linear prediction method: Application to neurophysiology *In Dynamical Systems Applications*; Awrejce-

- wicz, J., Kazmierczak, M., Olejnik, P., Mrozowski, J., Eds.; Wyd. Politech. Łódź.: Łódź, **2013**; Vol T2, pp 251-259.
32. Glushkov, A.V.; Khetselius, O.Yu.; Brusentseva, S.; Duborez, A. Modeling chaotic dynamics of complex systems with using chaos theory, geometric attractors, and quantum neural networks. *Proc. Intern. Geometry Center.* **2014**, 7(3), 87-94.
  33. Glushkov, A.V.; Bunyakova, Yu.Ya.; Zaichko, P.A. Geometry of Chaos: Consistent combined approach to treating chaotic dynamics atmospheric pollutants and its forecasting. *Proc. Intern. Geometry Center.* **2013**, 6(3), 6-14.
  34. Glushkov, A.V.; Lovett, L.; Khetselius, O.Yu.; Gurnitskaya, E.P.; Dubrovskaya, Yu.V.; Loboda, A.V. Generalized multiconfiguration model of decay of multipole giant resonances applied to analysis of reaction ( $\mu - n$ ) on the nucleus  $^{40}\text{Ca}$ . *Int. J. Modern Phys. A.* **2009**, 24(2-3), 611-615
  35. Khetselius, O.Yu.; Florko, T.A.; Svinarenko, A.A.; Tkach, T.B. Radiative and collisional spectroscopy of hyperfine lines of the Li-like heavy ions and Tl atom in an atmosphere of inert gas. *Phys. Scripta.* **2013**, T153, 014037
  36. Glushkov, A.V.; Malinovskaya, S.V.; Sukharev, D.E.; Khetselius, O.Yu.; Loboda, A.V.; Lovett, L. Green's function method in quantum chemistry: New numerical algorithm for the Dirac equation with complex energy and Fermi-model nuclear potential. *Int. Journ. Quant. Chem.* **2009**, 109, 1717-1727.
  37. Khetselius, O.Yu. Relativistic calculating the hyperfine structure parameters for heavy-elements and laser detecting the isotopes and nuclear reaction products. *Phys. Scripta.* **2009**, T135, 014023.
  38. Svinarenko, A.A. Study of spectra for lanthanides atoms with relativistic many-body perturbation theory: Rydberg resonances. *J. Phys.: Conf. Ser.* **2014**, 548, 012039
  39. Glushkov, A.V.; Malinovskaya, S.V.; Gurnitskaya, E.P.; Khetselius, O.Yu.; Dubrovskaya, Yu.V. Consistent quantum theory of recoil induced excitation and ionization in atoms during capture of neutron. *J. Phys.: Conf. Ser.* **2006**, 35, 425-430.
  40. Glushkov, A.V.; Ambroso, S.V.; Loboda, A.V.; Gurnitskaya, E.P.; Prepelitsa, G.P. Consistent QED approach to calculation of electron-collision excitation cross sections and strengths: Ne-like ions. *Int. J. Quantum Chem.* **2005**, 104, 562-569.
  41. Khetselius, O.Yu. Atomic parity non-conservation effect in heavy atoms and observing P and PT violation using NMR shift in a laser beam: To precise theory. *J. Phys.: Conf. Ser.* **2009**, 194, 022009.
  42. Glushkov, A.V.; Loboda, A.V.; Gurnitskaya, E.P.; Svinarenko, A.A. QED theory of radiation emission and absorption lines for atoms in a strong laser field. *Phys. Scripta.* **2009**, 135, 014022.
  43. Glushkov, A.V.; Ivanov, L.N. DC strong-field Stark effect: consistent quantum-mechanical approach. *J. Phys. B: At. Mol. Opt. Phys.* **1993**, 26, L379-386.
  44. Khetselius, O.Yu. *Hyperfine structure of atomic spectra.* Astroprint: Odessa, **2008**.
  45. Glushkov, A.V. Relativistic multiconfiguration time-dependent self-consistent-field theory for molecules. *Sov. Phys. Journal.* **1991**, 34(10), 871-876.
  46. Glushkov, A.V.; Khetselius, O.Yu.; Svinarenko, A.A. Theoretical spectroscopy of autoionization resonances in spectra of lanthanide atoms. *Phys. Scripta.* **2013**, T153, 014029.
  47. Glushkov, A.V. Spectroscopy of coop-

- erative muon-gamma-nuclear processes: Energy and spectral parameters *J. Phys.: Conf. Ser.* **2012**, 397, 012011
48. Khetselius, O.Yu. Spectroscopy of cooperative electron-gamma-nuclear processes in heavy atoms: NEET effect. *J. Phys.: Conf. Ser.* **2012**, 397, 012012.
  49. Glushkov, A.V.; Khetselius, O.Yu.; Loboda, A.V.; Svinarenko, A.A. QED approach to atoms in a laser field: Multi-photon resonances and above threshold ionization *In Frontiers in Quantum Systems in Chemistry and Physics, Series: Progress in Theoretical Chemistry and Physics*; Wilson, S., Grout, P., Maruani, J., Delgado-Barrio, G., Piecuch, P., Eds.; Springer: Dordrecht, **2008**; Vol. 18, pp 543-560.
  50. Malinovskaya, S.V.; Glushkov, A.V.; Khetselius, O.Y. New Laser-Electron Nuclear Effects in the Nuclear  $\gamma$  Transition Spectra in Atomic and Molecular Systems. *In Frontiers in Quantum Systems in Chemistry and Physics, Series: Progress in Theoretical Chemistry and Physics*; Wilson, S., Grout, P., Maruani, J., Delgado-Barrio, G., Piecuch, P., Eds.; Springer: Dordrecht, **2008**; Vol. 18, pp 525-541.
  51. Glushkov, A.V.; Malinovskaya, S.V.; Chernyakova Y.G.; Svinarenko, A.A. Cooperative laser-electron-nuclear processes: QED calculation of electron satellites spectra for multi-charged ion in laser field. *Int. Journ. Quant. Chem.* **2004**, 99, 889-893
  52. Glushkov, A.V. Negative ions of inert gases. *JETP Lett.* **1992**, 55, 97-100.
  53. Glushkov, A.V.; Ivanov, L.N.; Ivanova, E.P. Autoionization Phenomena in Atoms. *Moscow University Press, Moscow*, **1986**, 58-160
  54. Malinovskaya, S.V.; Glushkov, A.V.; Khetselius, O.Yu.; Lopatkin, Yu.M.; Loboda, A.V.; Nikola, L.V.; Svinarenko, A.A.; Perelygina, T.B. Generalized energy approach for calculating electron collision cross-sections for multicharged ions in a plasma: Debye shielding model, *Int. J. Quant.Chem.* **2011**, 111(2), 288-296.
  55. Buyadzhi, V.V. Laser multiphoton spectroscopy of atom embedded in Debye plasmas: multiphoton resonances and transitions. *Photoelectronics.* **2015**, 24, 128-133.
  56. Glushkov, A.V.; Malinovskaya, S.V.; Loboda, A.V.; Shpinareva, I.M.; Gurnitskaya, E.P.; Korchevsky, D.A. Diagnostics of the collisionally pumped plasma and search of the optimal plasma parameters of x-ray lasing: calculation of electron-collision strengths and rate coefficients for Ne-like plasma. *J. Phys.: Conf. Ser.* **2005**, 11, 188-198.
  57. Glushkov, A.V.; Khetselius, O.Yu.; Svinarenko, A.A. Relativistic theory of cooperative muon- $\gamma$  -nuclear processes: Negative muon capture and metastable nucleus discharge. *In Advances in the Theory of Quantum Systems in Chemistry and Physics, Series: Progress in Theoretical Chemistry and Physics*; Hoggan, P., Brändas, E., Maruani, J., Delgado-Barrio, G., Piecuch, P. Eds.; Springer: Dordrecht, **2012**; Vol. 22, pp 51-68.
  58. Glushkov, A.V.; Khetselius, O.Yu.; Lovett, L. Electron- $\beta$ -Nuclear Spectroscopy of Atoms and Molecules and Chemical Bond Effect on the  $\beta$ -Decay Parameters. *In Advances in the Theory of Atomic and Molecular Systems Dynamics, Spectroscopy, Clusters, and Nanostructures, Series: Progress in Theoretical Chemistry and Physics*; Piecuch, P., Maruani, J., Delgado-Barrio, G., Wilson, S., Eds.; Springer: Dordrecht, **2009**; Vol. 20, pp 125-152.
  59. Khetselius, O.Yu. Relativistic Energy Approach to Cooperative Electron- $\gamma$ -Nuclear Processes: NEET Effect *In Quantum Systems in Chemistry and Physics, Series: Progress in Theo-*

- retical Chemistry and Physics*; Nishikawa, K., Maruani, J., Brändas, E., Delgado-Barrio, G., Piecuch, P., Eds.; Springer: Dordrecht, **2012**; Vol. 26, pp 217-229.
60. Glushkov, A.V. Advanced Relativistic Energy Approach to Radiative Decay Processes in Multielectron Atoms and Multicharged Ions. In *Quantum Systems in Chemistry and Physics: Progress in Methods and Applications, Series: Progress in Theoretical Chemistry and Physics*; Nishikawa, K., Maruani, J., Brändas, E., Delgado-Barrio, G., Piecuch, P., Eds.; Springer: Dordrecht, **2012**; Vol. 26, pp 231–252.
  61. Khetselius, O.Yu. Relativistic perturbation theory calculation of the hyperfine structure parameters for some heavy-element isotopes. *Int. Journ. Quant.Chem.* **2009**, *109*, 3330-3335.
  62. Ignatenko, A.V. Probabilities of the radiative transitions between Stark sublevels in spectrum of atom in an DC electric field: New approach. *Photoelectronics*, **2007**, *16*, 71-74.
  63. Gurskaya, M.Yu.; Ignatenko, A.V.; Kvasikova, A.S.; Buyadzhi A.A. Advanced data for hydrogen atom in crossed electric and magnetic fields. *Photoelectronics*. **2017**, *26*, 148-155.
  64. Glushkov, A.V. *Atom in an electromagnetic field*. KNT: Kiev, **2005**.
  65. Glushkov, A.V. *Relativistic Quantum theory. Quantum mechanics of atomic systems*. Astroprint: Odessa, **2008**.
  66. Khetselius, O.Yu. *Quantum structure of electroweak interaction in heavy finite Fermi-systems*. Astroprint: Odessa, **2011**.
  67. Glushkov, A.V.; Buyadzhi, V.V.; Ponomarenko, E.L. Geometry of Chaos: Advanced approach to treating chaotic dynamics in some nature systems// Proc. Intern. Geom. Center. 2014 *7(1)*,24-30.
  68. Pettersson, A.; Koivisto, R.; Lindgren, P.; Lundevall, S; Royen, P.; Sassenberg, U.; Shi, W. Electric Dipole Moment of the  $B^1\Pi$  State of ZrO. *J. Mol. Spectr.* 2000, *200*, 65-71.
  69. Glushkov, A.V.; Khetselius, O.Yu.; Svinarenko, A.A.; Buyadzhi, V.V. Spectroscopy of autoionization states of heavy atoms and multiply charged ions (Odessa: TEC) -**2015**.
  70. Huber, K.P.; Herzberg, G. *Molecular spectra and molecular structure. IV. Constants of Diatomic Molecules*; Van Nostrand Reinhold Co.: New York, **1979**.

This article has been received in August 2018

PACS 31.15.-p; 33.20.-t

*A. A. Mashkantsev, A. V. Ignatenko, S. V. Kirianov, E. V. Pavlov*

## CHAOTIC DYNAMICS OF DIATOMIC MOLECULES IN AN ELECTROMAGNETIC FIELD

### Summary

Nonlinear chaotic dynamics of the diatomic molecules interacting with a resonant linearly polarized electromagnetic field is computationally modelled. It is presented an effective quantum-mechanical model for diatomic molecule in an electromagnetic field, based on the Schrödinger equation and model potential method. To detect the elements of a chaotic dynamics, we used the known chaos theory and non-linear analysis methods such as a correlation integral algorithm, the Lyapunov's exponents and Kolmogorov entropy analysis, prediction model etc. There are listed the data of computing dynamical and topological invariants such as the correlation, embedding and Kaplan-Yorke dimensions, Lyapunov's exponents, Kolmogorov entropy etc, for polarization time series of the ZrO molecule interacting with a linearly polarized electromagnetic field. The results obtained are in a physically reasonable agreement with the conclusions by Berman, Kolovskii, Zaslavsky, Zganh et al, Glushkov et al.

**Key words:** Nonlinear chaotic dynamics, diatomic molecules, electromagnetic field

PACS 31.15.-p; 33.20.-t

*A. A. Машканцев, А. В. Игнатенко, С. В. Кирьянов, Е. В. Павлов*

## ХАОТИЧЕСКАЯ ДИНАМИКА ДВУХАТОМНЫХ МОЛЕКУЛ В ЭЛЕКТРОМАГНИТНОМ ПОЛЕ

### Резюме

Моделируется нелинейная хаотическая динамика двухатомных молекул, взаимодействующих с резонансным линейно-поляризованным электромагнитным полем. Представлена эффективная квантово-механическая модель для двухатомной молекулы в электромагнитном поле, базирующаяся на использовании уравнения Шредингера и метода модельного потенциала. Для детектирования элементов хаотической динамики использованы методы теории хаоса и нелинейного анализа, такие как алгоритм корреляционного интеграла, анализ на основе показателей Ляпунова и энтропии Колмогорова, траекторная модель прогноза и др. Представлены данные вычисления динамических и топологических инвариантов таких как корреляционная размерность, размерности вложения и Каплана-Йорка, показатели Ляпунова, энтропия Колмогорова и т. д. для временной зависимости поляризации молекулы ZrO, взаимодействующей с линейно-поляризованным электромагнитным полем. Полученные результаты находятся в физически разумном согласии с качественными выводами Бермана, Коловского, Заславского, Згана, Глушкова и др.

**Ключевые слова:** нелинейная хаотическая динамика, двухатомная молекула, электромагнитное поле

*О. А. Машканцев, Г. В. Игнатенко, С. В. Кір'янов, Є. В. Павлов*

## **ХАОТИЧНА ДИНАМІКА ДВОАТОМНИХ МОЛЕКУЛ В ЕЛЕКТРОМАГНІТНОМУ ПОЛІ**

### **Резюме**

Моделюється нелінійна хаотична динаміка двоатомних молекул, взаємодіючих з резонансним лінійно-поляризованим електромагнітним полем. Представлена ефективна квантово-механічна модель для двоатомних молекули в електромагнітному полі, що базується на використанні рівняння Шредінгера і методу модельного потенціалу. Для детектування елементів хаотичної динаміки використані методи теорії хаосу і нелінійного аналізу, такі як алгоритм кореляційного інтеграла, аналіз на основі показників Ляпунова і ентропії Колмогорова, траєкторна модель прогнозу і ін. Представлені дані обчислення динамічних і топологічних інваріантів таких як кореляційна розмірність, розмірності вкладення і Каплана-Йорка, показники Ляпунова, ентропія Колмогорова і т. д. для часової залежності поляризації молекули  $ZrO$ , яка взаємодіє з лінійно-поляризованим електромагнітним полем. Отримані результати знаходяться в фізично розумній згоді з якісними висновками Бермана, Коловського, Заславського, Згана, Глушкова та ін.

**Ключові слова:** нелінійна хаотична динаміка, двоатомна молекула, електромагнітне поле

*A. A. Svinarenko<sup>2</sup>, V. B. Ternovsky<sup>1</sup>, I. S. Cherkasova<sup>1</sup>, D. A. Mironenko<sup>2</sup>*

<sup>1</sup>Odessa National Maritime Academy, Didrikhsona str. 4, Odessa, 65001

<sup>2</sup>Odessa State Environmental University, L'vovskaya str.15, Odessa, 65016

E-mail: ternovskyvb@gmail.com

## **THEORETICAL STUDYING SPECTRA OF YTTERBIUM ATOM ON THE BASIS OF RELATIVISTIC MANY-BODY PERTURBATION THEORY: DOUBLY EXCITED VALENCE STATES**

Theoretical studying spectrum of doubly excited valence states of the ytterbium is carried out within the relativistic many-body perturbation theory and generalized relativistic energy approach. The zeroth approximation of the relativistic perturbation theory is provided by the optimized Dirac-Kohn-Sham ones. Optimization has been fulfilled by means of introduction of the parameter to the Kohn-Sham exchange potentials and further minimization of the gauge-non-invariant contributions into radiation width of atomic levels with using relativistic orbital set, generated by the corresponding zeroth approximation Hamiltonian.

### **1. Introduction**

This paper goes on our work on theoretical studying spectra and spectroscopic parameters for heavy atoms, namely, lanthanides atoms (see, for example [1-3]). It is well known that an investigation of spectra, optical and spectral, radiative and autoionization characteristics for heavy elements atoms and multicharged ions is traditionally of a great interest for further development quantum atomic optics and atomic spectroscopy and different applications in plasma chemistry, astro-physics, laser physics etc. (see Refs. [1-31]).

The multi-configuration Dirac-Fock method is the most reliable version of calculation for multi-electron systems with a large nuclear charge. In these calculations the one- and two-particle relativistic and important exchange-correlation corrections are taken into account (see Refs. [1] and Refs. therein). However, one should remember about very complicated structure of spectra of the lanthanides atoms and necessity of correct accounting the different correlation effects such as polarization interaction of the valent quasi-particles and their mutual screening, iterations of a mass operator etc.). The known method of the model relativistic many-body perturbation

theory (RMBPT) has been earlier effectively applied to computing spectra of low-lying states for some lanthanides atoms [1] (see also [2-6]). We use an analogous version of the perturbation theory (PT) to study spectrum of doubly excited valence states of the ytterbium, however, the optimized zeroth approximation is generated within the Dirac-Kohn-Sham model.

### **2. Advanced relativistic many-body perturbation theory and energy approach**

As the method of computing is earlier presented in details, here we are limited only by the key topics [1-3]. Generally speaking, the majority of complex atomic systems possess a dense energy spectrum of interacting states with essentially relativistic properties. In the theory of the non-relativistic atom a convenient field procedure is known for calculating the energy shifts  $\Delta E$  of degenerate states. This procedure is connected with the secular matrix  $M$  diagonalization [26-30]. In constructing  $M$ , the Gell-Mann and Low adiabatic formula for  $\Delta E$  is used. In contrast to the non-relativistic case, the secular matrix elements are already complex in the second order of the electro-dynamical PT (first order of the interelectron interaction). Their imagi-

nary part of  $\Delta E$  is connected with the radiation decay (radiation) possibility. In this approach, the whole calculation of the energies and decay probabilities of a non-degenerate excited state is reduced to the calculation and diagonalization of the complex matrix  $M$ . In the papers of different authors, the  $\text{Re}\Delta E$  calculation procedure has been generalized for the case of nearly degenerate states, whose levels form a more or less compact group. One of these variants has been previously introduced: for a system with a dense energy spectrum, a group of nearly degenerate states is extracted and their matrix  $M$  is calculated and diagonalized. If the states are well separated in energy, the matrix  $M$  reduces to one term, equal to  $\dots$ . The non-relativistic secular matrix elements are expanded in a PT series for the interelectron interaction. The complex secular matrix  $M$  is represented in the form [2]:

$$M = M^{(0)} + M^{(1)} + M^{(2)} + M^{(3)}. \quad (1)$$

where  $M^{(0)}$  is the contribution of the vacuum diagrams of all order of PT, and  $M^{(1)}$ ,  $M^{(2)}$ ,  $M^{(3)}$  those of the one-, two- and three- quasiparticle diagrams respectively.  $M^{(0)}$  is a real matrix, proportional to the unit matrix. It determines only the general level shift. We have assumed  $M^{(0)} = 0$ . The diagonal matrix  $M^{(1)}$  can be presented as a sum of the independent one-quasiparticle contributions. For simple systems (such as alkali atoms and ions) the one-quasiparticle energies can be taken from the experiment. Substituting these quantities into (1) one could have summarized all the contributions of the one-quasiparticle diagrams of all orders of the formally exact QED PT. However, the necessary experimental quantities are not often available. The first two order corrections to  $\text{Re}M^{(2)}$  have been analyzed previously using Feynman diagrams (look Ref. in [2,3]). The contributions of the first-order diagrams have been completely calculated. In the second order, there are two kinds of diagrams: polarization and ladder ones. The polarization diagrams take into account the quasiparticle interaction through the polarizable core, and the ladder diagrams account for the im-

mediate quasiparticle interaction [11-20]. Some of the ladder diagram contributions as well as some of the three-quasiparticle diagram contributions in all PT orders have the same angular symmetry as the two-quasiparticle diagram contributions of the first order. These contributions have been summarized by a modification of the central potential, which must now include the screening (anti-screening) of the core potential of each particle by the two others. The additional potential modifies the one-quasiparticle orbitals and energies. Then the secular matrix is as follows:

$$\rightarrow \tilde{\dots} \tilde{\dots}, \quad (2)$$

where  $\tilde{M}^{(1)}$  is the modified one-quasiparticle matrix (diagonal), and  $\tilde{M}^{(2)}$  the modified two-quasiparticle one.  $\tilde{M}^{(1)}$  is calculated by substituting the modified one-quasiparticle energies, and  $\tilde{M}^{(2)}$  by means of the first PT order formulae for  $M^{(2)}$ , putting the modified radial functions of the one-quasiparticle states in the radial integrals..

Let us remind that in the QED theory, the photon propagator D(12) plays the role of this interaction. Naturally the analytical form of D(12) depends on the gauge, in which the electro-dynamical potentials are written. Interelectron interaction operator with accounting for the Breit interaction has been taken as follows:

$$V(r_i r_j) = \exp(i\alpha r_j) \cdot \frac{(1 - \hat{a}_i \hat{a}_j)}{r_j}, \quad (3)$$

where, as usually,  $\alpha_i$  are the Dirac matrices. In general, the results of all approximate calculations depended on the gauge. Naturally the correct result must be gauge-invariant. The gauge dependence of the amplitudes of the photo processes in the approximate calculations is a well known fact and is in details investigated by Grant, Armstrong, Aymar and Luc-Koenig, Glushkov-Ivanov et al (see [32-40] and numerous Refs. therein). Grant has investigated the gauge connection with the limiting non-relativistic form of the transition operator and has formulated the conditions for approximate functions of the states, in which the amplitudes

of the photo processes are gauge invariant [3]. These results remain true in the energy approach because the final formulae for the probabilities coincide in both approaches. Glushkov-Ivanov have developed a new relativistic gauge-conserved version of the energy approach [32]. In ref. [1] it has been developed its further generalization. Here we applied this approach for generating the optimized relativistic orbitals basis in the zeroth approximation of the many-body PT. Optimization has been fulfilled by means of introduction of the parameter to the Fock and Kohn-Sham exchange potentials and further minimization of the gauge-non-invariant contributions into radiation width of atomic levels with using relativistic orbital bases, generated by the corresponding zeroth approximation Hamiltonians. Other details can be found in Refs. [1-3,37-46].

### 3 Some illustration results and conclusion

The excited states of the ytterbium atom can be treated as the states with two-quasiparticles above the electron core  $[Xe]4f^{14}$ . In table 1 the energies (accounted from the Yb  $4f^{14}$  core energy): of the YbI excited states with doubly excited valence shell are listed:  $E1$ - the EA-MMBPT data (from refs. [31]);  $E2$ - the RMBPT data from [1,47];  $E3$  – our data.

Table 1.

### Energies (in $10^2\text{cm}^{-1}$ ) of some YbI excited states with doubly excited valence shell.

Config.	$J$	Theory			$Exp.$
		$E1$	$E2$	$E3$	
$6p_{1/2}^2$	0	-1067	-1064	-1062	-1062,7
$6p_{3/2}^2$	2	-987	-1004	-1003	-1008.9
$6p_{1/2}6p_{3/2}$	1	-1054	-1050	-1049	-1049.0
$6p_{1/2}6p_{3/2}$	2	-1032	-1036	-1035	-1039.5
$5d_{3/2}^2$	2	-1034	-1032	-1030	-1010.8
$5d_{3/2}5d_{5/2}$	2	-994	-995	-994	-994.6
$5d_{3/2}5d_{5/2}$	3	-1030	-1032	-1032	-1032.5

In table 2 our data listed for other similar states. All presented MMBPT, ROMBPT and our data on the energies are in the physically reasonable agreement with experimental data. However, comparison of the corresponding results for widths (will be listed in another paper) demonstrates again sufficiently large discrepancy. In our opinion, this fact is explained by insufficiently exact estimates of the radial integrals, using the non-optimized bases and some other additional calculation approximations.

Table 2.

### Theoretical energies (in $10^2\text{cm}^{-1}$ ) of the YbI excited states with doubly excited valence shell.

Config.	$J$	$E2$	Config.	$J$	$E2$
$6p_{1/2}^2$	0	-1062	$6p_{3/2}5d_{5/2}$	3	-961
$6p_{3/2}^2$	0	-917	$6p_{3/2}5d_{5/2}$	4	-1060
$6p_{3/2}^2$	2	-1003	$5d_{3/2}^2$	0	-981
$6p_{1/2}6p_{3/2}$	1	-1049	$5d_{3/2}^2$	2	-1031
$6p_{1/2}6p_{3/2}$	2	-1035	$5d_{5/2}^2$	0	-962
$6p_{1/2}5d_{3/2}$	1	-1071	$5d_{5/2}^2$	2	-968
$6p_{1/2}5d_{3/2}$	2	-1068	$5d_{5/2}^2$	4	-859
$6p_{1/2}5d_{5/2}$	2	-1002	$5d_{3/2}5d_{5/2}$	1	-981
$6p_{1/2}5d_{5/2}$	3	-1114	$5d_{3/2}5d_{5/2}$	2	-994
$6p_{3/2}5d_{3/2}$	0	-1016	$5d_{3/2}5d_{5/2}$	3	-1031
$6p_{3/2}5d_{3/2}$	1	-1011	$5d_{3/2}5d_{5/2}$	4	-1025
$6p_{3/2}5d_{3/2}$	2	-912	$7s_{1/2}6p_{1/2}$	0	-886
$6p_{3/2}5d_{3/2}$	3	-1034	$7s_{1/2}6p_{1/2}$	1	-885.6
$6p_{3/2}5d_{5/2}$	1	-947	$7s_{1/2}6p_{3/2}$	1	-849
$6p_{3/2}5d_{5/2}$	2	-1115	$7s_{1/2}6p_{3/2}$	2	-860

### References

1. Svinarenko, A.A. Study of spectra for lanthanides atoms with relativistic many- body perturbation theory: Ry-

- berg resonances. *J. Phys.: Conf. Ser.* **2014**, 548, 012039.
2. Khetselius, O.Yu. *Hyperfine structure of atomic spectra*. Astroprint: Odessa, **2008**.
  3. Glushkov, A.V. *Relativistic Quantum theory. Quantum mechanics of atomic systems*. Astroprint: Odessa, **2008**.
  4. Glushkov, A.V.; Malinovskaya, S.V.; Loboda, A.V.; Shpinareva, I.M.; Prepelitsa, G.P. Consistent quantum approach to new laser-electron-nuclear effects in diatomic molecules. *J.Phys.: Conf. Ser.* **2006**, 35, 420-424.
  5. Glushkov, A.V. Operator Perturbation Theory for Atomic Systems in a Strong DC Electric Field. In *Advances in Quantum Methods and Applications in Chemistry, Physics, and Biology, Series: Progress in Theoretical Chemistry and Physics*; Hotokka, M., Brändas, E., Maruani, J., Delgado-Barrio, G., Eds.; Springer: Cham, **2013**; Vol. 27, pp 161–177.
  6. Glushkov, A.V.; Ambrosov, S.V.; Ignatenko, A.V.; Korchevsky, D.A. DC strong field stark effect for nonhydrogenic atoms: Consistent quantum mechanical approach. *Int. Journ. Quant. Chem.* **2004**, 99, 936-939.
  7. Glushkov, A.V.; Kondratenko, P.A.; Buyadgi V.V.; Kvasikova, A.S.; Sakun, T.N.; Shakhman, A.S. Spectroscopy of cooperative laser electron- $\gamma$ -nuclear processes in polyatomic molecules. *J. Phys.: Conf. Ser.* **2014**, 548, 012025.
  8. Malinovskaya, S.V.; Dubrovskaya, Yu.V.; Vitavetskaya, L.A. Advanced quantum mechanical calculation of the beta decay probabilities. *AIP Conf. Proc.* **2005**, 796, 201-205.
  9. Glushkov, A.V.; Malinovskaya, S.V.; Chernyakova Y.G.; Svinarenko, A.A. Cooperative laser-electron-nuclear processes: QED calculation of electron satellites spectra for multi-charged ion in laser field. *Int. Journ. Quant. Chem.* **2004**, 99, 889-893.
  10. Glushkov, A.V.; Malinovskaya, S.V.; Prepelitsa, G.; Ignatenko, V. Manifestation of the new laser-electron nuclear spectral effects in the thermalized plasma: QED theory of co-operative laser-electron-nuclear processes. *J. Phys.: Conf. Ser.* **2005**, 11, 199-206.
  11. Glushkov, A.V.; Malinovskaya, S.V.; Loboda, A.V.; Shpinareva, I.M.; Gurnitskaya, E.P.; Korchevsky, D.A. Diagnostics of the collisionally pumped plasma and search of the optimal plasma parameters of x-ray lasing: calculation of electron-collision strengths and rate coefficients for Ne-like plasma. *J. Phys.: Conf. Ser.* **2005**, 11, 188-198.
  12. Glushkov, A.V.; Ambrosov, S.; Loboda, A.; Gurnitskaya, E.; Prepelitsa, G. Consistent QED approach to calculation of electron-collision excitation cross sections and strengths: Ne-like ions. *Int. J. Quantum Chem.* **2005**, 104, 562-569.
  13. Glushkov, A.; Loboda, A.; Gurnitskaya, E.; Svinarenko, A. QED theory of radiation emission and absorption lines for atoms in a strong laser field. *Phys. Scripta.* **2009**, T135, 014022.
  14. Florko, T.A.; Tkach, T.B.; Ambrosov, S.V.; Svinarenko, A.A. Collisional shift of the heavy atoms hyperfine lines in an atmosphere of the inert gas. *J. Phys.: Conf. Ser.* **2012**, 397, 012037.
  15. Buyadzhi, V.V. Laser multiphoton spectroscopy of atom embedded in Debye plasmas: multiphoton resonances and transitions. *Photoelectronics.* **2015**, 24, 128-133.
  16. Buyadzhi, V.V.; Chernyakova, Yu.G.; Smirnov, A.V.; Tkach, T.B. Electron-collisional spectroscopy of atoms and ions in plasma: Be-like ions. *Photoelectronics.* **2016**, 25, 97-101.
  17. Buyadzhi, V.V.; Chernyakova, Yu.G.; Antoshkina, O.; Tkach, T. Spectroscopy of multicharged ions in plasmas: Oscillator strengths of Be-like ion Fe.

- Photoelectronics*. **2017**, *26*, 94-102.
18. Karaçoban, B.; Özdem, L. Energies, Landé Factors, and Lifetimes for Some Excited Levels of Neutral Ytterbium. *Acta Phys.Pol.A*. **2011**, *119*, 342-353.
  19. Khetselius, O.Yu. Relativistic Energy Approach to Cooperative Electron- $\gamma$ -Nuclear Processes: NEET Effect *In Quantum Systems in Chemistry and Physics, Series: Progress in Theoretical Chemistry and Physics*; Nishikawa, K., Maruani, J., Brändas, E., Delgado-Barrio, G., Piecuch, P., Eds.; Springer: Dordrecht, **2012**; Vol. 26, pp 217-229.
  20. Khetselius, O.Yu. Relativistic perturbation theory calculation of the hyperfine structure parameters for some heavy-element isotopes. *Int. Journ. Quant.Chem.* **2009**, *109*, 3330-3335.
  21. Khetselius, O.Yu. Relativistic calculation of the hyperfine structure parameters for heavy elements and laser detection of the heavy isotopes. *Phys. Scripta*. **2009**, *135*, 014023.
  22. Khetselius, O.Yu. Optimized Perturbation Theory for Calculating the Hyperfine Line Shift and Broadening of Heavy Atoms in a Buffer Gas. *In Frontiers in Quantum Methods and Applications in Chemistry and Physics, Series: Progress in Theoretical Chemistry and Physics*; Nascimento, M., Maruani, J., Brändas, E., Delgado-Barrio, G., Eds.; Springer: Cham, **2015**; Vol. 29, pp. 55-76.
  23. Khetselius, O.Yu. *Quantum structure of electroweak interaction in heavy finite Fermi-systems*. Astroprint: Odessa, **2011**.
  24. Glushkov, A.V.; Malinovskaya S.V. Co-operative laser nuclear processes: border lines effects *In New Projects and New Lines of Research in Nuclear Physics*. Fazio, G., Hanappe, F., Eds.; World Scientific: Singapore, **2003**, 242-250.
  25. Glushkov, A.V. Spectroscopy of atom and nucleus in a strong laser field: Stark effect and multiphoton resonances. *J. Phys.: Conf. Ser.* **2014**, *548*, 012020
  26. Ivanov, L.N.; Ivanova, E.P. Atomic ion energies for Na-like ions by a model potential method  $Z = 25-80$ . *Atom. Data Nucl. Data Tabl.* **1979**, *24*, 95-109.
  27. Driker, M.N.; Ivanova, E.P.; Ivanov, L.N.; Shestakov, A.F. Relativistic calculation of spectra of 2-2 transitions in O- and F-like atomic ions. *J. Quant. Spectr. Rad. Transf.* **1982**, *28*, 531-535.
  28. Ivanova, E.P.; Ivanov, L.N.; Glushkov, A.V.; Kramida, A.E. High order corrections in the relativistic perturbation theory with the model zeroth approximation, Mg-Like and Ne-Like Ions. *Phys. Scripta* 1985, *32*, 513-522.
  29. Ivanov, L.N.; Ivanova, E.P.; Knight, L. Energy approach to consistent QED theory for calculation of electron-collision strengths: Ne-like ions. *Phys. Rev. A*. **1993**, *48*, 4365-4374.
  30. Glushkov, A.V.; Ivanov, L.N.; Ivanova, E.P. Autoionization Phenomena in Atoms. *Moscow University Press, Moscow*, **1986**, 58-160
  31. Bekov, G.I.; Vidolova-Angelova, E.P.; Ivanov, L.N.; Letokhov, V.S.; Mishin V.. Laser spectroscopy of narrow doubly excited autoionization states of ytterbium atoms. *JETP*. **1981**, *53*, 441-447
  32. Glushkov, A.V.; Ivanov, L.N. Radiation decay of atomic states: atomic residue polarization and gauge non-invariant contributions. *Phys. Lett. A* **1992**, *170*, 33-36.
  33. Glushkov, A.V. *Relativistic and Correlation Effects in Spectra of Atomic Systems*. Astroprint: Odessa, **2006**.
  34. Glushkov, A.V. Relativistic polarization potential of a many-electron atom. *Sov. Phys. Journal*. **1990**, *33(1)*, 1-4.

35. Glushkov, A.V. Negative ions of inert gases. *JETP Lett.* **1992**, *55*, 97-100.
36. Glushkov, A.V. Energy approach to resonance states of compound super-heavy nucleus and EPPP in heavy nuclei collisions *In Low Energy Antiproton Physics*; Grzonka, D., Czyzykiewicz, R., Oelert, W., Rozek, T., Winter, P., Eds.; AIP: New York, *AIP Conf. Proc.* **2005**, *796*, 206-210.
37. Glushkov, A.V. Spectroscopy of cooperative muon-gamma-nuclear processes: Energy and spectral parameters *J. Phys.: Conf. Ser.* **2012**, *397*, 012011
38. Glushkov, A.V. Advanced Relativistic Energy Approach to Radiative Decay Processes in Multielectron Atoms and Multicharged Ions. *In Quantum Systems in Chemistry and Physics: Progress in Methods and Applications, Series: Progress in Theoretical Chemistry and Physics*; Nishikawa, K., Maruani, J., Brandas, E., Delgado-Barrio, G., Piecuch, P., Eds.; Springer: Dordrecht, **2012**; Vol. 26, pp 231–252.
39. Glushkov, A. Multiphoton spectroscopy of atoms and nuclei in a laser field: relativistic energy approach and radiation atomic lines moments method// *Adv. Quant.Chem.* (Elsevier), **2018**, *78*, doi.org/10.1016/bs.aiq.2018.06.004
40. Khetselius, O. Optimized relativistic many-body perturbation theory calculation of wavelengths and oscillator strengths for li-like multicharged ions// *Adv. Quant. Chem.* (Elsevier) , **2018**, *78*, doi.org/10.1016/bs.aiq.2018.06.001.
41. Khetselius, O.Yu. Hyperfine structure of radium. *Photoelectronics.* **2005**, *14*, 83-85.
42. Glushkov A.V.; Ivanov, L.N. DC strong-field Stark effect: consistent quantum-mechanical approach. *J. Phys. B: At. Mol. Opt. Phys.* **1993**, *26*, L379-386.
43. Khetselius O.Yu.; Gurnitskaya, E.P. Sensing the hyperfine structure and nuclear quadrupole moment for radium. *Sensor Electr. and Microsyst. Techn.* **2006**, *2*, 25-29.
44. Khetselius, O.Yu. Atomic parity non-conservation effect in heavy atoms and observing P and PT violation using NMR shift in a laser beam: To precise theory. *J. Phys.: Conf. Ser.* **2009**, *194*, 022009
45. Glushkov, A.V.; Gurskaya, M.Yu.; Ignatenko, A.V.; Smirnov, A.V.; Serga, I.N.; Svinarenko, A.A.; Ternovsky, E.V. Computational code in atomic and nuclear quantum optics: Advanced computing multiphoton resonance parameters for atoms in a strong laser field. *J. Phys.: Conf. Ser.* **2017**, *905*, 012004.
46. Glushkov, A.; Khetselius, O.; Svinarenko, A.; Buyadzhi, V. *Spectroscopy of autoionization states of heavy atoms and multiply charged ions.* Odessa: TEC, **2015**.
47. Glushkov, A.V.; Khetselius, O.Yu.; Svinarenko A.A. Theoretical spectroscopy of autoionization resonances in spectra of lanthanides atoms. *Phys. Scripta.* **2013**, *T153*, 014029.

This article has been received in September 2018

PACS 32.30.-r

*A. A. Svinarenko, V. B. Ternovsky, I. S. Cherkasova, D. A. Mironenko*

**THEORETICAL STUDYING SPECTRA OF YTTERBIUM ATOM  
ON THE BASIS OF RELATIVISTIC MANY-BODY PERTURBATION THEORY:  
DOUBLY EXCITED VALENCE STATES**

**Summary**

Theoretical studying spectrum of doubly excited valence states of the ytterbium is carried out within the relativistic many-body perturbation theory and generalized relativistic energy approach. The zeroth approximation of the relativistic perturbation theory is provided by the optimized Dirac-Kohn-Sham ones. Optimization has been fulfilled by means of introduction of the parameter to the Fock and Kohn-Sham exchange potentials and further minimization of the gauge-non-invariant contributions into radiation width of atomic levels with using relativistic orbital sets, generated by the corresponding zeroth approximation Hamiltonian.

PACS 32.30.-r

*A. A. Свинаренко, В. Б. Терновский, И. С. Черкасова, Д. А. Мироненко*

**ТЕОРЕТИЧЕСКОЕ ИЗУЧЕНИЕ СПЕКТРА ИТТЕРБИЯ НА ОСНОВЕ  
РЕЛЯТИВИСТСКОЙ МНОГОЧАСТИЧНОЙ ТЕОРИИ ВОЗМУЩЕНИЙ:  
ДВАЖДЫ ВОЗБУЖДЕННЫЕ ВАЛЕНТНЫЕ СОСТОЯНИЯ**

**Резюме**

В рамках релятивистской многочастичной теории возмущений и обобщенного релятивистского энергетического подхода проведено теоретическое изучение спектра дважды возбужденных валентных состояний для атома иттербия. В качестве нулевого приближения релятивистской теории возмущений выбрано оптимизированное приближение Дирака-Кона-Шэма. Оптимизация выполнена путем введения параметра в обменные потенциалы Фока и Кона-Шэма и дальнейшей минимизацией калибровочно-неинвариантных вкладов в радиационные ширины атомных уровней с использованием релятивистского базиса орбиталей, сгенерированного соответствующим гамильтонианом нулевого приближения.

**Ключевые слова:** Релятивистская теория возмущений, оптимизированное нулевое приближение, иттербий

*А. А. Свиначенко, В. Б. Терновський, І. С. Черкасова, Д. А. Міроненко*

## **ТЕОРЕТИЧНЕ ВИВЧЕННЯ СПЕКТРУ ІТЕРБІЮ НА ОСНОВІ РЕЛЯТИВІСТСЬКОЇ БАГАТОЧАСТКОВОЇ ТЕОРІЇ ЗБУРЕНЬ: ДВІЧІ ЗБУДЖЕНІ ВАЛЕНТНІ СТАНИ**

### **Резюме**

В рамках релятивістської багаточастинкової теорії збурень і узагальненого релятивістського енергетичного підходу проведено теоретичне вивчення характеристик рідбергівських автоіонізаційних резонансів в спектрах атомів лантанідів (ітербію). В якості нульового наближення релятивістської теорії збурень обрано оптимізоване наближення Дірака-Кона-Шема. Оптимізація виконана шляхом введення параметра в обмінний потенціал Кона-Шема і подальшої мінімізації калібрувальних-неінваріантних вкладів в радіаційні ширини атомних рівнів з використанням релятивістського базису орбіталей, згенерованого відповідним гамільтоніаном нульового наближення.

**Ключові слова:** Релятивістська теорія збурень, енергії і ширини резонансів, оптимізоване нульове наближення, ітербій

*V. B. Ternovsky<sup>1</sup>, A.A. Kuznetsova<sup>1</sup>, A.V. Glushkov<sup>2</sup>, E.K. Plysetskaya<sup>2</sup>*

<sup>1</sup>National University “Odessa Maritime Academy”, Didrikhson str. 8, Odessa, Ukraine

<sup>2</sup>Odessa State Environmental University, L’vovskaya str. 15, Odessa, 65016, Ukraine

E-mail: ternovskyvb@gmail.com

## RELATIVISTIC OPERATOR PERTURBATION THEORY IN SPECTROSCOPY OF MULTIELECTRON ATOM IN AN ELECTROMAGNETIC FIELD

We present the theoretical basis of a new relativistic operator perturbation theory (OPT) approach to multielectron atom in an electromagnetic field combined with a relativistic many-body perturbation theory (RMBPT) formalism for a free multielectron atom. As illustration of application of the presented formalism, the results of energy and spectral parameters for a number of atoms are presented. The relativistic OPT method is tested for the multielectron systems such as Fr and Tm. New approach is elaborated for an accurate, consistent treatment of a strong field Stark effect in multielectron atoms.

**Keywords:** multielectron atom in a dc electric field – modified operator perturbation theory – Rydberg autoionization resonances

### 1. Introduction

An investigation of spectra, optical and spectral, radiative and autoionization characteristics for the rare-earth elements (isotopes) and corresponding ions is traditionally of a great interest for further development quantum optics and atomic spectroscopy and different applications in the plasma chemistry, astrophysics, laser physics, quantum and nano-electronics etc. (see Refs. [1–42]).

The calculation difficulties in description of the multielectron atoms in electromagnetic (electric) field inherent to the standard quantum mechanical approach are well known. Here one should mention the well-known Dyson phenomenon for a Strong Filed AC, DC Stark effect. Besides, in contrast to the hydrogen atom, the non-relativistic Schrödinger and relativistic Dirac equations for an electron moving in the field of the atomic core in many-electron atom and a uniform external electric field does not allow separation of variables in the parabolic coordinates.

The Wentzel-Kramers-Brillouin (WKB) approximation overcomes these difficulties for

the states lying far from the “new continuum” boundary. The detailed review of a modern states of art for spectroscopy of multielectron atoms in an electric (laser) field is presented in Refs. [8,16].

In this paper we present the theoretical basis of a new relativistic operator perturbation theory (OPT) approach to multielectron atom in an electromagnetic field combined with a relativistic many-body perturbation theory (RMBPT) formalism for a free multielectron atom. The relativistic OPT approach is tested for the multielectron systems such as francium Fr and thulium Tm.

The relativistic density-functional approximation with the Kohn-Sham potential is taken as the zeroth approximation in the RMBPT formalism. There have taken into account all exchange-correlation corrections of the second order and dominated classes of the higher orders diagrams (polarization interaction, quasiparticles screening, etc.). New form of the multi-electron polarization functional has been used.

As illustration of application of the presented formalism, new data on the energy and spectral parameters for two complex multielectron atoms in a electric (electromagnetic) field are presented.

## 2. Relativistic operator perturbation theory for multielectron atoms in an electromagnetic field

Here we present a new relativistic quantum approach to modeling the chaotic dynamics of atomic systems in a dc electric and ac electromagnetic fields, based on the theory of quasi-stationary quasienergy states, optimized operator perturbation theory, method of model-potential, a complex rotation coordinates algorithm method [16,43]. The universal chaos-geometric block will be used further to treat the chaotic ionization characteristics for a number of heavy atomic systems.

Let us remind that in the case of the electromagnetic field atomic Hamiltonian is usually as follows:

$$H = \frac{1}{2} p^2 + V_{at}(r) + zF_0 \cos(\omega t) \quad (1)$$

The field is periodic, of course one should use the Floquet theorem; then the eigen Floquet states and quasienergies  $E_j$  are defined as the eigen functions and eigen values of the Floquet Hamiltonian  $\hat{H}$ . In the general form with using the method of complex coordinates the problem reduces to the solution of stationary Schrödinger equation, which is as follows in the model potential approximation:

$$(-1/2 \cdot \nabla^2 + V_{at}(r) + \omega L_z + F_0 z) \Psi_E(r) = E \Psi_E(r) \quad (2)$$

i.e. to the stationary eigen value and eigen vectors task for some matrix A (with the consideration of several Floquet zones):  $(A - E_j B) |E_j\rangle = 0$ . As a decomposition basis, system of the Sturm functions of the operator perturbation theory basis is used.

In our new theory we start from the Dirac Hamiltonian (in relativistic units):

$$H = \alpha p + \beta - \alpha Z / r + \sqrt{\alpha} F z, \quad (3)$$

Here a field strength intensity is expressed in the relativistic units ( $F_{rel} = a^{5/2} F_{at.un.}$ ;  $a$  is the fine structure constant). One could see that a relativistic wave function in the Hilbert space is a bi-spinor. Using the formal transformation of co-ordinates  $r \rightarrow r \exp(i\theta)$  in the Hamiltonian (11), one could get:

$$H(\theta) = (\alpha p - Z/r) \exp(-i\theta) + \beta - \sqrt{\alpha} F z \exp(i\theta) \quad (4)$$

In comparison with an analogous non-relativistic theory, here there is arisen a technical problem. In formulae (11) there is term b, which can not be simply transformed. One of the solving receptions as a limitation of a sub-space of the Hamiltonian eigen-functions by states of the definite symmetry (momentum  $J$  and parity  $P$ ). These states can be described by the following functions:

$$\Psi_{PJ}^M = 1/r \begin{pmatrix} f(r) Y_{l'}^M(n, \sigma) \\ g(r) Y_{l'}^M(n, \sigma) \end{pmatrix} \quad (5)$$

Here  $l(l')$  and spin  $1/2$  in the coupling scheme give a state with the total momentum  $J$  and its projection  $M_J = M$ . Action of the Hamiltonian (11) on the functions (13) with definite  $J$  results in:

$$\begin{aligned} \hat{H}(\theta) \Psi_{PJ}^M &= \alpha_r (\hat{p}_r - \frac{i\omega(J+1/2)}{r}) \beta \exp(-i\theta) \Psi_{PJ}^M + \\ &+ (\beta - \frac{\alpha Z}{r} \exp(-i\theta) - \sqrt{\alpha} F z \exp(-i\theta)) \Psi_{PJ}^M \end{aligned} \quad (6)$$

$p_r = -i(1/r)(d/dr)r$ ,  $\vec{n} = \vec{r}/r$ ,  $\sigma$  – the Pauli matrices; parameter  $w = -1$ , if  $l = J - 1/2$  and  $w = 1$ , if  $l = J + 1/2$ .

In order to further diagonalize the Hamiltonian (6), we need to choose the correct basis of functions in the subspace (5), in particular, by choosing the following functions (the sitter or water-like type):

$$\Psi_{PJ}^{a,M} = 1/r \begin{pmatrix} F(r) Y_{l'}^M(n, \sigma) \\ 0 \end{pmatrix} \quad (7)$$

$$\Psi_{PJ}^{b,M} = 1/r \begin{pmatrix} 0 \\ iG(r) Y_{l'}^M(n, \sigma) \end{pmatrix} \quad (8)$$

It is easy to see that the matrix elements (6) will be no-zeroth only between the states with the same  $M_j$ . In fact this moment is a single limitation of the whole approach.

Transformation of co-ordinates in the Pauli Hamiltonian (in comparison with the Schrodinger equation Hamiltonian it contents additional potential term of a magnetic dipole in an external field) can be performed by the analogous way. However, procedure in this case is significantly simplified. They can be expressed through the set of one-dimensional integrals, described in details in Refs. [8,14,47].

In contrast to the hydrogen atom, the non-relativistic Schrödinger equation for an electron moving in the field of the atomic core in many-electron atom (in particular, an alkali element) and a uniform external electric field does not allow separation of variables in the parabolic coordinates  $x, y, z$  [14]. One of the ways this problem could be related to the use of effective potentials, chosen in such a way (for example, in the Miller-Green approximation (see [1,2]) that to achieve the separation of variables in the Schrödinger equation. Here the model potential approach or the quantum defect approximation can be used. One may introduce the ion core charge  $Z$  for the multielectron atom. According to standard quantum defect theory, the relation between quantum defect value  $\delta$ , electron energy  $E$  and principal quantum number  $n$  is:  $\mu_l = \delta - z^* (-2E)^{-1/2}$ . The quantum defect in the parabolic coordinates  $\delta(n, n_2, m)$  is connected to the quantum defect value of the free ( $\varepsilon = 0$ ) atom by the following relation [43]:

$$\delta(n, n_2, m) = (1/n) \sum_{l, m}^n (2l+1) C_{JM}^{lm} \mu_l \quad (9)$$

Such a scheme provides a general receipt to combine the OPT method with the RMBPT in spherical coordinates for a free atom. The details of the used method can be found in the references [8,16,43].

### 3. Method of relativistic many-body perturbation theory

Generally speaking, the energy spectra for the majority of complex atomic systems (naturally including the rare-earth elements) are characterized by a great density. Moreover, these spectra have essentially relativistic properties. So, correct theoretical method of their studying can be based on the convenient field procedure, which includes computing the energy shifts DE of the degenerate electron states. More exactly, speech is about constructing secular matrix  $M$  (with using the Gell-Mann and Low adiabatic formula for DE), which is already complex in the relativistic theory, and its further diagonalization [26-32]. In result one could compute the energies and decay probabilities of a non-degenerate excited state for a complex atomic system [26]. The secular matrix elements can be further expanded into a PT series on the inter-electron interaction. Here the standard Feynman diagrammatic technique is usually used.

Generally speaking, the secular matrix  $M$  can be represented as follows:

$$M = M^{(0)} + M^{(1)} + M^{(2)} + M^{(3)} + \dots + M^{(k)} \quad (10)$$

where  $M^{(0)}$  is the contribution of the vacuum diagrams of all PT orders (this contribution determines only the general levels spectrum shift);  $M^{(1)}$ ,  $M^{(2)}$ ,  $M^{(3)}$  are contributions of the 1-, 2- and 3- quasiparticle (QP) diagrams respectively. The matrix  $M^{(1)}$  can be presented as a sum of the independent one-QP contributions. Substituting these quantities into (1) one could have summarized all the one-QP diagrams contributions. In the empirical methods here one could use the experimental values of one-electron energies, however, the necessary experimental quantities (especially for the rare-earth and other elements) are not often available. The detailed procedure for computing  $\text{Re} M^{(2)}$  is presented, for example, in Ref. [3].

We will describe an atomic multielectron system by the relativistic Dirac Hamiltonian (the atomic units are used) as follows [41-43]:

$$H = \sum_i \{ \alpha c p_i - \beta c^2 - Z / r_i \} + \sum_{i>j} \exp(i | \omega | r_{ij}) (1 - \alpha_i \alpha_j) / r_{ij} \quad (11)$$

where  $Z$  is a charge of nucleus,  $a_i, a_j$  are the Dirac matrices,  $w_{ij}$  is the transition frequency,  $c$  – the velocity of light. The interelectron interaction potential (second term in (3)) takes into account the retarding effect and magnetic interaction in the lowest order on parameter of the fine structure constant. In the PT zeroth approximation it is used ab initio mean-field potential:

$$V^{DKS}(r) = [V_{Coul}^D(r) + V_X(r) + V_C(r|a)], \quad (12)$$

with the standard Coulomb, exchange Kohn-Sham  $V_X$  and correlation Lundqvist-Gunnarsson  $V_C$  potentials (look details in Refs. [46-49]). An effective approach to accounting the multi-electron polarization contributions is described earlier and based on using the effective two-QP polarizable operator, which is included into the PT first order matrix elements.

In order to calculate the radiation decay probabilities and autoionization energies and widths a gauge invariant relativistic energy approach (version [43]) is used. In particular, a width of the state, connected with an autoionization decay, is determined by a coupling with the continuum states and calculated as square of the matrix element [43]:

$$V_{\beta_1 \beta_2; \beta_4 \beta_3} = \sqrt{(2j_1+1)(2j_2+1)(2j_3+1)(2j_4+1)} \times \sum_{a\mu} (-1)^\mu \begin{pmatrix} j_1 & j_3 & a \\ m_1 - m_3 & \mu \end{pmatrix} \begin{pmatrix} j_2 & j_4 & a \\ m_2 - m_4 & \mu \end{pmatrix} \times \times Q_a(n_1 l_1 j_1 n_2 l_2 j_2; n_4 l_4 j_4 n_3 l_3 j_3) \quad (13)$$

Here  $= Q_a^{Quil} + Q_a^B$ , where  $Q_a^{Quil}$ ,  $Q_a^B$  correspond to the Coulomb and Breit parts of the relativistic interelectron potential in (3) and express through Slater-like radial integrals and standard angle coefficients. Other details can be found in Refs. [44-57].

The most complicated problem of the relativistic PT computing the complex multielectron elements spectra is in an accurate, precise

accounting for the multi-electron exchange-correlation effects (including polarization and screening effects, a continuum pressure etc), which can be treated as the effects of the PT second and higher orders. Using the standard Feynman diagrammatic technique one should consider two kinds of diagrams (the polarization and ladder ones), which describe the polarization and screening exchange-correlation effects. The detailed description of the polarization diagrams and the corresponding analytical expressions for matrix elements of the polarization QPs interaction (through the polarizable core) potential is presented in Refs. [34-36]. An effective approach to accounting of the polarization diagrams contributions is in adding the effective two-QP polarizable operator into the PT first order matrix elements. In Ref. [27] the corresponding non-relativistic polarization functional has been derived. More correct relativistic expression has been presented in the Refs. [2] and used in our computing. The contribution of the ladder diagrams (these diagrams describe the immediate QPs interaction) is summarized by a modification of the PT zeroth approximation mean-field central potential (look below), which include the screening (anti-screening) of the core potential of each particle by the two others. The details of this contribution can be found in Refs. [44-57].

#### 4. Results and Conclusions

In the framework of the development of spectroscopy of the AS of heavy atoms in the external field, a quantitative study of the effects of the non-conductive electric field on the parameters of the AS in the spectra of the lanthanide atoms was performed. Based on our theory, for the first time, the widths of the autoionization states for the Tm  $4f^{13} 7/2, 5/2 6s_{1/2} (3, 2) ns, np$  i  $4f^{13} 5/2 6s_{1/2} (2) nsp_{1/2} [3/2]$  ( $n=26, 30$ ) i Yb  $4f^{13} [^2F_{7/2}] 6s^2 np [5/2]_2 4f^{13} [^2F_{7/2}] 6s^2 nf [5/2]_2$ . In Table 1 we list our data on the widths of the  $4f^{13} 7/2, 5/2 6s_{1/2} (3, 2) ns, np$  states, which are mixed with the resonances of the opposite parity in a rather weak DC electric field.

Table 1.  
**The widths  $\Gamma$  (cm<sup>-1</sup>) of autoionization states of the Tm  $4f^{13}_{7/2}6s_{1/2}(3)ns,np$ , which are mixed with resonances of opposite parity for different DC electric fields**

F(V/cm)		$\frac{4f^{13}_{7/2}6s_{1/2}(3)ns[5/2]}{n=26} \quad \frac{}{n=30}$	
$\Gamma$	F=0	1.13D-5	6.12D-6
$\Gamma$	F =50	1.11D-04	5.88D-5
$\Gamma$	F =100	4.05D-04	2.15D-4
$\Gamma$	F =150	8.15D-04	4.13D-4
F(V/cm)		$\frac{4f^{13}_{7/2}6s_{1/2}(3)np_{3/2}[3/2]}{n=26} \quad \frac{}{n=30}$	
$\Gamma$	F=0	4.22D-5	2.42D-5
$\Gamma$	F =50	4.07D-4	2.36D-4
$\Gamma$	F =100	1.56D-3	8.88D-4
$\Gamma$	F =150	3.08D-3	1.76D-3
F(V/cm)		$\frac{4f^{13}_{5/2}6s_{1/2}(2)np_{1/2}[3/2]}{n=26} \quad \frac{}{n=30}$	
$\Gamma$	F=0	2.36D-5	1.27D-5
$\Gamma$	F =50	2.23D-4	1.22D-4
$\Gamma$	F =100	8.37D-3	4.28D-4
$\Gamma$	F =150	1.64D-3	8.63D-3

Note: 1.13D-5=1.13×10<sup>-5</sup>;

From these data one could see that in this case there is the effect of a giant broadening of the resonance widths. For the first time, for Tm, the possibility of such an effect was foreseen in the papers by Glushkov-Ivanov-Letokhov, which was later confirmed in the known ISAN experiments by V.S. Letokhov etal (look details in Refs. [3,8]). Similar data are obtained for Yb, for which we first detected the effect of strong amplification of the AU .

We also present our results of numerical modelling ionization dynamics for Rydberg atoms Rb, Cs, Fr (Rb:  $n=50-80$ ; Cs, Fr:  $n=60-80$ ) in a microwave field ( $F=(1.2-3.2)\times 10^{-9}$  a.u.;  $w/2p=8.87, 36$  HGz). The preliminary estimate a dependence of the Rb ionization probability P upon the F, interaction time “atom-field”

and comparison with available data by Krug-Buchleitner [19] and Glushkov-Ternovsky etal [49] shows that all listed data are in a reasonable agreement with experiment, however, the best accuracy is provided by relativistic theory. In Table 2 we firstly present new data on dependence of the Fr ionization probability upon the F value, interaction time “atom-field”. Unfortunately, here there are no any alternative theoretical or experimental data.

Table 2.  
**Our data for ionization probability P for Fr ( $l_0=0, m_0=0, n_0=76-80$ ) in dependence on  $n_0$  F (at.units; field parameters:  $t = 327\times 2p/w$ ; frequency  $w_c=w/2p=36$  GHz, 8.87 GHz)**

$n_0$ ↓	Our data	Our data	Our data	Our data
F=	2.8× 10 <sup>-9</sup>	3.1× 10 <sup>-9</sup>	2.8× 10 <sup>-9</sup>	3.1× 10 <sup>-9</sup>
$w_c=$	36GHz	36GHz	8.87GHz	8.87GHz
77	0.47	0.50	0.43	0.46
80	0.58	0.61	0.54	0.56
83*	0.56	0.60	0.51	0.53
86	0.67	0.69	0.62	0.66

In whole, our modeling relativistic dynamics of ionization Rb, Cs, Fr Rydberg states in the electromagnetic field shows that there are the local violations of probability smooth growth associated with the complex Floquet spectrum, link between the quasi-stationary states and a continuum, the growing influence of multiphoton resonances. The picture becomes by more complicated due to the single-photon near-resonance transitions with quasi-random detuning from resonance and quantum phase shift due to scattering Rydberg electron on the atomic core.

## References

1. Landau, L.D.; Lifshitz, E.M. *Quantum Mechanics*. Pergamon: Oxford, **1977**.
2. Glushkov, A.V. *Atom in an electromagnetic field*. KNT: Kiev, **2005**.
3. Glushkov, A.V. *Relativistic Quantum*

- theory. *Quantum mechanics of atomic systems*. Astroprint: Odessa, **2008**.
4. Lisitsa, V.S. New results on the Stark and Zeeman effects in the hydrogen atom. *Sov. Phys. Usp.* **1987**, *30*, 927-960.
  5. Ivanov, L.N.; Letokhov, V.S. Selective ionization of atoms by a light and electric field. *Quant. Electr.*(in Russian) **1975**, *2*, 585-590.
  6. Ivanov, L.N.; Letokhov, V.S. Spectroscopy of autoionization resonances in heavy elements atoms. *Com.Mod. Phys.D.:At.Mol.Phys.* **1985**, *4*, 169-184.
  7. Letokhov, V.S. ; Hurst, G.S. Resonance Ionization Spectroscopy. *Phys. Today*. **1994**, Oct., 38-45.
  8. Glushkov, A.V. Operator Perturbation Theory for Atomic Systems in a Strong DC Electric Field. *In Advances in Quantum Methods and Applications in Chemistry, Physics, and Biology, Series: Progress in Theoretical Chemistry and Physics*; Hotokka, M., Brändas, E., Maruani, J., Delgado-Barrio, G., Eds.; Springer: Cham, **2013**; Vol. 27, pp 161–177.
  9. Glushkov, A.V. Advanced Relativistic Energy Approach to Radiative Decay Processes in Multielectron Atoms and Multicharged Ions. *In Quantum Systems in Chemistry and Physics: Progress in Methods and Applications, Series: Progress in Theoretical Chemistry and Physics*; Nishikawa, K., Maruani, J., Brandas, E., Delgado-Barrio, G., Piecuch, P., Eds.; Springer: Dordrecht, **2012**; Vol. 26, pp 231–252.
  10. Moiseyev, N. Quantum theory of resonances: calculating energies, widths and cross-sections by complex scaling *Phys. Rep.* **1998**, *302*, 211-293
  11. Glushkov, A.V. *Relativistic and Correlation Effects in Spectra of Atomic Systems*; Astroprint: Odessa, **2006**.
  12. Rao, J.; Liu, W.; Li, B. Theoretical complex Stark energies of hydrogen by a complex-scaling plus B-spline approach. *Phys. Rev. A.* **1994**, *50*, 1916-1919 (1994).
  13. Rao, J.; Li, B. Resonances of the hydrogen atom in strong parallel magnetic and electric fields. *Phys. Rev. A.* **1995**, *51*, 4526-4530.
  14. Glushkov A.V.; Ivanov, L.N. DC strong-field Stark effect: consistent quantum-mechanical approach. *J. Phys. B: At. Mol. Opt. Phys.* **1993**, *26*, L379-386
  15. Glushkov, A.V.; Ternovsky, V.B.; Buyadzhi, V.V.; Prepelitsa, G.P. Geometry of a Relativistic Quantum Chaos: New approach to dynamics of quantum systems in electromagnetic field and uniformity and charm of a chaos. *Proc. Intern. Geom. Center.* **2014**, *7(4)*, 60-71.
  16. Kuznetsova, A.A.; Glushkov, A.V.; Ignatenko, A.V.; Svinarenko, A.A.; Ternovsky V.B. Spectroscopy of multielectron atomic systems in a DC electric field. *Adv. Quant. Chem.* (Elsevier) **2018**, *78*,  
1. [doi.org/10.1016/bs.aiq.2018.06.005](https://doi.org/10.1016/bs.aiq.2018.06.005)
  17. Hehenberger, M.; McIntosh, H.V.; Brändas, E. Weyl's theory applied to the Stark effect in the hydrogen atom. *Phys. Rev. A* **1974**, *10 (5)*, 1494-1506.
  18. Khetselius, O.Yu. *Hyperfine structure of atomic spectra*. Astroprint: Odessa, **2008**
  19. Krug, A.; Buchleitner, A., Microwave ionization alkali-metal Rydberg states in a realistic numerical experiment. *Phys. Rev. A.* **2002**, *66*, 053416,
  20. Gallagher, T.; Mahon, C.; Dexter, J.; Pillet, P. Ionization of sodium and lithium Rydberg atoms by 10-MHz to 15-GHz electric fields, *Phys. Rev. A.* **1991**, *44*, 1859-1872.
  21. Buyadzhi, V.V. Laser multiphoton spectroscopy of atom embedded in Debye plasmas: multiphoton resonances and transitions. *Photoelectronics.* **2015**, *24*, 128-133.

22. Glushkov, A.V. Spectroscopy of cooperative muon-gamma-nuclear processes: Energy and spectral parameters *J. Phys.: Conf. Ser.* **2012**, *397*, 012011
23. Glushkov, A.V. Spectroscopy of atom and nucleus in a strong laser field: Stark effect and multiphoton resonances. *J. Phys.: Conf. Ser.* **2014**, *548*, 012020
24. Glushkov, A.V.; Ambrosov, S.V.; Ignatenko, A.V.; Korchevsky, D.A. DC strong field stark effect for nonhydrogenic atoms: Consistent quantum mechanical approach. *Int. Journ. Quant. Chem.* **2004**, *99*, 936-939.
25. Buyadzhi, V.V.; Glushkov, A.V.; Lovett, L. Spectroscopy of atom and nucleus in a strong laser field: Stark effect and multiphoton resonances. *Photoelectronics.* **2014**, *23*, 38-43.
26. Ivanov, L.N.; Ivanova, E.P.; Aglitsky, E.V. Modern trends in the spectroscopy of multicharged ions. *Phys. Rep.* **1988**, *166*, 315-390.
27. Ivanova, E.P.; Glushkov, A.V. Theoretical investigation of spectra of multicharged ions of F-like and Ne-like isoelectronic sequences. *J. Quant. Spectr. Rad. Transfer.* 1986, *36*, 127-145.
28. Glushkov, A.V.; Ivanov, L.N.; Ivanova, E.P. Autoionization Phenomena in Atoms. *Moscow University Press, Moscow*, **1986**, 58-160
29. Vidolova-Angelova, E.; Ivanov, L.N.; Ivanova, E.P.; Angelov, D.A. Relativistic perturbation theory method for investigating the radiation decay of highly excited many electron atomic states. Application to the Tm atom. *J. Phys. B: At. Mol. Opt. Phys.* **1986**, *19*, 2053-2069.
30. Khetselius, O. Relativistic perturbation theory calculation of the hyperfine structure parameters for some heavy-element isotopes. *Int. Journ. Quant. Chem.* **2009**, *109*, 3330-3335.
31. Khetselius, O.Yu. Relativistic calculation of the hyperfine structure parameters for heavy elements and laser detection of the heavy isotopes. *Phys. Scripta.* **2009**, *135*, 014023.
32. Glushkov, A.V.; Loboda, A.V.; Gurnitskaya, E.P.; Svinarenko, A.A. QED theory of radiation emission and absorption lines for atoms in a strong laser field. *Phys. Scripta.* **2009**, *T135*, 014022
33. Ignatenko, A.V. Probabilities of the radiative transitions between Stark sublevels in spectrum of atom in an DC electric field: New approach. *Photoelectronics*, **2007**, *16*, 71-74.
34. Glushkov, A.V.; Ambrosov, S.V.; Ignatenko, A.V. Non-hydrogenic atoms and Wannier-Mott excitons in a DC electric field: Photoionization, Stark effect, Resonances in ionization continuum and stochasticity. *Photoelectronics*, **2001**, *10*, 103-106.
35. Glushkov, A.V. Negative ions of inert gases. *JETP Lett.* **1992**, *55*, 97-100.
36. Glushkov, A.V.; Malinovskaya, S.V.; Loboda, A.V.; Shpinareva, I.M.; Prepelitsa, G.P. Consistent quantum approach to new laser-electron-nuclear effects in diatomic molecules. *J.Phys.: Conf. Ser.* **2006**, *35*, 420-424.
37. Glushkov, A.V.; Malinovskaya S.V. Co-operative laser nuclear processes: border lines effects *In New Projects and New Lines of Research in Nuclear Physics.* Fazio, G., Hanappe, F., Eds.; World Scientific: Singapore, **2003**, 242-250.
38. Glushkov, A.V. Energy approach to resonance states of compound superheavy nucleus and EPPP in heavy nuclei collisions *In Low Energy Anti-proton Physics;* AIP: New York, *AIP Conf. Proc.* **2005**, *796*, 206-210.
39. Glushkov, A.V.; Malinovskaya, S.V.; Prepelitsa, G.P.; Ignatenko, V. Manifestation of the new laser-electron nuclear spectral effects in the thermalized plasma: QED theory of co-oper-

- ative laser-electron-nuclear processes. *J. Phys.: Conf. Ser.* **2005**, *11*, 199-206.
40. Glushkov, A.V.; Malinovskaya, S.V.; Loboda, A.V.; Shpinareva, I.M.; Gurnitskaya, E.P.; Korchevsky, D.A. Diagnostics of the collisionally pumped plasma and search of the optimal plasma parameters of x-ray lasing: calculation of electron-collision strengths and rate coefficients for Ne-like plasma. *J. Phys.: Conf. Ser.* **2005**, *11*, 188-198.
  41. Glushkov, A.V.; Ambrosov, S.V.; Loboda, A.V.; Gurnitskaya, E.P.; Prepelitsa, G.P. Consistent QED approach to calculation of electron-collision excitation cross sections and strengths: Ne-like ions. *Int. J. Quantum Chem.* **2005**, *104*, 562-569.
  42. Khetselius, O.Yu. Relativistic Energy Approach to Cooperative Electron- $\gamma$ -Nuclear Processes: NEET Effect *In Quantum Systems in Chemistry and Physics, Series: Progress in Theoretical Chemistry and Physics*; Nishikawa, K., Maruani, J., Brändas, E., Delgado-Barrio, G., Piecuch, P., Eds.; Springer: Dordrecht, **2012**; Vol. 26, pp 217-229.
  43. Glushkov, A.; Khetselius, O.; Svinarenko, A.; Buyadzhi, V.; Ternovsky, V.; Kuznetsova, A.; Bashkarev, P. Relativistic perturbation theory formalism to computing spectra and radiation characteristics: Application to heavy elements *Recent Studies in Perturbation Theory*; Uzunov, D. Ed.; InTech, **2017**; pp 131-150
  44. Khetselius, O.Yu. Relativistic Hyperfine Structure Spectral Lines and Atomic Parity Non-conservation Effect in Heavy Atomic Systems within QED Theory. *AIP Conf. Proceedings*. **2010**, *1290(1)*, 29-33.
  45. Khetselius, O.Yu. Spectroscopy of cooperative electron-gamma-nuclear processes in heavy atoms: NEET effect. *J. Phys.: Conf. Ser.* **2012**, *397*, 012012
  46. Khetselius, O.Yu. Atomic parity non-conservation effect in heavy atoms and observing P and PT violation using NMR shift in a laser beam: To precise theory. *J. Phys.: Conf. Ser.* **2009**, *194*, 022009.
  47. Buyadzhi, V.V.; Chernyakova, Yu.G.; Smirnov, A.V.; Tkach, T.B. Electron-collisional spectroscopy of atoms and ions in plasma: Be-like ions. *Photoelectronics*. **2016**, *25*, 97-101.
  48. Buyadzhi, V.V.; Chernyakova, Yu.G.; Antoshkina, O.A.; Tkach, T.B. Spectroscopy of multicharged ions in plasmas: Oscillator strengths of Be-like ion Fe. *Photoelectronics*. **2017**, *26*, 94-102.
  49. Glushkov, A.V.; Ternovsky, V.B.; Buyadzhi, V.; Prepelitsa, G.P. Geometry of a Relativistic Quantum Chaos: New approach to dynamics of quantum systems in electromagnetic field and uniformity and charm of a chaos. *Proc. Intern. Geom. Center*. **2014**, *7(4)*, 60-71.
  50. Glushkov, A.V.; Kondratenko, P.A.; Buyadgi, V.V.; Kvasikova, A.S.; Sakun T.N.; Shakhman, A.S. Spectroscopy of cooperative laser electron- $\gamma$ -nuclear processes in polyatomic molecules. *J. Phys.: Conf. Ser.* **2014**, *548*, 012025.
  51. Svinarenko, A.A. Study of spectra for lanthanides atoms with relativistic many-body perturbation theory: Rydberg resonances. *J. Phys.: Conf. Ser.* **2014**, *548*, 012039.

This article has been received in September 2018

PACS 31.15.A-

*V. B. Ternovsky, A. A. Kuznetsova, A. V. Glushkov, E. K. Plysetskaya*

## **RELATIVISTIC OPERATOR PERTURBATION THEORY IN SPECTROSCOPY OF MULTIELECTRON ATOM IN AN ELECTROMAGNETIC FIELD**

### **Summary**

We present the theoretical basis of a new relativistic operator perturbation theory (OPT) approach to multielectron atom in an electromagnetic field combined with a relativistic many-body perturbation theory (RMBPT) formalism for a free multielectron atom. As illustration of application of the presented formalism, the results of energy and spectral parameters for a number of atoms are presented. The relativistic OPT method is tested for the multielectron systems such as Fr and Tm. New approach is elaborated for an accurate, consistent treatment of a strong field Stark effect in multielectron atoms.

**Keywords:** multielectron atom in a dc electric field – modified operator perturbation theory – Stark resonances

PACS 31.15.A-

*В. Б. Терновский, А. А. Кузнецова, А. В. Глушков, Е. К. Плисецкая*

## **РЕЛЯТИВИСТСКАЯ ОПЕРАТОРНАЯ ТЕОРИЯ ВОЗМУЩЕНИЙ В СПЕКТРОСКОПИИ МНОГОЭЛЕКТРОННОГО АТОМА В ЭЛЕКТРОМАГНИТНОМ ПОЛЕ**

### **Резюме**

Изложены теоретические основы нового аппарата релятивистской операторной теории возмущений (ОТВ) в спектроскопии многоэлектронного атома в электромагнитном поле, объединенного с формализмом релятивистской многочастичной теории возмущений для свободного многоэлектронного атома. В качестве иллюстрации тестирования представленного подхода представлены результаты оценки энергетических и спектральных параметров для ряда атомов. Релятивистский метод ОПТ тестируется для таких многоэлектронных систем как Fr и Tm. Новый подход разработан для последовательного описания эффекта Штарка в многоэлектронных атомах в сильном внешнем электромагнитном поле.

**Ключевые слова:** Многоэлектронный атом в электрическом поле - модифицированная операторная теория возмущений – штарковские резонансы

*В. Б. Терновський, Г. О. Кузнецова, О. В. Глушков, Є. К. Плисецька*

## **РЕЛЯТИВІСТСЬКА ОПЕРАТОРНА ТЕОРІЯ ЗБУРЕНЬ В СПЕКТРОСКОПІЇ БАГАТОЕЛЕКТРОННОГО АТОМА В ЕЛЕКТРОМАГНІТНОМУ ПОЛІ**

### **Резюме**

Викладені теоретичні основи нового апарату релятивістської операторної теорії збурень (ОРЗ) в спектроскопії багатоелектронного атома в електромагнітному полі, об'єднаного з формалізмом релятивістської багаточастинкової теорії збурень для вільного багатоелектронного атома. В якості ілюстрації можливостей представленого підходу представлені результати оцінки деяких енергетичних і спектральних параметрів для ряду атомів. Релятивістський метод ОРЗ тестується для таких багатоелектронних систем як Fr і Tm. Новий підхід розроблений для послідовного опису ефекту Штарка в багатоелектронних атомах в сильному зовнішньому електромагнітному полі.

**Ключові слова:** багатоелектронний атом у електричному полі - модифікована операторна теорія збурень – штарківські резонанси

*V. V. Halyan<sup>1</sup>, I. D. Olekseyuk<sup>2</sup>, I. A. Ivashchenko<sup>2</sup>, A. H. Kevshyn<sup>1</sup>, P. V. Tishchenko<sup>2</sup>,  
M. V. Shevchuk<sup>3</sup>*

<sup>1</sup>Department of Experimental Physics and Technologies for Information Measuring, Lesya Ukrainka Eastern European University, 13 Voli Avenue, Lutsk 43009, Ukraine

<sup>2</sup>Department of Inorganic and Physical Chemistry of Lesya Ukrainka Eastern European University, 13 Prospect Voli, Lutsk 43009, Ukraine

<sup>3</sup>Lutsk National Technical University, 75 Lvivska Street, Lutsk 43000, Ukraine  
e-mail: halyanv@ukr.net

## OPTICAL PROPERTIES OF THE $\text{Ag}_{28}\text{Ga}_{28}\text{Ge}_{532}\text{Er}_2\text{S}_{1123}$ AND $\text{Ag}_{12}\text{Ga}_{12}\text{Ge}_{228}\text{Er}_2\text{S}_{483}$ GLASSES

Absorption spectra of the glasses  $\text{Ag}_{28}\text{Ga}_{28}\text{Ge}_{532}\text{Er}_2\text{S}_{1123}$  and  $\text{Ag}_{12}\text{Ga}_{12}\text{Ge}_{228}\text{Er}_2\text{S}_{483}$  in the 450–1050 nm range at room temperature were investigated. PL bands with maxima at 980 and 1540 nm were recorded under laser excitation with 800 nm wavelength. PL emission mechanism is analyzed from energy transfer processes, taking into account partial cluster formation of erbium ions and energy transition diagram of  $\text{Er}^{3+}$ .

Keywords: absorption spectra, photoluminescence, erbium ion, cluster formation, emission mechanism.

### 1. INTRODUCTION

Over the past two decades, substantial research interest was attracted to the study of the optical properties of semiconductors doped with rare-earth metals (RE). This is due to the growing needs of the industry in optoelectronic devices operating in the spectral range compatible with telecommunication gadgets. The most commonly used RE is erbium that has an intensive emission band near 1.5  $\mu\text{m}$  and low energy losses in fiber optics at this wavelength. Additionally, erbium-doped crystalline and amorphous materials can be used as active media in laser technology [1], displays, optical amplifiers, photonic devices [2], non-contact temperature [3, 4] and g-irradiation sensors [5, 6, 7].

Phase equilibria in the reciprocal system  $\text{AgGaS}_2 + \text{GeSe}_2 \hat{=} \text{AgGaSe}_2 + \text{GeS}_2$  were investigated, and the glass formation region was determined [8]. An alloy with the composition  $\text{Ag}_{0.05}\text{Ga}_{0.05}\text{Ge}_{0.95}\text{S}_2$  is characterized by the largest transparency window in this system. It was doped with 0.18 and 0.42 mol.%  $\text{Er}_2\text{S}_3$  (samples

$\text{Ag}_{28}\text{Ga}_{28}\text{Ge}_{532}\text{Er}_2\text{S}_{1123}$  and  $\text{Ag}_{12}\text{Ga}_{12}\text{Ge}_{228}\text{Er}_2\text{S}_{483}$ , respectively).

In our previous works on these glasses, we investigated the main structural units of the glass-forming matrix by Raman spectroscopy, as well as photoluminescence spectra under excitation by 532 and 980 nm wavelengths [4, 9]. Partial clustering of erbium ions was established from EPR and static magnetization studies, and the effect of g-irradiation on glass photoluminescence was analyzed [5].

The objective of this work is to investigate the absorption spectra and the mechanism of PL emission under laser excitation at 800 nm wavelength.

### 2. EXPERIMENTAL

The alloys were synthesized from elemental components (Ag, Ga, Ge, Se – 99.997 wt.% purity, S, 99.999 wt.%, Er, 99.9 wt.%) in evacuated thin-walled quartz ampoules in two stages. To prevent condensation losses of the vapor phase, the free volume of the container

was thermostated with asbestos cord. The residual pressure in ampoules was 0.1 Pa. Initially, the ampoules were heated in oxygen-gas burner flame for the binding of elemental sulfur. Then they were placed in a shaft-type furnace and heated at a rate of 20 K/hr to the maximum temperature of 1273 K. After holding at this temperature for 10 hours, the alloys were quenched into 25% aqueous saline solution at room temperature. The glassy state of the alloys was examined by X-ray diffraction at a DRON 4-13 diffractometer, CuK $\alpha$  radiation (Fig. 1).

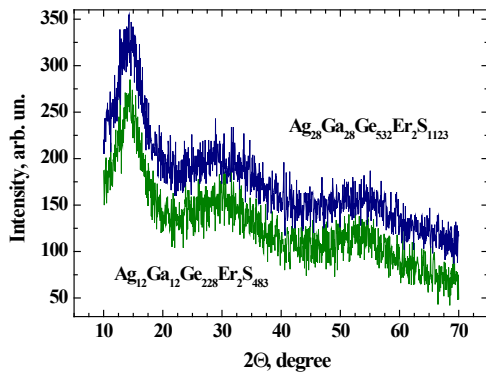


Fig. 1. X-ray diffraction patterns of the glasses.

The study of absorption spectra and photoluminescence utilized an MDR-206 monochromator with Si and PbS photodetectors. Luminescence excitation was performed by a laser at 800 nm wavelength and 400 mW power. The photoluminescence signal was received from the same sample surface as the excitation. The sample thickness was 0.5 mm.

### 3. RESULTS AND DISCUSSION

The absorption spectra of glasses were investigated at room temperature in the 450–1050 nm range (Fig. 2). The recorded absorption bands with maxima at 520, 550, 660, 805, and 980 nm correspond to the transitions in the  $f$ -shell of Er<sup>3+</sup> ions from the ground state to the excited states  $^2H_{11/2}$ ,  $^4S_{3/2}$ ,  $^4F_{9/2}$ ,  $^4I_{9/2}$ ,  $^4I_{11/2}$ , respectively. The intensity of the absorption bands increases with erbium content, while their position does not change. We established in a previous work [9] that the absorption coefficient decreases

with the increase in erbium concentration. This is due to the structural ordering of glass and, as it follows from Raman spectroscopy studies, to the decrease in the number of structural units  $[S_3Ge(Ga)-(Ga)GeS_3]$  and the increase of the  $[Ge(Ga)S_4]$  units.

The photoluminescence spectra (PL) of glasses in the 600–2000 nm range were investigated at room temperature under excitation by 800 nm wavelength (Figs. 3, 4). Two maxima at about 980 and 1540 nm were recorded in the near infrared spectral region.

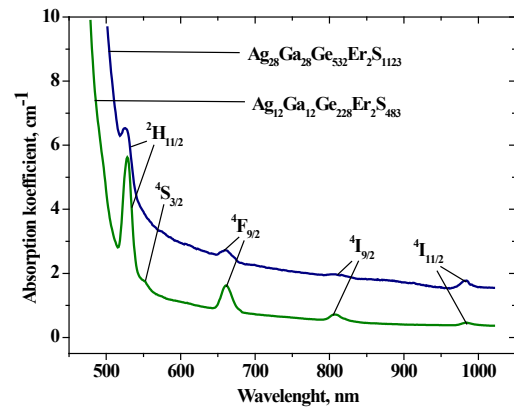


Fig. 2. Absorption spectra of the glasses at room temperature.

The emission efficiency of the band at 1540 nm wavelength is important for the use in telecommunication devices. A parameter of the effective bandwidth ( $\Delta\lambda_{\text{eff}}$ ) is used since the band is asymmetrical. It is calculated by the formula [10]:

$$\Delta\lambda_{\text{eff}} = \frac{\int I(\lambda)d\lambda}{I_{\text{max}}} \quad (1)$$

where  $I(\lambda)$  is the emission intensity at wavelength  $\lambda$ ;  $I_{\text{max}}$  is the maximum emission intensity.

The calculated  $\Delta\lambda_{\text{eff}}$  values for the glasses are 63 and 66 nm for  $Ag_{28}Ga_{28}Ge_{532}Er_2S_{1123}$  and  $Ag_{12}Ga_{12}Ge_{228}Er_2S_{483}$ , respectively. Clearly, not only PL intensity increases with erbium content but also does the effective width of the emission band. Additionally, the  $\Delta\lambda_{\text{eff}}$  values for the excitation at 800 nm is higher for these glasses than for the 980 nm excitation [11].

In our previous work [9], the excitation of these samples by 980 nm wavelength yielded in the visible range a green (520 nm) and a red (660 nm) PL band. However, no PL was detected in the visible spectral range when excited by 800 nm wavelength.

This is due to the fact that anti-Stokes PL (under 980 nm excitation) is associated with the absorption of two photons by  $\text{Er}^{3+}$  ions which are promoted from the ground state  $^4\text{I}_{15/2}$  to the excited state  $^4\text{F}_{7/2}$  ( $^4\text{I}_{15/2} + h\nu_{980} \rightarrow ^4\text{I}_{11/2} + h\nu_{980} \rightarrow ^4\text{F}_{7/2}$ ) with subsequent non-radiative relaxation to the state  $^2\text{H}_{11/2}$ . Since

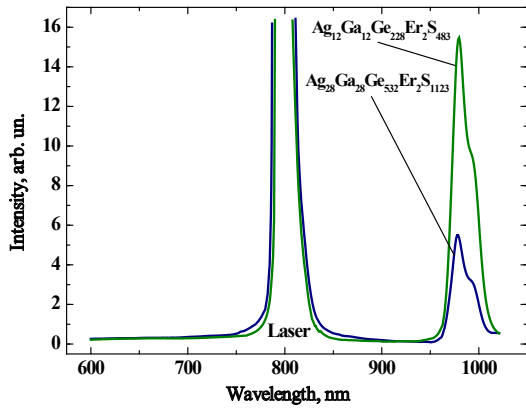


Fig. 3. PL spectra of the glasses excited with 800 nm laser (600–1050 nm range).

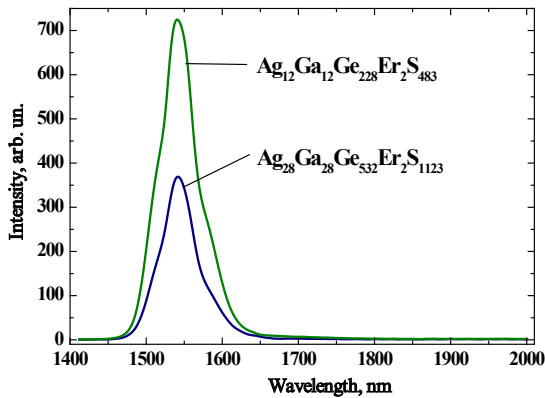


Fig. 4. PL spectra of the glasses excited with 800 nm laser (1400–2000 nm range).

the excitation at 800 nm has higher energy compared to 980 nm, the absorption of two photons promotes erbium ions to the excited state  $^2\text{H}_{9/2}$  ( $^4\text{I}_{15/2} + h\nu_{800} \rightarrow ^4\text{I}_{9/2} + h\nu_{800} \rightarrow ^2\text{H}_{9/2}$ )

located above the absorption edge (Fig. 2) in the conduction band.

The emission mechanism in these glasses can be determined from the transition chart for  $\text{Er}^{3+}$  ions (Fig. 5). Erbium ions in the state  $^4\text{I}_{13/2}$  are promoted due to absorption of 800 nm photons or energy transfer (ET) from adjacent ions in the state  $^4\text{I}_{9/2}$  to the state  $^2\text{H}_{11/2}$ . These erbium ions can non-radiatively relax to the state  $^4\text{S}_{3/2}$ . However, erbium ions can not relax non-radiatively to lower energy states because of the large energy gap and low phonon energy (about 300-400  $\text{cm}^{-1}$  [9]). Excited states  $^4\text{I}_{11/2}$  and  $^4\text{I}_{13/2}$  which yield PL bands with maxima at 980 and 1540 nm result from cross-relaxation  $\text{CR}_1$ ,  $\text{CR}_2$  (Fig. 5):

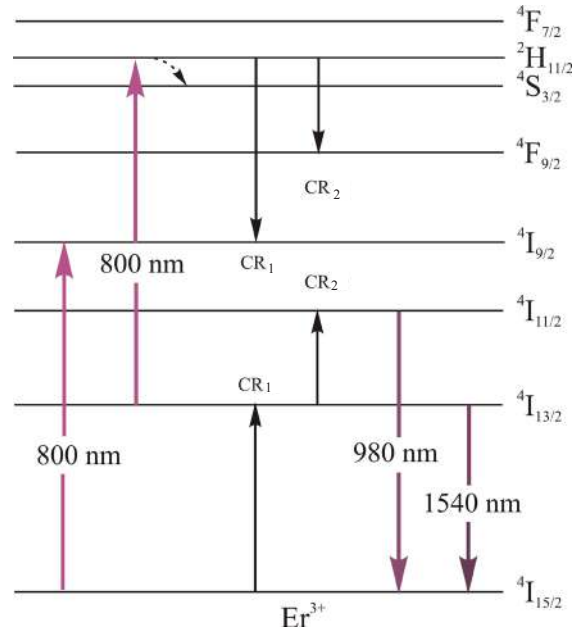
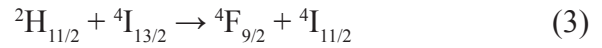
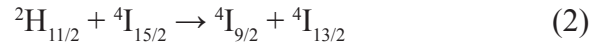


Fig. 5. Diagram of energy levels in  $\text{Er}^{3+}$  ions.

Therefore, an important role in the PL mechanism is played by the energy exchange (ET or CR) between the neighboring  $\text{Er}^{3+}$  ions. Such processes are typical of erbium ions which are involved in the formation of clusters [12]. It was established in our previous work [5] that clusters of up to  $10^3$  erbium ions form in the  $\text{Ag}_{0.05}\text{Ga}_{0.05}\text{Ge}_{0.95}\text{S}_2\text{-Er}_2\text{S}_3$  glasses.

#### 4. CONCLUSIONS

Absorption spectra in the glasses  $\text{Ag}_{28}\text{Ga}_{28}\text{Ge}_{532}\text{Er}_2\text{S}_{1123}$  and  $\text{Ag}_{12}\text{Ga}_{12}\text{Ge}_{228}\text{Er}_2\text{S}_{483}$  were investigated. Recorded absorption bands with maxima at 520, 550, 660, 805, 980 nm correspond to the transitions in 4f intra-shell transitions from the ground state to the excited states  $^2\text{H}_{11/2}$ ,  $^4\text{S}_{3/2}$ ,  $^4\text{F}_{9/2}$ ,  $^4\text{I}_{9/2}$ ,  $^4\text{I}_{11/2}$ , respectively. Stokes PL with maxima at 980 and 1540 nm was recorded upon laser excitation at 800 nm wavelength. A model explaining PL emission mechanism was elucidated from the energy level diagram of  $\text{Er}^{3+}$  ions.

#### REFERENCES

1. V.P.Gapontsev, S.M.Matitsin, A.A.Isineev, V.B.Kravchenko, Erbium glass lasers and their applications // Optics & Laser Technology V. 14, 1982, P. 189-196.
2. B. J. Eggleton, B. Luther-Davies, K. Richardson, Chalcogenide photonics // Nature Photonics. 2011. V. 5. P. 141–148.
3. Danilo Manzani, João Flávio da Silveira Petrucci, Karina Nigoghossian, Arnaldo Alves Cardoso, Sidney J. L. Ribeiro, A portable luminescent thermometer based on green up-conversion emission of  $\text{Er}^{3+}/\text{Yb}^{3+}$  co-doped tellurite glass / Scientific Reports 7 (2017) 41596
4. V.V. Halyan, I.V. Kityk, A.H. Kevshyn, I.A. Ivashchenko, G. Lakshminarayana, M.V. Shevchuk, A. Fedorchuk, M. Piasecki, Effect of temperature on the structure and luminescence properties of  $\text{Ag}_{0.05}\text{Ga}_{0.05}\text{Ge}_{0.95}\text{S}_2\text{-Er}_2\text{S}_3$  glasses / Journal of Luminescence. – 2017. V. 181. – P. 315-320.
5. V.V. Halyan, A.A. Konchits, B.D. Shanina, S.V. Krasnovyd, O.O. Lebed, A.H. Kevshyn, M.V. Shevchuk, A.V. Bodnaruk, V.O. Yukhymchuk, EPR of  $\gamma$ -induced defects and their effects on the photoluminescence in the glasses of the  $\text{Ag}_{0.05}\text{Ga}_{0.05}\text{Ge}_{0.95}\text{S}_2\text{-Er}_2\text{S}_3$  system / Radiat. Phys. Chem. 115 (2015) 189.
6. I.V. Kityk, V.V. Halyan, A.H. Kevshyn, I.A. Ivashchenko, I.D. Olekseyuk, O.O. Lebed, G. Lakshminarayana, M. Piasecki,  $(\text{Ga}_{54.59}\text{In}_{44.66}\text{Er}_{0.75})_2\text{S}_{300}$  single crystal: novel material for detection of  $\gamma$ -radiation by photoinduced nonlinear optical method / Journal of Materials Science: Materials in Electronics. – 2017. – V. 28. – P. 14097–14102
7. I.V. Kityk, V.O. Yukhymchuk, A. Fedorchuk, V.V. Halyan, I.A. Ivashchenko, I.D. Oleksieyuk, M.A. Skoryk, G. Lakshminarayana, A.M. El-Naggar, A.A. Albassam, O.O. Lebed, M. Piasecki, Laser stimulated piezo-optics of  $\gamma$ -irradiated  $(\text{Ga}_{55}\text{In}_{45})_2\text{S}_{300}$  and  $(\text{Ga}_{54.59}\text{In}_{44.66}\text{Er}_{0.75})_2\text{S}_{300}$  single crystals // Journal of Alloys and Compounds. – 2017.V. 722. – P. 265–271
8. V.V. Halyan, M.V. Shevchuk, G.Ye. Davydyuk, S.V. Voronyuk, A.H. Kevshyn, V.V. Bulatetsky. Glass formation region and X-ray analysis of the glassy alloys in  $\text{AgGaSe}_2+\text{GeS}_2$ – $\text{AgGaS}_2+\text{GeSe}_2$  system / Semicond. Phys. Quant. Electron. Optoelectron. 12 (2009) 138.
9. V.V. Halyan, V.V. Strelchuk, V.O. Yukhymchuk, A.H. Kevshyn, G.Ye. Davydyuk, M.V. Shevchuk, S.V. Voronyuk. Role of structural ordering on optical properties of the glasses  $\text{Ag}_{0.05}\text{Ga}_{0.05}\text{Ge}_{0.95}\text{S}_2\text{-Er}_2\text{S}_3$  / Physica B. 411 (2013) 35.
10. I.I. Opera, H. Hesse, K. Betzler. Luminescence of erbium-doped bismuth-borate glasses // Optical Materials V. 28, 2006, P. 1136-1142
11. V.V. Halyan, A.H. Kevshyn, G.E. Davydyuk, M.V. Shevchuk, S.V. Voronyuk, Influence of the Er Concentration on the Bandwidth of Photoluminescence in the  $\text{Ag}_{0.05}\text{Ga}_{0.05}\text{Ge}_{0.95}\text{S}_2\text{-Er}_2\text{S}_3$  Glasses // Ukr. Fiz. Zh., 55 (2010) 1278

12. K. Koughia, M. Munzar, D. Tonchev, C.J. Haugen, R.G. Decorby, J.N. McMullin, S.O. Kasap, Photoluminescence in Er-doped Ge–Ga–Se glasses //

Journal of Luminescence. – 2005. V. 112. – P. 92-96.

This article has been received in September 2018

UDC 621.315.592

*V. V. Halyan, I. D. Olekseyuk, I. A. Ivashchenko, A. H. Kevshyn, P. V. Tishchenko, M. V. Shevchuk*

### OPTICAL PROPERTIES OF THE $\text{Ag}_{28}\text{Ga}_{28}\text{Ge}_{532}\text{Er}_2\text{S}_{1123}$ AND $\text{Ag}_{12}\text{Ga}_{12}\text{Ge}_{228}\text{Er}_2\text{S}_{483}$ GLASSES

Absorption spectra of the glasses  $\text{Ag}_{28}\text{Ga}_{28}\text{Ge}_{532}\text{Er}_2\text{S}_{1123}$  and  $\text{Ag}_{12}\text{Ga}_{12}\text{Ge}_{228}\text{Er}_2\text{S}_{483}$  in the 450–1050 nm range at room temperature were investigated. PL bands with maxima at 980 and 1540 nm were recorded under laser excitation with 800 nm wavelength. PL emission mechanism is analyzed from energy transfer processes, taking into account partial cluster formation of erbium ions and energy transition diagram of  $\text{Er}^{3+}$ .

**Keywords:** absorption spectra, photoluminescence, erbium ion, cluster formation, emission mechanism.

УДК 621.315.592

*В. В. Галян, І. Д. Олексюк, І. А. Іващенко, А. Г. Кевшин, П. В. Тищенко, М. В. Шевчук*

### ОПТИЧНІ ВЛАСТИВОСТІ СТЕКОЛ $\text{Ag}_{28}\text{Ga}_{28}\text{Ge}_{532}\text{Er}_2\text{S}_{1123}$ ТА $\text{Ag}_{12}\text{Ga}_{12}\text{Ge}_{228}\text{Er}_2\text{S}_{483}$

Досліджено спектри поглинання стекол  $\text{Ag}_{28}\text{Ga}_{28}\text{Ge}_{532}\text{Er}_2\text{S}_{1123}$  та  $\text{Ag}_{12}\text{Ga}_{12}\text{Ge}_{228}\text{Er}_2\text{S}_{483}$  в діапазоні 450 – 1050 нм за кімнатної температури. Зафіксовано смуги ФЛ із максимумами 980 та 1540 нм при збудженні лазером із довжиною хвилі 800 нм. На основі процесів обміну енергією, враховуючи часткову кластеризацію іонів Ербію та діаграму енергетичних переходів в іонах  $\text{Er}^{3+}$ , проаналізовано механізм випромінювання ФЛ.

**Ключові слова:** спектр поглинання, фотолюмінесценція, іон Ербію, кластеризація, механізм випромінювання.

*В. В. Галян, И. Д. Алексеюк, И. А. Иващенко, А. Г. Кевшин, П. В. Тищенко, М. В. Шевчук*

### **ОПТИЧЕСКИЕ СВОЙСТВА СТЕКОЛ $\text{Ag}_{28}\text{Ga}_{28}\text{Ge}_{532}\text{Er}_2\text{S}_{1123}$ И $\text{Ag}_{12}\text{Ga}_{12}\text{Ge}_{228}\text{Er}_2\text{S}_{483}$**

Исследованы спектры поглощения стекол  $\text{Ag}_{28}\text{Ga}_{28}\text{Ge}_{532}\text{Er}_2\text{S}_{1123}$  и  $\text{Ag}_{12}\text{Ga}_{12}\text{Ge}_{228}\text{Er}_2\text{S}_{483}$  в диапазоне 450 – 1050 нм при комнатной температуре. Зафиксировано полосы ФЛ с максимумами 980 и 1540 нм при возбуждении лазером с длиной волны 800 нм. На основе процессов обмена энергией, учитывая частичную кластеризацию ионов эрбия и диаграмму энергетических переходов в ионах  $\text{Er}^{3+}$ , проанализирован механизм излучения ФЛ.

**Ключевые слова:** спектр поглощения, фотолюминесценция, ион эрбия, кластеризация, механизм излучения.

## ВАЛЕНТИНУ АНДРІЙОВИЧУ СМИНТИНІ – 70!

*8 вересня 2018 р. виповнилося 70 років від дня народження зав. кафедрою експериментальної фізики Одеського національного університету імені І. І. Мечникова, керівника фізико-технічного центру НАН України та МОН України, радника ректора ОНУ імені І. І. Мечникова,*

*доктора фізико-математичних наук, професора, Заслуженого діяча науки і техніки України, лауреата Державної премії України в галузі науки і техніки*

### СМИНТИНИ ВАЛЕНТИНА АНДРІЙОВИЧА



По закінченню з відзнакою фізичного факультету і аспірантури Одеського державного університету імені І. І. Мечникова В. А. Сминтина з 1974 р. до теперішнього часу постійно працює там науковим співробітником, заступником декана фізичного факультету з наукової роботи, проректором (1992-1995) та ректором (1995-2010). Під його керівництвом ОНУ здобуває статус національного (2000 р.), нагороджений

Почесною Грамотою Кабінету Міністрів України (2000 р.) та посів перше місце у рейтингу класичних університетів (2005 р.).

В. А. Сминтина – відомий і авторитетний фізик, праці якого визнані в Україні та за її межами. Він є автором 15 наукових монографій (6 без співавторів), понад 300 статей у провідних закордонних виданнях (30 без співавторів), 38 авторських свідоцтв та патентів (7 без співавторів) та 15 підручників (7 без співавторів), рекомендованих МОН України. Всього наукових публікацій понад 700.

Основні наукові результати отримані В. А. Сминтиною в області фізики поверхневих явищ та сенсорики при дослідженні поверхні плівок, шарів, складних макро-, мікро- та нанопоруватих структур і квантових точок напівпровідників. Він розв'язав принципово важливу фізичну проблему цілеспрямованого впливу на адсорбційні властивості поверхні; розвинув теорію універсального визначення адсорбційної чутливості матеріалів, методів її прогнозування і формування. Вперше запропонував метод елементної діагностики складу поверхні, який базується на результатах взаємодії між біографічними та адсорбованими атомами поверхні. Виявив новий тип неоднорідності на поверхні – хемосорбційно-електричний домен, який відповідає за комплекс вперше ним вивчених поверхневих явищ: хемосорбційно стимульовані коливання струму, від'ємний диференційний опір та насичення ВАХ, сенсibiлізація та десенсибилізація поверхні як наслідок хемосорбційної генерації і розпаду центрів fotocутливості. Вперше встановив фізичний механізм невідтворюваності властивостей поверхні плівок  $A_2B_6$ , розробив й впровадив методику управління їх адсорбційними властивостями, розкрив фізичні закономірності немонотонної пошарової зміни хімічного складу їх поверхні, зробив вагомий внесок у розвиток фізичних основ процесів формування кластерних та сіткових структур нестехіометричних поверхневих атомів, запропонував експрес-методи встановлення природи як центрів адсорбції, так й адсорбованих частинок на поверхні. Ним

створено і передано замовникам серію нових адсорбційно чутливих елементів. Цей комплекс робіт, разом з іншими, відзначений у 2007 р. Державною премією України з науки і техніки.

В результаті досліджень явищ на поверхні та на межі розділу під керівництвом В. А. Сминтини отримані принципово нові наукові результати стосовно поверхневих ефектів, встановлені фізичні механізми направленного формування функціональних параметрів поверхні епітаксціальних структур мікро- і наногетеропереходів, квантових точок в їх складі; створені нові гетеросистеми реєстрації зображення; розвинуто теорію переносу заряду в неідеальних гетероструктурах.

В результаті аналізу й моделювання поверхневих електронно-молекулярних, електрофізичних процесів під керівництвом В. А. Сминтини створені нові мікроелектронні сенсори для інтелектуальних систем контролю фізичних, хімічних, біологічних та екологічних об'єктів.

В області нанобіофізики складних структур і систем В. А. Сминтиною отримані вагомні наукові результати, що є значним внеском у розвиток досліджень нанобіофізичних сенсорів, наногетеропереходів, наноламініатів, нанострижнів, нанодротів та інших структур. У створених за новою розробленою під його керівництвом технологією нанобіофізичних сенсорах встановлено механізм взаємодії квантових точок CdS з біологічною матрицею, в якій вони виконують роль трансдюсера неелектричного сигналу у фотолюмінісцентне випромінювання, визначена роль наноболонки ZnS на нанокристалах CdS та встановлено її значення у формуванні їх сенсорних властивостей у складі наногетеропереходу ZnS-CdS. Квантові точки CdS та наноболонка ZnS виготовлені за розробленою під його керівництвом новітньою технологією.

Під керівництвом В.А. Сминтини розроблена нова технологічна платформа та на її основі виготовлені нанобіофізичні сенсорні складні структури на базі наноламініатів (atomic layer deposition), нанострижнів, нанодротів, інших наноматеріалів у вигляді склад-

них композицій AlZnO-TiO<sub>2</sub> та інших оксидів металів. Ним визначені фізичні механізми чутливості складних структур до біологічних об'єктів, зокрема, до лейкозу ВРХ та сальмонели, встановлена природа центрів чутливості створених під його керівництвом нанобіофізичних сенсорів до біологічних субстанцій як в області екситонної, так й дефектної люмінесценції базових наноструктур. Методами XPS, SEM, AFM та іншими засобами прямих досліджень морфології та елементного складу поверхні нанобіофізичних сенсорів визначено характерні особливості технологічної платформи для їх створення.

За допомогою нового розробленого під керівництвом В. А. Сминтини методу неелектролітичного травлення Si створені оригінальні нано- та мезопоруваті біофізичні сенсори, чутливість яких до біологічних об'єктів підвищена нанесенням на поверхню та в пори Si (10-15 нм) методом atomic layer deposition наночастинок TiO<sub>2</sub>.

Методом поверхневого плазмонного резонансу (ППР) визначені адсорбційно чутливі властивості наночастинок SnO<sub>2</sub> та квантових точок Ag. За допомогою ППР встановлені оптимальні розміри квантових точок Ag, які успішно застосовані як складові антисептика та як фактор стимулювання загоєння пошкодженої шкіри.

Найважливіші результати захищені у 10 докторських та багатьох кандидатських дисертаціях, отримали нагороди на міжнародних та вітчизняних виставках, відзначені трьома Державними Преміями України в галузі науки і техніки (2007, 2009 та 2011 рр.).

В. А. Сминтина є визнаним керівником наукової школи з фізики поверхні напівпровідників, яка визначає стан даної галузі на Півдні України і впливає на її розвиток в Україні. Він ефективно керує створеним ним фізико-технічним центром НАН України та МОН України, є головою спеціалізованої ради по захисту докторських дисертацій, заступником голови Наукової Ради з фізики напівпровідників при Президії НАНУ, був віце-президентом Українського Фізичного Товариства, членом Комітету з Державних премій України, за-

ступником Голови Південного наукового центру НАНУ. Завдяки його зусиллям в останні роки Одеський науковий регіон став одним з відомих наукових центрів в галузі фізики, зокрема, фізики наноструктур.

Він головний редактор журналів «Фотоелектроніка», «Сенсорна електроніка та мікросистемні технології» (входять до наукометричної бази «Index Copernicus») та організатор Всеукраїнського з'їзду «Фізика в Україні», I і III Всеукраїнських конференцій з фізики напівпровідників, восьми Міжнародних конференцій «Сенсорна електроніка та мікросистемні технології», конгресів EUROSENSOR.

В. А. Сминтина створив науково-дослідну лабораторію сенсорної електроніки, відкрив навчально-науковий центр медичної та біологічної фізики, фізико-технічний центр подвійного підпорядкування НАНУ та МОН України, якими успішно керує.

В. А. Сминтина – єдиний від України постійний член відбіркового комітету EUROSENSOR, член Європейського фізичного товариства та Оптичного Товариства Америки, керівник та учасник наукових програм в національних центрах досліджень Італії, Франції, Німеччини, Фінляндії, Португалії та ін., в деяких з них започатку-

вав нові напрямки досліджень в галузі фізики поверхневих явищ. Він ефективно керує роботою українських груп у європейських науково-дослідних програмах FP-6, FP-7.

В. А. Сминтина на високому науковому рівні читає розроблені ним новітні спецкурси «Поверхневі явища у напівпровідниках», «Фізико-хімічні явища на поверхні твердих тіл» й «Фотоелектричні процеси у напівпровідниках» та фундаментальні курси

«Оптика», «Фізика атома» та «Фізика сенсорів» ефективно керує підготовкою магістрів, аспірантів, докторів філософії і докторантів з фізики поверхні та експериментальної фізики, як запрошений професор читає курси лекцій за кордоном.

Діяльність В. А. Сминтини у галузі науки та освіти відзначена багатьма державними нагородами. Він – Заслужений діяч науки і техніки України, Лауреат Державної Премії України в галузі науки і техніки, кавалер ордену «За заслуги» III ступеня, його нагороджено також Почесними Грамотами Верховної Ради України та Кабінету Міністрів України, Почесними відзнаками НАН України «За наукові досягнення» та «За підготовку наукової зміни», відзнаками МОН України. Валентин Андрійович Сминтина також відзначений нагородами 7 країн світу.

## Інформація для авторів наукового збірника «Photoelectronics»

У збірнику "Photoelectronics " друкуються статті, що містять відомості про наукові дослідження і технічні розробки в напрямках:

- \* фізика напівпровідників;
- \* гетеро- і низькорозмірні структури;
- \* фізика мікроелектронних приладів;
- \* лінійна і нелінійна оптика твердого тіла;
- \* оптоелектроніка та оптоелектронні прилади;
- \* квантова електроніка;
- \* сенсорика

Збірник "Photoelectronics видається англійською мовою. Рукопис подається автором у двох примірниках англійською і російською мовами.

### **Електронна копія статті повинна відповідати наступним вимогам:**

1. Для тексту дозволяються наступні формати - MS Word (rtf, doc).
2. Рисунки приймаються у форматах – EPS, TIFF, BMP, PCX, JPG, GIF, CDR, WMF, MS Word I MS Gif, Micro Calc Origin (obj).

### **Рукописи надсилаються за адресою:**

Відп. секр. Куталовій М. І., вул. Пастера, 42. фіз. фак. ОНУ, м. Одеса, 65082

E-mail: photoelectronics@onu.edu.ua

тел. 0482 - 726 6356 .

Збірники "Photoelectronics" знаходяться на сайті: <http://photoelectronics.onu.edu.ua>

### **До рукопису додаються:**

1. Коди РАС і УДК. Допускається використання декількох шифрів, що розділяються комами.
2. Прізвища і ініціали авторів.
3. Установа, повна поштова адреса, номер телефону, номер факсу, адреси електронної пошти для кожного з авторів.
4. Назва статті.
5. Резюме обсягом до 200 слів пишеться англійською, російською і (для авторів з України) – українською мовами.

*Текст* друкувати шрифтом 14 пунктів через два інтервали на білому папері формату А4. Назва статті, а також заголовки підрозділів друкуються прописними літерами. .

*Рівняння* необхідно друкувати в редакторі формул MS Equation Editor. Необхідно давати визначення величин, що з'являються в тексті вперше.

*Посилання* на літературу друкувати через два інтервали, нумеруватися в квадратних дужках послідовно, у порядку їхньої появи в тексті статті. Посилатися необхідно на літературу, що видана пізніше 2000 року.

*Підписи* до рисунків і таблиць друкуються в тексті рукопису в порядку їхньої ілюстрації.

*Резюме* обсягом до 200 слів друкується англійською, російською і українською мовами (для авторів з України). Перед текстом резюме відповідною мовою вказуються УДК, прізвища та ініціали всіх авторів, назва статті.

## **Информация для авторов Научного сборника «Photoelectronics»**

В сборнике "Photoelectronics" печатаются статьи, которые содержат сведения о научных исследованиях и технических разработках в направлениях:

- \* физика полупроводников;
- \* гетеро- и низкоразмерные структуры;
- \* физика микроэлектронных приборов;
- \* линейная и нелинейная оптика твердого тела;
- \* оптоэлектроника и оптоэлектронные приборы;
- \* квантовая электроника;
- \* сенсорика

Сборник "Photoelectronics" издаётся на английском языке. Рукопись подается автором в двух экземплярах на английском и русском языках.

**Электронная копия статьи должна отвечать следующим требованиям:**

1. Для текста допустимы следующие форматы - MS Word (rtf, doc).
2. Рисунки принимаются в форматах – EPS, TIFF, BMP, PCX, JPG, GIF, CDR, WMF, MS Word И MS Gif, Micro Calc Origin (orj).

**Рукописи присылаются по адресу:**

Отв. секр. Куталовой М. И., ул. Пастера. 42. физ. фак. ОНУ, г. Одесса, 65026  
E-mail: photoelectronics@onu.du.ua тел. 0482 - 726 6356 .

Статьи сб. "Photoelectronics" находятся на сайте: <http://photoelectronics.onu.edu.ua>

**К рукописи прилагается:**

1. Коды РАС и УДК. Допускается использование нескольких шифров, которые разделяются запятой.
2. Фамилии и инициалы авторов.
3. Учреждение, полный почтовый адрес, номер телефона, номер факса, адреса электронной почты для КАЖДОГО ИЗ АВТОРОВ.
4. Название статьи.
5. Резюме объемом до 200 слов пишется на английском, русском языках и (для авторов из Украины) – на украинском.

*Текст* должен печататься шрифтом 14 пунктов через два интервала на белой бумаге формата А4. Название статьи, а также заголовки подразделов печатаются прописными буквами и отмечаются полужирным шрифтом.

*Уравнения* необходимо печатать в редакторе формул MS Equation Editor. Необходимо давать определение величин, которые появляются в тексте впервые.

*Ссылки* на литературу должны печататься через два интервала, нумероваться в квадратных скобках последовательно, в порядке их появления в тексте статьи. Ссылаться необходимо на литературу, которая издана позднее 2000 года.

*Подписи* к рисункам и таблицам печатаются в тексте рукописи в порядке их иллюстрации.

*Резюме* объемом до 200 слов печатается на английском, русском языках и на украинском (для авторов из Украины). Перед текстом резюме соответствующим языком указываются УДК, фамилии и инициалы всех авторов, название статьи.

## **Information for contributors of «Photoelectronics» articles**

“Photoelectronics” Articles publishes the papers which contain information about scientific research and technical designs in the following areas:

- Physics of semiconductors;
- Physics of microelectronic devices;
- Linear and non-linear optics of solids;
- Optoelectronics and optoelectronic devices;
- Quantum electronics;
- Sensorics.

“Photoelectronics” Articles is defined by the decision of the Highest Certifying Commission as the specialized edition for physical-mathematical and technical sciences and published and printed at the expense of budget items of Odessa I.I. Mechnikov National University.

«Photoelectronics» Articles is published in English. Authors send two copies of papers in English. The texts are accompanied by 3.5» diskette with text file, tables and figures. Electronic copy of a material can be sent by e-mail to the Editorial Board and should meet the following requirements:

1. The following formats are applicable for texts – MS Word (rtf, doc).

2. Figures should be made in formats – EPS, TIFF, BMP, PCX, JPG, GIF, WMF, MS Word I MS Gif, Micro Calc Origin (opj). Figures made by packets of mathematical and statistic processing should be converted into the foregoing graphic formats.

The papers should be sent to the address:

Kutalova M.I., Physical Faculty of Odessa I. I. Mechnikov National University, 42 Pastera str, 65026 Odessa, Ukraine, e-mail: wadz@mail.ru, tel. +38-0482-7266356. Information is on the site: <http://www.photoelectronics.onu.edu.ua>

### **The title page should contain:**

1. Codes of PACS
2. Surnames and initials of authors
3. TITLE OF PAPER
4. Name of institution, full postal address, number of telephone and fax, electronic address

An abstract of paper should be not more than 200 words. Before a text of summary a title of paper, surnames and initials of authors should be placed.

Equations are printed in MS Equation Editor.

References should be printed in double space and should be numbered in square brackets consecutively throughout the text. References for literature published in 2000-2009 years are preferential.

Illustrations will be scanned for digital reproduction. Only high-quality illustrations will be taken for publication. Legends and symbols should be printed inside. Neither negatives, nor slides will be taken for publication. All figures (illustrations) should be numbered in the sequence of their record in text.

For additional information please contact with the Editorial Board.



---

Верстка – О. І. Карлічук

Підп.до друку 02.11.2018. Формат 60×84/8. Ум.-друк.арк. 16,74. Тираж 300 прим. Замов. № 1831.

**Видавець і виготовлювач**  
**«Одеський національний університет імені І. І. Мечникова»**  
Свідоцтво ДК № 4215 від 22.11.2011 р.

65082, м. Одеса, вул. Єлісаветинська, 12, Україна  
Тел.: (048) 723 28 39, e-mail: [druk@onu.edu.ua](mailto:druk@onu.edu.ua)